THE SEISMIC BEHAVIOUR OF EXISTING HOLLOWCORE SEATING CONNECTIONS PRE AND POST RETROFIT

A Thesis
submitted in partial fulfilment
of the requirements for the Degree
of
Master of Engineering
at the
University of Canterbury
by
James Jensen

University of Canterbury
Christchurch, New Zealand
2006

Abstract

This investigation was part of a greater research initiative regarding the seismic vulnerability of precast hollowcore floor systems. The primary focus throughout the research programme has been to investigate the susceptibility to loss of vertical support of the floor system, from the seating beam. Previous research firstly focussed on identifying and understanding preconceived deficiencies with existing seating connection details. This was followed by the validation of amended, superior performing, 'new' seating connection details. However, little consideration has been given to retrofit techniques for already existing buildings, with potentially poor performing existing seating connections. A two-dimensional, single hollowcore unit, seating connection sub-assembly is used to experimentally investigate the seismic behaviour of previously un-tested existing seating connections pre- and post-retrofit. Three existing seating connection configurations, with the hollowcore unit seated directly on the bare concrete seating ledge and with varying seating lengths were tested. These tests were followed by a fourth retrofitted specimen. Both relative rotation between the hollowcore unit and seating beam, and beam elongation 'pull-off' deformations (resulting from the supporting frame deformations) were imposed on the test specimens. In conjunction with this experimental investigation and with prior knowledge from previous investigations, three primary failure mechanisms for existing hollowcore seating connections are summarised. A suite of conceptual retrofit techniques which target the critical structural weaknesses attributed to causing the primary failure mechanisms are outlined. In general, unfavourable performance was exhibited by the existing seating connections in the experimental investigation, resulting in loss of vertical support of the hollowcore unit under imposed 'pull-off' effects. In contrast, when the retrofit strategy was implemented, a higher level of seismic performance, leading to collapse prevention was achieved. A review is carried out into existing beam elongation numerical models, which are simple and involve only hand-type calculation procedures. The aim of this was to investigate potential methods for predicting the 'pull-off' effects on suspended floor systems. From this, a modification is made to an existing, loading dependent method developed by Matthews (2004). The modified method aimed to more accurately represent the loading dependant nature of beam elongation (and the resulting 'pull-off' effects) as described by Lee and Watanabe (2003). A number of beam elongation predictions for a suite of experimental beam elongation data sets were carried out with the modified method. Good agreement was generally seen, both in terms of prediction of the magnitude of elongation and the shape of the elongation profile.

This page is blank

Acknowledgements

The research presented in this thesis was carried out at the Department of Civil Engineering at the University of Canterbury under the supervision of Professor Des Bull and Dr Stefano Pampanin. I would sincerely like to express my gratitude to both Des and Stefano for the guidance and encouragement throughout this project and my university studies.

I would like to thank the following companies and organisations for providing financial assistance and resources for this project: University of Canterbury; Foundation for Research Science and Technology (FRST): Retrofit Solutions for New Zealand Multi Storey Buildings; The New Zealand Society for Earthquake Engineering Inc. (NZSEE): 2005 Research Scholarship, PRECAST NZ Ltd; Stresscrete; Pre-Cast Components Ltd.; Firth Industries Ltd.

Thanks must also be given to the technical staff in the Department of Civil Engineering for their guidance and friendship. In particular, I would like to recognise the significant time and effort put into my project by Russell McConchie, it would have not been possible without his experience and knowledge. I would also like to acknowledge the time and effort of John Marshall from Stresscrete Christchurch.

I would also like to express my thanks to my postgraduate colleagues, particularly Matt Ireland, Ben Hayward and Dion Marriot. Without the advice, encouragement and general good times shared with these guys my postgraduate experience would not have been the same. In addition I would like to thank Dr Jeff Matthews, Renee Brook (Lindsay) and Cameron MacPherson for going out of their way to supply me with data and information from their research.

Finally I would like to thank my friends and family for their ongoing support, encouragement, and numerous enjoyable times throughout my university career. In particular I would like to thank my father and his partner Donna for their unwavering support and encouragement during my studies.

This page is blank

Table of Contents

This page is blank

List of Figures

List of Tables

This page is blank

1 Research Review and Outline

1.1 Introduction

Post-earthquake reconnaissance and experimental investigations have highlighted uncertainties regarding the seismic performance of existing precast hollowcore floor systems when coupled with ductile seismic resisting frames (Norton et al. 1994; Iverson and Hawkins 1994; Holmes and Somers 1995; Herlihy 1999; Bull and Matthews 2003; Liew 2004; Matthews 2004). These uncertainties are associated with the structural detailing and resulting behaviour of connections around the floor perimeter. The foremost of these uncertainties is the issue of maintaining vertical support of the one-way floor system at the end floor to seating beam connection during a seismic event.

The gravity load carrying capacity of the end seating connection can be jeopardised by incompatibilities between the intrinsic behaviour of the individual floor and frame systems. The frame behaviour of concern is the elongation of plastic hinges in beams running parallel to the one-way floor system; and relative rotation between the floor system and the supporting end seating beam; both of which result under the lateral drift of a ductile seismic resisting frame. The conflicting intrinsic floor properties are the one-way, brittle, and unreinforced nature of the prestressed, concrete hollowcore floor units.

As a result of these incompatibilities, the end seating connection must accommodate both 'pull-off' and rotational deformation from beam elongation and seating beam rotation to maintain vertical support. The general connection philosophy adopted for typical existing seating connections has been shown to be deficient in both of these facets through insufficient seating ledges and excess rotational fixity. Consequently, the structural integrity and performance of the floor system, both in gravity support and lateral load transfer can be jeopardised.

Research has since shown that through a number of simple structural modifications to the end seating and longitudinal perimeter connection details, much higher levels of performance can be achieved by such systems (Lindsay 2004; MacPherson 2005). The primary aim of these modifications was to maintain the vertical gravity support of the floor system. Alternative seating connections have been tested in a full-scale, three-dimensional floor and frame

super-assembly, showing a higher performance when compared with typical existing seating connections. As a result, two acceptable solutions for hollowcore seating connections have been amended within NZS3101:1995 (NZS3101:1995, Amendment 3 2004) and NZS3101:2006 for use in 'new' construction practice in New Zealand.

However, there has been little research carried out investigating retrofit procedures for existing buildings designed prior to the implementation of amended connection details. This, therefore, is the motivation for this investigation, being part of an ongoing research programme regarding the seismic performance of hollowcore floor systems. Focus is primarily given to the hollowcore end seating connection. Failure of this connection has by far the greatest implication on seismic performance of such buildings with potential for substantial loss of life.

1.2 Previous Research Base

Previous research that focussed on the interaction between seismic resisting frame and proprietary precast hollowcore floor systems has highlighted and further confirmed a number of issues and incompatibilities between the two systems. These incompatibilities can potentially jeopardise structural integrity of the floor diaphragm system locally at individual connections on individual floors, and globally of a number of floors in a 'pancake' manner. Considerable advances in the understanding of these issues and further identified questions are discussed, from which the motivation, background and foundation for this research is based upon. Particular focus is given to hollowcore to seating beam connections as this area has the most relevance to this research project.

1.3 'Pull-Off' Sub-Assembly Investigations

A succession of simplified hollowcore seating connection sub-assembly tests were carried out at the University of Canterbury to investigate concerns regarding structural incompatibilities of such systems. The particular connection of concern was the vertical support seating connection between the precast hollowcore floor units and frame seating beams which support these units. The series of 'pull-off' type tests were carried out on a variety of seating connection details and were tested under a range monotonic and cyclic axial tension and/or monotonic vertical load, designed to pull the flooring unit off the supporting beam (Herlihy 1999; Mejia-McMaster 1994; Oliver 1998). The aim was to investigate the amount

of ‘pull-off’ (resulting from plastic hinging in beams running parallel to the one-way floor system) that was required to induce loss of seating. Further to this, the aim was to investigate what vertical load carrying capacity remained following the loss of seating due to additional tie reinforcement, bond between the units and cast *in-situ* concrete topping, and interlock at the failure surface. Figure 1-1 shows the test rig typical of early ‘pull-off’ style hollowcore sub-assembly tests.

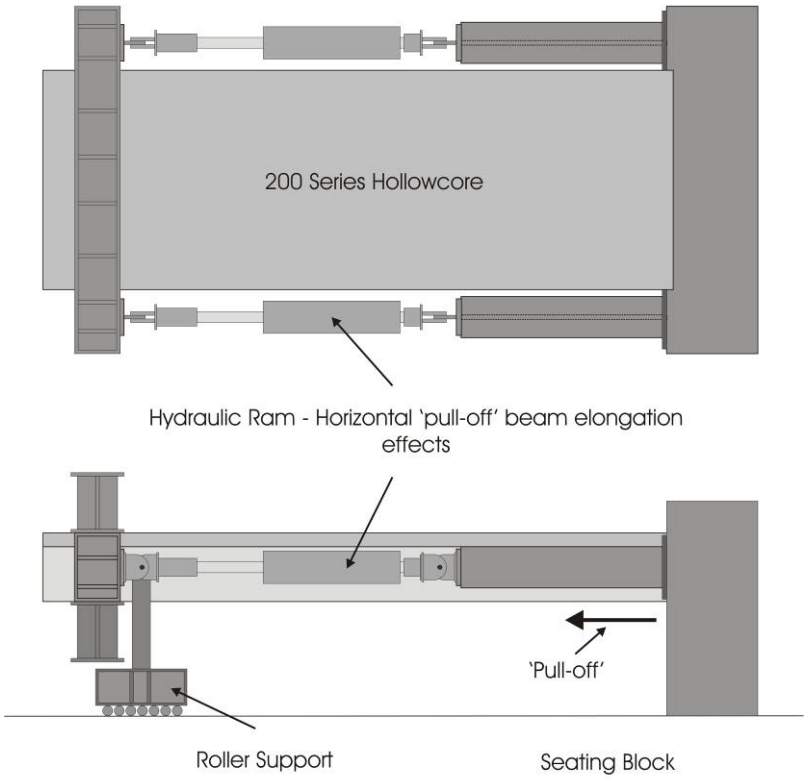

Figure 1-1 Typical ‘pull-off’ type test setup used to investigate the effect of beam elongation on seating connection integrity after Herlihy (1999)

Mejia-McMaster (1994) investigated three hollowcore seating connections with varying tie reinforcement between the precast hollowcore units and supporting seating beam. The aim was to investigate the shear capacity of the hollowcore unit to seating beam interface and quantify the potential for vertical support due to tie reinforcement should loss of seating occur. Figure 1-2 shows the nature of the connections and tie reinforcement tested by Mejia-McMaster (1994).

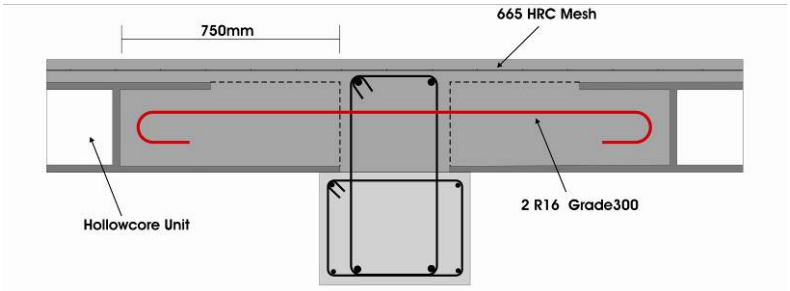

a) Detail 1

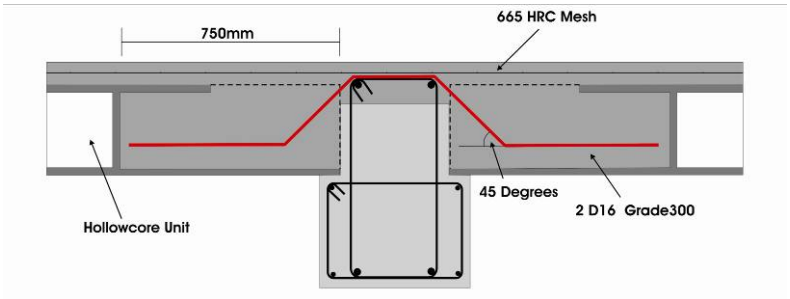

b) Detail 2

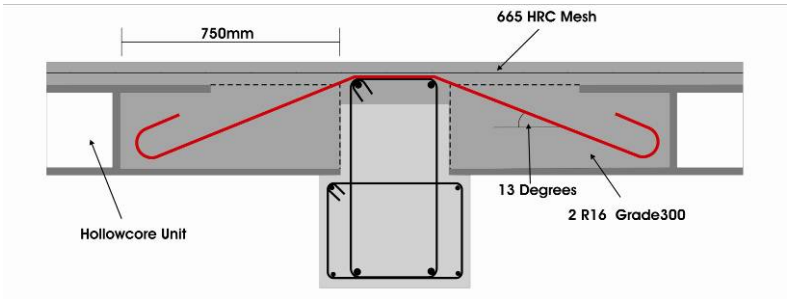

c) Detail 3

Figure 1-2 Additional tie reinforcement details tested by Mejia-McMaster (1994)

Additional tie reinforcement was found to provide sufficient vertical support to maintain support of the units following loss of seating under vertical loads greater than the seismic design gravity loads. However, the amount of elongation and the nature of tie reinforcement significantly affected the ability of the floor to supporting beam connection to deal with the elongation of the neighbouring beam. The use of plain round bars was seen to increase the deformation capacity of the connection due to early de-bonding of the tie reinforcement and hence higher levels of strain penetration along the tie bar. Under greater levels of elongation the shear capacity was provided solely through kinking of the tie bars in the absence of any shear friction between the end of the unit and seating beam due to the opening of a large crack at the hollowcore unit to beam interface.

Herlihy (1999) carried out a number of sub-assembly tests investigating a range of behavioural issues associated with the support and continuity of typical hollowcore seating

connection details. Emphasis was given to the 'pull-off' effects of beam elongation on the seating connection and the ability of the cast *in-situ* concrete topping and tie reinforcement to provide vertical support. Loss of seating tests showed that typical starter bar and mesh details in cast *in-situ* toppings provide no vertical support or control over potential loss of seating. Figure 1-3 from Herlihy (1999) shows the delamination surface between the unit and cast *in-situ* topping resulting in a lack of support.

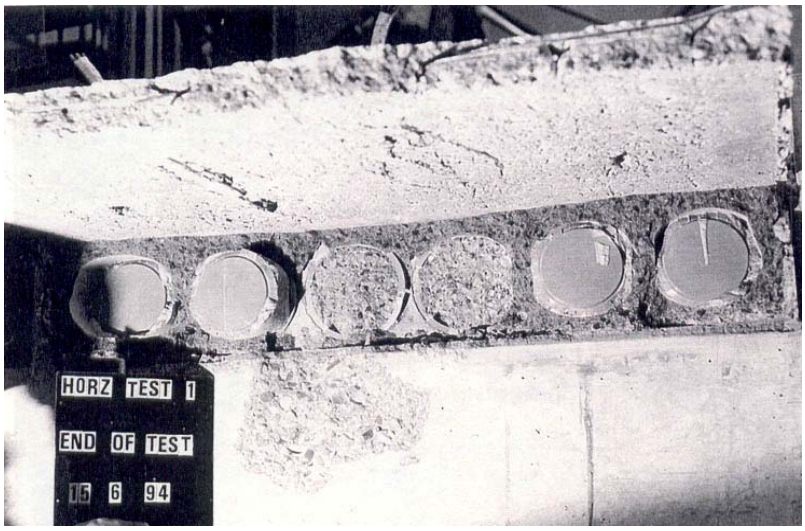

Figure 1-3 Loss of seating test after Herlihy (1999)

It was found that the bond between the hollowcore units and topping in the region of the seating connection was also likely be lost or severely deteriorated prior to sudden loss of seating due to yielding of the starter bars progressing into (strain penetration) and stretching the topping; this resulted in breaking the bond between the topping and unit. In addition, it was concluded that a provided length of seating can not necessarily be relied upon due to spalling of the un-reinforced seat.

Herlihy (1999) investigated the use of a hairpin-type tie reinforcement detail as an alternative to traditional tie reinforcement configurations. It was concluded such a tie can achieve ductile behaviour at the floor to beam connection interface when exposed to beam elongation 'pull-off'. Figure 1-4 below shows the hairpin type detail tested by Herlihy (1999).

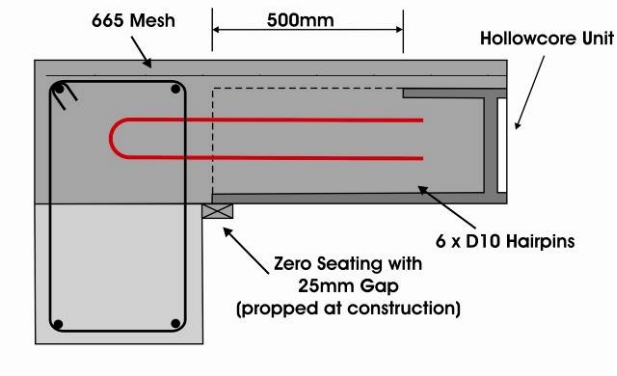

Figure 1-4 Hairpin type tie reinforcement detail tested by Herlihy

In support of Mejia-McMaster (1994), Herlihy (1999) also concluded that the use of deformed bars as tie reinforcement reduced the elongation ductility of the connection, and plain round bars were more suited to the 'pull-off' behaviour of the connection. In addition to this, it was found that when tie reinforcement was used, due to *in-situ* topping concrete passing down into the open voids (cores) at the ends of the hollowcore units, the topping was less likely to delaminate and fracture. A paperclip tie reinforcement detail was recommended by Herlihy (1999) as an alternative to the tested hairpin tie reinforcement configuration, illustrated in Figure 1-5.

Oliver (1998) investigated the use of a similar paperclip type tie reinforcement detail proposed by Herlihy (1999) and the use of steel fibre reinforced concrete (SFRC) in the addition to traditional topping reinforcement. Figure 1-5 below shows the paperclip type tie reinforcement connection detail tested by Oliver (1998).

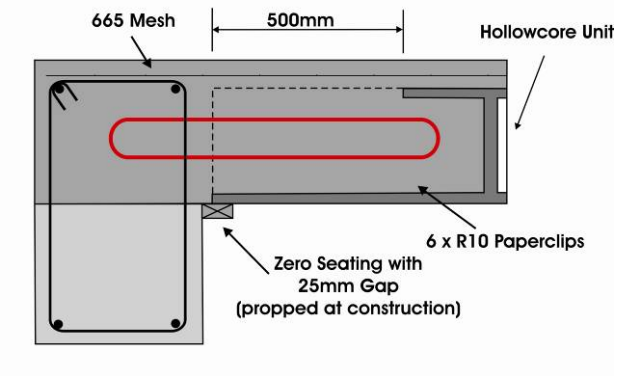

Figure 1-5 Paperclip tie reinforcement connection proposed by Herlihy (1999), tested by Oliver (1998)

Oliver (1998) concluded that the deformation capacity of paperclip tie reinforcement may not be sufficient where extreme elongation is expected. Such elongation occurs in corner regions

of seismic frame systems directly adjacent to elongating beam plastic hinges. It was also found that the use of SFRC can increase the tensile capacity of the topping and core concrete resulting in higher sustainable elongation 'pull-off' effects.

1.4 'Rotation' Sub-Assembly Investigations

Following the initial sequence of 'pull-off' tests, the relative rotation between the seating beam and hollowcore units was identified as a potential primary damage causing mechanism (Matthews 2004). This changed the approach in hollowcore research to focus on the damage to the units themselves, as well as previously identified loss of seating issues. In terms of sub-assembly type investigations, a sequence of tests were carried out which were 'rotation-focused' (Bull and Matthews 2003; Liew 2004). Figure 1-6 shows the hollowcore sub-assembly test rig used to apply relative rotation at the hollowcore seating connection. Rotation was induced through fixing the supporting seating beam and articulating the hollowcore unit using a hydraulic ram.

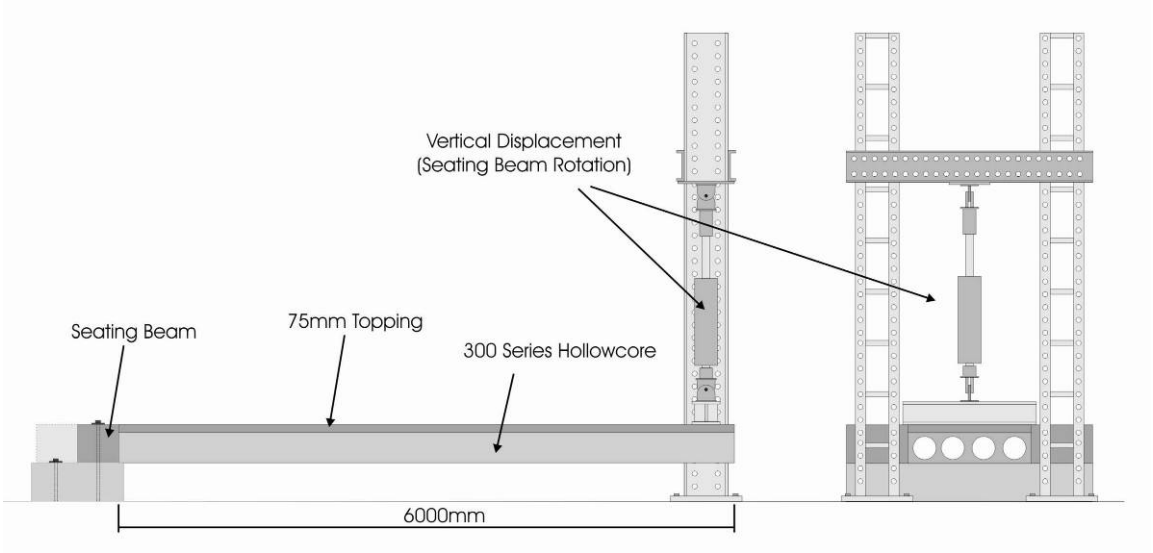

Figure 1-6 Initial hollowcore sub-assembly test rig for applying relative rotation after Bull and Matthews (2003)

The sub-assembly test rig was developed by Bull and Matthews (2003) for the purpose of efficient and indicative testing of hollowcore seating connection details. To verify the representativeness of the sub-assembly, an existing seating connection consistent with Matthews (2004) full-scale, three-dimensional super-assembly test (discussed in Section 1.6) was tested to verify compatibility between the super and sub-assembly test rigs. Good agreement was found between the two tests thus justifying the sub-assembly approach for

investigating seating connection seismic performance. There were a number of simplifications introduced into the sub-assembly test system; however the identified fundamental relative rotation damage causing mechanism was sufficiently replicated. The benefit of the sub-assembly was that results representative of realistic connection performance could be achieved at a connection level much quicker and for much less cost than the full super-assembly test. The sub-assembly approach also had a unique advantage in terms of understanding the connection performance by isolating the main damage causing mechanisms.

In the series of tests carried out by Bull and Matthews (2003), four seating connections where investigated as shown in Figure 1-7. Two of these were control specimens representing typical existing seating connections and the two remaining connections were new alternative seating connection details proposed by a Precast Suspended Floor Technical Advisory Group (NZ Technical Advisory Group on Suspended Concrete Floors, chaired by Dene Cook of CCANZ, (TAG)) aimed at improving seating connection performance in new buildings. The purpose of testing the alternative connection details was to efficiently trial new proposed seating connection details before testing the detail in the full super-assembly.

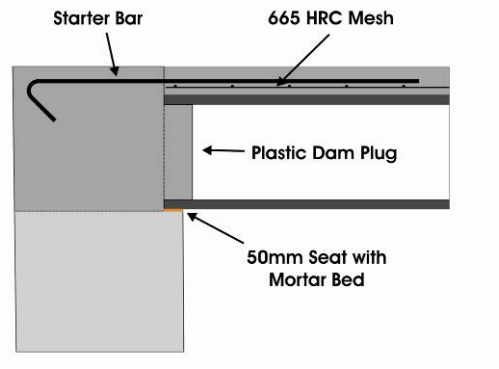

a) HC1 Control Specimen connection detail for 300 and 200 Series Hollowcore

b) HC1 300 Series flexure-shear failure mechanism

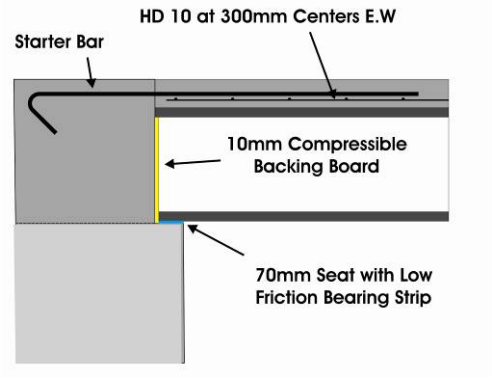

c) HC2 - TAG Proposed 'Pinned' connection

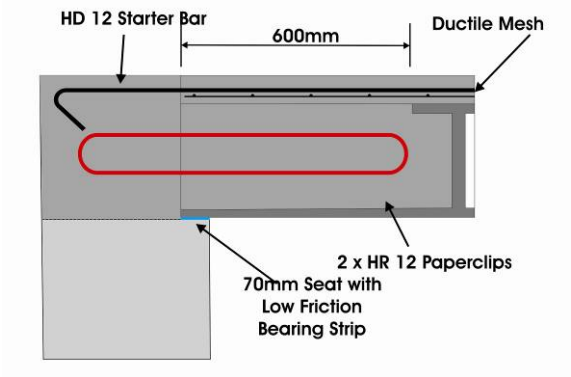

d) HC3 - TAG Proposed 'rigid' connection

Figure 1-7 Seating connection tests carried out by Bull and Matthews (2003)

The performance of the two existing connections exhibited a flexure-shear failure mechanism whereby diagonal shear cracks induced by initial flexure rupture in the soffit of the unit up through the hollowcore section in front of the seating beam. This stemmed from connection fixity imposing seating beam rotation on the floor system, consistent with Matthews' (2004) super-assembly test, as shown in Figure 1-7 b). From the control specimen tests it also concluded that the failure mechanism was consistent between 300 and 200 series hollowcore units.

The performance of the two alternative seating connection details was seen to be superior in comparison to the typical existing control specimen tests. Much higher levels of drift were achieved and loss of support and damage to the hollowcore units prevented through the connection detail modifications. The first connection modification isolated the unit from the face of the seating beam by placing a compressible backing board between the ends of the

unit and seating beam. In addition the unit was seated on a larger seating ledge (70mm as opposed to 50mm previously) with a low friction bearing strip as seen in Figure 1-7 c). The combination of which resulted in significantly reducing the rotational fixity of the connection by isolating the unit from the seating, therefore accommodating seating beam rotation.

The second modification approach reinforced the unit with a 'paperclip' type reinforcement detail in combination with an increased seating ledge length and low friction bearing strip as seen in Figure 1-7 d). The first of these connections represented a simple 'pinned' connection and the second a 'semi-rigid' type connection and both were seen as 'acceptable solutions' for new construction practice. The first of the connections was later tested and its performance verified using the full scale super-assembly test rig by Lindsay (2004) as discussed in Section 1.6. A similar 'semi-rigid' type connection was also later tested by McPherson (2005), employing the same general modification principle as the 'semi-rigid' connection but with slightly different tie reinforcement details.

Liew (2004) continued the research carried out by Bull and Matthews (2003) using the 'rotation-focussed' sub-assembly and carried out three tests. The first tests were paperclip type tie reinforcement details (one with a negative seating) aimed at representing common construction practice when seating is deficient upon erection of the floor system. These were followed by a conceptual retrofit solution for typical existing connections as tested by Bull and Matthews (2003) and Matthews (2004). The three connection details are shown in Figure 1-8 a), b) and c).

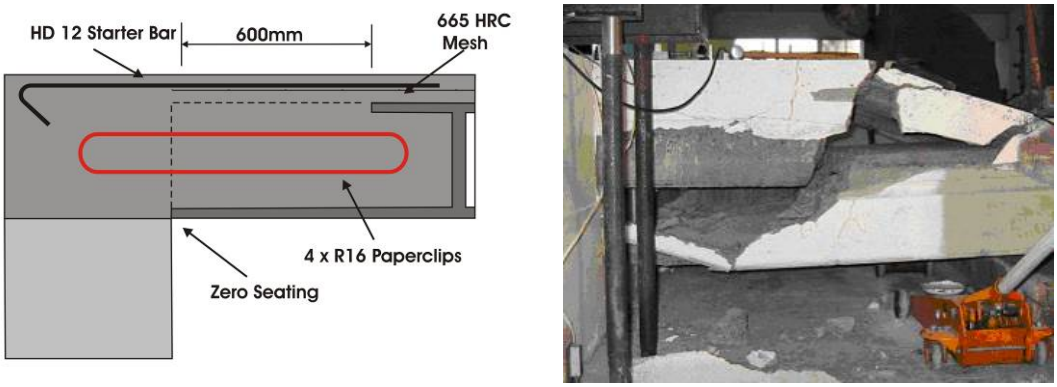

a) Negative seated paperclip seating connection detail

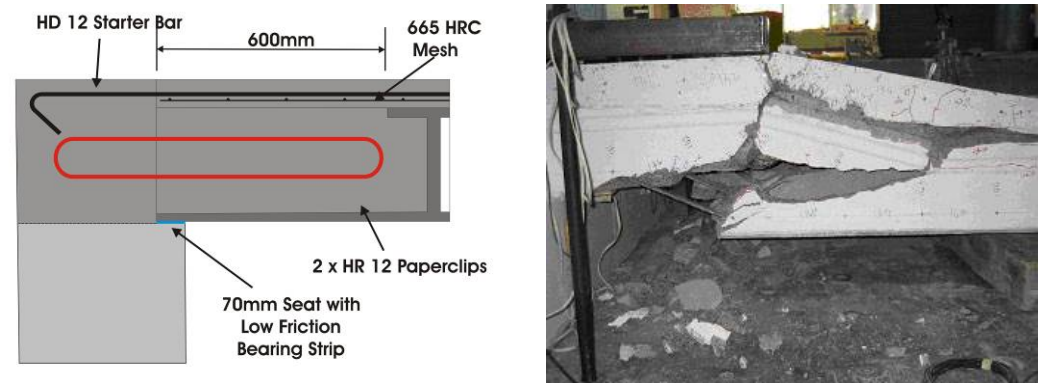

b) Seated paperclip seating connection detail

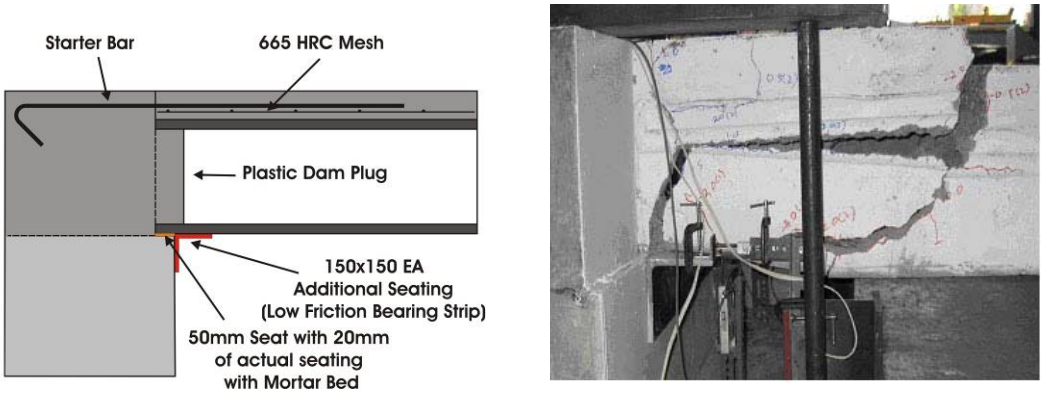

c) Retrofitted seating connection

Figure 1-8 Seating connections tested by Liew (2004)

Liew (2004) concluded that the amount of reinforcement placed in the cores can significantly affect the failure mechanism. It was found that over-reinforcement of the cores resulted in shifting the location of the previously observed flexure-shear failure mechanism from the interface between the unit and seating beam along the hollowcore unit and occurring at the termination of the reinforced core region. The connection with zero seating and paperclip tie

reinforcement in the cores performed particularly poorly, with early failure due to flexure-shear rupture of the hollowcore unit at the termination of the reinforced cores. This was of concern as the nature of this detail was similar to that used in practice when seating was not sufficient. The specific aspect of concern is the use of tie or "paperclip" reinforcement of varying densities placed centrally in the cores of the hollowcore units. More recently tie reinforcement is required to be set in the bottom of the hollowcore unit and significant consideration given to the density of the tie reinforcement and the effect his can have on overall connection flexural strength (NZS3101:2006). Further to this, the potential for over-reinforcement is increased with core reinforcement seen as beneficial to seating connection performance based on a crude 'more steel is stronger' premise.

The addition of a steel angle under the soffit of the unit as a retrofit concept aimed at increasing the provided seating length resulted in clamping the unit, leading to the unit failure under hogging moments. The seat served to provide vertical support following initial failure. However, it was concluded that clearance should be provided between the unit and additional seat to avoid further rotational restriction being imposed on the hollowcore unit (Liew 2004).

1.5 'Rotation-Elongation' Sub-Assembly Investigations

Following initial rotation-focussed sub-assembly tests, further similar tests were carried out which advanced the testing regime by incorporating both elongation and rotation on the seating connection, thus effectively combining the two previous sub-assembly test approaches. To achieve this a horizontal hydraulic ram was used similar to the 'pull-off' test method in conjunction with a vertical hydraulic ram as used in the 'rotation-focussed' sub assembly tests as seen in Figure 1-9. The aim of this was to further replicate the *in-situ* actions imposed on the precast hollowcore floor in a full-scale, three-dimensional super assembly.

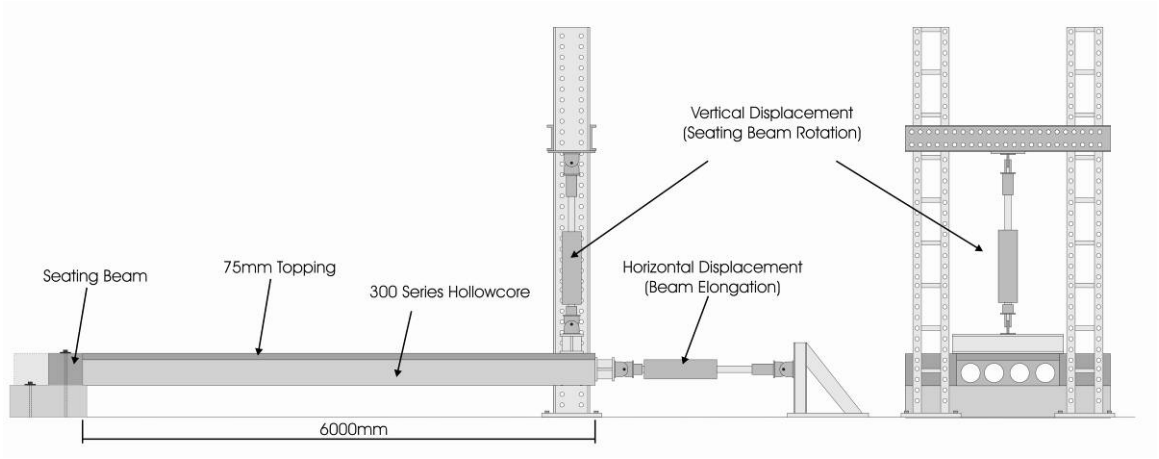

Figure 1-9 'Rotation–Elongation' sub-assembly test setup

Two tests have been carried out using this approach which trialled two alternative 'semi-rigid' type seating connections. These connections incorporated a capacity design approach to the seating connection philosophy to protect the integrity of the floor system. The first of these tests carried out by Trowsdale (2004) who tested the proposed 'acceptable solution' shown in Figure 1-10 a), specified in Amendment 3 to NZS 3101:1995 (and more recently NZS 3101:2006) and MacPherson (2005) tested a very similar detail with slightly different reinforcement details as shown in Figure 1-10 b).

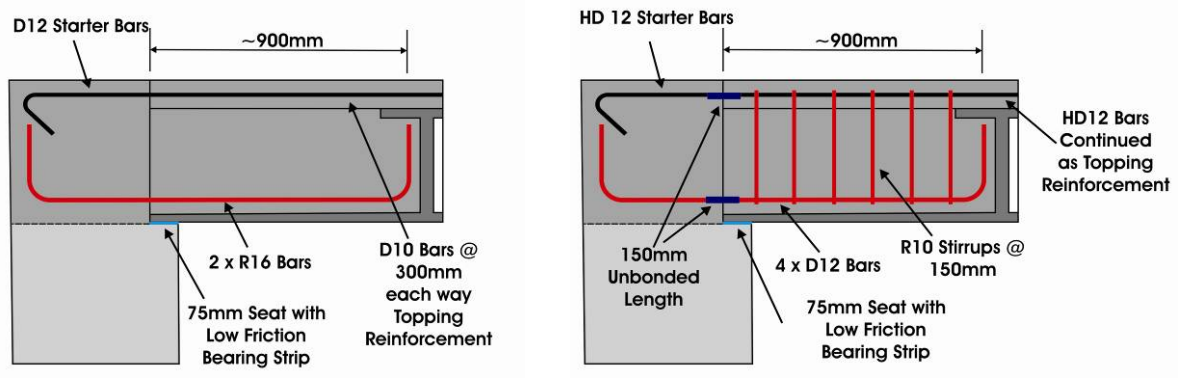

a) Trowsdale sub-assembly seating connection **b) MacPherson sub-assembly seating connection**

Figure 1-10 Seating connections tested by Trowsdale (2004) and MacPherson (2005)

The connection tested by Trowsdale (2004) was seen to out-perform previous existing and amended seating connection tests, achieving rotational drift levels of +/-4.0% with little damage to the seating beam and unit. The intended semi-rigid connection behaviour was observed whereby tension and compression yielding of the tie steel occurred at the critical hollowcore unit to seating beam interface. The resulting ductile behaviour allowed rotation to

occur between the unit and seating beam whilst also providing vertical support through tie reinforcement passing between the unit end and seating beam.

The second connection tested by MacPherson (2005) using 500 grade reinforcing did not perform as well as the connection tested by Trowsdale (2004). A moment capacity significantly greater than Trowsdale (2004) was achieved in the connection due to the use of higher grade steel, which in turn placed significantly more force demand on the unit and seating connection elements.

1.6 Super-Assembly Frame and Floor Slab Investigations

To comprehensively investigate identified uncertainties with the performance of these connections between precast hollowcore floor diaphragms and seismic resisting frame systems, a series of full-scale, three-dimensional super-assembly tests were carried out at the University of Canterbury. This sequence of tests was carried out following the initial 'pull-off' sub-assembly tests and in concurrence with the later 'rotation-focussed' and 'rotation-elongation' tests. The aim was to investigate the issues associated with hollowcore seating and perimeter connections to include three dimensional and second order effects, and how this affected the overall seismic performance of the combined structural system. Discussion is predominantly focused on hollowcore seating connection performance relevant to this investigation.

Three super-assembly tests have been carried out; the first of these by Matthews (2004) investigating then current practice (termed 'existing' in this investigation) to form a control specimen benchmark; this was followed by two tests carried out by Lindsay (2004) and MacPherson (2005) who investigated alternative construction details. The main differences were in the seating connection details aimed at remedying the shortcomings identified by Matthews (2004). This section outlines the super-assembly test rig and its advancement over previous test rigs, followed by the test details and outcomes from individual tests.

1.6.1 Lau: Precast Prestressed floors and Seismic Resisting Frames

Prior to super-assembly tests at the University of Canterbury, Lau (2001) carried out an investigation into the influence of precast prestressed floor systems on the seismic performance of reinforced concrete perimeter frames. Although not specifically looking at hollowcore floor systems, this was one of the first investigations into combined

super-assembly precast floor and frame systems seismic performance. The two-dimensional frame and floor system assembly test comprised of a four bay seismic resisting frame and precast floor system as illustrated in Figure 1-11.

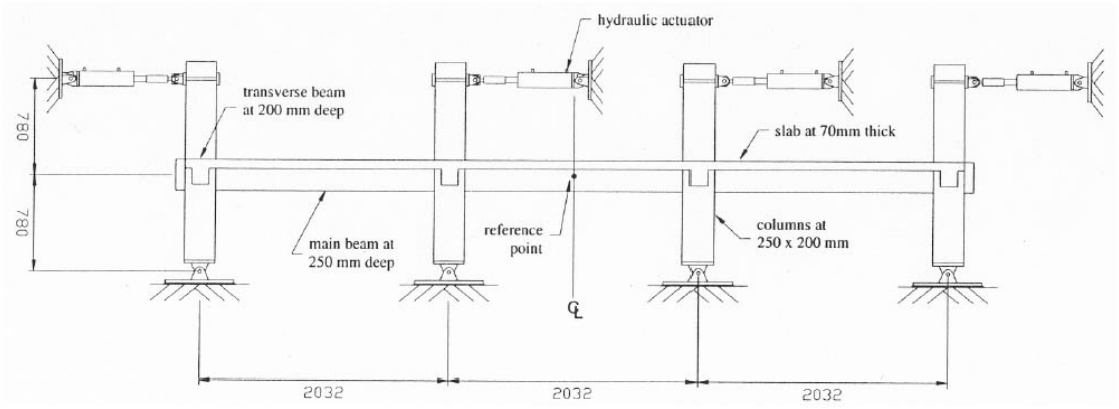

Figure 1-11 Frame and floor assembly used by Lau (2001)

Lau (2001) found interaction between the precast floor system and perimeter frame at the longitudinal perimeter connection resulted in significantly higher frame stiffness and strength than assumed for the independent frame system. A significant amount of damage was observed in connection region between the floor and frame systems. This was attributed to conflicting deformations between the floor and frame systems along the connection interface.

1.6.2 'Canterbury' Precast Floor and Frame Super Assembly

The super-assembly devised by Matthews (2004) at the University of Canterbury consisted of a two by one bay corner segment of a reinforced concrete moment resisting frame and precast hollowcore floor system that was representative of some New Zealand practices throughout the 1980's and 1990's. The nature and origin of the sub-assembly is shown in Figure 1-12.

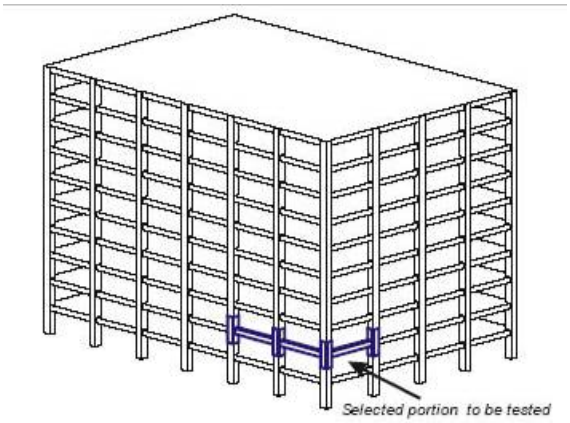

a) Prototype Building

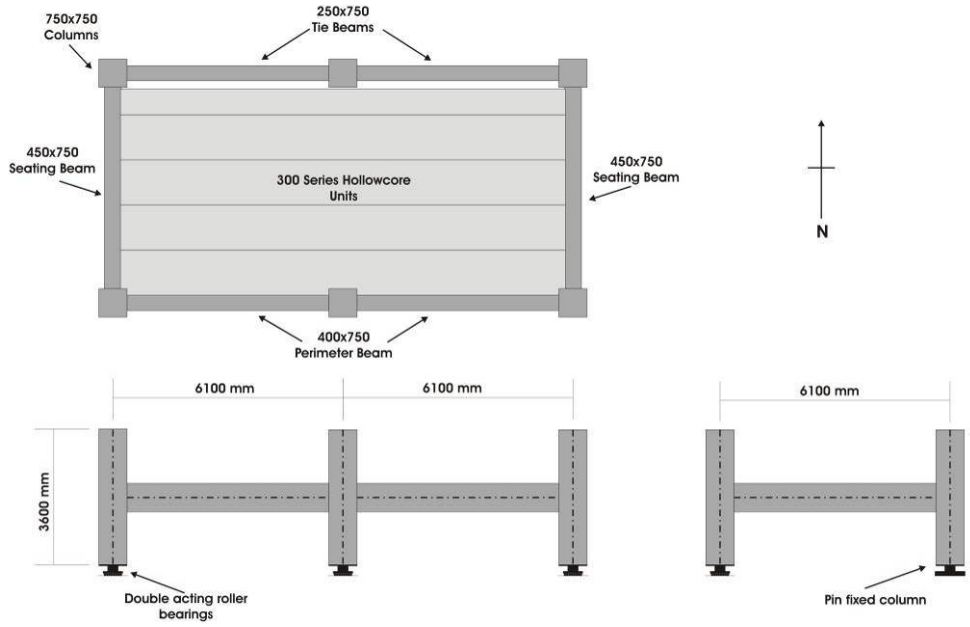

b) Super-assembly elevations

Figure 1-12 Nature and origin of the super-assembly test rig after Matthews (2004)

The seismic resisting frame system was designed and constructed using a precast emulation of a monolithic reinforced concrete seismic resisting frame assembly. The floor system was comprised of 300 series Hollowcore units and cast *in-situ* concrete topping which spanned the full length of the specimen (running parallel to the two bay length of the frame). The variations between the three tests carried out were primarily in the detailing of the connections between the individual floor and frame structural systems. The advantage of the super-assembly test setup was that through using a full-scale and three-dimensional test it was possible to construct the specimen using the same construction techniques used in practice. This significantly minimised any uncertainty associated with common simplifications in

laboratory tests. Such simplifications include scaling, reduction of the number degrees of freedom and most importantly the simplification of boundary conditions. This is particularly relevant for boundaries at connections between the floor and frame systems, which was one of the primary interests of the investigation.

Of particular relevance with respect to boundary conditions was the use of sliding column base supports and test loading rig design to provide no restraint to beam elongation. This was particularly important when considering the effect of beam elongation 'pull-off' on the hollowcore floor diaphragm system. This was a significant advancement from previous fixed base, elongation restraining test rigs. The loading frames and sliding base are illustrated in Figure 1-13.

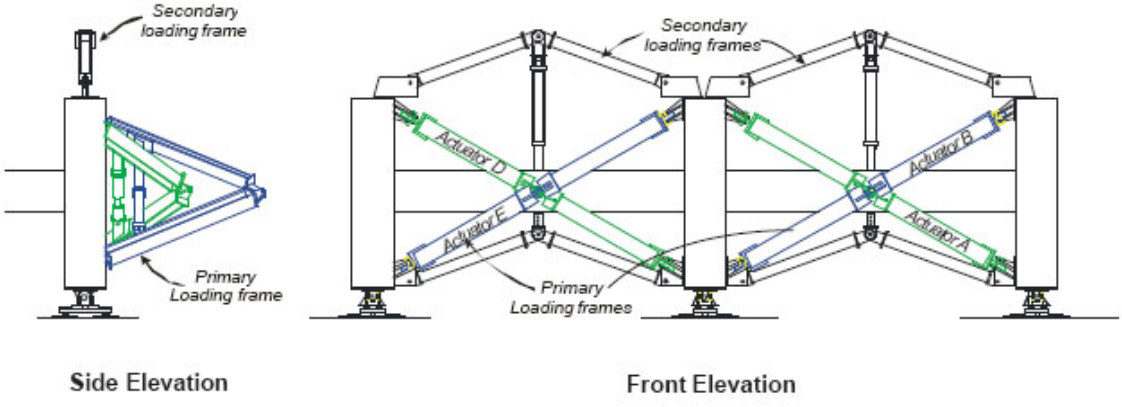

Figure 1-13 Sliding base boundary conditions and loading mechanism after Matthews (2004)

1.6.3 Matthews: Existing Design, Details and Construction Practice

Matthews (2004) was the first in the series of three super assembly tests and adopted traditional structural design, details and construction practice in order to form a control specimen. The aim was to investigate perceived behavioural deficiencies of precast hollowcore relevant to New Zealand practice. Of particular interest was the seating connection used, shown in Figure 1-14. It was found that this seating detail (considered one of the common details adopted in current construction practice in New Zealand at the time) performed very poorly. Matthews (2004) observed that the relative rotation between the seating beam and hollowcore units was the primary damage causing mechanism resulting in a snapping action as a result of a flexure induced shear failure occurring at the face of the seating beam as shown in Figure 1-14 b).

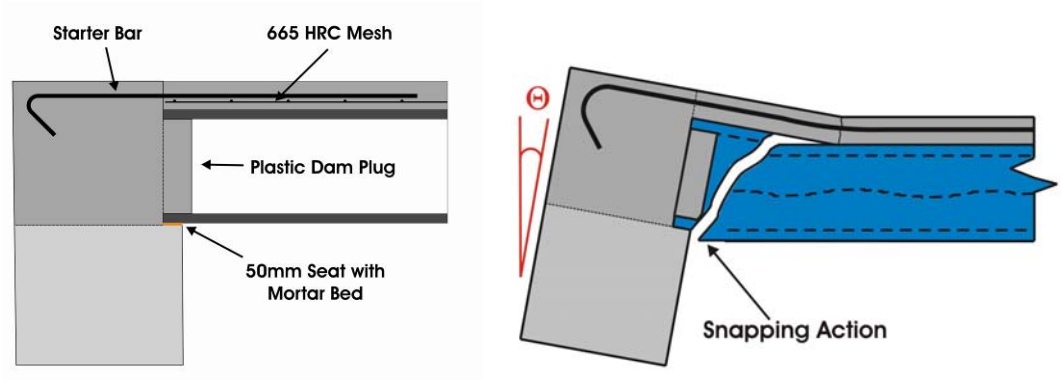

a) Seating connection detail **b) Flexure-shear failure mechanism**

Figure 1-14 Seating connection and observed failure mechanism adapted from Matthews (2004)

This failure mechanism which was influenced by the seating connection details resulted in significant damage to the floor system leading to premature collapse both locally and globally as seen in Figure 1-15 a) and b). This highlighted that not only was loss of seating through beam elongation an issue, but also the structural integrity of the hollowcore units could be jeopardised by the nature of the seating connection.

a) Seating connection failure mechanism **b) Floor collapse**

Figure 1-15 Local failure mechanism and global floor collapse as a result of local failure mechanism Matthews (2004)

A number of other issues associated with not only hollowcore floor diaphragm performance but also diaphragm and seismic frame performance in general were discovered and highlighted by Matthews (2004).

Matthews (2004) confirmed a number of issues consistent with investigations by Lau (2001). The presence of a floor diaphragm significantly affected the behaviour of the seismic resisting frame structural system. The main aspect of this was the effect the diaphragm had on the

flexural behaviour of the adjacent beams. It was found that significantly higher beam flexural strengths were achieved in the beams due to the floor system axially restraining the beams (induced axial loads) and also activation of topping reinforcement. Both of these phenomenon could detrimentally affect the local and global performance of the structural frame system. This is because the initial capacity design assumptions would underestimate the actions being applied the columns, as the design is based on the nominal beam flexural strength alone.

A number of issues associated with beam elongation and the effects this has on floor diaphragm performance were perceived prior to Matthews (2004) test. One of the foremost issues was the effect of the resulting 'pull-off' on the floor system, leading to potential loss of seating, for which two possible loss of seating mechanisms were conceived (illustrated in Figure 1-16). The first being loss of seating confined to the plastic hinge zones (Mode 1), or alternatively along the entire length of a frame bay (Mode 2).

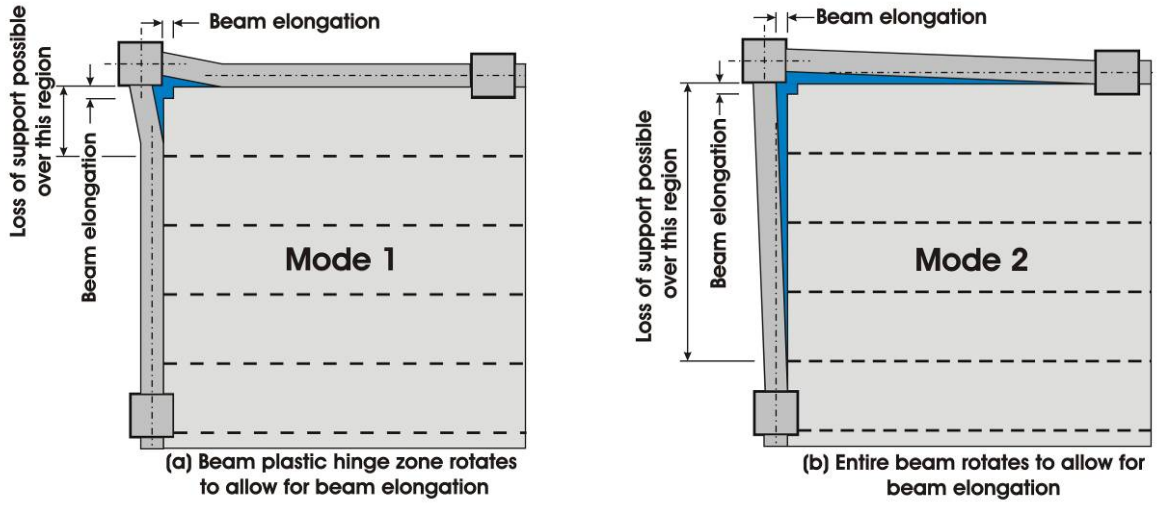

Figure 1-16 Beam elongation resulting in loss of seating after Matthews (2004)

However, Matthews (2004) found as a result of beam elongation the internal column of the super-assembly displaced laterally away from the floor diaphragm. This created a large tear in the floor diaphragm which significantly affected the in-plane transfer and inertia load paths within the diaphragm, to and between the lateral resisting frame systems. This subsequently affected the seismic performance of the global structural system. This behaviour was termed Mode 3 and is illustrated in Figure 1-17. This was the result of the absence of tie

reinforcement between the column and floor system to restrict the outward lateral movement of the column.

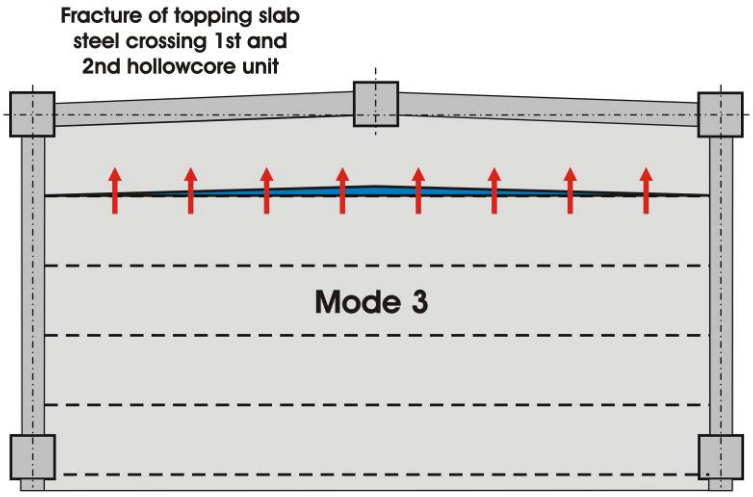

Figure 1-17 Mode 3 frame-floor behaviour due to beam elongation after Matthews (2004)

Vertical displacement incompatibility along the longitudinal perimeter was seen to cause significant damage to the first unit adjacent to the perimeter frame. This was attributed to conflicting displacement patterns of the frame beams and precast floor system. The simply supported floor system sags in single curvature between points of support (seating beams) and the frame beams deform in double curvature between points of fixture (columns) as shown in Figure 1-18.

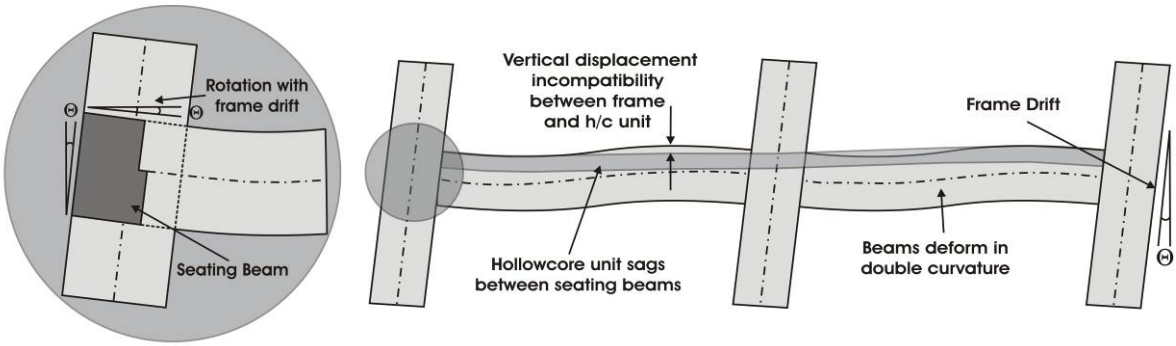

Figure 1-18 Vertical displacement incompatibility after Matthews (2004)

Matthews (2004) highlighted the torsional stiffness of the seating beam as a critical structural performance aspect. The issue raised was related to the extent of floor slab reinforcing activation and the effect this had on the frame behaviour. It can be seen that this would also affect the extent of rotation demand on the floor system at the end seating connection.

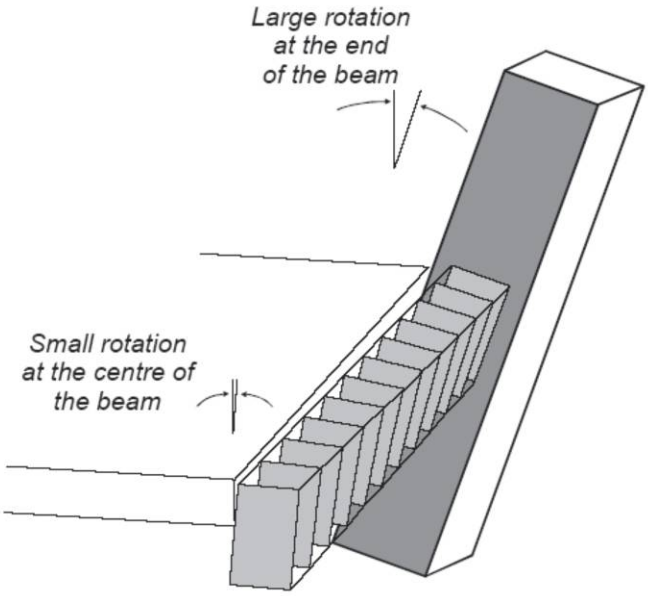

Figure 1-19 Seating beam torsion after Matthews (2004)

1.6.4 Lindsay: NZS 3101:1995 Amendment 3(Acceptable Solution 1)

Lindsay (2004) repaired Matthews (2004) frame system and replaced the floor system with a number of modifications to the structural detailing aimed at addressing the behavioural deficiencies observed by Matthews (2004). The most significant of these changes was the modification to the end seating connection according to recommendations from TAG and Bull and Matthews (2003) trial 'rotation-focussed' sub-assembly tests. The connection detail tested is illustrated in Figure 1-20.

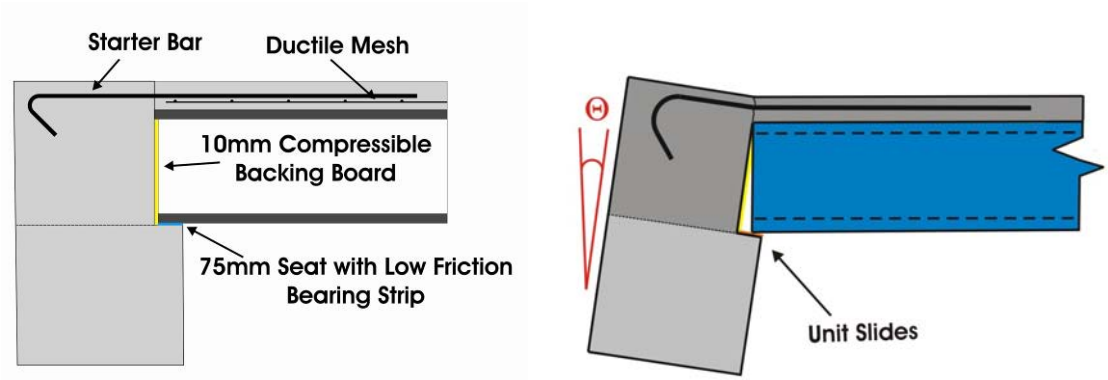

a)Seating connection detail **b) Behaviour mechanism**

Figure 1-20 Observed behaviour of the amended seating connection detail after Lindsay (2004)

An increased seating length, compressible backing board and low friction bearing strip were introduced to target the observed structural deficiencies of existing seating connections. The aim was to isolate the hollowcore units from the seating beam and allow the unit to slide,

preventing any damage being introduced into the floor system because of the rotation of the seating beam. A number of other modifications were made to the structural details to address more general hollowcore and diaphragm performance issues at the longitudinal perimeter connection.

Lindsay (2004) found the seating connection detail performed well, with the method of isolating the hollowcore units from the seating beam working effectively. Much higher levels of performance were achieved in the structural system with the floor system effectively performing to the same high levels of drift as the frame system. Concern was raised however over the connections lack of vertical support, should excessive elongation induce loss of seating.

Lindsay (2004) also showed that torsional strength and stiffness of the seating beam can significantly affect the extent of rotation imposed on the floor system. Lindsay (2004) observed that once the seating beam was softened torsionally, the relative rotation between the seating beam and floor system can be greater than the imposed frame drift. This was a result of the eccentric gravity loading of the floor system on the seating beam. Figure 1-21 shows a graph taken from Lindsay (2004) illustrating the variation between frame drift (termed joint in the figure) and relative rotation imposed on the hollowcore units along the length of the seating beam. This demonstrates that under positive frame drift positive rotation (soffit of the unit pulling away from the seating beam) imposed on the floor system can exceed frame drift. In addition to this, as a result of torsional softening of the seating beam, the relative rotation imposed on the floor system can be less than the overall frame drift. This suggests the relationship between overall frame drift and the relative rotation imposed on the end seating connection of the floor system is complicated. It is therefore simplistic to assume relative rotations imposed on the floor system relate directly to frame drift.

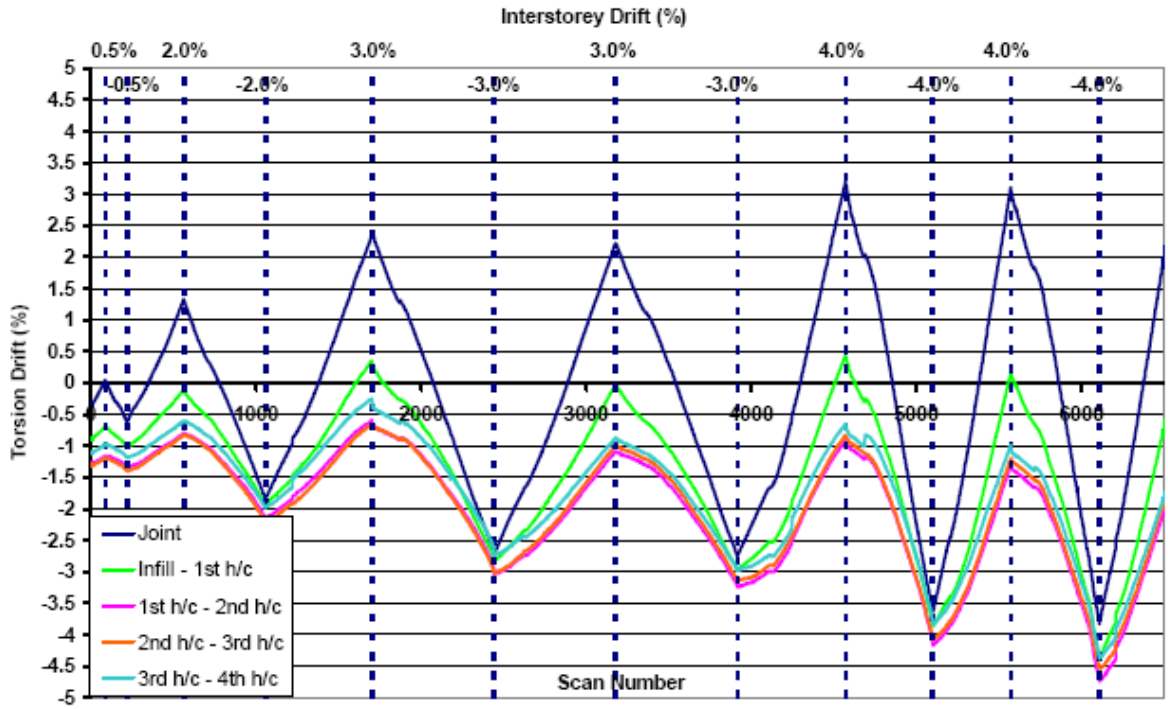

Figure 1-21 Relationship between relative rotation imposed on the floor system and frame drift as a result of seating beam torsion from Lindsay (2004) (the graph is for Phase 3 of the experimental procedure)

1.6.5 MacPherson: NZS 3101:1995 Amendment 3(Acceptable Solution 2)

MacPherson (2005) refined again the general structural floor and frame system details following Lindsay (2004) and tested a second alternative seating connection 'acceptable solution' recommended by the TAG and trialled using a 'rotation-elongation' based sub-assembly test by Trowsdale (2004). The seating connection detail and the intended behaviour are shown in Figure 1-22.

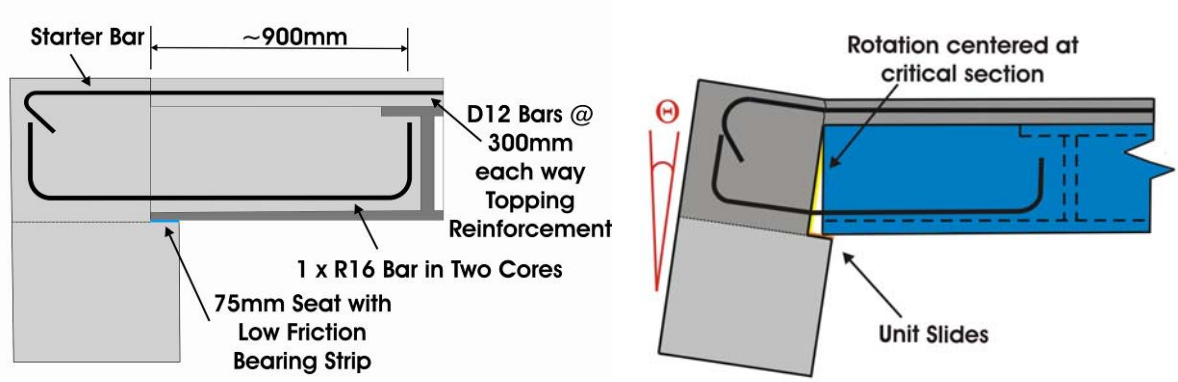

a)Seating connection detail **b) Behaviour mechanism**

Figure 1-22 Observed behaviour of connection adapted from MacPherson (2005)

The seating connection incorporated an increased seating and low friction bearing strip in the same way as the connection tested by Lindsay (2004). However, in addition to this tie reinforcement was placed in the bottom of selected cores of the units tying the unit into the seating beam and reinforcing the end of the unit. A capacity design approach was adopted to ensure any seating beam rotation was accommodated through tension and compression yielding of topping reinforcement and that of the tie reinforcement at the seating beam to hollowcore unit interface or 'critical section'.

MacPherson (2005) found this seating connection detail performed very well, sustaining only minor levels of damage up to drift levels of +/- 5%. The connection was seen to behave as intended with seating beam rotation being confined to the intended 'critical section' at the face of the seating beam. The important advancement of this connection from the previous connection tested by Lindsay (2004) was the introduction of tie reinforcement and vertical support redundancy into the seating connection system.

1.7 Current Research Outline

Previous research has shown that there are a number of potential issues associated with the interaction between precast hollowcore floor systems and seismic resisting frame systems. This interaction produces incompatibilities in local deformation which result in undesired damage in connection regions between the two systems. The seating connection region is the most concerning of these with potential collapse of the floor system through loss of vertical support as the likely outcome. Extensive investigations have made significant ground in assessing the problem and providing solutions for future construction. However, currently there has been very little consideration given to how to retrofit the existing stock of buildings with hollowcore floor systems.

This is where the motivation for this research has been derived. It is firstly planned to carry out an investigation looking specifically at the performance of typical existing seating connections. Based on this investigation, and in conjunction with knowledge applicable from previous research, a retrofit approach will be developed aimed at bringing performance of existing seating connections towards the more ideal performance of the amended connection details. This is seen the most critical issue which needs addressing given the uncertainty and extreme consequences of poor seating connection behaviour during a seismic event.

An experimental investigation involving a series of 'rotation-elongation' type hollowcore sub-assembly tests were carried out. These tests firstly looked at variants of potential existing seating connection details and behaviour. This was then followed by the implementation of a conceptual retrofit approach on an existing seating connection detail. Although only one retrofit concept was experimentally trialled, a broader retrofit procedure or framework was suggested which could be tailored to a variety of existing seating connections.

1.8 References

Centre for Advanced Engineering, 1999, *Guidelines for the use of structural precast concrete in buildings*, Centre for Advanced Engineering, University of Canterbury, Christchurch, New Zealand.

Bull D.K, Matthews J.G, 2003, *Proof of concept tests for hollow-core floor unit connections*, Precast NZ report, Feb 2003.

Herlihy M.D, 1999, *Precast concrete floor support and diaphragm action*, PhD Thesis, Department of Civil Engineering, University of Canterbury, Christchurch, New Zealand.

Fenwick R.C, Deam B.L, Bull D.K, 2004, *Failure Modes for Hollowcore Flooring Units,* Journal of the Structural Engineering Society of New Zealand (SESOC), Vol. 17, No. 1.

Holmes W.T and Somers P, 1995, *Northridge Earthquake of January 17, 1994, Reconnaissance Report Vol. 2*, Earthquake Spectra, Vol.11.

Iverson J.K and Hawkins N.M, 1994, *Performance of Precast/Prestressed Concrete Building Structures During Northridge Earthquake*, PCI Journal, March-April, Vol. 39, No. 2.

Lau D.B.N, 2001, *The influence of precast-prestressed flooring on the seismic performance of reinforced concrete perimeter frame buildings*, Department of Civil and Resource Engineering, University of Auckland, Auckland, New Zealand.

Liew H.Y, 2004, *Performance of hollow-core floor seating connection details*, Masters Thesis, Department of Civil Engineering, University of Canterbury, Christchurch, New Zealand.

Lindsay R.A, 2004, *Experiments on the seismic performance of hollow-core floor systems in precast concrete buildings*, Masters Thesis, Department of Civil Engineering, University of Canterbury, Christchurch, New Zealand.

MacPherson C.J, 2005, *Seismic performance and forensic analysis of a precast concrete hollow-core floor super-assemblage*, Masters Thesis, Department of Civil Engineering, University of Canterbury, Christchurch, New Zealand.

Matthews J.G, 2004, *Hollow-core floor slab performance following a severe earthquake*, PhD Thesis, Department of Civil Engineering, University of Canterbury, Christchurch, New Zealand.

Meija-McMaster J.C, 1994, Precast *concrete hollowcore floor unit support and continuity*, Masters Thesis, Department of Civil Engineering, University of Canterbury, Christchurch, New Zealand.

Norton, J. A, King, A. B, Bull, D. K, Chapman, H. E, McVerry, G. H, Larkin, T. J, and Spring, K. C, (1994), *Northridge Earthquake Reconnaissance Report*, Bulletin of the NZNSEE, Vol. 39,No. 4.

NZS3101:1995, 1995, *Concrete Structures Standard, NZS3101, Parts 1 & 2*, Standards New Zealand, Wellington, New Zealand.

NZS3101:1995, 2004, Amendment No. 3 to 1995 Standard (NZS3101), Standards New Zealand, Wellington, New Zealand.

NZS3101:2006, 2006, *Concrete Structures Standard, NZS3101, Parts 1 & 2*, Standards New Zealand, Wellington, New Zealand.

NZ Technical Advisory Group on Suspended Concrete Floors (Chairman: Cook, D.), 2002, *The Seismic Performance of Flooring Systems – Executive Summary*, Journal of the Structural Engineering Society of New Zealand (SESOC), Vol. 15, No. 2.

Oliver S.J, 1998, *The performance of concrete topped precast hollow-core flooring systems reinforced with and without Dramix steel fibres under simulated seismic loading*, Masters Thesis, Department of Civil Engineering, University of Canterbury, Christchurch, New Zealand.

Taylor L.J, 2004, *Vertical Displacement Incompatibility between Floor Slabs and Seismic Resisting Systems*, Final Year Project, Department of Civil Engineering, University of Canterbury, Christchurch, New Zealand.

Trowsdale J, 2004, *Seismic Performance of Hollowcore Seating Detail Specified by Amendment No 3 NZS 3101:1995*, Final Year Project, Department of Civil Engineering, University of Canterbury, Christchurch, New Zealand.

2 Experimental Investigation Outline

The end seating connection between precast hollowcore floor and frame systems can be a potential weak link in the overall combined structural system. The experimental use of a two-dimensional, single hollowcore unit and seating beam connection sub-assembly test-rig has been shown to replicate the predominant damage causing mechanisms of concern (Bull and Matthews 2003). The experimental investigation presented in this thesis utilised the sub-assembly approach to investigate the behaviour of three typical existing seating connections, followed by a retrofitted seating connection solution. This section outlines the details of the sub-assembly test rig, the loading protocol used, the seating connection details tested, instrumentation, and the limitations of the sub-assembly test procedure.

2.1 Hollowcore Sub-Assembly

The sub-assembly test rig originates from the University of Canterbury full-scale, three-dimensional super assembly floor and frame system used by Matthews (2004), Lindsay (2004) and MacPherson (2005). The aim of the sub-assembly test rig was to induce the two most predominant damage causing actions on the hollowcore unit seating, namely the relative seating beam rotation and longitudinal beam elongation.

The reduction from a super-assembly to sub-assembly was carried out by taking half the span of the floor and reducing this half span of floor to a single flooring unit and *in-situ* concrete topping. This isolated hollowcore unit was then seated on a length of seating beam and supported and loaded at the pseudo mid-span by hydraulic rams. Figure 2-1 below shows the origin of the sub-assembly, all member dimensions are identical to the super assembly.

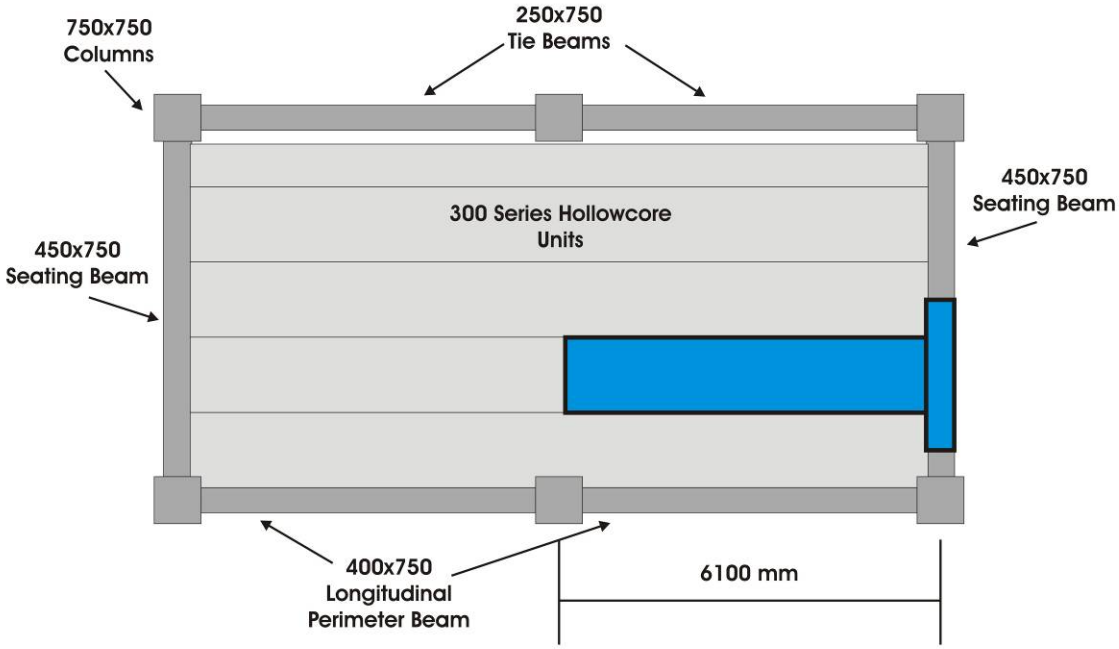

Figure 2-1 Hollowcore sub-assembly origin

The sub-assembly can represent any unit along the length of the seating beam except for the first unit immediately adjacent to the parallel frame. Figure 2-1 shows the second unit from the perimeter frame, which was the focus of the sub-assembly test rather than the first adjacent unit. The first unit is significantly influenced by the deformation characteristics of the beams parallel to it (see Figure 1-18). The sub-assembly test rig can not replicate these actions on the unit. Therefore the sub-assembly tests are taken as representative of units further into the floor.

The seating beam was modified in order to carry out two tests on the same combined base block. This was made up of two 450mm by 750mm seating beams cast back to back and tied together by a tie stirrup within the half beam. This was also beneficial in generating a stable base block. Previous researchers found it difficult to restrain a base block with a smaller footprint of a single seating beam (Bull and Matthews 2003; Liew 2004; Trowsdale 2004).

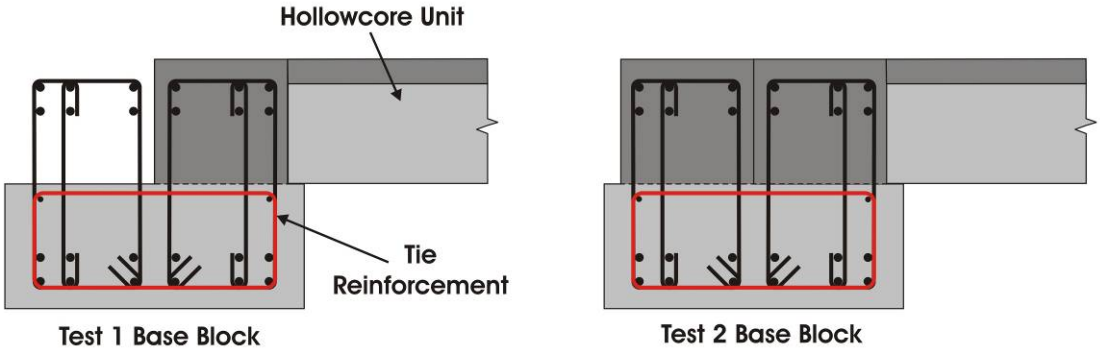

Figure 2-2 Sub-assembly back-to-back seating beam base block

The reason for modelling the sub-assembly closely on the super-assembly test rig was to promote compatibility of results between the simplified sub-assembly and more realistic super-assembly.

The 'rotation-elongation' sub-assembly uses two hydraulic rams to apply loading. The loading was aimed to represent deformation actions experienced by the floor system in the full scale building system. One ram applies relative rotation between the seating beam and floor system and the other the 'pull-off' due to longitudinal perimeter beam elongation. Both of which are quasi-static, displacement controlled, and applied at the pseudo mid-span of the hollowcore unit.

Seating beam rotation was applied by the vertical ram displacement acting over the 6m span of the hollowcore unit. Elongation was applied by applying tension to the unit according to an elongation profile taken from that recorded by Matthews (2004). The point of physical control of the sub-assembly loading was located at the end of the hollowcore unit, as this allowed the test rig to fit within physical restraints of the laboratory. However, this complicated the test system in terms of defining the loading protocol (this is discussed in Section 2.2). Figure 2-3 shows the hollowcore sub-assembly, with the vertical ram for applying seating beam rotation and a horizontal ram for applying beam elongation 'pull-off'.

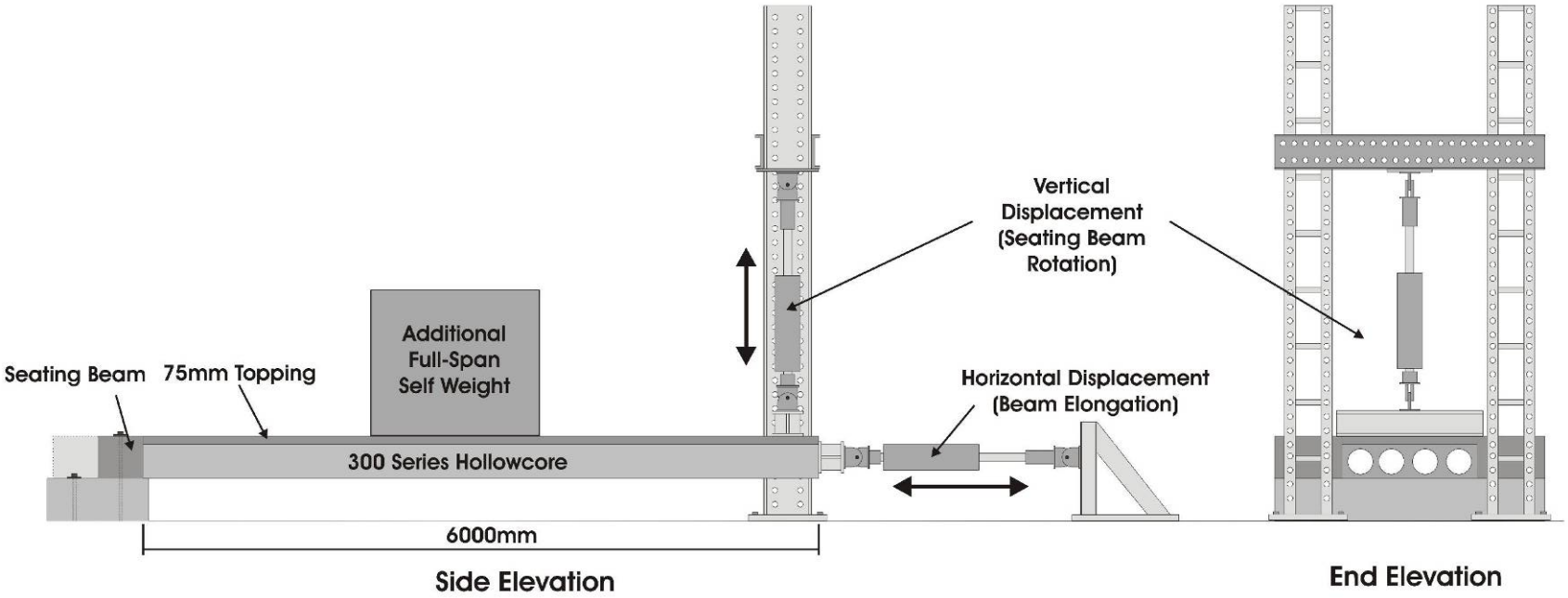

Figure 2-3 Hollowcore sub-assembly test setup

Additional gravity load was applied to the sub-assembly system in order to generate a shear gradient and vertical seating support reaction consistent with the equivalent full-span floor system. The application of additional gravity load was carried out assuming simply supported conditions in the sub-assembly. This was contrary to what would have been significant initial fixity of the floor to beam connection. The reason for this was that very early during the test, rupture of the unreinforced seating connection, combined with elongation resulted in conditions at the seating connection that were close to a simply supported state. Therefore the shear distribution was best matched for the majority of the test assuming simply supported conditions. Figure 2-4 illustrates the assumed bending moment distributions for the respective sub- and super-assembly systems before and after initial rupture. The parabolic bending moment shape would not be strictly maintained in the case of the sub assembly, this is due to the additional gravity load being applied by a point load.

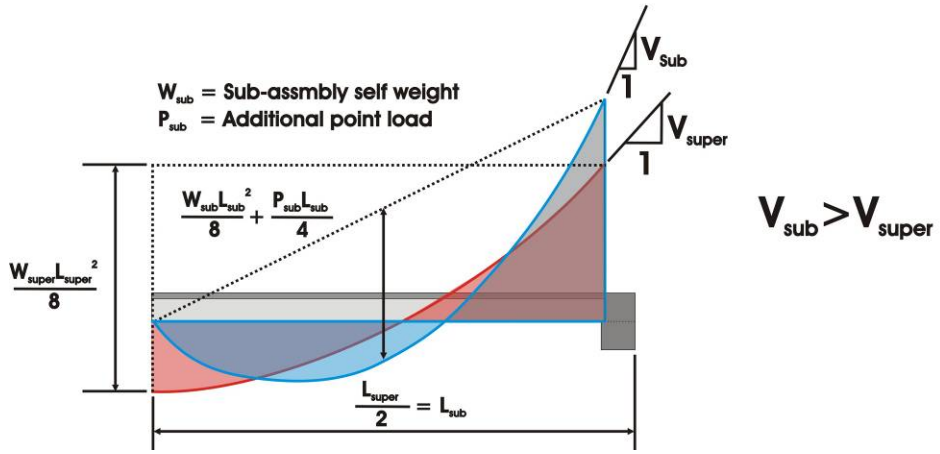

a) Pre-rupture bending moment distribution

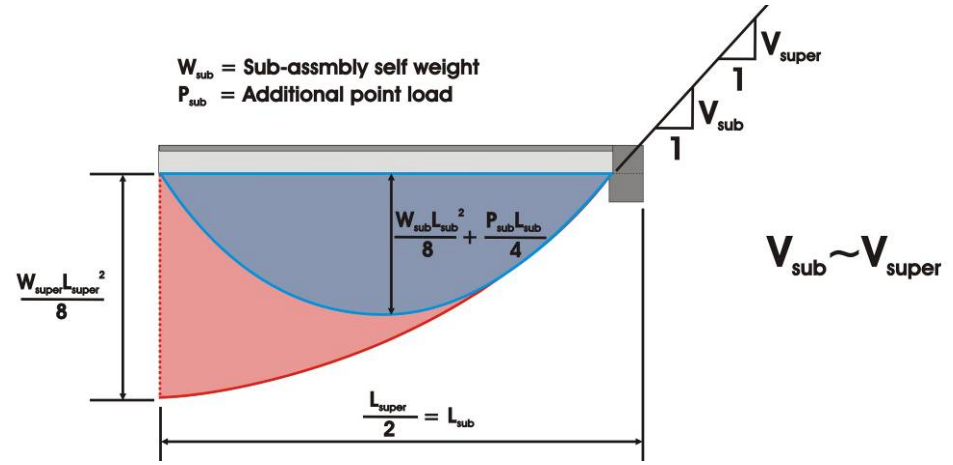

a) Post-rupture bending moment distribution

Figure 2-4 Assumed bending moment diagram of the floor system before and after rupture

Figure 2-5 below shows how the additional load modifies the shear force distribution to represent the equivalent full span assuming simply supported conditions.

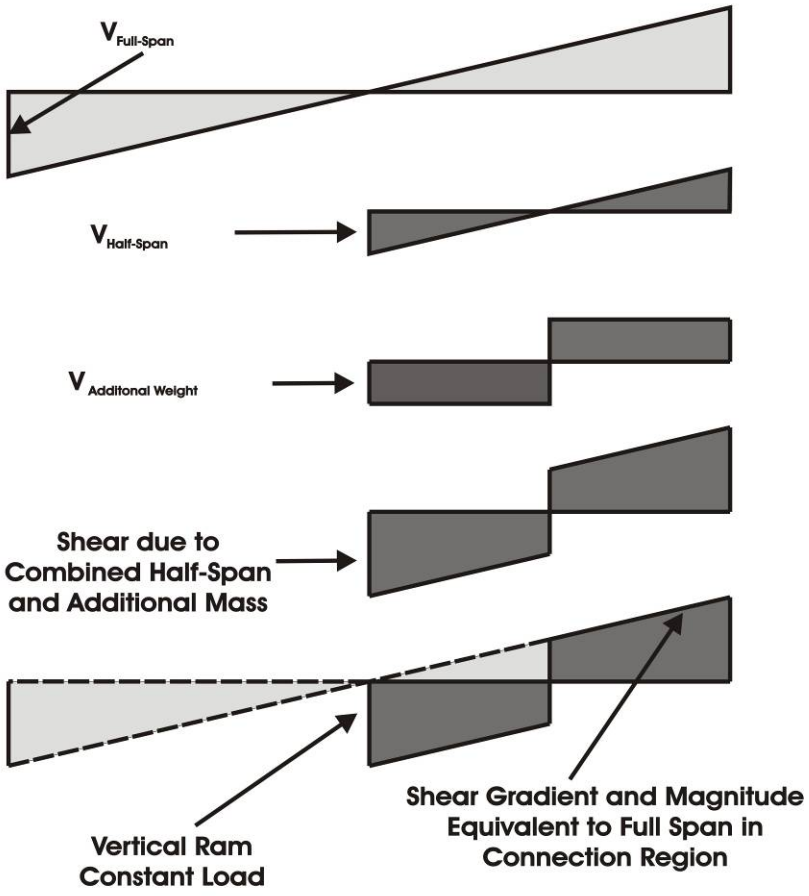

Figure 2-5 Additional load application and shear force distribution to account for half-span to full-span consistency

Two alternative gravity load configurations were applied. The first represented only self weight of the full-span, consistent with previous tests. The second was as specified by the G&Qu&E seismic design load case (NZS1170:2005). The second of these produced a larger shear distribution on the unit as the additional weight was added to incorporate superimposed dead loads and live loads as defined by G&Qu&E. The lesser load addition was used for the first two tests (HC1 and HC2), and the larger G&Qu&E for the later two tests (HC3 and HC4)

2.2 Loading Protocol Development

The experimental investigation focused on the seismic assessment and retrofit of existing hollowcore seating connections. Therefore, typical quasi-static drift histories used to test 'new' structures were not considered appropriate because they are generally excessive for this situation of assessment and retrofit. For this reason, and also due to significant uncertainty surrounding theoretical beam elongation prediction procedures, the drift history and corresponding measured experimental beam elongation from the Matthews (2004) super-assembly test was used.

Matthews (2004) investigation was based on an existing structure and the drift history used was developed from a series of non-linear time history studies. The earthquake records used were scaled to 10% in 50 years (DBE) and 2% in 50 years (MCE) magnitudes. As a result the drift history used was refined to represent more realistic seismic demand. In addition to this, by using the measured beam elongation behaviour, any uncertainty regarding predicting beam elongation was negated. This approach appealed because using measured experimental results from the Matthews (2004) super-assembly test further promoted consistency between the super and sub-assembly investigations. This enabled the load applied to the sub-assembly to best represent the *in-situ* actions that should be realistically experienced.

Two similar variations of the loading profile were used as illustrated in Figure 2-6. The first of these was the original profile from Matthews (2004). The second omitted the initial elastic 0.25% drift cycle. The reason for this was that it was found in early tests that the 0.25% drift cycle coincided with first cracking of the seating connection system. And for investigation purposes it was desired to induce loading which passed first cracking drift in the first cycle. The original drift profile shown in Figure 2-6 a) was used for the first two tests (HC1 and HC2). The profile shown in Figure 2-6 b) was used for the latter two tests (HC3 and HC4).

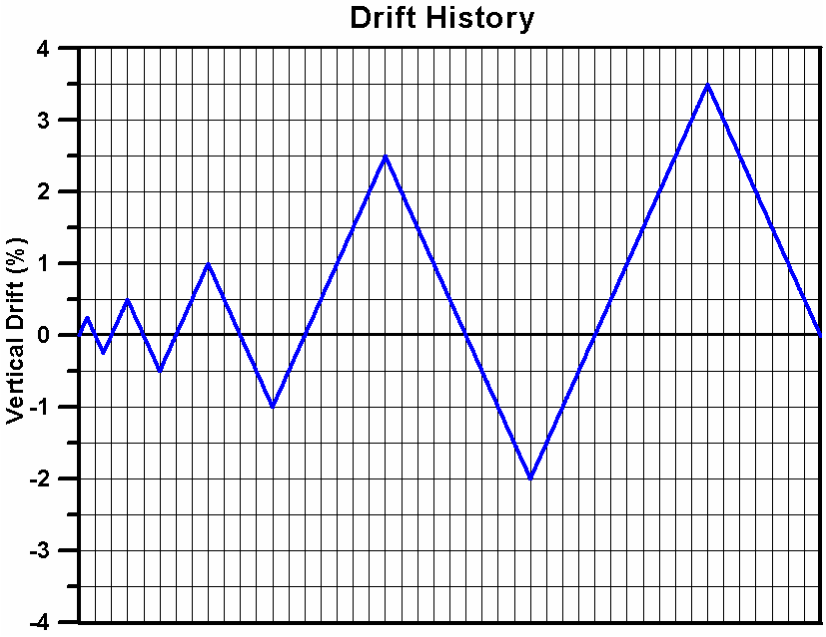

a) Drift history for HC1 and HC2 tests

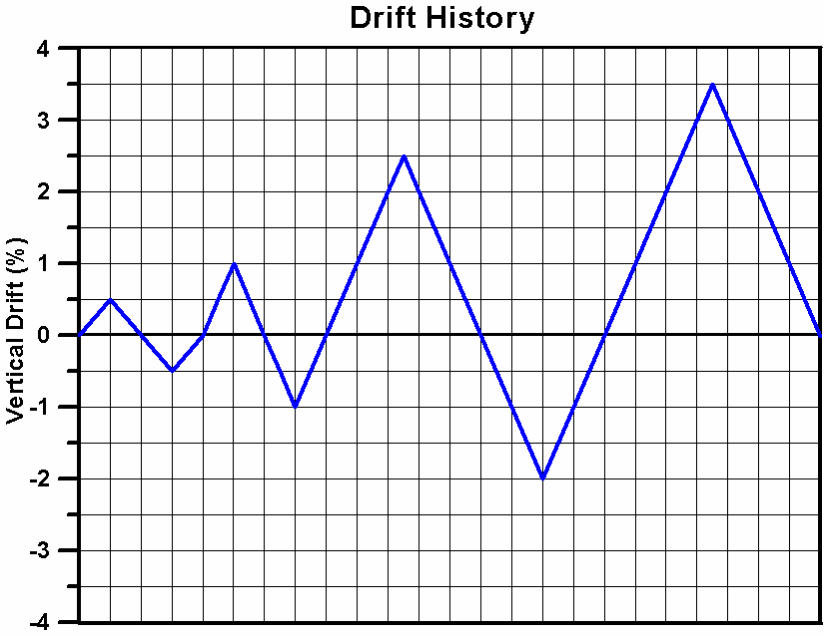

b) Drift history for HC3 and HC4 tests

Figure 2-6 Rotational drift loading profile adapted from Matthews (2004)

Modifications were made to both the drift and elongation profiles adapted from Matthews (2004). The reason for this was to convert the loading profile from the three dimensional super-assembly to be used in the two-dimensional sub-assembly. Matthews (2004) original drift history was intended for three-dimensional testing and applied in three phases. An initial profile applied in a longitudinal direction (which was used in this investigation), followed by a transverse profile, and then a second longitudinal profile. Due to

the two dimensional nature of the sub-assembly, and requiring continuity in rotational drift and respective measured beam elongation, the loading which could be adapted from Matthews (2004) was limited to the first longitudinal phase.

To account for this, the first phase loading history was modified with the addition of a +3.5% drift cycle to increase the demand closer to the original three-phase loading history, which included DBE and MCE drift magnitudes. This involved theoretically determining the respective beam elongation for this cycle, which was carried out using theory proposed by Matthews (2004). Figure 2-7 below shows the measured elongation versus drift data from Matthews (2004) up to a rotational drift level of 2.5%. This was then smoothed and extended for the additional 3.5% drift cycle. The two elongation profiles shown in Figure 2-7 are for the two variations in drift profile (including and excluding the initial 0.25% cycle).

The measured experimental elongation values used from the Matthews (2004) test were for one of the two bays of the super-assembly test specimen. This involved the summation of the elongation contribution from one external plastic hinge and one internal plastic hinge. As a result, the elongation profile is best representative of a frame and floor system for which the hollowcore units span past an intermediate column. However, the contribution of the internal plastic hinge to the overall elongation is significantly smaller than that from the external plastic hinge. This is due to the axial restraint provided to the plastic hinge by the floor system. For this reason the elongation profile can also be considered applicable for assessment of frame and floor systems which the floor spans only one bay.

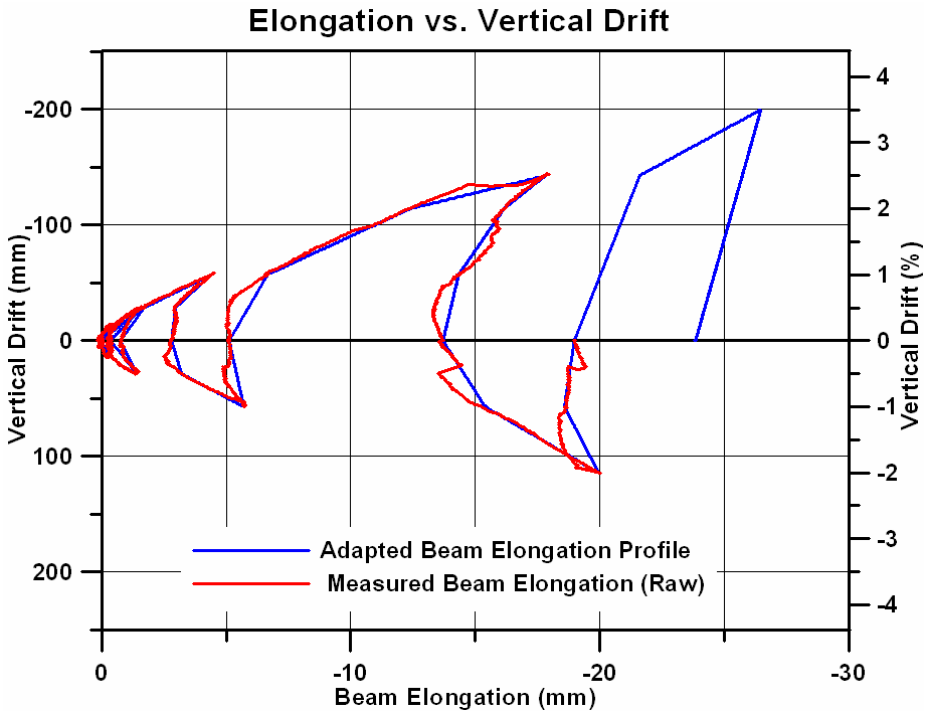

a) Elongation profile including elastic 0.25% drift cycle

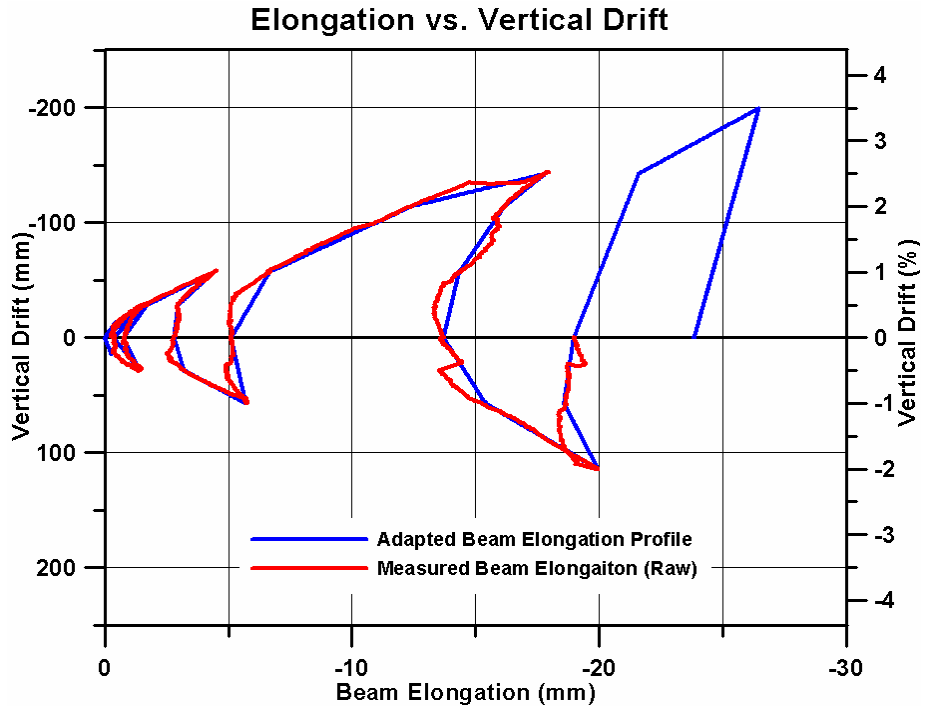

b) Elongation profile excluding elastic 0.25% drift cycle

Figure 2-7 Beam elongation history adapted from Matthews (2004)

To achieve the desired seating beam rotation and beam elongation 'pull-off' at the seating ledge, the appropriate control information for the hydraulic rams had to be determined. This was complicated due to geometric constraints as a result of the rotation and elongation deformation being applied at the pseudo mid-span of the test specimen, rather than the seating connection (as in a full building). This resulted in geometric interaction between the vertical and horizontal hydraulic rams acting at a 6m lever-arm (the length of the hollowcore unit) from the seating connection. In addition to this the actuators were controlled by displacement along their line of action. Therefore, due to the vertical and horizontal movement of hollowcore unit during the test, these lines of action did not coincide with the global vertical and horizontal axis, which the rotation and 'pull-off' actions were described in (at the seating connection). The three stages in the development of the loading history based on the raw vertical drift (seating beam rotation) and beam elongation histories are outlined below:

Stage 1: Determine seating ledge 'pull-off' demand

The elongation demand on the hollowcore unit along the provided seating ledge ('pull-off' effect) was broken into two components. The first is the geometric and recoverable component imposed on the hollowcore unit at the level of the seating ledge. This 'pull-off' component results from the lateral drift of the frame columns relative to the longitudinal frame beams as illustrated in Figure 2-8. The magnitude of the contribution to the 'pull-off' depends on the location of the seating ledge (and the hollowcore unit soffit) relative to the instantaneous centre of rotation (ICR) of the adjoining longitudinal beam. The greater the distance between the seating ledge and the ICR, the greater the resulting 'pull-off' for a given frame drift (or rotation). Figure 2-8 shows the rotation of longitudinal beams about the assumed beam ICR's, as determined by Matthews (2004) (based on full frame and floor system).

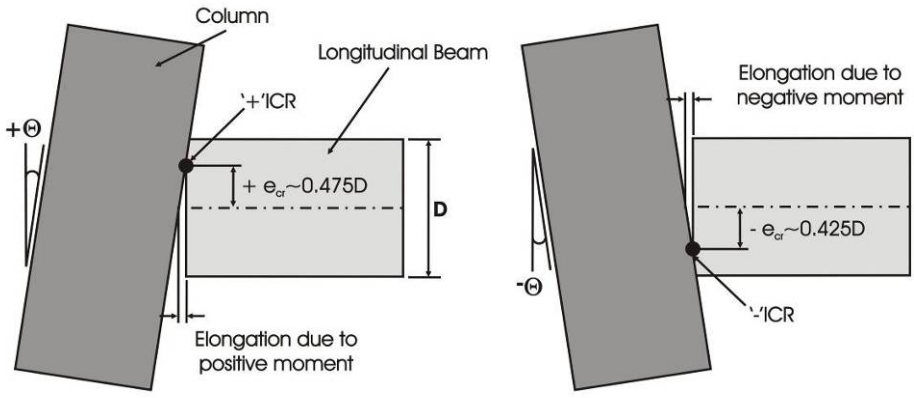

Figure 2-8 Beam elongation schematic after Matthews (2004)

The second component is the beam elongation (data taken from Matthews (2004) super-assembly test) of longitudinal perimeter beams, acting along the horizontal plane of the floor system at the centreline of the longitudinal beam. The combination of the geometric and beam elongation 'pull-off' components can result in elongation demand greater than the beam elongation component alone, depending on drift direction and equal to the beam elongation alone component at zero drift.

Due to misinterpretation of the measured beam elongation data when developing the loading protocol, the resulting 'pull-off' demand was overestimated. This was a result of the seating ledge for the sub-assembly coinciding with the centreline of the longitudinal beam affecting the geometric 'pull-off' contribution. However, fortunately this had little or no bearing on the test specimens as there was significant slack between the imposed and achieved 'pull-off' in the experiment test setup. This resulted in the achieved 'pull-off' equating closely to, if not being less than the prescribed beam elongation 'pull-off' alone. This is illustrated by a comparison of the elongation observed in the HC4 test specimen (as outlined in Section 2 and Section 5) at +2.5% drift and the equivalent beam elongation demand (excluding geometric effects). The comparison shows a measured elongation value in the order of 15-18mm, compared with a prescribed beam elongation of approximately 17mm. As a result, it can be shown that the slack in the system accounted for the initial and conservative assumption of including geometric elongation effects.

Stage 2: Conversion of rotation and 'pull-off' demand to hydraulic ram pin movements

Using the combined seating beam rotation and 'pull-off' of the hollowcore unit on the seating ledge, global vertical and horizontal vector movements of the hydraulic ram pins (point of load application) were determined geometrically. Movement was assumed about an instantaneous centre of rotation (ICR) at the end of the hollowcore unit and topping section, at the level of the seating ledge, as illustrated in Figure 2-9 . The reason the ICR's in both rotation directions coincided was due to the assumption of ideal sliding of the hollowcore unit soffit along the seating ledge under combined elongation and rotation actions (ie contact between the seating ledge and hollowcore unit soffit was maintained, providing vertical support to the hollowcore unit) .

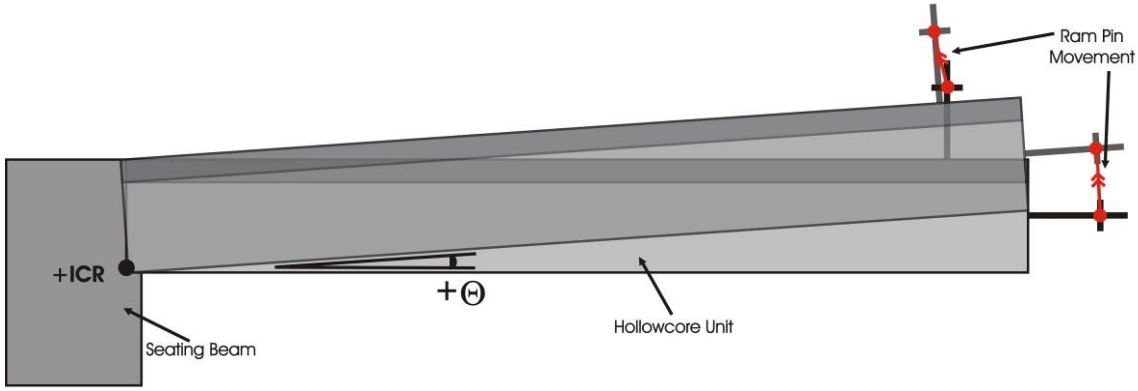

a) Ram pin movement for positive drift

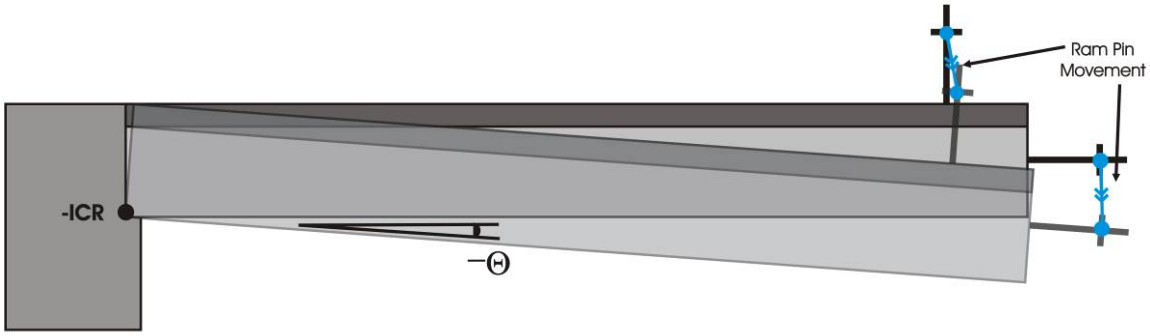

b) Ram pin movement for negative drift

Figure 2-9 Schematic used to determine ram pin movement for loading

Figure 2-10 illustrates the geometric relationship of the hollowcore sub-assembly used to determine the hydraulic ram pin movements (Δ_x (RAM X), Δ_y (RAM X), Δ_x (RAM Y), Δ_y (RAM Y)) on the end of the hollowcore unit. Figure 2-10 shows the relationship for positive drift only. The same relationship was used for negative seating beam rotation (vertical drift); only it varied slightly due to downward rather than upward movement of the hollowcore unit.

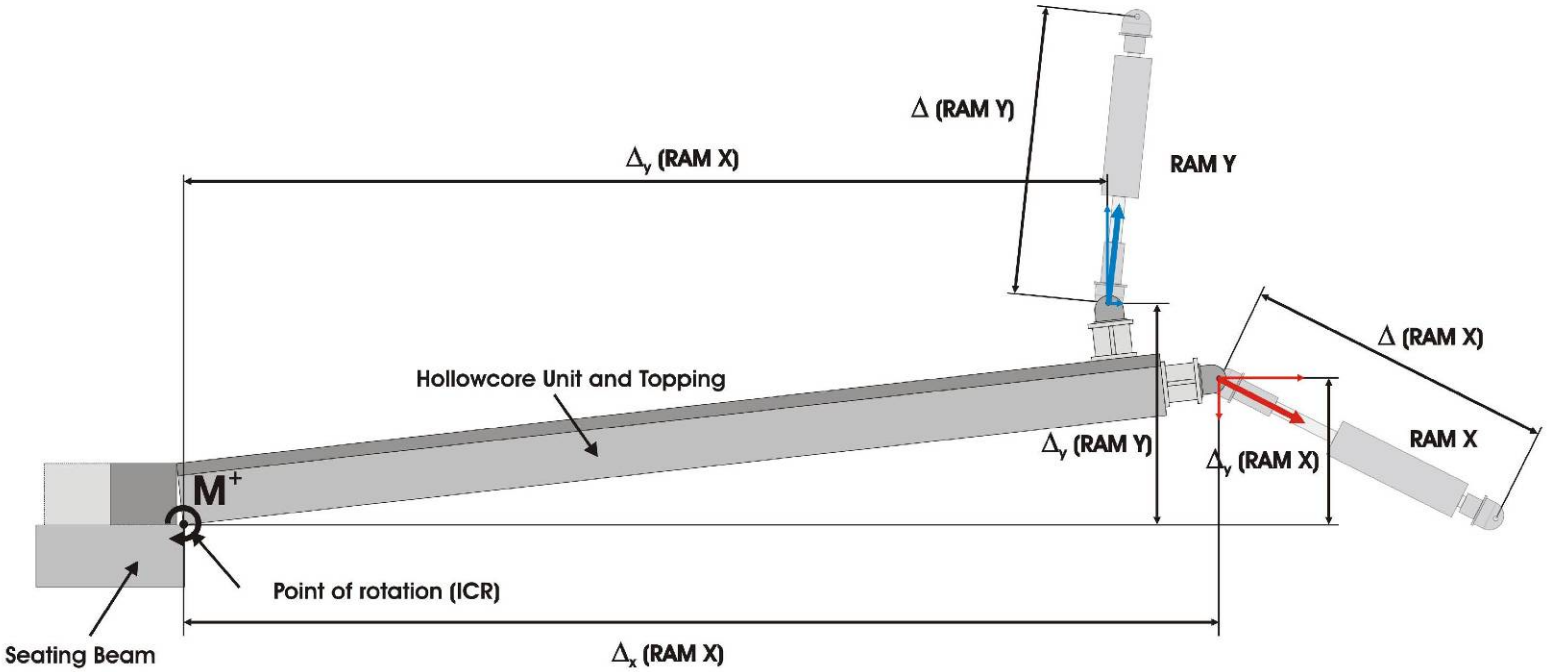

Figure 2-10 Hollowcore sub-assembly geometric displacement relationships

Stage 3: Conversion of ram pin movements to hydraulic ram displacements

The pin movements on the end of the hollowcore unit were then geometrically converted to ram extensions or contractions (the change in Δ(RAMX) and Δ(RAMY) shown in Figure 2-10). This was carried out using geometer based on the hydraulic rams rotating about the pinned end of the hydraulic rams attached to reaction frames and the laboratory strong floor and the initial ram lengths. This is illustrated in Figure 2-11, which shows the change in hydraulic ram length as a function of movement of the hollowcore unit with respect to the initial position of the hydraulic rams.

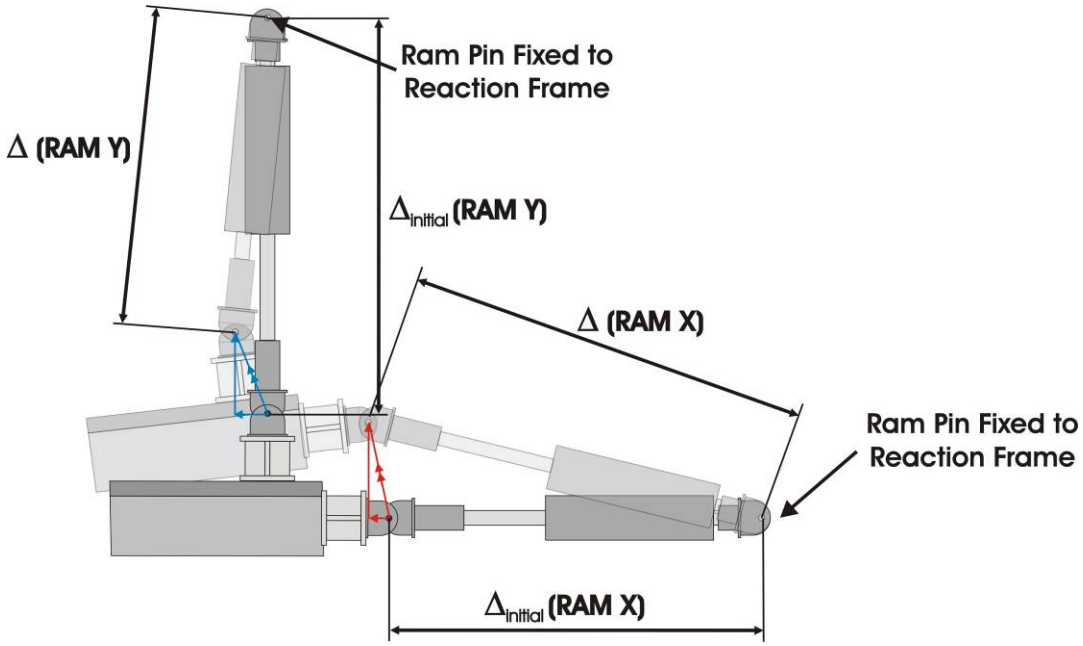

Figure 2-11 Conversion of hydraulic ram pin movement to hydraulic ram displacements

The process for converting the desired rotation and elongation demand into the control displacements for the hydraulic rams was later used in a reverse manner to determine the moment verses rotation relationships for the seating connection tests (at the ICR). This was carried out by converting the measured local forces and displacements in the hydraulic rams into global horizontal and vertical force components and lever arms with respect to the ICR. Moments were then summed about the ICR accordingly according to the varying drift levels.

Figure 2-12 shows the beam elongation, combined beam and geometric elongation (net 'pull-off' of the hollowcore unit soffit on seating), and the horizontal ram displacement protocol to achieve the desired 'pull-off' demand on the hollowcore unit. The variation in horizontal ram control displacement due to geometric constraints can clearly be seen. The

vertical ram displacement control is not shown as it does not vary from the raw vertical drift profile shown in Figure 2-6. This is due to the elongation movement being so small in comparison to length of the vertical hydraulic ram. The loading protocol development was verified using trial hollowcore unit movements on full-scale drawings in AutoCAD (2005) draughting software.

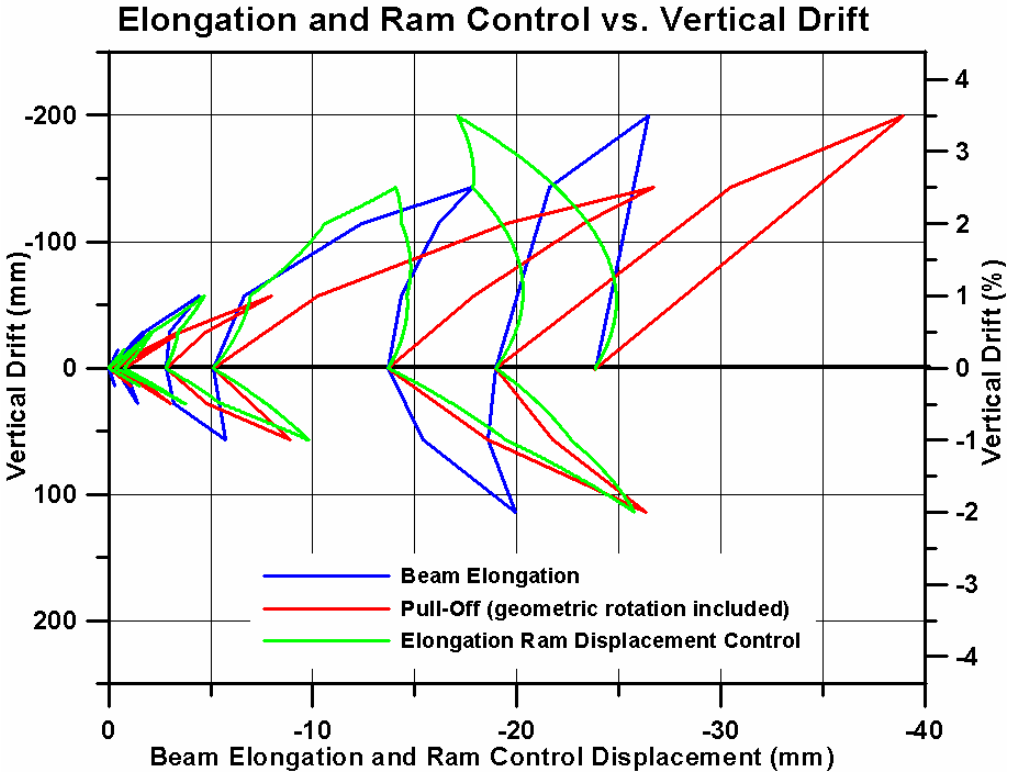

Figure 2-12 Comparison of beam elongation alone, pull off including geometric component, and horizontal ram control

2.3 Test Specimens and Material Properties

This section describes the connection details which were tested. HC1, HC2 and HC3 were control specimens and HC4 was a retrofitted seating connection detail. All connection details tested were variations based around fundamental details typical of existing hollowcore seating connections. 'Existing' refers to design and construction practice prior to Matthews (2004) super-assembly tests, and the introduction of Amendment 3 to NZS 3101:1995 in 2004 regarding the use of precast flooring systems.

The consistent structural details include the use of Grade 300 (f_y=300MPa, where f_y is the lower characteristic yield stress) deformed starter bars, all of the same length and non-ductile HRC 665 mesh topping reinforcement. The use of Grade 300 starter bars is in place of Grade

430 (f_y=430MPa). The reason for this is Grade 430 bars were not available. All the units were seated directly on the bare concrete seating ledge. This was significant as all previous control specimens have used a mortar bed between the unit and seating ledge, for which significant debate has arisen regarding the effect this had on connection performance and how often this particular detail was actually employed. All seating connections used 75mm dam plugs which resulted in a core of concrete being formed in the end of the unit cores. The standard concrete properties specified for the seating beams and toppings were: a compressive strength of 30MPa to 45MPa (test dependent), 19mm aggregate and a slump of 100mm. More specific details of achieved concrete strengths for each test are reported in the respective section on each specimen. The nature and origin of the units used for each test are discussed in the individual connection details sections. Full construction drawings are shown in Appendix A.

2.3.1 HC1 – Control Specimen

The HC1 seating connection detail shown in Figure 2-13 aimed to represent and investigate the performance of typical existing seating connections which have insufficient seating length. The purpose of this was to represent construction tolerances and shrinkage and creep resulting in units being shorter then desired upon arrival on site. The provided seating length was 35mm of an available 50mm. This decision to specify a 35mm provided seating was based on the 6m long units representing half a span, arriving approximately 5mm short. In addition, observation of Matthews' (2004) super-assembly specimen showed provided seating lengths of 20mm and 40mm resulted when constructed in a consistent manner with industry practice.

The hollowcore unit used was determined to be a 'new' unit originating from an extruding machine which began operation in the early 2000's. The 'new' units were therefore not representative of targeted existing hollowcore units (1980's-1990's), designated as 'old' units, which originate from a number of extruding machines which produce units of varying geometric and physical properties. The extent of the differences between the "new" and "old" hollowcore units was not explicitly investigated in this investigation. Only a simple comparison of the relative compressive strength (f'_c) and modulus of rupture (f_r) of the concrete making up the individual hollowcore units was considered. These parameters were determined using standard laboratory testing procedures, the results of which are shown in Appendix A.

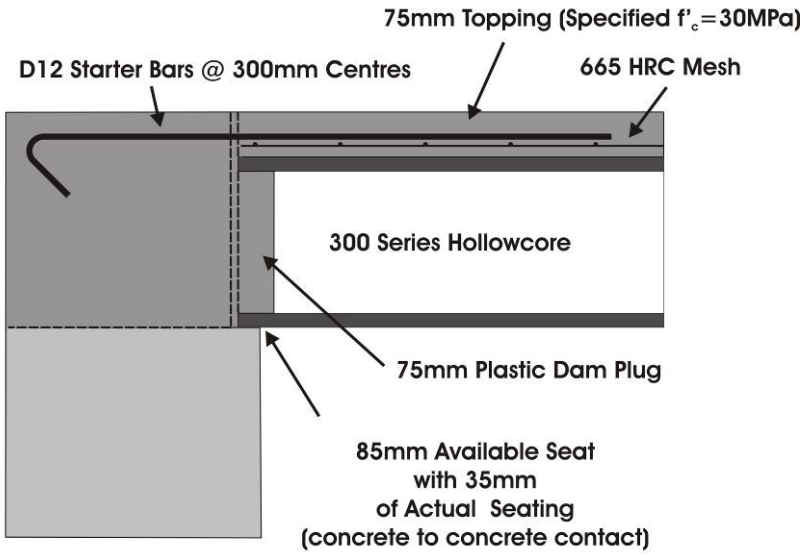

Figure 2-13 HC1 control specimen seating connection detail

Tested material properties of the seating beam and topping concrete and reinforcement for HC1 are in Table 2-1 and Table 2-2. The compressive strength of the concrete seating ledge (half beam) was under strength. Table 2-3 shows the concrete properties of the hollowcore unit. The concrete compressive strength f'_c was obtained from 75mm (diameter) core samples so was likely conservative. The modulus of rupture (f_r) was determined experimentally for the 'new' and 'old' hollowcore units used. This was carried out using a simply supported, two point flexural beam test on small portions of the hollowcore units. The experimental procedure and results are outlined in more detail in Appendix A. Any yield stress (f_y) values not reported were due to the reinforcing not having a yield plateau; any 28 day concrete compressive strengths not reported was a result of the test occurring within the 28 days.

Table 2-1 HC1 reinforcement material properties

	f_y (MPa)	f_u(MPa)
D12 Starter Bars	326	436
HRC 665 Mesh	-	548

Table 2-2 HC1 concrete compressive strengths

	28 Day f'_c(MPa)	Test Day f'_c(MPa)
Half Beam	20.3	21.0
Full Beam/Topping	33.2	39.2

Table 2-3 HC1 'new' unit concrete properties

f'_c(MPa)	f_r(MPa)
50.0	6.0

2.3.2 HC2 – Control Specimen

The HC2 seating connection detail aimed to investigate the effect a large provided seating had on connection performance. A seating length of 75mm was used, which was governed by the available seating length of approximately 85mm to the seating beam transverse reinforcement. This specimen also used a 'new' unit not representative of typical existing units.

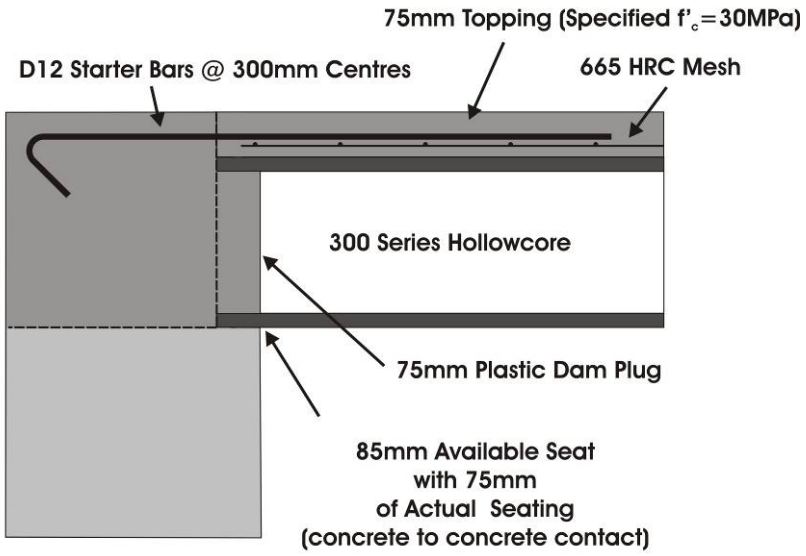

Figure 2-14 HC2 control specimen seating connection detail

Tested material properties of the seating beam and topping concrete and reinforcement for HC2 are shown in Table 2-4 and Table 2-5 below. Table 2-6 outlines the hollowcore unit concrete properties. The material properties were determined using the same techniques as those employed for specimen HC1.

Table 2-4 HC2 reinforcement material properties

	f_y (MPa)	f_u(MPa)
D12 Starter Bars	326	436
HRC 665 Mesh	-	548

Table 2-5 HC2 concrete compressive strengths

	28 Day f'_c(MPa)	Test Day f'_c(MPa)
Half Beam	20.3	23.0
Full Beam/Topping	37.6	38.9

Table 2-6 HC2 'new' unit concrete properties

f'_c(MPa)	f_r(MPa)
50.0	6.0

2.3.3 HC3 – Control Specimen

The HC3 seating connection detail incorporated a hollowcore unit from an older extrusion machine which was hoped to be more representative of units exiting in nature. The detail had a 50mm provided seating length. Tested material properties of the seating beam and topping concrete, reinforcement, and hollowcore unit for HC3 are shown in Table 2-7, Table 2-8 and below. A seating length of 50mm was adopted which fell between HC1 and HC2 lower and upper bound seating lengths. The specified *in-situ* topping concrete strength was increased from previous tests to 45MPa. This was to represent the strength development given the age of existing seating connections.

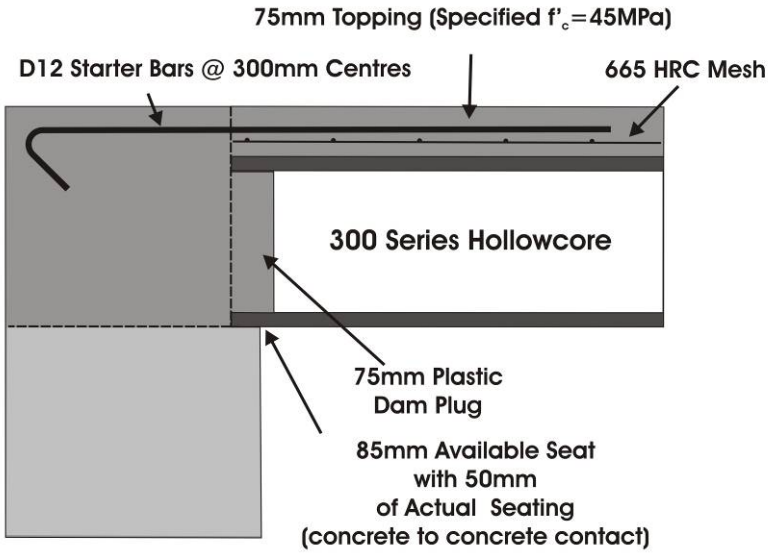

Figure 2-15 HC3 control specimen seating connection detail

Table 2-7, Table 2-8, and Table 2-9 show the material properties for seating connection elements. The observed compressive strength of the 'old' hollowcore unit was found to be

extremely high (twice that of the typical design strength of 40MPa). Again this value likely underestimated the actual strength, as is often the case with core samples.

Table 2-7 HC3 Reinforcement material properties

	f_y (MPa)	f_u(MPa)
D12 Starter Bars	326	436
HRC 665 Mesh	-	548

Table 2-8 HC3 concrete compressive strengths

	28 Day f'_c(MPa)	Test Day f'_c(MPa)
Half Beam	37.6	38.4
Full Beam/Topping	-	46.9

Table 2-9 HC3 'old' unit concrete properties

f'_c(MPa)	f_r(MPa)
85.0	7.6

2.3.4 HC4 – Retrofit Specimen

The HC4 seating connection detail was an attempted retrofit solution applied to same existing connection detail as HC3. The retrofit modification involved fixing a steel rectangular hollow section (RHS) to the face of the seating beam, combined with a plane of weakness immediately behind the hollowcore unit produced by intermittent drilling of holes (16mm in diameter, at approximate 50mm centres). The aim of this retrofit approach was to provide further additional seating, confine the existing seating ledge to suppress the spalling of the seating, and isolating the unit end from the seating beam. More specific details of the retrofit philosophy are outlined in Section 5. An 'old' unit was used in this test.

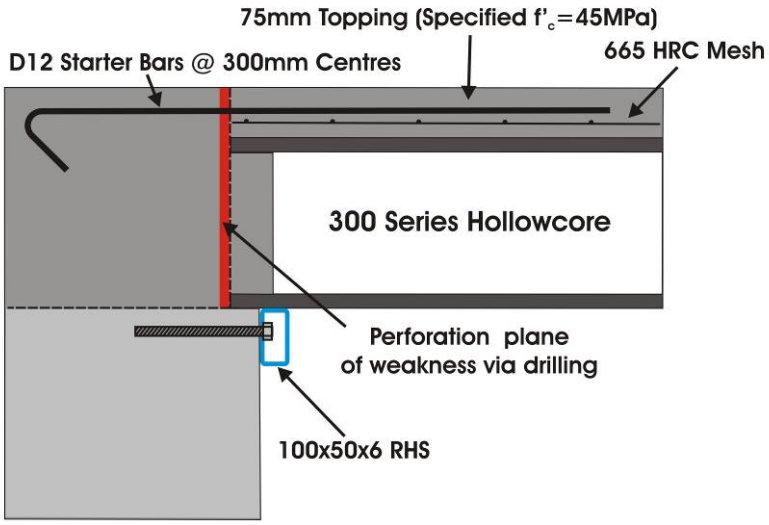

Figure 2-16 HC4 control specimen seating connection detail

Tested material properties of the seating beam and topping concrete, hollowcore unit, and reinforcement for HC4 are shown in Table 2-10, Table 2-11, and Table 2-12 below.

Table 2-10 HC3 reinforcement material properties

	f_y (MPa)	f_u(MPa)
D12 Starter Bars	326	436
HRC 665 Mesh	-	548

Table 2-11 HC3 concrete compressive strengths

	28 Day f'_c(MPa)	Test Day f'_c(MPa)
Half Beam	37.6	38.7
Full Beam/Topping	-	44.8

Table 2-12 HC4 'old' unit concrete properties

f'_c (MPa)	f_r(MPa)
85.0	7.6

2.4 Instrumentation

Primary instrumentation for this investigation focused on the seating connection region of the test specimen. Further secondary instrumentation was used to control and monitor the hydraulic rams. The focus of the discussion is given to primary instrumentation.

Potentiometers were used to monitor rotation and sliding of the base block, capturing any loss of implied rotation or elongation applied to the system. This was carried out using the strong floor as a reference point and movement tracked between the floor and base as a whole, and between the half-beam and full-beam. The setup typical of each test specimen (slight variations occurred between individual tests) is shown in Figure 2-17.

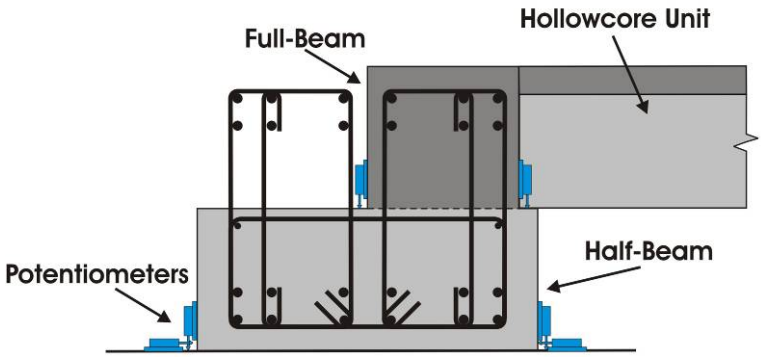

Figure 2-17 Seating beam instrumentation

In order to monitor the behaviour of the hollowcore unit on the seating beam, two sets of potentiometers were used. Potentiometers were fixed between the soffit of the unit and the face of the seating half-beam to monitor the amount of elongation and any vertical drop of the unit. Potentiometers were also fixed down one side of the unit and to the face of the full-beam to monitor the relative rotation and elongation between the unit and seating beam interface. Figure 2-18 shows the two sets of pots between the seating beam and hollowcore unit.

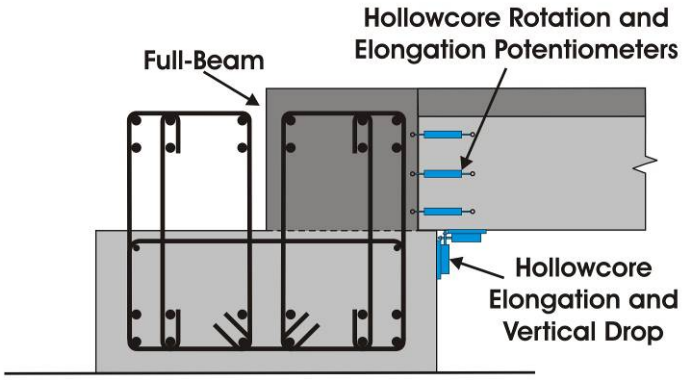

Figure 2-18 Hollowcore unit to seating beam interface instrumentation

In order to determine the strain demand on the starter bars both potentiometers and strain gauges were used. Potentiometers were used across the hollowcore unit to seating beam interface on each of the starter bars, and along the full length of one of the starter bars. The reason for this was that the interface was the region where potentially significant cracking and strain was expected. Potentiometers were the most reliable method for measuring strain in such cases. Also the strain determined was an average strain over the potentiometers length of application and was preferred to the discrete and limited measurement of a strain gauge. Figure 2-19 and Figure 2-20 show the starter bar pot configurations; it is important to note that there was a cavity created around each of the potentiometer fixing points to negate any restricting interference of the topping concrete.

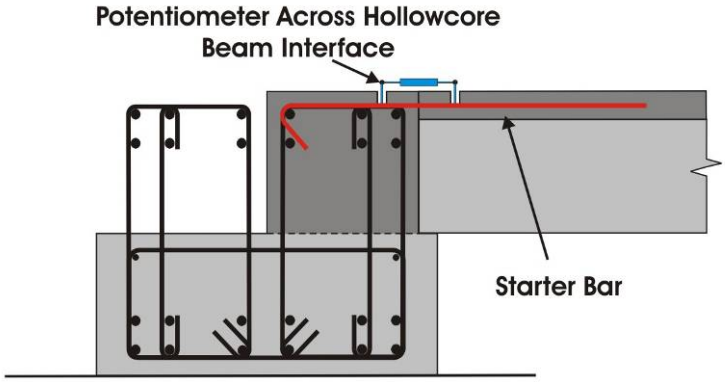

Figure 2-19 Potentiometers on starter bars across hollowcore unit and seating beam interface

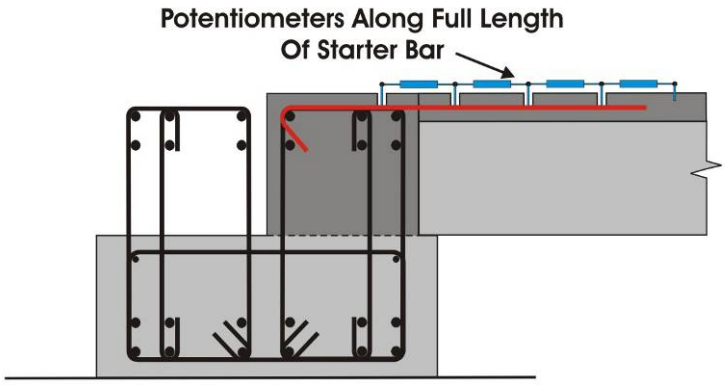

Figure 2-20 Potentiometers along full length of North starter bar on the outside of the hollowcore unit

In addition to potentiometers, strain gauges were placed on all starter bars as indicated in Figure 2-21. The strain gauges were approximately straddled by the potentiometers, leading to the strain gauges measuring discrete strain values in the middle of the potentiometer range. Strain gauges were also placed on the topping mesh to coincide with the two strain gauges closet to the end of the starter bars.

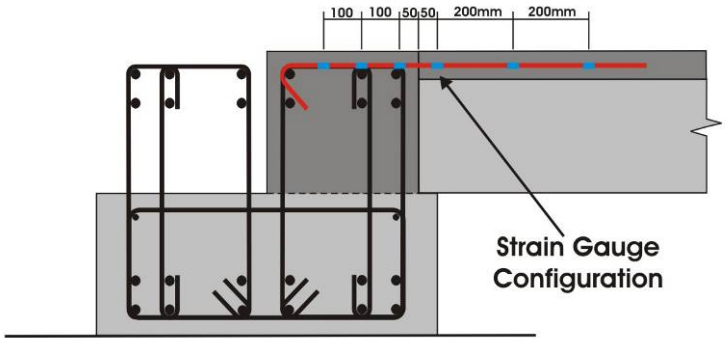

Figure 2-21 Typical starter bar strain gauge configuration

2.5 Sub-Assembly Limitations

A number of simplifications were introduced into the experimental test system through the reduction from a three-dimensional floor and frame super-assembly to a two-dimensional, single hollowcore unit and seating beam sub-assembly. This simplification was justified by focussing the investigation on what have been identified as the two mechanisms that caused the predominant damage; namely: relative rotation between the seating beam and floor system, and 'pull-off' effects as a result of beam elongation. This section discusses the aspects neglected by the sub-assembly and the potential influence on the inferred performance of the seating connection.

2.5.1 Seating Beam Behaviour – Bi-Directional Loading

The subassembly test rig was two dimensional. As a result torsional displacement (rotation) of the seating beam and elongation effects resulting from bi-directional loading are neglected. These effects have the potential to significantly modify the connection performance.

Torsion along the length of the seating beam due to interaction with the floor system results in varying levels of relative rotation between the seating beam and floor system. As a result of torsion affects, the relative seating beam rotation can vary from the frame drift, which is the source of the rotation. For simplicity and due to practical limitations, during this investigation the frame drift or rotation was considered equal to relative seating beam-to-floor system rotation, without any loss or gain due to seating beam torsion effects. This was also partly justified as the rupture of existing seating connections occurs at very low drifts. From which point connection performance is governed by beam elongation 'pull-off', which is unaffected by seating beam torsion.

The sub-assembly test procedure does not account for the effects of inelastic behaviour (plastic hinges) in potential plastic hinge zones (PPHZ) in the supporting beam. Inelastic hinging of the seating beam occurs under bi-directional loading, specifically when lateral loading acts perpendicular to the span of the floor system. This results in typical seismic frame beam vertical deformation and elongation behaviour being induced under the seating of the floor units. As hollowcore units are prestressed, one-way systems and significant stress interference and distribution could potentially result from such actions. This could have a damaging effect on the already complex stress conditions at the end of the floor system. Damage causing un-even bearing of the seated hollowcore units would also likely result.

2.5.2 Dynamic Effects

The sub-assembly test approach is quasi-static; therefore the dynamic effects of seismic events are not represented. Given the substantial mass of a floor system, an important aspect of these dynamic effects are the vertical accelerations associated with a seismic event. This is particularly relevant given the prestressed nature of hollowcore floor units making them sensitive to vertical acceleration induced inertia forces (Ho 2001). In terms of the seating connection, vertical inertia forces would significantly increase the vertical support reaction on the provided seat. This would be undesirable and would likely detrimentally affect the

performance of the seating connection because of the higher induced vertical stresses, both in the hollowcore unit itself and in the unreinforced concrete seating ledge.

2.5.3 Pre-Existing Stress Conditions

Due to the investigation being focussed on retrofit options the existing seating connections of interest can be up to 25 years old (constructed in the 1980-1990's). The aged nature of the connections was not represented by the sub-assembly test specimens. This is important given the prestressed, composite nature of hollowcore floor systems. In particular how time dependant stress effects such as creep and shrinkage affect strain conditions in the seating connection region of hollowcore unit and *in-situ* topping (Fenwick et al 2004). It is likely these would detrimentally affect the performance of the seating connection.

2.5.4 Shift in Gravity Load

Artificial gravity load was added to the sub-assembly test system representing the full floor span gravity load. The manner with which this was carried out was discussed in Section 2.2. The gravity load generates inaccuracies in the load data recorded from vertical ram, which supports the pseudo mid-span of the floor unit. This inaccuracy was due to substantial loss in strength and stiffness at initial rupture of the seating connection. This loss in seating connection fixity shifted a higher proportion of gravity load to the vertical ram supporting the unit. This inaccuracy is represented by an offset in moment versus rotation relationships of the test specimens. Effectively the increase in vertical load due to changing seating connection conditions results in a perceived increase in the rotational strength of the connection. For this reason, hysteretic properties of the seating connections are not entirely representative following initial rupture.

2.6 Conclusions

The sub-assembly testing procedure, motivation for the specimens tested, origin and nature of the rotation and elongation loading protocol, and instrumentation was discussed. An attempt has been made to describe the methods used and the justification of these methods. The general theme behind the experimental investigation of the existing seating connection was first to build on previous research and further understand potential failure mechanisms of the existing seating connections (HC1, HC2, HC3).

The sub-assembly approach is simplistic as a result of the omission of influential factors described above. This provides both deficiencies and benefits in the testing procedure. The exclusion of factors such as three dimensional frame behaviour, dynamic effects, and pre-existing stress states in the floor system the testing procedure are not entirely accurate and are considered un-conservative. However, through the simplifications involved in the sub-assembly test, the major damage causing mechanisms (being seating beam rotation and longitudinal beam elongation) are highlighted. This enabled a clearer understanding of the effects these aspects have on the seismic performance of hollowcore seating connections to be established.

2.7 References

Bull D.K, Matthews J.G, 2003, *Proof of concept tests for hollow-core floor unit connections*, Precast NZ report, Feb 2003.

Fenwick R.C, Deam B.L, Bull D.K, 2004, *Failure Modes for Hollowcore Flooring Units,* Journal of the Structural Engineering Society of New Zealand (SESOC), Vol. 17, No. 1.

Ho D.T, 2001, *Performance of hollow-core floor systems under earthquake induced vertical acceleration*, Masters Thesis, Department of Civil Engineering, University of Canterbury, Christchurch, New Zealand.

Ireland M.G, 2006, *Concept and Implementation of a Selective Weakening Approach for the Seismic Retrofit of R.C. Buildings*, NZSEE Conference Proceedings, Napier, New Zealand.

Liew H.Y, 2004, *Performance of hollow-core floor seating connection details*, Masters Thesis, Department of Civil Engineering, University of Canterbury, Christchurch, New Zealand.

Lindsay R.A, 2004, *Experiments on the seismic performance of hollow-core floor systems in precast concrete buildings*, Masters Thesis, Department of Civil Engineering, University of Canterbury, Christchurch, New Zealand.

MacPherson C.J, 2005, *Seismic performance and forensic analysis of a precast concrete hollow-core floor super-assemblage*, Masters Thesis, Department of Civil Engineering, University of Canterbury, Christchurch, New Zealand.

Matthews J.G, 2004, *Hollow-core floor slab performance following a severe earthquake*, PhD Thesis, Department of Civil Engineering, University of Canterbury, Christchurch, New Zealand.

NZS3101:1995, 1995, *Concrete Structures Standard, NZS3101, Parts 1 & 2*, Standards New Zealand, Wellington, New Zealand.

NZS3101:1995, 2004, Amendment No. 3 to 1995 Standard (NZS3101), Standards New Zealand, Wellington, New Zealand.

NZS3101:2006, 2006, *Concrete Structures Standard, NZS3101, Parts 1 & 2*, Standards New Zealand, Wellington, New Zealand.

AutoCAD, 2005, Computer program library, Department of Civil Engineering, University of Canterbury, Christchurch, New Zealand.

3 Experimental Observations and Results: Existing Seating Connections

This section discusses the behaviour and performance observed in the existing seating connection control specimen tests. Results are presented through discussion of photographs of the connections during and after testing. Instrumented results such as overall connection hysteretic behaviour and strain demand on the starter bars were also used to assess the behaviour of the connections. The aims of the control specimen tests were to investigate and further develop the understanding of pre-conceived and observed structural weaknesses in existing hollowcore seating connections.

3.1 HC1 – Control Specimen

The HC1 seating connection detail represented existing seating connections which are seating deficient. The provided seating was 35mm and the unit sat directly on the bare concrete seating ledge, a 'new' hollowcore unit was used for the HC1 specimen (discussed in Section 2.3.1). Additional gravity load represented the self weight of the equivalent full-span floor system only. Figure 3-1 illustrates the HC1 connection detail.

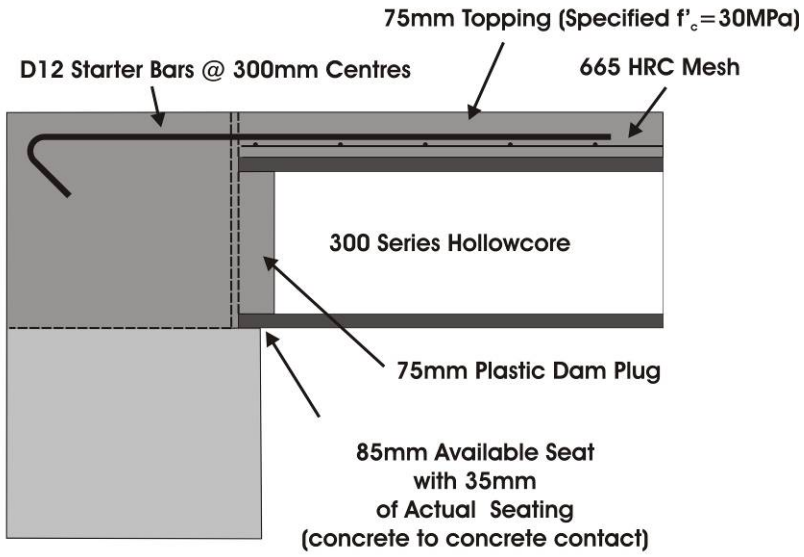

Figure 3-1 HC1 connection detail

3.1.1 Test Visual Performance Indicators

For discussion regarding the seating connection behaviour positive rotation or drift refers to the hollowcore unit soffit pulling away from the seating ledge; conversely negative rotation or drift refers to the top of the unit pulling away from the seating beam, this is illustrated in Figure 2-8.

Upon completion of the first positive and negative drift cycles of 0.25% small near-vertical hairline cracks appeared at the hollowcore unit to seating beam interface. Later observation of the moment rotation hysteretic behaviour following this cycle showed no strength or stiffness degradation as a result of this cracking. At a drift level of +0.25%, during the following +0.5%, cycle a large crack opened behind the hollowcore unit in a sudden and brittle manner. The crack ran from the face of the provided seating, through the lower corner regions of the hollowcore unit soffit, and up through the hollowcore-to-seating beam interface and topping. The location of this crack can be seen in Figure 3-2 and Figure 3-3.

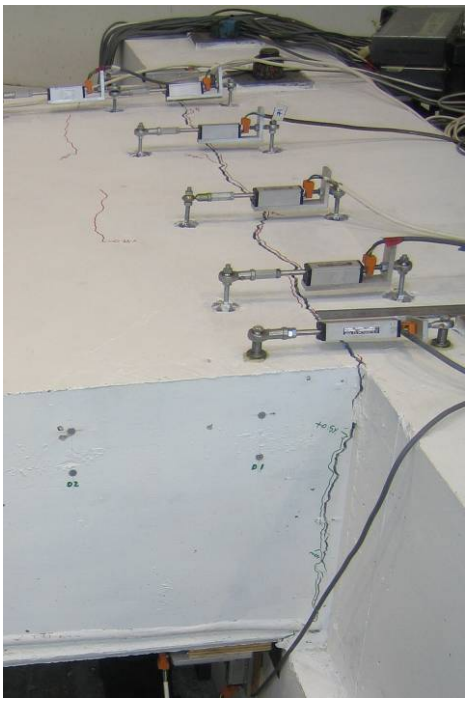

Figure 3-2 HC1 interface crack initiation at -1.0% drift

This initial near vertical crack surface formed a failure plane which the unit progressively slid down under increasing drift and elongation demand. At initial rupture, spalling of the seating ledge had been initiated. This spalling contributed to the hollowcore unit-to-seating beam

rupture interface. As a result the failure surface extended below the level of the seating ledge in some regions.

Following the 1.0% drift cycle, the seating beam interface crack was approximately 3mm wide. At the completion of the 2.0% drift cycle the unit had dropped approximately 13mm. As the drop of the unit increased, a horizontal crack opened along the hollowcore interface between hollowcore unit and the *in-situ* concrete topping. The crack interface originated from the near vertical seating interface crack region as illustrated in Figure 3-3.

At a drift level of approximately +3.1%, and an elongation of approximately 25mm, loss of seating occurred and the unit lost support and dropped off the cracked failure plane. When the unit fell, the topping delaminated from the upper surface of the unit and ruptured at the termination of the starter bars. This is illustrated in Figure 3-3 which shows the progressive dropping of the unit and final collapse and delamination of the topping during the +3.5% drift cycle.

Figure 3-3 Failure sequence of HC1 control specimen during 3.5% drift cycle

3.1.2 Post-Test Visual Performance Indicators

Following the test, the end of the unit and the beam section of the interface between the unit and seating beam were exposed. A number of observations were made which helped describe the connection behaviour.

A combination of seat spalling and the trapped corner portions of the hollowcore unit soffit resulted in there being no provided seating ledge following initial rupture. This is illustrated in Figure 3-4 a) and c). The regions of trapped unit and spalled seat can be seen on the seating beam interface. In Figure 3-4 c) regions shaded in red highlight seat spalling and green regions highlight the trapped portions of hollowcore unit. The red and green regions meet almost the full length of the provided seating illustrating the extent of the failure surface and lack of any provided horizontal seating. Figure 3-4 b) and d) illustrate the unit side of the rupture interface. The damage to the end of the hollowcore unit resulting from the trapping of the soffit can be seen shaded in green.

Figure 3-4 a) and c) illustrate the delaminated portion of topping hanging from the seating beam. This portion of the topping contains the starter bars still tied into the seating beam. Figure 3-4 c) and d) show the top surface of the unit where delamination has led to separation of the *in-situ* topping concrete from the top of the hollowcore unit, shaded in blue. The failure sequence shown in Figure 3-3 illustrates the onset of delamination prior to final collapse as the horizontal crack grows under increasing downward slip of the unit.

Figure 3-4 shows the near vertical failure plane passes behind the end of the hollowcore unit and through the concrete stubs cast inside the end of the hollowcore unit. The snapped ends of the stubs can be seen trapped in the end of the unit. This suggests that until rupture occurs these stubs are a source of initial connection fixity, and therefore, resist rotation of the hollowcore unit. As the stubs are unreinforced the extent of this fixity would be governed by the tensile strength of the *in-situ* beam and topping concrete.

a) Exposed seating beam

b) Exposed hollowcore unit end

c) Exposed seating beam – critical regions highlighted

d) Exposed hollowcore unit end – critical regions highlighted

Figure 3-4 Damage mechanism and failure surfaces HC1

3.1.3 Instrumental Performance Indicators

Figure 3-5 shows the moment versus rotation hysteretic behaviour of the seating connection. Relationships were determined for the individual vertical drift (vertical ram) component and elongation component (horizontal ram), as shown in Figure 3-5 a) and b). The combined net moment versus rotation relationship is shown in Figure 3-5 c). The individual relationships were determined using the geometric relationships established for the sub-assembly test rig, and discussed in Section 2 (shown in fig 2-10), to determine the loading protocol (only in a reverse sense). This converted the measured forces and displacements along the lines of action of the hydraulic rams into global horizontal and vertical force components applied to the system at the hydraulic ram pins. The respective lever arms from the hydraulic ram pins to the ICR were then used to determine the resulting moments at varying drift levels.

Observing the vertical and net moment versus rotation relationship of the seating connection (illustrated in Figure 3-5 b) and c)) it can be seen the connection is initially relatively stiff. This stiff initial phase was seen in both negative and positive drift directions. The rupture of the connection occurred at a peak strength of 70kNm, and a drift of +0.25%. This is highlighted by the sudden drop in moment (strength) representing the sudden brittle nature of the rupture. Following this, a residual strength of approximately 15kNm was observed under increasing positive drift cycles. The true residual strength was likely much less due to the shift in gravity load (discussed in Section 2) giving an inaccurate indication of the true connection flexural strength. In the negative drift direction, a higher residual moment of approximately 50kNm was maintained due to activation of the starter bars. Figure 3-5 a) illustrates the moment induced in the connection due to elongation actions from the horizontal ram.

The behaviour of the connection following initial cracking is considered to be ideal in terms of limiting forces imposed on the hollowcore unit through the connection. However this is only ideal provided that the vertical support is sufficient and reliable, which in this case was not seen due to the location of the initial crack resulting in zero provided seating.

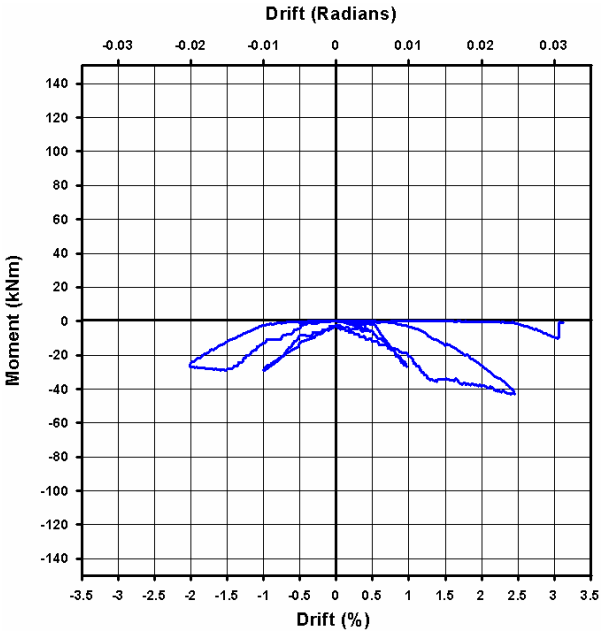

a) Horizontal elongation induced moment versus rotation

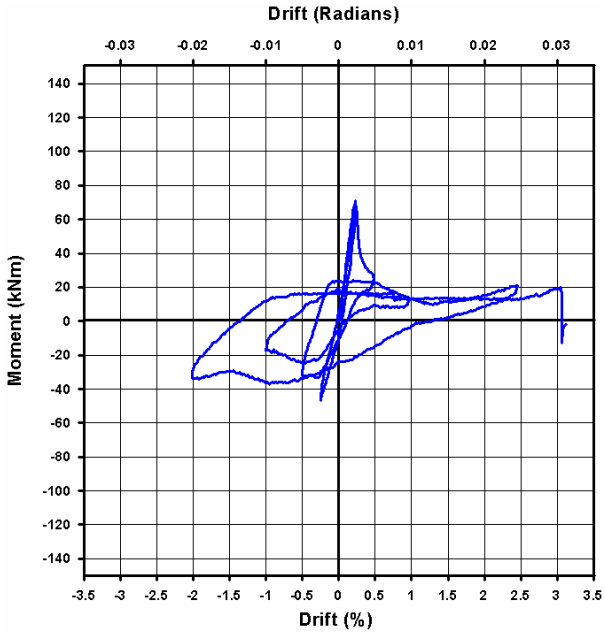

b) Vertical drift induced moment versus rotation

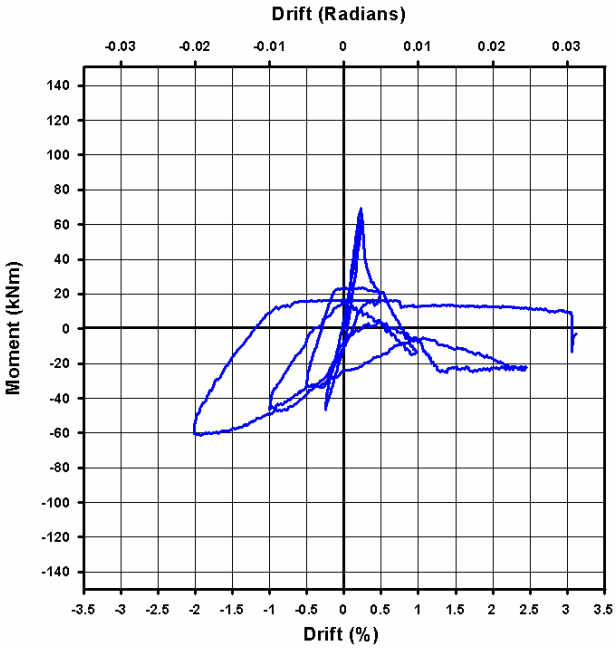

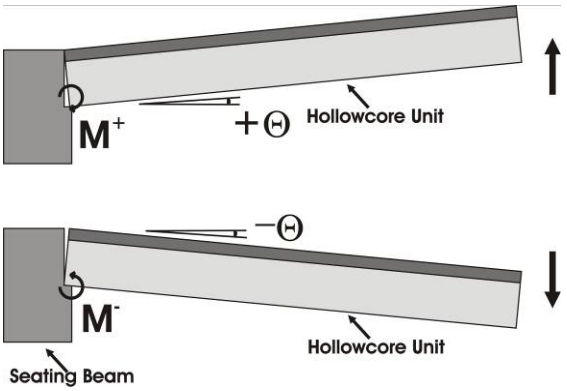

c) Net moment versus rotation

Figure 3-5 HC1 moment versus rotation

Figure 3-6 shows the average strain in the four starter bars across the interface between the seating beam and hollowcore unit. The strain profile shows the 'walking' nature of stretching demand on the starter bars due to the combined rotation and beam elongation demand. This strain was inferred using the change in length of a potentiometer over an initial gauge length of approximately 200mm which straddled the crack interface. The strain was an average

value and could be significantly higher locally within the potentiometer length, depending on the amount of strain penetration.

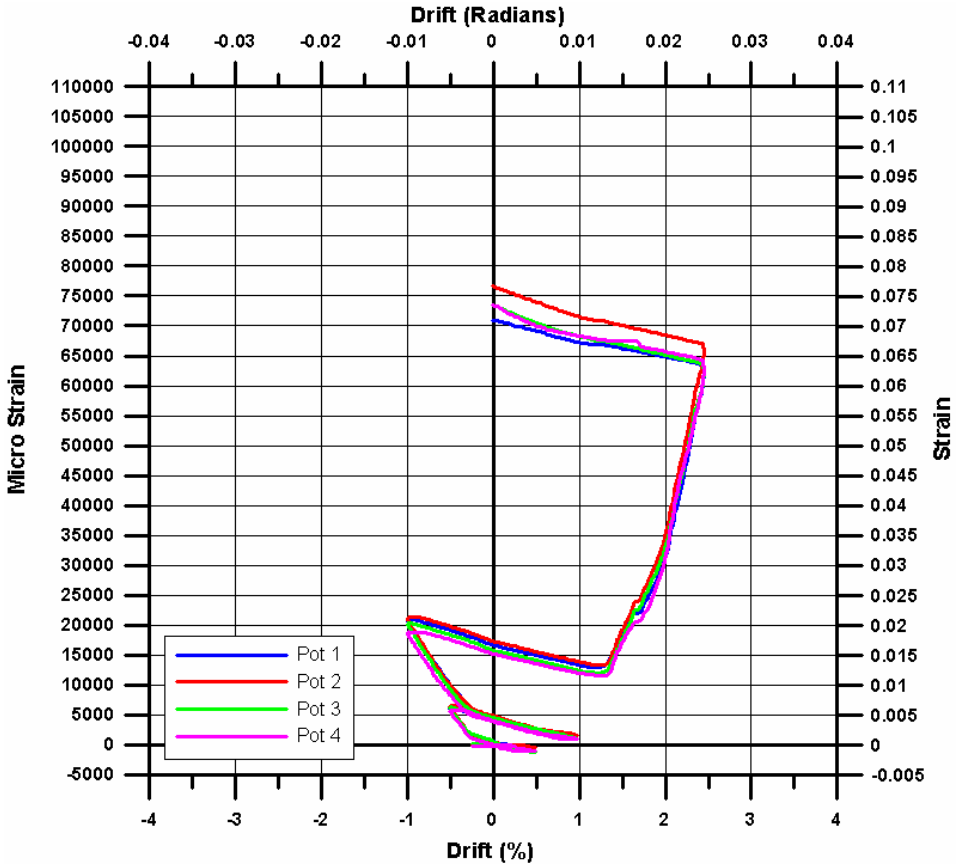

Figure 3-6 HC1 Starter bar Strain across crack interface

Strain gauge readings taken approximately 50mm either side of the crack interface are shown in Appendix B. The magnitude of strain values along the length of the starter bars confirmed the presence of strain penetration. An approximate integration assuming a linear change in strain between discrete strains, inferred from the strain gauges within the potentiometer length, accounted for a large proportion of the average strain. This suggests that the average value was representative and not largely skewed by strain concentration at the crack interface. Strain penetration along the length of the starter bars would have been helped by, or in fact contributed to, the progressive topping delamination observed.

Figure 3-7 shows the desired ('T') and measured ('M') end profile of the hollowcore unit at peak drift levels up until instrumentation was removed (-1.0% drift). The vertical axis represents the depth of the combined hollowcore unit and topping section, 0mm corresponds to the level of the hollowcore unit soffit (and seating ledge) and 375mm the level of the

topping floor surface. It was observed that the desired levels of elongation were not achieved, which was likely due to slack in the ram connection system and trying to impose such small elongation movements (in the order of millimetres on the system). Through visual observation during the test this slack was seen to be less evident at higher drift levels where elongation values were much larger than indicated in Figure 3-7. It can be seen however that desired vertical drift levels (slopes of the profiles) were achieved to sufficient accuracy.

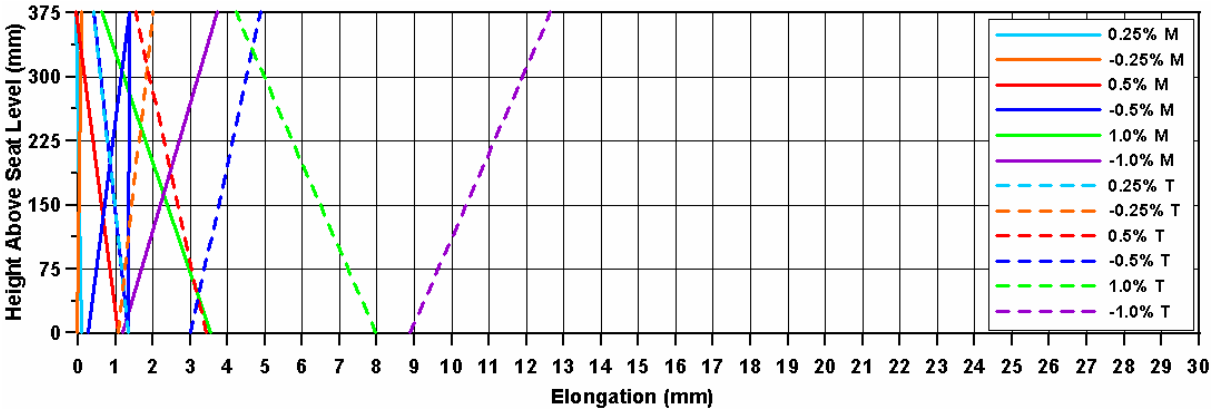

Figure 3-7 HC1 hollowcore unit end displacement profile

3.1.4 Key Implications of Connection Performance

There were a number of issues highlighted in this test which contributed to the observed loss of seating failure mechanism. Rupture of the hollowcore unit-to-seating beam interface resulted in a near vertical crack forming behind the end of the hollowcore unit. The crack originated from the face of the provided seating ledge and passed through corner portions of the unit soffit, *in-situ* concrete stubs and topping. In areas of substantial spalling of the existing seating ledge, the failure plain passed below the level of the provided seating. This raises performance concerns due to the location of the crack interface, the susceptibility of the supporting seating to spalling, and the inherently unquantifiable nature of the crack formation.

Due to the location of the near vertical failure plane any provided seating ledge was negated. This was a result of small trapped corner portions of the unit soffit, in addition to large amounts of seat spalling. Consequently the unit was supported only by interlock and friction between the damaged unit end and seating beam interface. At low drift and elongation levels some vertical support may have be provided by the topping starter bar reinforcement. However, this would only be true prior to significant yield penetration and topping delamination and therefore cannot be relied upon. As a result of the near vertical nature of the

failure interface, the unit was seen to slide down the failure plane under vertical drift and elongation loading, finally resulting in collapse.

The unreinforced nature of the seating connection resulted in the rupture of the interface being unpredictable, without a clearly defined or calculable hierarchy of strength. The elements which make up the combined connection are the hollowcore unit, surrounding *in-situ* topping and concrete stubs, and seating ledge. Of particular concern was the way the concrete stubs key into the end of the unit, and restraint on the soffit from the seating ledge. These two elements promote fixity of the connection prior to rupture. Potentially, if the strength of the unit was lower than the combined stubs, surrounding topping and seating ledge, then the rupture could occur in the hollowcore unit. This would be an undesirable hierarchy of strength and failure mechanism, as was observed by Matthews (2004).

The substantial amount of spalling of the seating ledge had a large contribution to the lack of any support of the unit. Spalling was attributed to a combination of the unit bearing weight and the pulling of the soffit across the seating ledge. This highlights a concern over typical existing seating connections which rely on the unreinforced cover concrete of the beam to provide seating. These types of seating connections are susceptible to loss of gravity support as a result of spalling.

The presence of trapped soffit of the hollowcore unit also suggests sitting the unit directly on the bare concrete seating ledge (as an alternative to using a mortar bed) had little effect on aiding the unit to slide. This is further emphasised given the provided seating ledge was relatively small, at 35mm, but still managed to trap portions of the unit. In addition, the peak connection strength (under positive drift) prior to rupture was comparable to that of a similar test using a mortar bed by Bull and Matthews (2003) (70kNm compared with 68kNm).

High levels of strain were observed in the starter bars due to both direct tensile elongation and negative unit rotation. Strain penetration in the starter bars was evident and likely prevented starter bar rupture. It is likely that strain penetration also contributed to the extent of delamination of the topping through aiding in breaking the bond between the unit and topping. This was particularly evident at high drift and elongation demand.

3.2 HC2 – Control Specimen

This section outlines the major visual and instrumental observations from the HC2 seating connection detail. The seating connection was based around typical structural details as was HC1. However, in contrast to HC1 a larger seating ledge length of 75mm was used. The reason for this was to investigate the effect a large seating has on the connection performance as an upper bound configuration. Additional gravity load represented the self weight of the equivalent full-span floor system only. A 'new' hollowcore unit was also used in the HC2 test specimen, consistent with HC1. Figure 3-8 shows the HC2 connection detail.

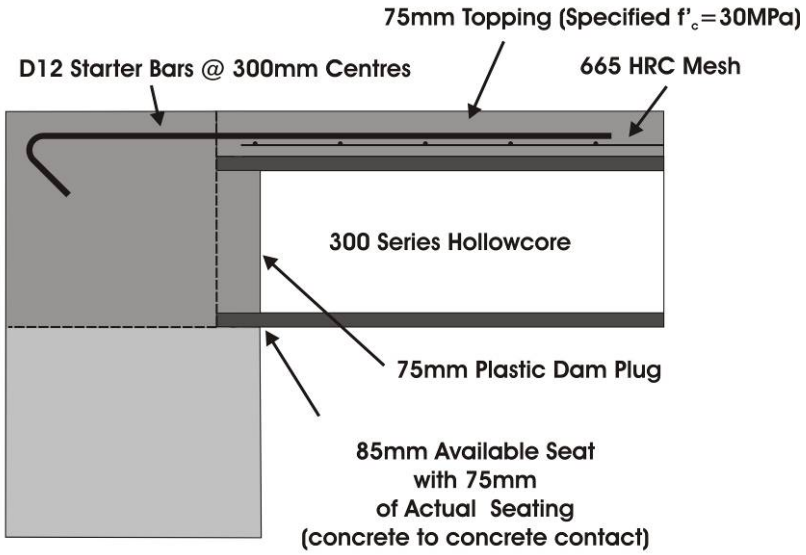

Figure 3-8 HC2 connection detail

3.2.1 Test Visual Performance Indicators

The HC2 seating connection specimen behaved in a manner consistent with the HC1 test specimen, only hairline cracks, and no significant loss of strength or stiffness was observed to a drift of +0.25% . In the negative cycle to 0.25% drift, cracking behind the end of the hollowcore unit (seating beam interface) was more substantial. However, this was not as sudden and complete as HC1, suggesting only partial or onset of rupture had occurred at this point. Early in the following +0.5% drift cycle (+0.25%) rupture of the hollowcore unit-to-seating beam interface was completed. Upon completion of +/-0.5% drift cycle the hollowcore-to-seating beam crack interface was fully developed with a crack width of approximately 1.0mm. Following this drift cycle, spalling of the seating ledge had initiated

and a number of lateral cracks running across the topping were observed, as illustrated in Figure 3-9.

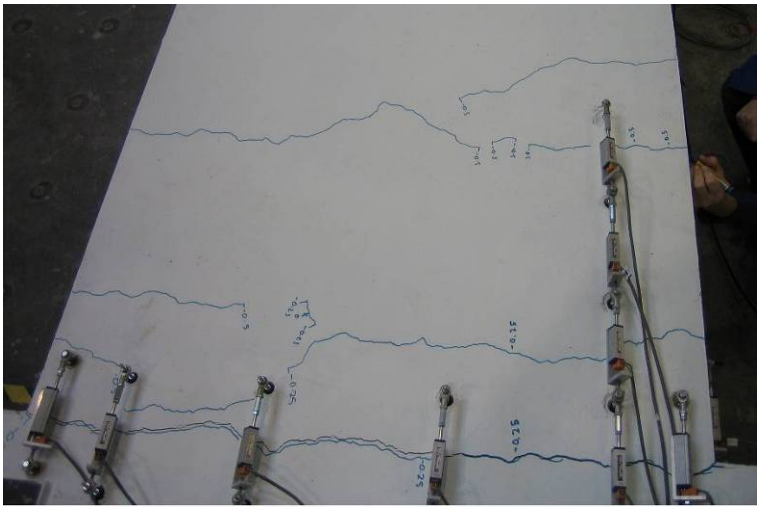

Figure 3-9 HC2 Lateral topping cracking after +/-0.5% drift cycle

As drift levels increased the hollowcore unit to seating beam crack interface was seen to widen in a 'walking out' manner under imposed rotation and elongation demand. This behaviour is illustrated in Figure 3-10 which shows the seating beam interface crack under peak drifts of +2.5%, -2.0% and +3.5%. The interface crack widths following theses cycles were approximately 9mm, 17.5mm and 20mm respectively. Upon completion of the test, no vertical displacement (drop) of the hollowcore unit was observed. Throughout the test considerable spalling of the seating ledge occurred, following initiation at early drift levels

.Due to the vertical support of the hollowcore unit being maintained to the completion of the test, the combined drift and elongation loading protocol was repeated. The position of the hollowcore unit at the completion of the first loading procedure was used as the starting point of the second loading procedure. On completion of the second loading cycle an elongation of approximately 40mm had been applied to the unit and a vertical displacement (drop) of the hollowcore unit in the order of 40mm was observed. Following this, monotonic elongation was imposed on the hollowcore unit in the 0% drift position, resulting in rupture of the starter bars and final loss of support, under and overall elongation of approximately 55-60mm. Throughout the test only small amounts of delamination were observed in close proximity to the seating beam. This was in contrast to the extensive delamination observed in the HC1 test specimen.

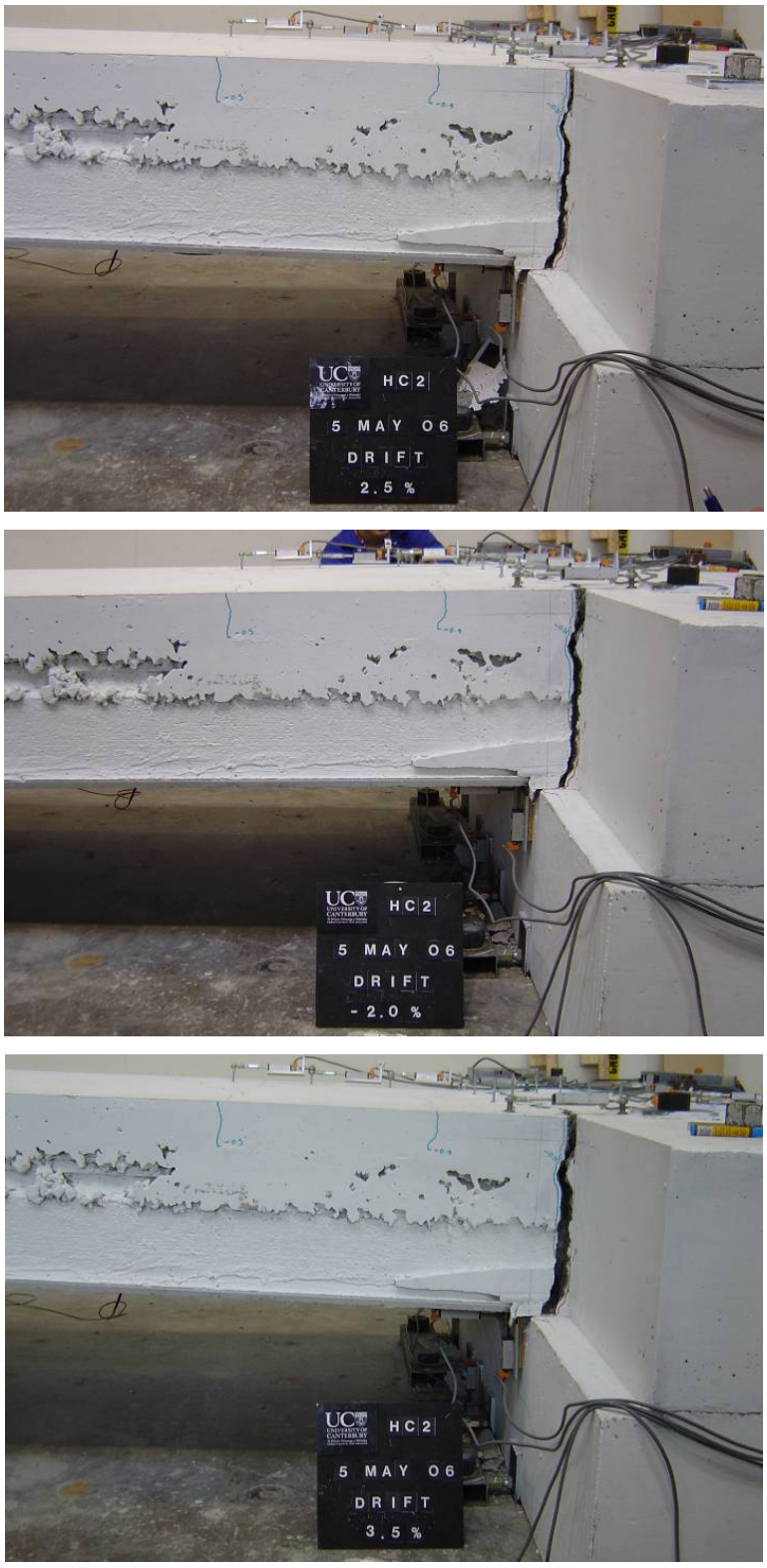

Figure 3-10 Final behaviour sequence of HC2 Control Specimen

3.2.2 Post-Test Visual Performance Indicators

Figure 3-11 shows the exposed seating beam interface and hollowcore unit following the test. A damaged crack interface much like that of HC1 was observed. The crack ran near vertical from the seating ledge, through the concrete stubs in the cores of the unit, and through the *in-situ* topping. However, due to the larger seating ledge there were regions of horizontal ledge surface remaining where the crack interface originated from within the provided seating length. This provided vertical support to the unit consequently preventing the loss of seating from occurring. This is illustrated in Figure 3-11 a) and c) where gaps between regions of trapped unit shaded in green and spalled seating regions in red can be seen.

As a result of the larger seating ledge, no sudden loss of support for the floor occurred under the prescribed loading protocol (additional loading was later applied, resulting in loss of support). In addition to this, there was no obvious or sudden separation of the *in-situ* topping from the unit as a result of delamination. However, Figure 3-11 b) and d) show the exposed hollowcore unit with some delamination evident shaded in blue. It was likely delamination was initiated during the test as suggested by the lateral cracking across the topping as shown in Figure 3-9.

Consistent with HC1, all stubs within the cores of the hollowcore unit were ruptured forming a significant portion of the seating beam crack interface. This further confirms the potential influence the strength of these cores has on the performance of the connection. Potentially, the greater the strength of the concrete cores the greater the overall connection flexural strength. This is of concern given the overall connection strength controls the magnitude of undesired flexure and shear forces imposed on the floor system. Large amounts of seat spalling were observed, as illustrated in Figure 3-11 c), shaded in red.

a) Exposed seating beam

b) Exposed hollowcore unit end

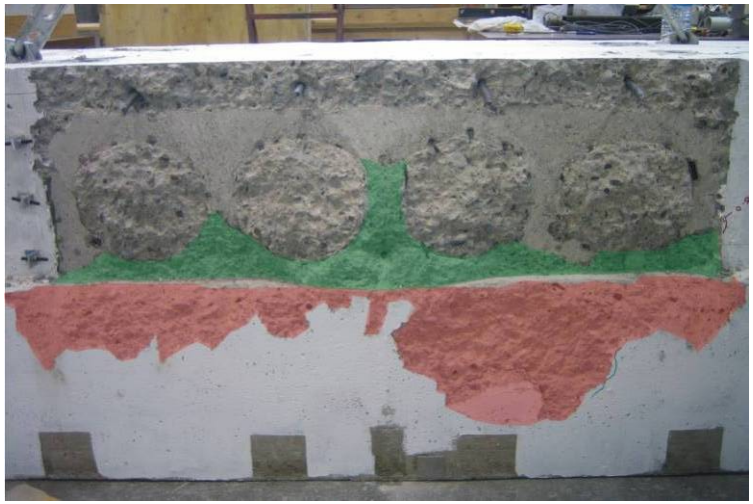

c) Exposed seating beam – critical regions highlighted

d) Exposed hollowcore unit end – critical regions highlighted

Figure 3-11 Damage mechanism and failure surfaces HC2

Exposing the HC2 seating beam interface revealed a large portion of the soffit of the hollowcore unit trapped the full depth of the 75mm seating ledge. This was important as enough of the unit was broken off to expose a prestressing strand from the hollowcore unit which had been anchored into the seating beam. Figure 3-12 a) shows the end of the hollowcore unit with the exposed and 'kinked' pre-stressing strand. Figure 3-12 b) shows the portion of hollowcore unit clearly trapped between two ruptured concrete stubs. This suggests larger seating ledges increase the overall connection flexural strength, increasing the potential for undesired flexure and shear actions being imposed on the floor system..

a) Kinked prestressing strand protruding from hollowcore unit

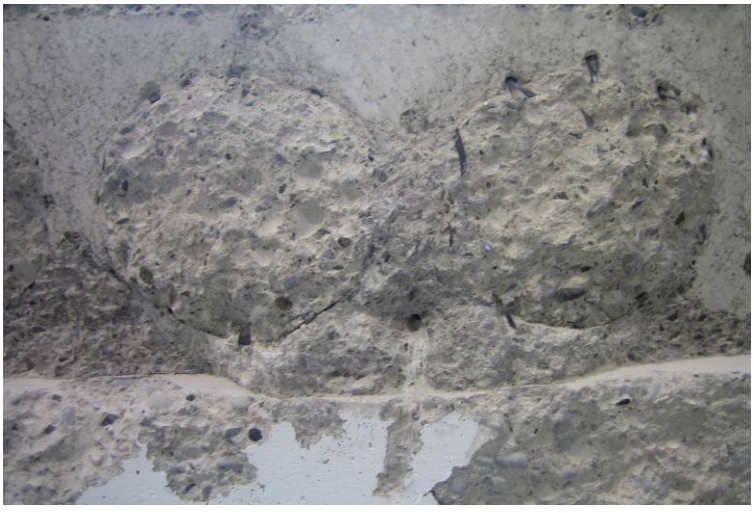

b) Trapped portion of hollowcore unit on the seating ledge (showing the void left by the prestressing strand)

Figure 3-12 HC2 Trapped portion of hollowcore unit

3.2.3 Instrumental Performance Indicators

Figure 3-13 shows the individual vertical, elongation, and the combined net moment versus rotation relationships for the seating connection. The hysteretic behaviour resembles that described for the HC1 seating connection, with high initial stiffness followed by sudden rupture at a drift of approximately +0.25%. A slight variation was observed as a small drop in strength on the first -0.25% drift cycle occurred prior to complete rupture. A peak positive strength of approximately 85kNm was reached. This increase, when compared with the peak strength of HC1, was attributed to the larger provided seating length. A peak negative moment of approximately 50kNm was reached before partial rupture of the hollowcore unit to seating beam interface. The elongation induced moment shown in Figure 3-13 a) illustrates regions of positive moment, indicating compressive elongation forces were required to compress previously stretched starter bars.

A large offset in moment was observed with a residual moment of approximately 20kNm at zero drift levels. This was likely caused by the transfer of gravity load to the vertical hydraulic ram as a result of loss of fixity at the seating connection. Figure 3-13 shows the seating connection exhibits ductile behaviour under negative drifts as a result of the presence of the starter bars.

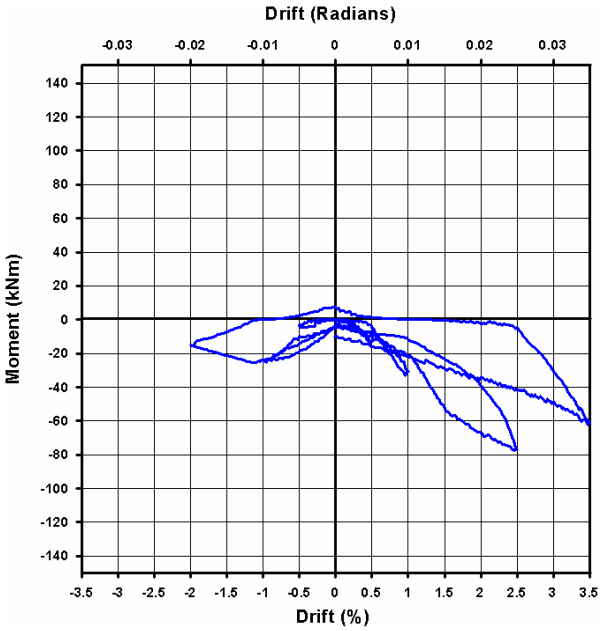

a) Horizontal elongation induced moment versus rotation

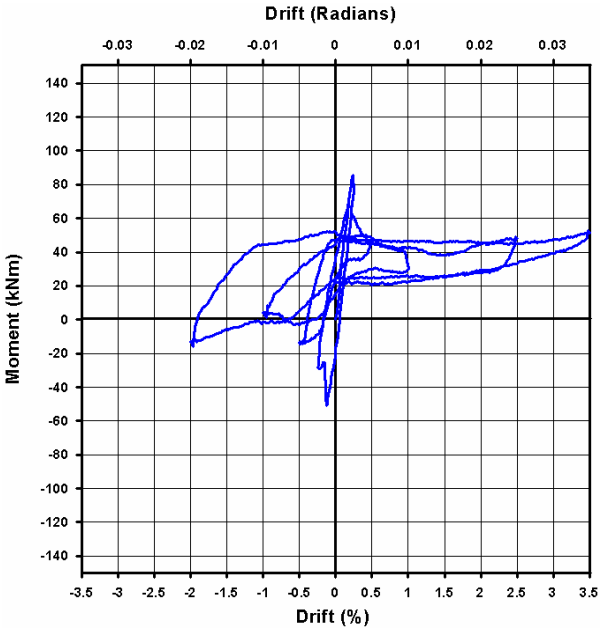

b) Vertical drift induced moment versus rotation

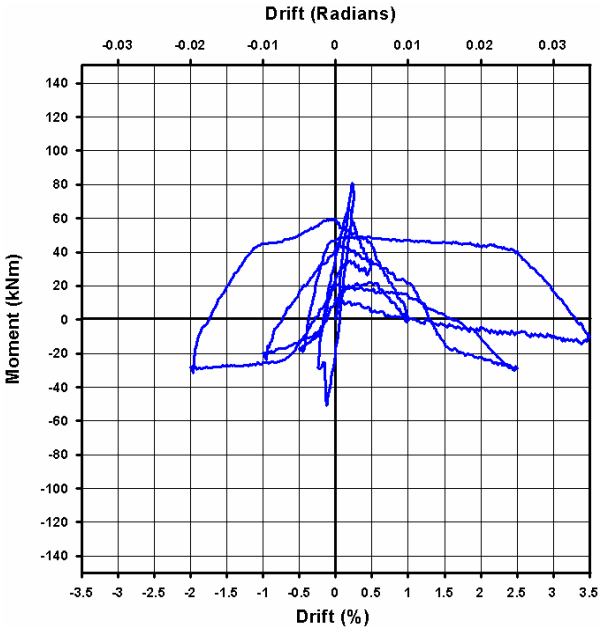

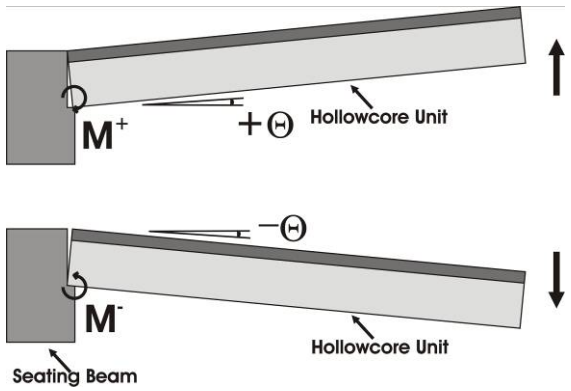

c) Net moment versus rotation

Figure 3-13 HC2 Moment versus rotation

Figure 3-14 shows the strain in the starter bars determined using potentiometers and as a function of drift. Again, approximate strain integration of values obtained from strain gauges from within the potentiometer length suggested that the average strain values were representative.

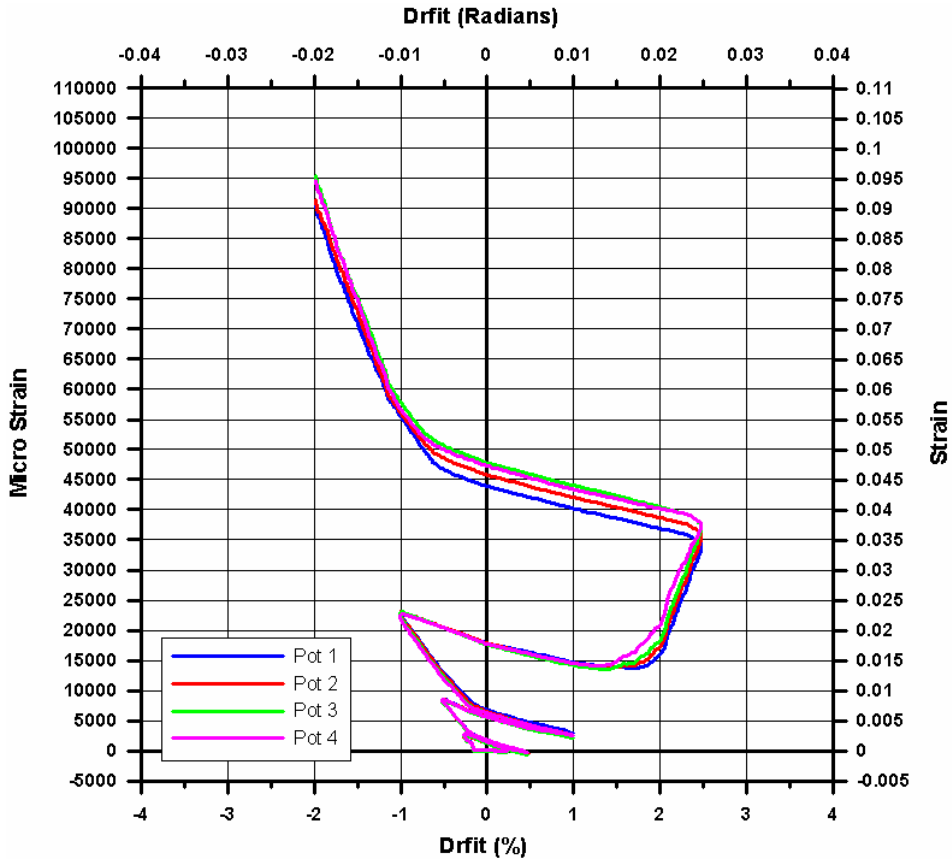

Figure 3-14 HC2 average starter bar strain determined using potentiometers

Figure 3-15 shows the desired ('T') and measured ('M') end profile of the hollowcore unit at peak drift levels up until instrumentation was removed (-1.0% drift), some slack in elongation was observed. The slack was seen to be less than in HC1 and good agreement between desired and achieved vertical drift (seating beam rotation) was achieved.

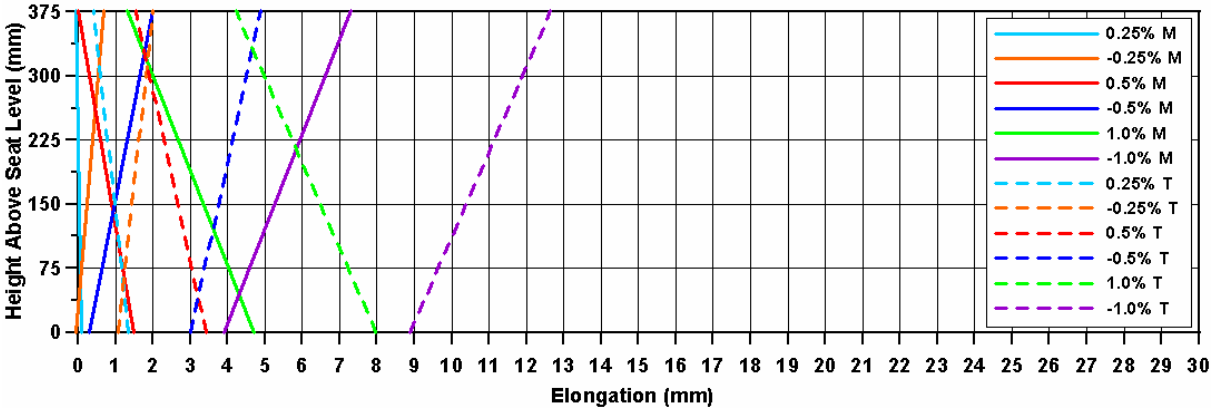

Figure 3-15 HC2 hollowcore unit end displacement profile

3.2.4 Key Implications of Connection Performance

The performance of HC2 was consistent with HC1 and many of the same conclusions can be drawn from the test. The connection was initially very stiff prior to rupture of the hollowcore to seating beam interface at a +0.25% drift. As with HC1 ruptured stubs, trapped unit soffit and substantial seat spalling were observed. Due to the larger provided seating loss of support did not occur at the completion of the prescribed loading protocol (a peak drift level of 3.5%, and an applied elongation of approximately 20mm). Further loading was subsequently applied to the test specimen and eventual loss of support occurred under an elongation of approximately 55-60mm

The larger provided seating highlighted the potential clamping effect a larger seating ledge can have on the hollowcore unit. This was evident as a higher rupturing moment was achieved in comparison with HC1 (an increase in the order of 20% was observed). As a result, a large portion of trapped hollowcore unit was observed. This behaviour highlights the unpredictable nature of the failure plane. This further suggests that a bare concrete ledge can provide substantial soffit restraint, and the mortar bedding material used by Bull and Matthews (2003) and Matthews (2004) was not a performance variable in the observed flexure-shear failures.

Delamination was not as obvious as in HC1 due to the additional seating preventing the unit from dropping and pulling away from the topping. However through observed lateral cracking in the topping and observed separation of the topping near the end of the unit some delamination had occurred, only to a lesser extent than was observed in HC1.

HC2 test observations further highlighted that an available seating ledge (geometrically) was not reliable as a result of seat spalling. In association with this, the strength of the seat for both HC1 and HC2 tests was significantly under-strength. This may have provided a weak link which limited the strength of the seating connection and how much demand could be placed on the unit.

3.3 HC3 – Control Specimen

The HC3 seating connection detail was a control specimen representative of typical existing seating connections, as illustrated in Figure 3-16. A provided seating of 50mm was used to fit between the previous upper and lower bound ledge lengths (35mm and 75mm). As with HC1 and HC2 the unit was seated on a bare concrete seat. Stronger, 45MPa topping concrete was used to represent the aged nature of the system.

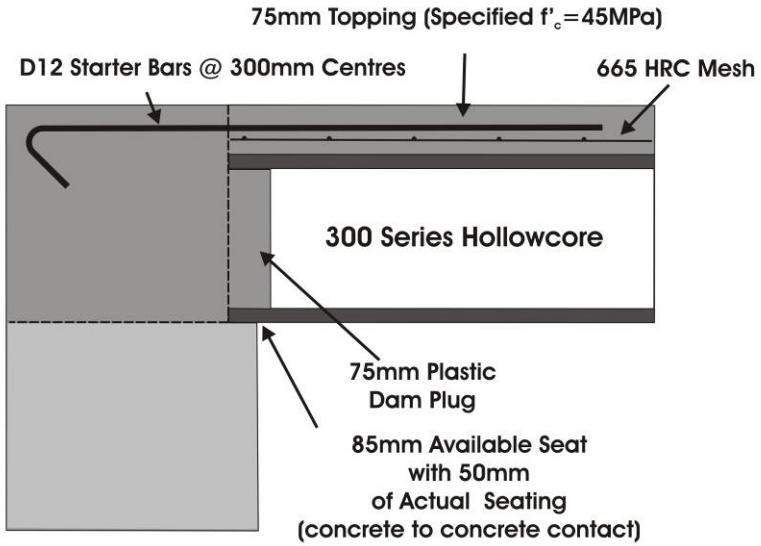

Figure 3-16 HC3 connection detail

An 'old' (produced by an old extrusion machine) hollowcore unit was used for the HC3 test specimen. This aimed at being more representative of the hollowcore units in existing buildings. Core samples of the unit later showed concrete strength in excess of 85MPa, significantly stronger than expected. HC1 and HC2 tests used 'new' units as currently produced. The variation between 'new' and 'old' is a function of the type of extrusion machine, the vibration method and mix design used.

HC3 incorporated a larger gravity load than HC1 and HC2, which included seismic live load and superimposed dead load (G&Qu&E load case). HC1 and HC2 tests included only self weight of the floor system.

3.3.1 Test Visual Performance Indicators

The HC3 seating connecting exhibited rupture of the interface between the hollowcore unit and seating beam at a drift of approximately 0.25%. The nature of the rupture and location was consistent with both HC1 and HC2 tests. At a drift level of -0.5% the width of the crack at the interface between the hollowcore unit and seating beam was approximately 2mm. Figure 3-17 illustrates the crack interface at -0.5% drift. It was noticed that no lateral cracking developed further into the topping of the floor system as in previous tests, suggesting delamination was not occurring and starter bar strains were likely concentrated at the crack interface.

Figure 3-17 HC3 crack interface at -0.5% drift

Significant spalling of the seating ledge was noticed from early drift levels and at a drift level of 1.0%, spalling resulted in the loss of instrumentation between the seating beam and hollowcore unit. At 1.0% drift the crack at the interface was approximately 5mm wide. Figure 3-18 illustrates the amount of spalling of the seating ledge during the 2.5% drift cycle; the interface gap behind the unit could clearly be seen from the underside of the unit. At a drift of 2.5% the south end of the unit had dropped approximately 15mm and the crack at the interface was approximately 15mm wide.

Figure 3-18 Seat spalling during test unit vertical slip initiated

Nearing -2.0% drift the unit had dropped significantly (in the order of 25mm) and seat spalling had resulted in the loss of the majority of the provided seating. At this point, three of the four starter bars ruptured and the unit lost vertical support and collapsed. Figure 3-19 shows specimen at 1.0%, 2.5%, and collapse at -2.0% drift.

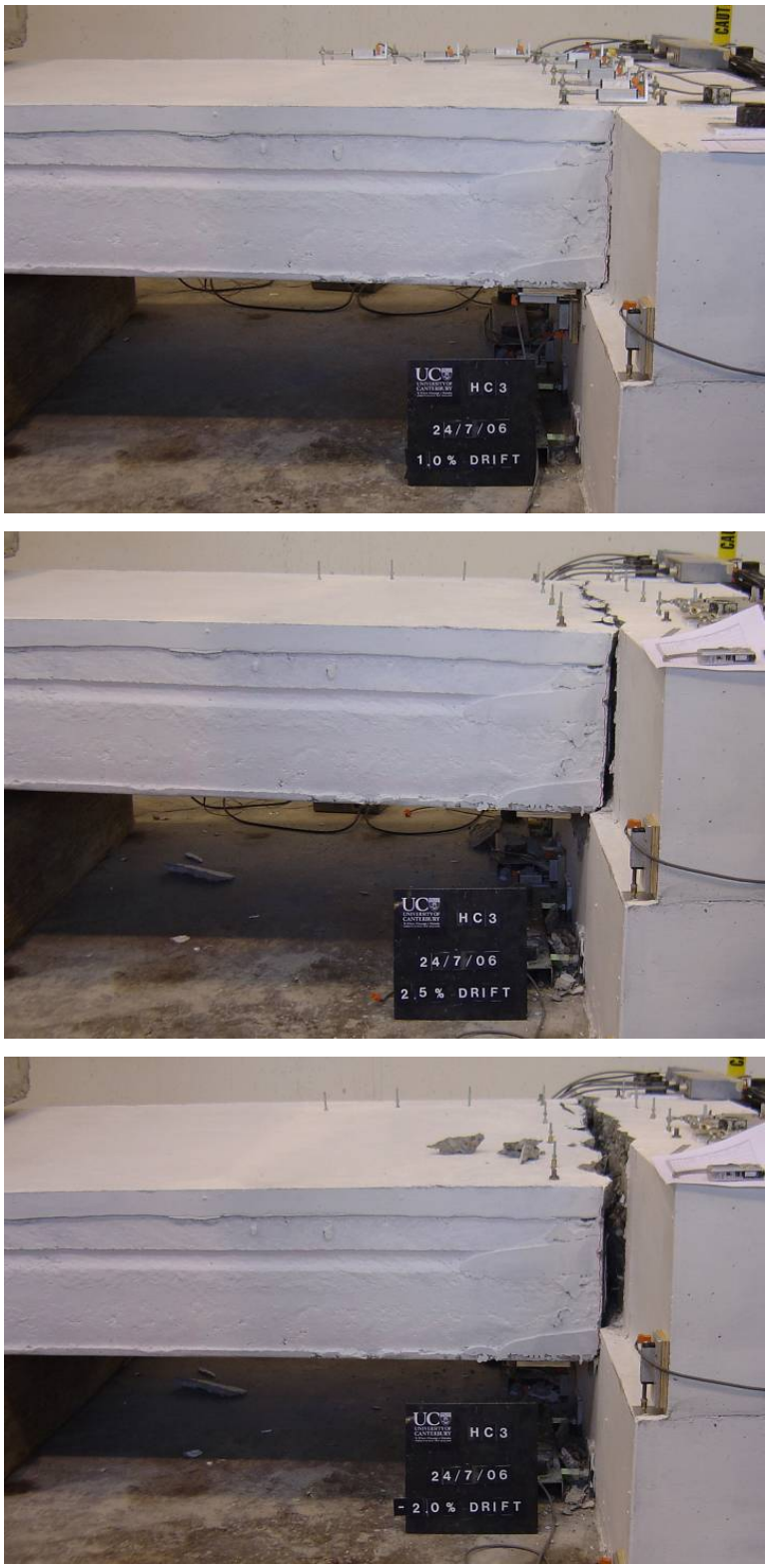

Figure 3-19 Failure sequence of HC3 Control Specimen

3.3.2 Post-Test Visual Performance Indicators

Figure 3-20 illustrates interface between the hollowcore unit and supporting beam following collapse. The regions shaded blue in Figure 3-20 b) highlight the three ruptured starter bars, while the fourth is intact. It was observed during the test that loss of vertical support and collapse coincided with the rupturing of the starter bars. It was likely the starter bars were providing significant vertical support as there was no evidence of delamination. The absence of delamination also likely resulted in strain demand in the starter bars being confined to the crack at the interface, therefore leading to rupture of the starter bars at lower drifts than in the previous tests that exhibited varying degrees of delamination.

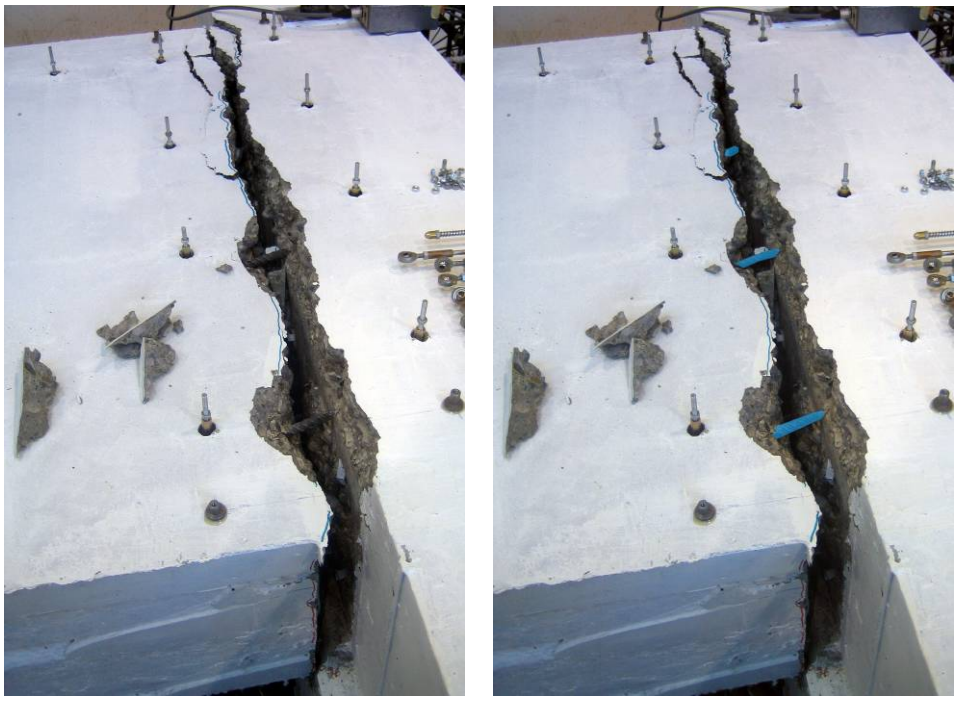

a) Seating beam interface

b) Seating beam interface – ruptured starter bars highlighted

Figure 3-20 Ruptured starter bars

Figure 3-21 shows the exposed interface of the seating beam interface and end of the unit, Figure 3-21 c) and d) illustrate regions of the trapped unit (shaded in green) and seat spalling (shaded in red). The boundaries of the two shaded regions meet the full length of the seating connection, demonstrating the lack of horizontal seating ledge. The crack interface shows the ruptured concrete stubs consistent with HC1 and HC2 tests.

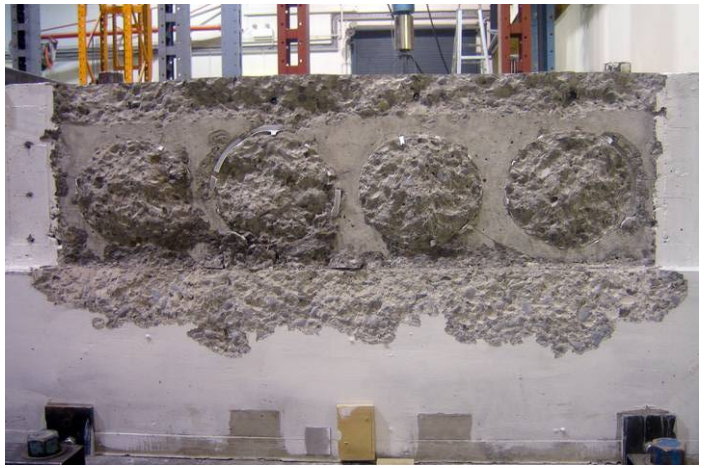

a) Exposed seating beam

b) Exposed hollowcore unit end

c) Exposed seating beam – critical regions highlighted

d) Exposed hollowcore unit end – critical regions highlighted

Figure 3-21 Damage mechanism and failure surfaces HC3

Figure 3-21 b) and d) illustrate the observed absence of any topping delamination where there is no gap or crack observed between the hollowcore unit and topping. Topping delamination of varying degrees was observed in both HC1 and HC2. This suggested that either the higher strength of the topping concrete or the dry cement rich nature of the 'old' hollowcore unit resulted in the prevention of starter bar strain penetration and delamination.

3.3.3 Instrumental Performance Indicators

Figure 3-22 shows the vertical, horizontal (elongation) and the combined net moment versus rotation relationships for the seating connection. The observed hysteretic behaviour was consistent with HC1 and HC2. High initial stiffness and rupture of the interface between the hollowcore unit and seating beam was observed at a drift of approximately +0.25%. A peak moment of approximately 110kNm was reached (under positive drift); this was in the order of 75% greater then HC1 and HC2. This was probably due to the higher concrete strength of the seating ledge and the 'old' hollowcore unit when compared with HC1 and HC2 specimens. There is also a possibility that the increased gravity load contributed to the increase in flexural strength of the seating connection.

No stiff, elastic, negative drift cycle was observed due to the omission of the 0.25% drift cycle from the loading protocol. As a result, rupture occurred in the first positive drift push. The residual and peak negative moments were extremely skewed due to shift in gravity load described earlier. The larger gravity load amplified this offset. Figure 3-22 a) shows positive elongation moment at higher drift levels as previously stretched starter bars were compressed.

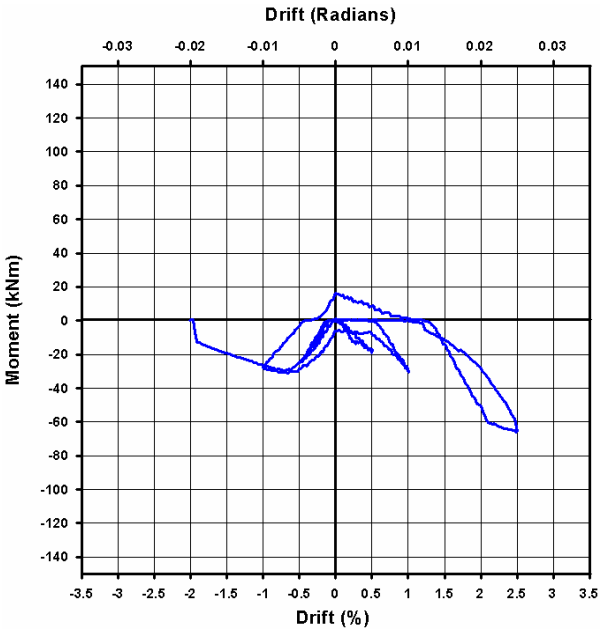

a) Horizontal elongation induced moment versus rotation

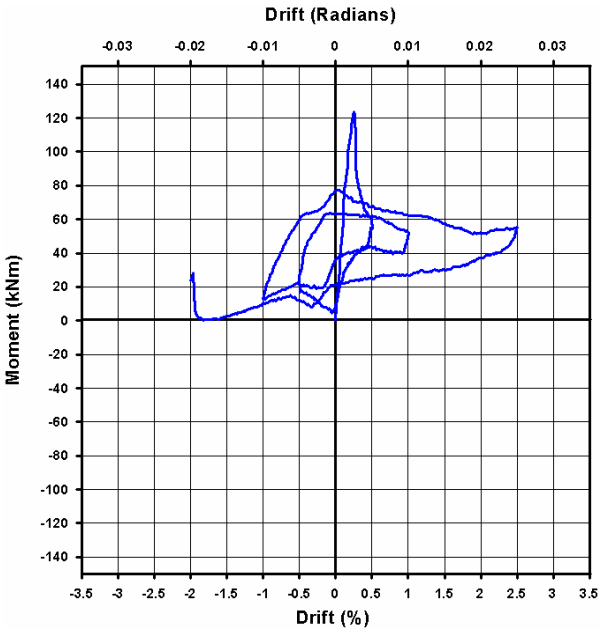

b) Vertical drift induced moment versus rotation

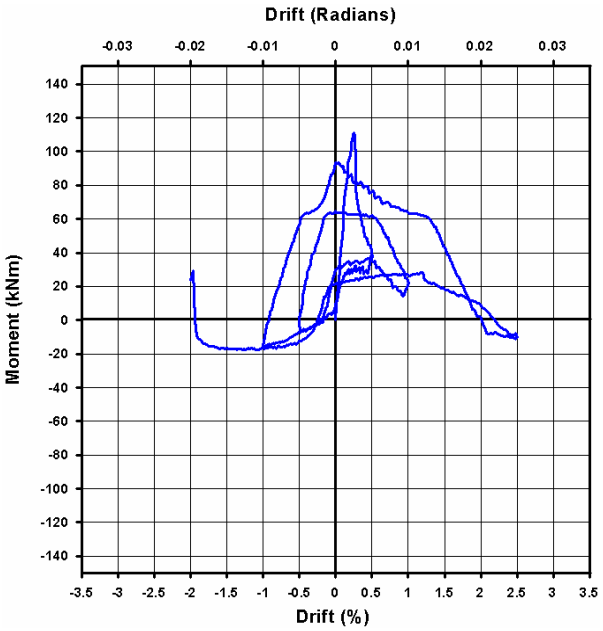

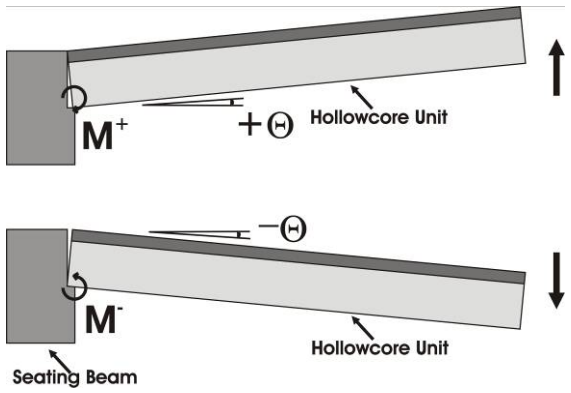

c) Net moment versus rotation

Figure 3-22 HC3 Moment versus rotation relationships

Figure 3-23 shows the average starter bar strain across the cracked interface between the hollowcore unit and seating beam. HC3 shows much higher levels of strain at the same drift levels than were exhibited by HC1 and HC2. This confirms the observation of lack of topping delamination and strain penetration, resulting in strain concentration at the cracked

interface between the hollowcore unit and seating beam. At 1.0% drift, HC1 and HC2 had strain values of approximately 20,000 microstrain, compared with approximately 40,000 microstrain for HC3 (twice that of the HC1 and HC2). Given these higher strain levels it makes sense that the starter bars ruptured much earlier than in HC1 and HC2.

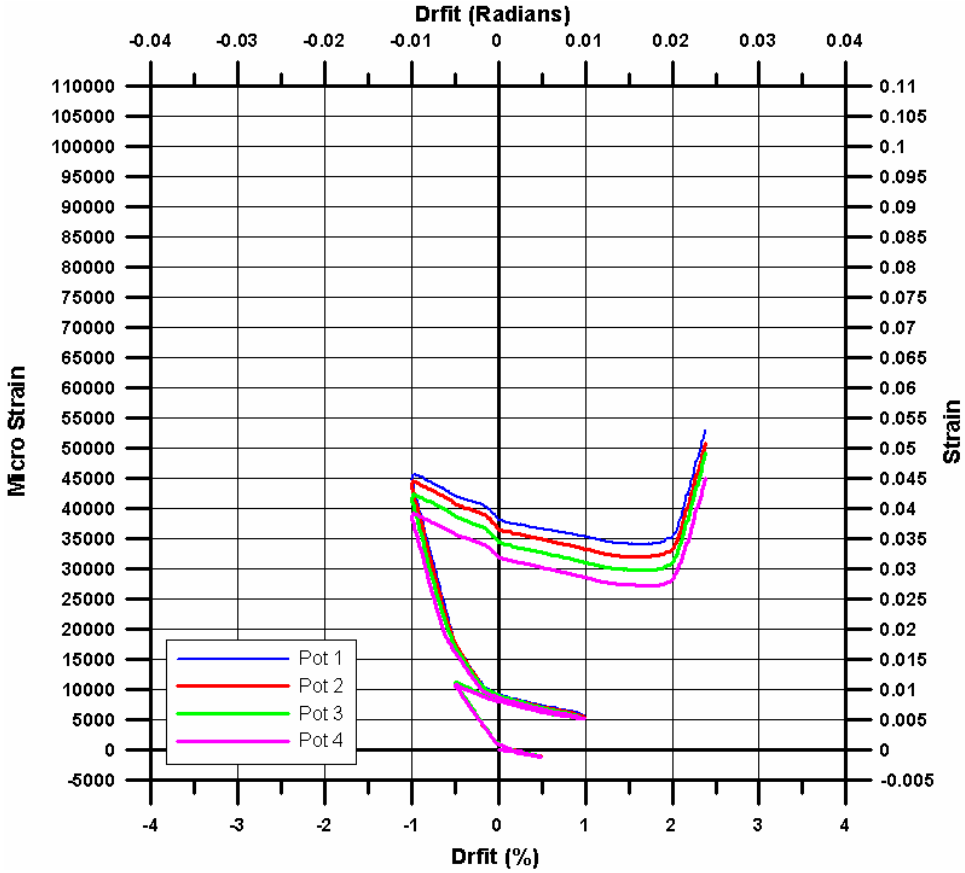

Figure 3-23 HC3 average starter bar strain determined using potentiometers

Strain values measured using strain gauges along the length of the starter bars also show very small strain levels (shown Appendix B). This again confirms the limited amount of strain penetration and increased strain concentration at the hollowcore to seating beam interface.

Figure 3-24 shows the desired ('T') and measured ('M') end profile of the hollowcore unit at peak drift levels up until instrumentation was removed (2.5% drift).. As with HC1 and HC3 some elongation slack and good vertical drift agreement was observed in the system. However, in the HC3 test, instrumentation was maintained to a higher drift than HC1 and HC2. The desired and measured displacement profile at 2.5% shows the lessening influence of the elongation slack once higher drifts (and larger elongations) are imposed in the system.

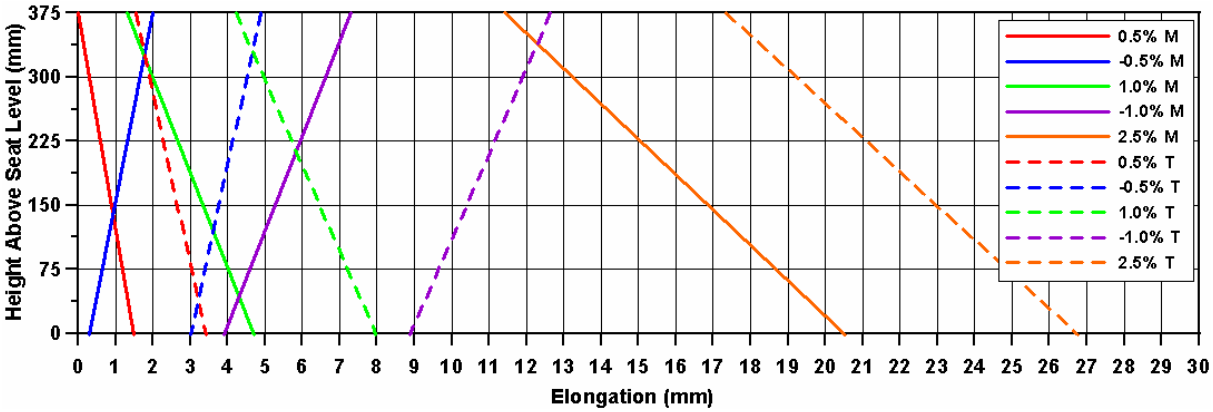

Figure 3-24 HC3 hollowcore unit end displacement profile

3.3.4 Key Implications of Connection Performance

The failure of this seating connection exhibited very similar characteristics to HC1 and HC2 tests. These characteristics include: early cracking of the interface between the hollowcore unit and seating beam, rupturing of the concrete stubs cast in the end of the unit, substantial spalling of the seating ledge and trapped portions of the soffit of the hollowcore unit in the seating region.

The concrete strength of the seating, stubs and topping was higher for the HC3 specimen than for the HC1 and HC2 specimens. As a result, a higher flexural strength, at the point of rupture, was achieved and was very close to the theoretical strength of the hollowcore unit itself. This confirmed the hierarchy of strength of typical existing seating connections is a function of the relative strengths of the seating, concrete stubs, topping and the hollowcore unit itself. This further suggests that bare concrete ledges can provide sufficient soffit restraint to induce flexure-shear failure in the hollowcore unit.

A large amount of spalling of the seating ledge was observed, which protruded further into the provided seating ledge than was observed in HC1 and HC2. The increased gravity load most likely increased the vertical stresses in the unreinforced seating ledge and promoted spalling. In addition, the concrete strength of the seating ledge was higher than HC1 and HC2 which resulted in significantly more spalling of larger concrete segments. This was in contrast to the more ‘crumbly’ spalling exhibited by weaker concrete seating ledges of the HC1 and HC2 specimens.

In the absence of topping delamination, strain penetration was limited and resulted in significant concentration of strain demand at the interface between the hollowcore unit and supporting seating beam. This lead to rupture of the starter bars, suggesting starter bars should not be relied upon for vertical support of hollowcore floor systems. This also suggests that some delamination could be beneficial in terms of maintaining the action of the floor acting as a diaphragm (transferring forces to and from the lateral force resisting systems).

3.4 Bull and Matthews (2003) Equivalent Sub-Assembly Test

In a series of sub-assembly tests carried out by Bull and Matthews (2003) a seating connection test was carried out which was very similar in nature to the details in HC1, HC2 and HC3 (without 'pull-off' effects). Figure 3-25 illustrates the seating connection detail tested by Bull and Matthews (2003). The main variation was the use of a mortar bed on the seating ledge, where a bare concrete ledge was used in this investigation.

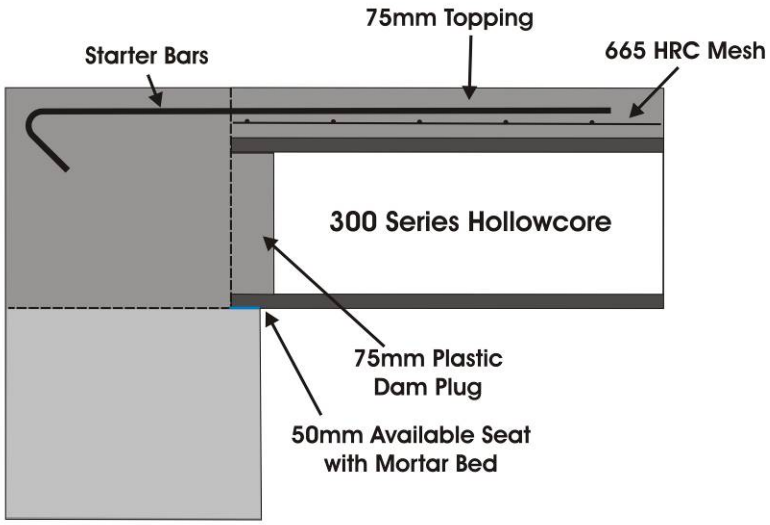

Figure 3-25 HC1 seating connection specimen from Bull and Matthews (2003)

The observed failure in this test was a flexure-shear failure in the hollowcore unit, consistent with Matthews' (2004) super assembly specimen with the same seating connection details. For comparison the failure mechanism is shown in Figure 3-26.

a) Photo of flexure shear failure mechanism from Bull and Matthews (2003)

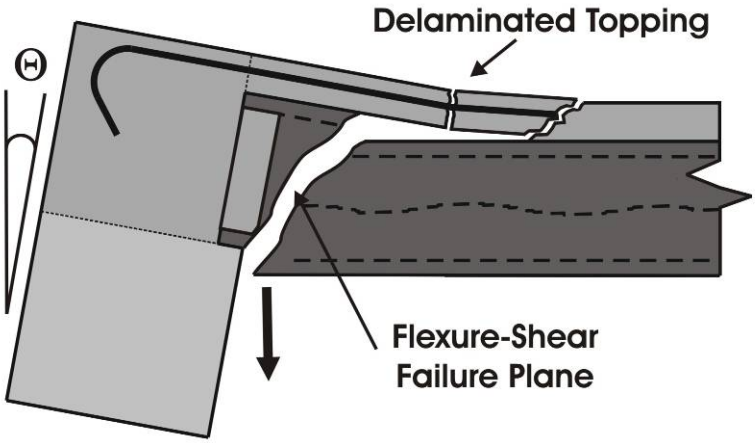

b) Flexure shear schematic after Matthews (2004)

Figure 3-26 Flexure shear failure mechanism from Bull and Matthews (2003) and Matthews (2004)

The moment versus rotation hysteretic behaviour of the Bull and Matthews (2003) connection in Figure 3-27 shows the peak strength of approximately 68kNm. This was lower than all peak strengths reached by seating connections in this investigation (70kNm, 85kNm and 110kNm for HC1, HC2 and HC3 respectively).

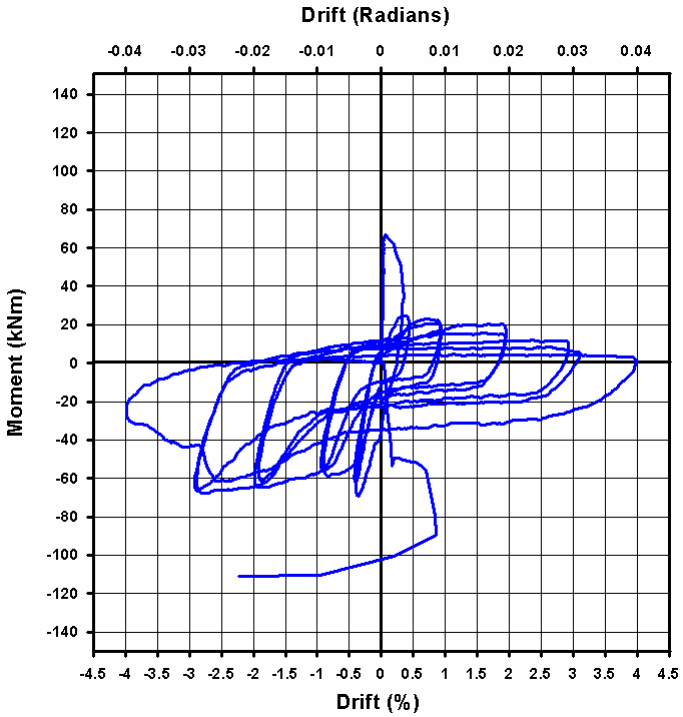

Figure 3-27 Moment versus rotation behaviour for Bull and Matthews (2003) seating connection

3.5 Conclusions

A common behavioural mechanism was observed in all three benchmark tests of existing seating connections. All specimens had relatively high initial stiffness, followed by sudden rupture of the interface between the hollowcore unit and supporting beam. This rupture acted as a release mechanism for the drift induced forces imposed on the hollowcore unit, and accommodated the rotation of the floor system relative to the seating beam. For two of these connections the nature of this behaviour resulted in loss of seating and collapse under the prescribed drift and elongation demands. The failure mechanism that resulted in loss of seating (loss of gravity support) of the hollowcore unit varied from the previously observed flexure-shear failure mechanism in the hollowcore unit (Bull and Matthews 2003; Matthews 2004).

The variation in failure mechanism between this and previous investigations can be explained by an increase in strength of the hollowcore units between the tests. All peak strengths in HC1, HC2 and HC3 in this investigation were higher than that reached by Bull and Matthews (2003). HC3 reached a flexural strength of 110kNm, approximately 75% greater than the 68kNm peak of Bull and Matthews (2003). The higher peak strengths achieved in HC1, HC2 and HC3 compared with that of the Bull and Matthews (2003) test, suggests that a bare concrete seating ledge can produce a degree of fixity sufficient enough to induce a

flexure-shear failure in the hollowcore unit. This suggests the mortar bedding material used by Bull and Matthews (2003) did not contribute significantly to the seating connection fixity, as previously thought.

The loss of seating failure illustrated a number of individual detailing aspects contributed to the failure mechanism. These included: substantial spalling of the seating ledge, trapped portions of the soffit of the hollowcore unit, delamination of the *in-situ* topping, and rupturing of starter bars.

A combination of spalled seating ledge and trapped soffit of the hollowcore unit negated any provided horizontal seating ledge, forming a near-vertical failure surface behind the end of the hollowcore unit (the interface between the hollowcore unit and supporting beam). Following rupture at this interface, the floor system was supported by a combination of friction and interlock at the damaged interface. Additional support was provided by the starter bars at in combination with the topping in the absence to topping delamination prior to rupture. As a result, the elongation required to induce loss of seating was substantially less than the length of the provided seating ledge (in the case of the HC3 specimen, this occurred under approximately 20mm of elongation, significantly less than the provided setting ledge length of 50mm). Due to the relatively early loss of the intended mechanism for gravity support of the hollowcore unit, that is the concrete seating ledge, a higher gravity demand was placed on bond between the *in-situ* topping and hollowcore unit. This increased the potential for topping delamination and starter bar rupture, depending on the amount of strain penetration along the starter bars.

Excess positive fixity (unit soffit restrained from pulling away from the seating beam) was a preconceived weakness in existing hollowcore seating connections. The elements which contributed to positive connection strength were the strength and length of the unreinforced concrete seating ledge and *in-situ* concrete stubs cast in the end of the unit. The positive connection strength was seen to be governed by the concrete tensile strength of the two elements. This resulted in an unpredictable overall connection hierarchy of strength, governing the location of the failure which potentially can be either behind the hollowcore unit or in the hollowcore unit itself. Should the restraint from the unit soffit and stubs exceed the strength of the unreinforced end of the hollowcore unit, a failure in the hollowcore unit itself, as highlighted by Matthews (2004) would result. Connection strength in the negative

direction was seen to be substantially less due to the absence of soffit restraint. Negative rotation of the floor system resulted in a more ductile response due to the presence of topping reinforcement (starter bars).

In the absence of topping delamination, high strain levels were induced into the topping starter bars. This was due to the combination of elongation and rotation demand. For this reason topping delamination in connection regions can be beneficial in limiting strain concentration in the starter bars at the interface between the hollowcore units and supporting beam due to strain penetration. As a result, a ductile link develops which is capable of transferring lateral floor diaphragm forces to and between the seismic resisting systems results. This is ideal as lateral force transfer is the fundamental purpose of the combined topping and starter bars in a precast floor system. Starter bars should not be used for providing vertical support in retrofit applications, or assumed to contribute vertical support for existing seating connections though the bond between the topping to hollowcore unit.

3.6 References

Bull D.K, Matthews J.G, 2003, *Proof of concept tests for hollow-core floor unit connections*, Precast NZ report, Feb 2003.

Matthews J.G, 2004, *Hollow-core floor slab performance following a severe earthquake*, PhD Thesis, Department of Civil Engineering, University of Canterbury, Christchurch, New Zealand.

4 Experimental Hollowcore Seating Connection Seismic Behaviour and Assessment Issues

Based on the performance of tests of existing seating connections in this investigation and previous investigations, (Matthews 2004; Bull and Matthews 2003; and Liew 2004) a summary of the performance of typical existing seating connection details was developed. From this database primary failure mechanisms and secondary performance issues for existing hollowcore floor seating connections were identified. This section outlines the primary failure mechanisms and contributing factors associated with the respective seating connection details. Secondary issues associated with the primary failure mechanisms, which can affect general diaphragm seismic performance are also highlighted.

The reason for categorising potential primary failure mechanisms was to later develop a suite of retrofit approaches which target the identified deficiencies. Discussion is given in context to existing seating connections prior to Matthews' (2004) super-assembly test and common practice at the time, no reference was intended to current practice.

4.1 Primary Failure Mechanisms

Three potential primary failure mechanisms have been identified. Primary failure mechanisms can result in loss of vertical support of individual hollowcore units, entire bays of hollowcore units, and potentially a number of floors in a 'pancake' type failure. These failure mechanisms stem from the intrinsic properties of the supporting lateral force resisting frame (in this case a ductile reinforced concrete (RC) seismic frame) being imposed on the floor system through the rigid, monolithic connections linking the floor and frame systems. In terms of the vertical support providing seating connection, the two frame properties of most concern are the 'pull-off' effect from beam elongation (of beams running parallel to one-way the floor system) and rotation of the supporting (seating) beam relative to the floor system. These frame deformations conflict with, and jeopardise, the structural integrity of hollowcore floor system through the initiation of the primary failure mechanisms. In general the primary failure mechanisms are further promoted by both the unreinforced brittle nature of the hollowcore units and the inability of the general seating connections to accommodate combined cyclic rotation and elongation demand.

Specific structural details of a seating connection can govern what failure mechanism the connection is most susceptible to. The predominant details are the strength of the hollowcore unit, the strength and length of the provided seating ledge, the presence of core tie reinforcement, and the strength of the *in-situ* concrete end stubs and topping concrete.

4.1.1 Loss of Seating (LOSD and LOS)

Loss of seating is associated directly with deficiencies in the detailing of the existing seating connections. The critical connection deficiencies are: insufficient provided seating length and seating ledges consisting of unreinforced cover concrete (of the supporting seating beam). The provided seating length deficiency is often a result of, or worsened by, tolerances associated with construction practice. Loss of seating is an inevitable result for seating connections which are deficient in length of seating, should enough elongation 'pull-off' be imposed on the floor system, regardless of the type of precast flooring unit.

Tests in this investigation found the susceptibility of existing seating connections to loss of seating was heightened due to the combination of trapped portions of the hollowcore unit soffit and spalling of the seating ledge. This resulted in a continuous near vertical failure surface between the hollowcore unit and seating beam, which negated the vertical support provided by the seating ledge, as illustrated in Figure 4-1. Following this rupture, vertical support of the hollowcore unit was provided by interlock and friction on the near vertical failure surface. Contribution to the vertical support was seen in the absence of topping delamination in some cases; however this should not be relied upon. Therefore the elongation required to induce loss of seating was much less than the initial provided seating length. The potential for loss of seating is higher in the absence of core tie reinforcement because the bond between *in-situ* topping and hollowcore unit and starter bars can not be relied upon to provide vertical support.

Loss of seating was observed in two of the three sub-assembly tests carried out in this investigation. Two variants of loss of seating were observed, namely loss of seating with and without delamination of the *in-situ* topping, termed LOSD and LOS respectively. In the case of topping delamination, strain demand was distributed further along the starter bars due to strain penetration, and rupture of the starter bars was prevented. In the absence of strain penetration, rupture of the starter bars was induced at the interface between the hollowcore unit and seating beam, at which point loss of support occurred. Figure 4-1 illustrates LOSD,

the near vertical failure plane negating any provided seating ledge as a result of trapped portions of hollowcore unit soffit and spalling of the seating ledge are shown in Figure 4-1 a) and Figure 4-1 b) respectively.

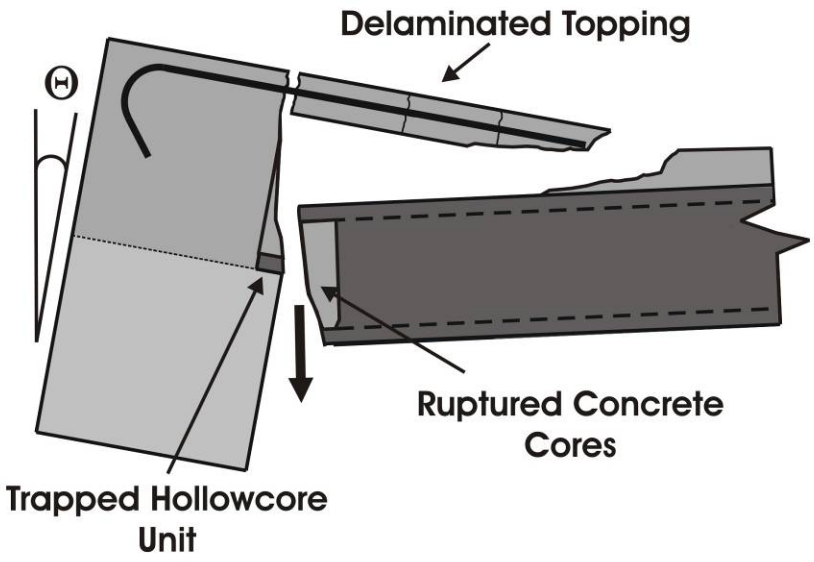

a) Trapped Hollowcore unit soffit

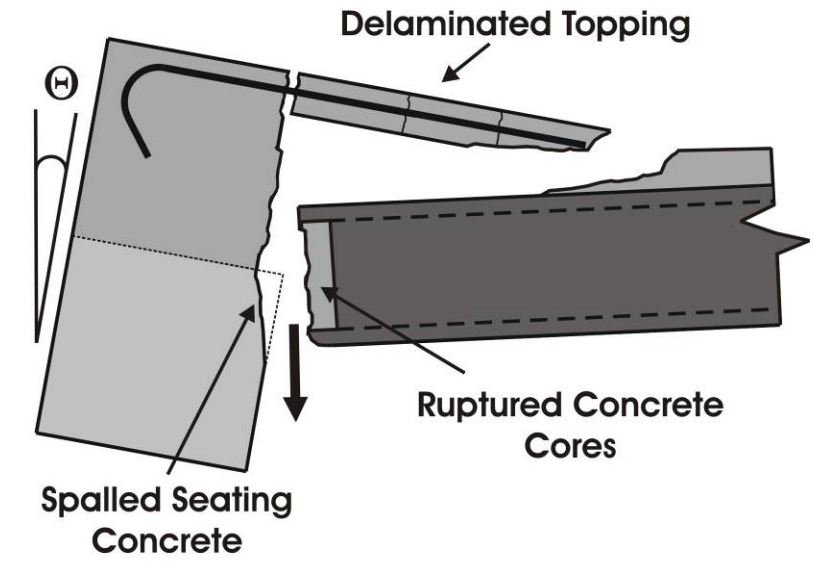

b) Spalled seating ledge concrete

Figure 4-1 LOSD primary failure mechanism with topping delamination

Figure 4-2 illustrates LOS (no topping delamination), resulting in rupture of the topping starter bars at the hollowcore unit to seating beam interface. As with LOSD, a combination of trapped portions of hollowcore unit soffit and spalled seating ledge along the length of seating

connection negated the provided seating ledge. Figure 4-2 a) and Figure 4-2 b) illustrate the trapped portions of hollowcore unit soffit and spalling of the seating ledge respectively.

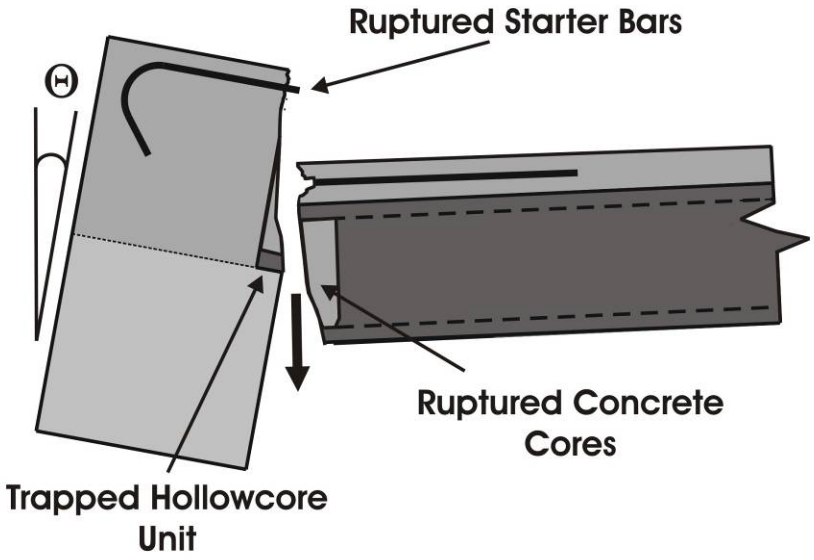

a) Trapped Hollowcore unit soffit

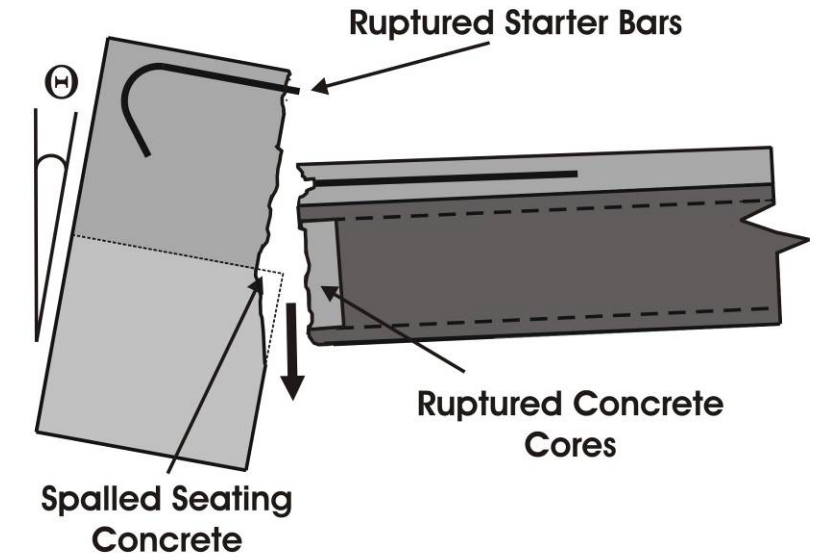

b) Spalled seating ledge concrete

Figure 4-2 LOS primary failure mechanism without topping delamination

Examining the LOSD and LOS failure mechanisms, it is clear there is a need to target two specific aspects of seating connections of this nature (seating deficient). The most important of these is to provide vertical support to prevent collapse of the floor system. The second target, taking a performance-based approach, is to prevent the trapping of the hollowcore unit

soffit and spalling of the seating ledge, protecting the structural integrity of the hollowcore unit and seating beam. This suggests a hierarchy of strength intervention is applicable, focusing attention on protecting the hollowcore unit by limiting or controlling the imposed frame deformations (and resulting forces) imposed on the floor system.

4.1.2 Flexure-Shear Failure (FSF)

Flexure-shear failure (FSF) is a direct result of the inability of the unreinforced hollowcore units to resist force actions imposed on the floor system by the rotation of the seating beam relative to the floor system. Force actions are transferred from the seating beam to the floor system due to fixity in the seating connection.

FSF results when overall connection fixity is sufficient enough to induce flexure and shear demand which exceeds the capacity of the hollowcore unit. Such a failure mechanism was identified by Matthews (2004) and Bull and Matthews (2003). It was suggested that the mortar bedding product used on the seating ledge in these tests resulted in excess fixity, contributing to the cause of the failure mechanism. However, the peak strengths achieved in control specimen tests in this investigation (seated on the bare concrete ledges) exceeded that of the peak strength seen by Bull and Matthews (2003). This suggests the strength of the hollowcore unit (specifically the concrete modulus of rupture, f_r) was the dominant behavioural variable between the tests.

The failure mechanism was termed flexure-shear as rupture in the hollowcore unit soffit at the face of the seating beam is initiated by flexural cracking, from which a shear failure is subsequently initiated. FSF is exhibited through diagonal cracking in the hollowcore unit, originating from the face of the seating beam and passing through the hollowcore unit as illustrated in Figure 4-3. The outcome of such a failure mechanism is loss of vertical support, with the same consequences as LOS.

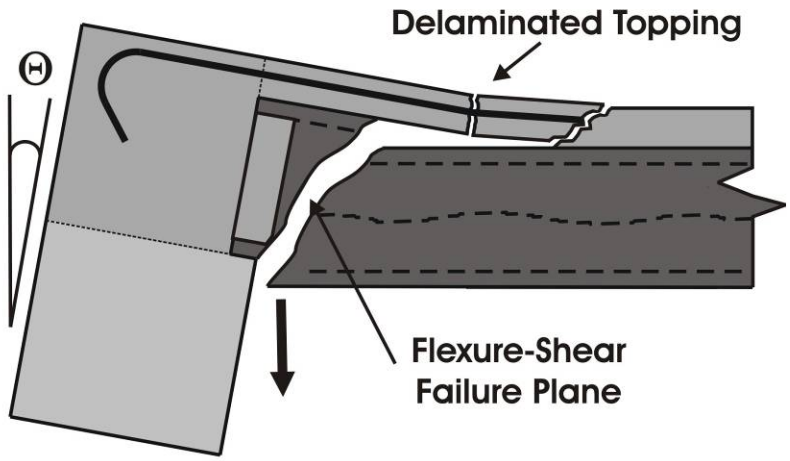

Figure 4-3 Flexure-Shear primary failure mechanism adapted from Matthews (2004)

Based on the observed FSF mechanism it can be seen that the risk of such a failure is heightened by the intrinsic properties of both the connection system and hollowcore unit. The rational behind existing seating connections results in unpredictable and often excess connection fixity. This is a result of the 'keyed-in' nature of the connection by surrounding concrete elements, particularly restraint on the hollowcore unit soffit from the seating ledge, as illustrated in Figure 4-4. This suggests that the strength of the surrounding elements and seating ledge (including seating ledge length) are dominant variables which effect seating connection fixity. If additional core tie reinforcement is present, further fixity will result as discussed in section 4.1.3.

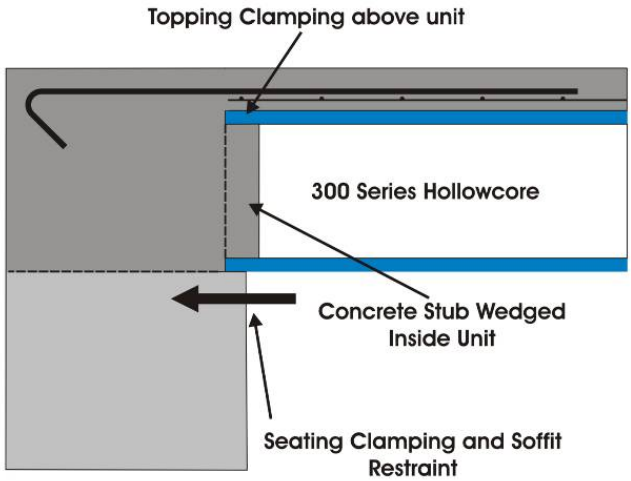

Figure 4-4 Excess fixity mechanism of typical existing seating connections

On the other side of the hierarchy of strength for the seating connection is the capacity of the floor system. Hollowcore units are designed under the assumption of a simply supported seating condition, which is clearly not the case, and with no provision of transverse reinforcement for shear resistance. Further, the rupture occurs well inside the development length of the prestressing tendons and, as a result, the design flexural strength of the hollowcore unit is not achieved in the critical region. This results in the flexural capacity of the hollowcore unit being governed by the strength of the concrete alone, which is significantly less than the full hollowcore unit capacity (including prestressing effects).

Further, the stress conditions at the seated end of a hollowcore unit are significantly disturbed due to the presence of prestressing reinforcement, creep and shrinkage effects, and stress flow associated with local bearing effects. These effects become particularly important given the passing of time, as in the case of existing seating connections (Herlihy 1999; Fenwick et al. 2004), which can be in the order of 10-20 years old. As a result, the shear capacity of such elements is unreliable and potentially lower than expected. Further, due to the absence of transverse reinforcement, the strength capacity of the hollowcore is governed largely by the strength to the concrete of the hollowcore units, which also can be highly variable.

Hollowcore units are susceptible to the both positive and negative flexure and the respective shear forces associated with the relative seating beam rotation imposed on the floor system (Matthews 2004; Bull and Matthews 2003; Fenwick et al 2004). The risk of FSF under these actions is higher if seating connection conditions result in either excess imposed demand on the floor system (excess overall connection flexural strength), or lower than expected hollowcore unit flexural capacity. In terms of FSF, focus of this investigation was given to positive moment demand (hollowcore unit soffit pulling away from the seating beam).This focus was driven by what had been observed experimentally (Matthews 2004; Bull and Matthews 2003). Also there is more potential for positive connection strengths to be excessive due to the restraint of the hollowcore unit soffit from the seating ledge. In Section 4.1.3 offset flexure-shear failure (OFSF) is discussed in terms of negative (hogging) moment demand.

The discussed critical structural deficiencies suggest that an appropriate retrofit approach to target the FSF mechanism is to isolate the hollowcore unit from the seating beam. Doing so

could modify the hierarchy of strength in a manner that would protect the floor system from imposed seating beam behaviour. Through creating a weak link at the interface between the hollowcore unit and seating beam the uncertainties associated with the extent of connection fixity and strength capacity of the hollowcore units could be negated. This is a favorable approach and conforms to the rational commonly held in earthquake engineering of dictating the failure mechanism and overall structural behavior under seismically imposed deformations.

4.1.3 Offset Flexure-Shear Failure (OFSF)

Offset flexure-shear failure (OFSF) is a specific case of a FSF when tie reinforcement is placed within the open cores at the end of the hollowcore unit and cast into the unit with the *in-situ* topping concrete. The OFSF mechanism was highlighted by tests carried out by Liew (2004). Such a connection detail is generally an unplanned variation during construction when seating is deficient as a result of construction tolerances. Critical tolerances include the length of the hollowcore units (affected by creep, shrinkage and cutting tolerances), and tolerances associated with the seating beams the units span between. When seating was deficient, it was common practice (prior to Amendment 3 of NZS3101:1995 in 2004) to prop the hollowcore units, cut open the cores in the connection region, place reinforcement in the cores which is tied into the seating beam and fill the cores when the topping concrete was poured. Such a technique was also used when no seating was available, termed 'negative seating' by participants on the construction industry.

Normally seated and negatively seated hollowcore units that had cores reinforced with bars and in-filled with concrete were tested by Liew (2004). In the case of OFSF it was observed that the flexure rupture occurred under negative seating beam rotation (top of the hollowcore unit in tension) induced hogging moments (Liew 2004). This contrasted with the positive flexure (tension in the hollowcore unit soffit) induced rupture observed by Matthews (2004). This may be explained, as the offset of the rupture surface resulted in shifting the critical region along the hollowcore unit, well into (if not beyond) the development length of the prestressing tendons. As a result, the hollowcore unit has developed sufficient positive (sagging) design moment capacity. However, the hollowcore unit is still susceptible to negative flexure due to the design assumption of simply supported end seating conditions. Fenwick et al (2004) also highlighted the potential for flexure-shear failure as a result of

negative (hogging) moments of this nature. Seated and negative seated OFSF failure mechanisms are illustrated in Figure 4-5 respectively.

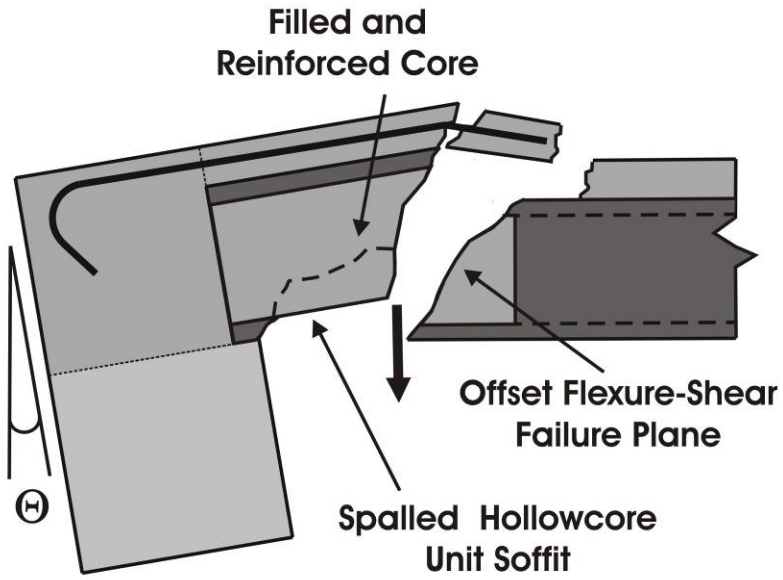

a) Seating deficient

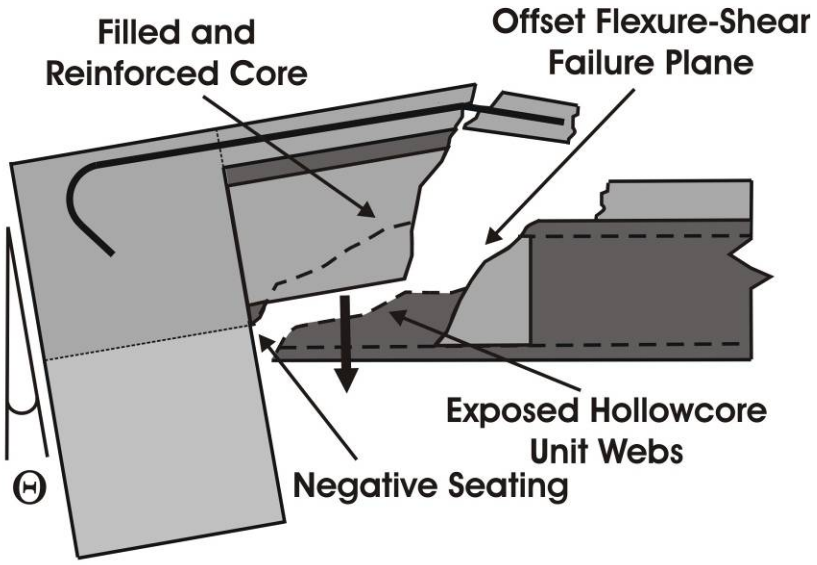

b) negative seating

Figure 4-5 Offset Flexure-Shear primary failure mechanism adapted from Liew (2004)

The aim of this connection modification was to bridge between the seating beam and hollowcore unit, providing vertical support to the floor system. What resulted was a rigid link between the seating beam and hollowcore unit which offset the failure plane out along the

hollowcore unit by the length of the reinforced, concrete unfilled section of the hollowcore unit.

In terms of retrofit approaches for OFSF failure, it can be seen intervention is needed at the interface between the hollowcore unit and seating beam to eliminate the effect of the rigid link and to provide additional seating. This suggests a combined approach from LOS and FSF mechanisms would be suitable. The difficult task is identifying connections which would be susceptible to OFSF failure as it is unlikely that there will be obvious external indication as to whether the cores are filled or not.

4.2 Secondary Performance Issues

In addition to the primary failure mechanisms, there are also secondary performance issues associated with existing seating connections. These issues have been termed secondary because they concern general hollowcore floor diaphragm behaviour rather than specifically loss of support at the seating connection. These issues include vertical displacement incompatibility along the longitudinal perimeter connection, longitudinal web splitting of the hollowcore unit, and delamination of the *in-situ* topping from the hollowcore unit.

4.2.1 Vertical Displacement Incompatibility

Vertical displacement incompatibility is a problem associated primarily with the two outside units (units further into the floor system are also potentially affected) of the floor system, directly adjacent to longitudinal perimeter beams. This problem is due to the outside units being fixed to both seating and longitudinal perimeter connections by topping starter bars. Previous research has shown seating connection behaviour can affect the extent of incompatibility along the longitudinal connection and resulting level of damage (Taylor 2004; MacPherson 2005). Vertical displacement incompatibility occurs due to the differing deformation modes of the frame and floor systems. Frame beams deform in double curvature, and the adjacent hollowcore unit acts in a near simply supported manner (seating connection dependant), deforming in single curvature (as illustrated in Figure 4-6). The hollowcore units are forced to deform with the frame beams due to the continuous monolithic connection between the two systems. The hollowcore units are not designed for such actions (Matthews 2004). Significant damage to the hollowcore unit can result in the form of web splitting in the hollowcore units and topping delamination.

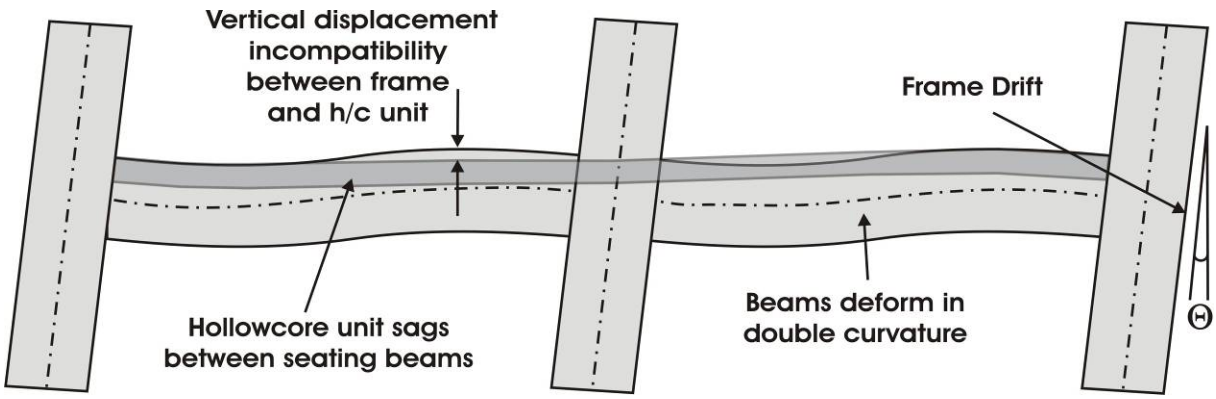

Figure 4-6 Vertical displacement incompatibility after Matthews (2004)

Retrofitting of such a secondary failure mechanism was not the focus of this investigation. This discussion was given only to highlight the interaction with primary failure mechanisms of the seating connections and to generate a broader perspective of how global behavior can be influenced by seating connection behavior.

4.2.2 Longitudinal Web Splitting

Longitudinal splitting of the hollowcore unit webs has been seen to result in the separation and collapse of the bottom half of individual hollowcore units (Matthews 2004). This is of most concern for hollowcore units directly adjacent to longitudinal perimeter frames. Vertical displacement incompatibility actions are the primary contributor to longitudinal web splitting. Figure 4-7 illustrates the extent of web splitting in Matthews (2004) super-assembly test, the unit pictured is directly adjacent to the longitudinal perimeter frame.

Figure 4-7 Web splitting of hollowcore unit adjacent to longitudinal perimeter connection observed by Matthews (2004)

The behaviour at the seating connection, particularly the presence of *in-situ* concrete stubs, can potentially initiate this splitting at the seated ends of the hollowcore units (Fenwick et al. 2004). This is a concern as the separated portion of the hollowcore unit drops onto the floor below, causing danger to building inhabitants and the floor system below. Isolating the floor system from the seating beam (previously suggested as an approach to target primary failure mechanisms) could potentially mitigate the contribution of the seating connection rotation to longitudinal web splitting.

4.2.3 Topping Delamination

Topping delamination is a result of rotation, elongation and vertical displacement incompatibilities at seating and longitudinal perimeter connection regions. Delamination occurs because of the inelastic behaviour in connection regions, specifically tensile strain penetration in topping starter bar reinforcement, breaking the bond between hollowcore units and cast *in-situ* topping (Herlihy 1999; Matthews 2004). It has previously been recognised that bonding of the topping to the hollowcore units should not be relied upon to provide vertical support of the floor system. With this in mind, topping delamination can be seen as beneficial for overall diaphragm performance. The reason for this is that delamination

reduces strain concentration in starter bars through strain penetration that would otherwise occur at the interface between the hollowcore unit and supporting beam, thereby helping prevent rupture of the starter bars. This effectively creates a ductile link between the floor diaphragm and seismic resisting frame system. This is beneficial in maintaining floor diaphragm force transfer to and between lateral force resisting systems.

4.3 Assessment of Existing Seating Connections

Experimental tests carried out representing existing seating connections have shown that seating connection performance is sensitive to the individual seating connection details. The most significant details are the seating length, presence and nature of core reinforcement and the strength of the concrete forming the individual elements such as the seating ledge, *in-situ* topping and concrete core stubs.

The biggest challenge faced in assessing the nature of individual detailing aspects is the existing nature of the connection. This is a result of a number of factors: the details are likely to vary from specified plans due to construction tolerances, in extreme cases changes may be made to the planned connection details during the construction process (placement of core tie reinforcement when units are short), and the majority of important aspects or detailing are hidden.

4.3.1 Existing Seating Ledge

The existing seating length is potentially one of the most important attributes to identify in the seismic assessment of existing hollowcore seating connections. This is because the available seating length has a significant influence on the likely primary failure mechanism. If seating is seen to be deficient, loss of seating is more likely, and if seating is not deficient flexure-shear failure (FSF) is more likely. In cases where seating is seen to be extremely deficient or even have negative seating (as discussed in Section 4.1.3) the likelihood that the cores were reinforced upon placement is higher, therefore suggesting offset flexure-shear failure (OFSF) is more likely. However, there are significant complications associated with what failure mechanism a specific connection is most susceptible to. The most significant of these is the strength and quality of the hollowcore unit itself. Theoretically, even seating deficient seating connections can result in FSF if the strength (and quality) of the hollowcore unit is low enough. For this reason the use of intervention at the interface between the

hollowcore unit and the seating beam is attractive, as this uncertainty over the hollowcore unit flexural strength can be negated.

In order to identify whether a seating connection is deficient in seating ledge length, the provided seating should firstly be compared with current code requirements. In addition to this, some consideration of the expected amount of beam elongation should be made. Estimating the amount of elongation accurately is a difficult task due to the lack of theoretical methods available which are simple enough to be used in practice. For the purpose of seating connection assessment, the most appropriate estimation is to use simple relationships based on the depths of the beams in the lateral frame system. The suggested typical overall elongation values are in the order of 2-4% of the beam depth per contributing plastic hinge (Fenwick and Megget 1993; Restrepo et al 1993). The upper bound of 4% should be used to be conservative. The suggested simple distribution of the number of contributing plastic hinges to beam elongation 'pull-off' on individual seating connections is illustrated in Figure 4-8.

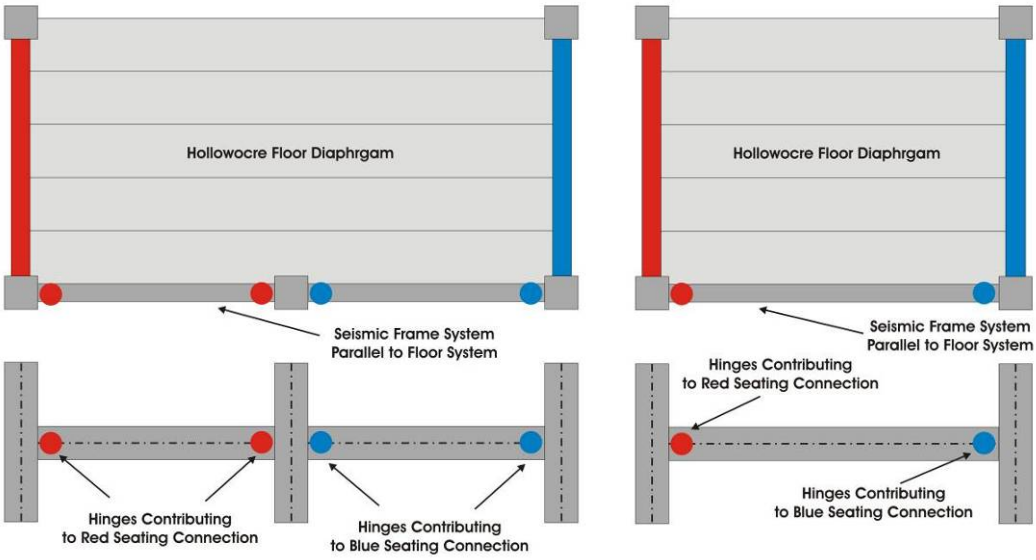

a) Floor system spans two frame bays **b) Floor system spans one frame bay**

Figure 4-8 Plastic hinge contribution to beam elongation 'pull-off' on a hollowcore floor system seating connections

It is thought that some indication of the provided seating length can be ascertained through inspection of the underside of the seating connection. In regions between units, and around the ends of units, it is likely topping and half beam concrete has not completely penetrated to

the face of the seating beam, therefore giving some indication as to the seating length. In the case of negative seating it might be possible see where the hollowcore unit end terminates against the *in-situ* beam concrete away from the face of the seating beam.

4.3.2 Presence of Core Reinforcement

The presence of core reinforcement is a unique variation of typical existing seating connections. Such a detail is directly associated with the offset flexure-shear failure mechanism (OFSF). The problem with such a detail is the difficulty in recognising the presence of filled and reinforced cores which are concealed.

The seating ledge length can however give an initial indication of the presence of core reinforcement. Common practice was to reinforce cores when seating was deficient upon placement of the hollowcore units. Therefore if little or no seating is observed it is likely that at least every second core of the hollowcore unit is reinforced. A suggested method to further identify reinforced cores is to drill small investigation holes through into the cores to determine whether cores are filled or not.

4.3.3 Strength of Individual Connection Elements

The strength of the hollowcore unit and surrounding concrete elements which make up the seating connection can have a significant influence on the likely failure mechanism. The strength of the hollowcore unit compared with that of the surrounding elements determines where the initial rupture occurs. If the hollowcore unit strength is insufficient (or conversely overall connection strength excessive), rupture would occur in the hollowcore unit itself (FSF and OFSF); alternatively if the hollowcore unit strength exceeds the over all connection strength then loss of support would occur (as was observed in this investigation, HC1 and HC3 specimens). Therefore the strength of the concrete used in the hollowcore units becomes important. This is because the critical region is within the provided seating length from the end of the hollowcore unit, well inside the development length of the prestressing reinforcement. As a result, the flexural strength is largely governed by the modulus of rupture of the concrete (f_r). An exception to this is when the cores are over-reinforced and filled (OFSF) where the failure plane is offset from the face of the seating beam and negative strength demand is the critical case.

The inability to determine these *in-situ* strengths generates significant uncertainty regarding the failure mechanism which is most likely to occur. This further supports the approach to intervene in the connection hierarchy of strength and isolate the hollowcore unit from the imposed seating beam deformations.

4.3.4 Assessment of Expected Rotation of the Seating Beam

The assessment of the expected rotation of the seating beam relative to the floor system, which is a function of frame inter-storey drift, is an important aspect of the seismic assessment of existing hollowcore seating connections. The rotation of the seating beam has been identified as one of the major damage causing mechanisms for existing seating connections (Matthews 2004).

Experimental tests in this and previous investigations (Matthews 2004; Bull and Matthews 2003; Liew 2004) highlighted the early onset of primary failure mechanisms through rupturing of either the hollowcore unit (FSF and OFSF) or the interface between the hollowcore unit and seating beam (LOSD and LOS). The relative rotation between the seating beam and floor system at which this occurs is in the order of 0.2-0.30%. This rotation is well under typical frame design level drifts (approx 2.5% based on code limits (NZS 1170.5:2004)), and even typical frame yield drifts of approximately 0.5%. This suggests there is a high probability of rupture occurring in existing seating connections even under low seismic intensity. Following initial rupture, further connection damage is primarily elongation induced. Due to this, an upper bound elongation value is the most important seismic assessment demand variable. For this reason the number and magnitude of seating beam rotation cycles becomes important. This is because these factors control the magnitude of beam elongation, and the resulting 'pull-off' imposed on the floor system.

A possible approach to account of beam elongation is to develop a frame drift profile using non-linear time history analysis and using theory discussed in Section 7 to estimate a loading dependant (plastic hinge rotation) elongation profile. Alternatively, a simplistic approach should be to assume 2-5% as suggested in Section 4.3.1. The recoverable geometric seating beam elongation component of the elongation (discussed in Section 2) must also be included; previously in earlier researching this has not been addressed. This then gives a more accurate estimate of the 'pull-off' the floor system has to undergo.

When assessing the seating beam rotation based on the drift of the frame running parallel to the one-way floor system (orthogonal to the seating beam supporting the floor system), it is suggested for simplicity to assume the seating beam rotation equates directly to frame drift. In reality this is not the case because torsion about the seating beams longitudinal axis can effect how much seating beam rotation results from a given frame drift (Matthews 2004; Lindsay 2003; MacPherson 2005) as discussed in Section 2. Figure 4-9 illustrates the way seating beam rotation is induced from orthogonal frame drift, assuming no loss or gain due to seating beam torsion.

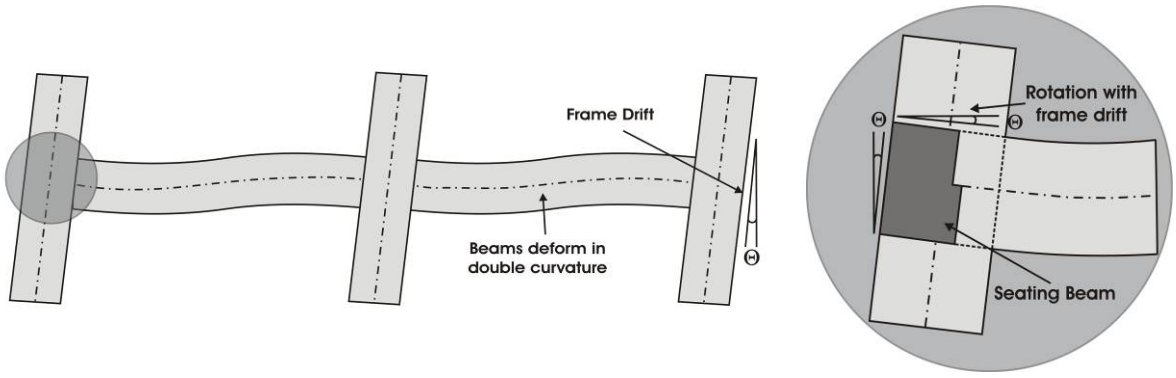

a) Assumed frame drift profile **b) Seating beam rotation**

Figure 4-9 Assumed seating beam rotation and inter-storey frame drift relationship

Figure 4-10 illustrates the observed seating beam torsional behaviour from Matthews (2004).

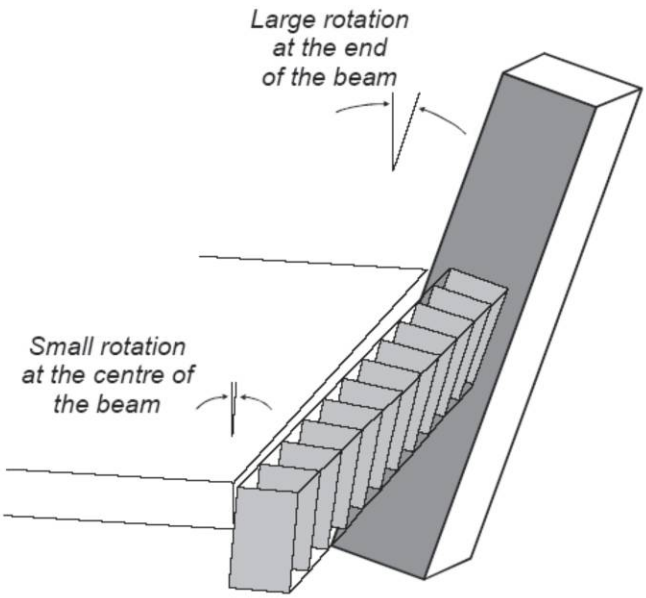

Figure 4-10 Seating beam torsion after Matthews (2004)

4.4 Existing Stress Conditions

This section is a summary and discussion of ideas presented by Fenwick et al (2004), it was considered important to highlight the relevance of existing stress conditions when assessing existing seating connections and the limitation this placed on experimental tests.

A limitation faced by all experimental tests was the maturity of the test specimens. All experimental tests have been in the order of 1-6 months old. This does not represent the time effects experienced by *in-situ* seating connections which can be up to 20 years old. Time dependent behaviour of existing connections could potentially have a negative effect on the performance of the floor system (Fenwick et al 2004). There are a number of reasons for this, all of which are associated with time-dependent stress conditions in seated ends of the composite hollowcore and *in-situ* topping floor system.

The prestressed nature of the hollowcore units results in a highly disturbed stress state in the end regions of the hollowcore units. The reason for this is the prestressing tendon force development and transfer to the hollowcore unit over the 600-750mm tendon development length. As a result, tensile and compressive transverse stresses are induced in the section orthogonal to the prestressing tendons due to bond development. Figure 4-11 from Fenwick et al (2004) illustrates the stresses resulting from prestressing force transfer in the end development length region of a hollowcore unit. Such existing stress conditions could potentially have a substantial effect on the expected primary failure mechanism. The likely outcome is a higher probability of flexure-shear failure (FSF).

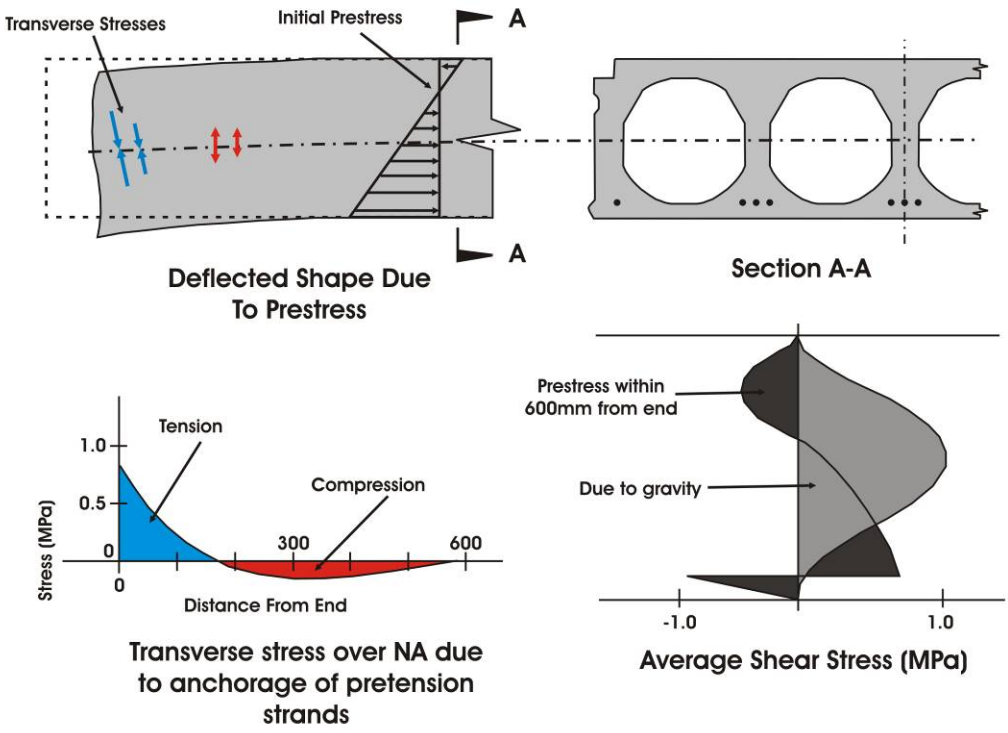

Figure 4-11 Stresses induced in hollowcore units by prestressing tendons from Fenwick et al (2004)

As a result of the induced tensile stresses, combined with shear stresses due to gravity loads, the net shear strength of the hollowcore units end regions can be reduced. The problem associated with this is that the end regions are the regions of greatest shear demand from combined seismic and gravity actions. This is recognised in the shear design process of prestressed slabs in Section 9 of NZS3101:1995 and Section 19 in NZS3101:2006, which identify induced principle stresses and potential web splitting at the end regions of simply supported prestressed members. However, in these standards, the complexity due to additional seismic induced stresses, time effects such as creep and shrinkage, and the composite nature of final floor system are not considered.

Creep and shrinkage of the prestressed hollowcore units following placing of the *in-situ* topping concrete can also affect the stress state in the combined floor system. It has been suggested that due to differential creep and shrinkage between the hollowcore unit and topping, redistribution of prestressing force occurs in the composite floor section. This results in the introduction of tensile stresses in the topping and reduced compressive stresses in the hollowcore unit as illustrated in Figure 4-12 from Fenwick et al (2004). It was suggested as a result the negative flexural strength (top of the hollowcore unit in tension, important for OFSF) can be reduced by as much as 60% in regions of negligible dead load bending moment

(critical end connection regions). This raises concern in the case of existing seating connections, which can have flexural strength capable of transferring substantial moment and shear demand in the hollowcore unit.

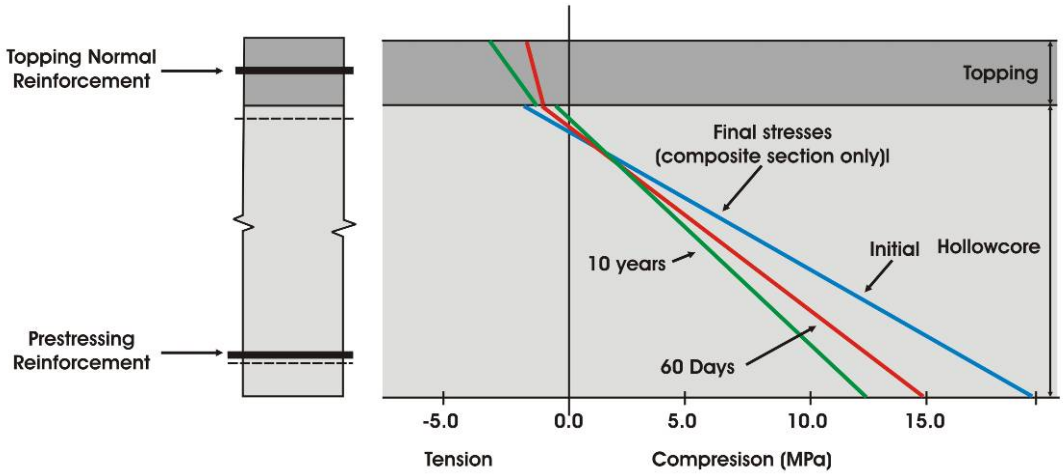

Figure 4-12 Existing stress states of composite hollowcore floor section due to creep and shrinkage from Fenwick et al (2004)

4.5 Conclusions

Based on experimental tests in this investigation and previous investigations (Matthews 2004; Bull and Matthews 2003; Liew 2004) a suite of three potential primary failure mechanisms have been identified. These failure mechanisms are associated with either the deficiencies of the hollowcore units locally, or the inability of existing seating connection details to accommodate induced seating beam rotation relative to the floor system. The three primary failure mechanisms are loss of seating (LOSD & LOS), flexure-shear failure (FSF) and offset flexure-shear failure (OFSF), all of which result in loss of gravity support of the floor system. The concern with such failures is the resulting collapse of individual units, entire floors, and potentially a 'pancake' type collapse from floor to floor of an entire building.

Secondary performance issues associated with the primary failure mechanisms have been highlighted concerning general diaphragm performance. These include vertical displacement incompatibility, longitudinal web splitting and topping delamination. The last of which has been highlighted as potentially beneficial in maintaining floor diaphragm force transfer to and between lateral resisting systems (aiding the overall seismic performance of the combined frame and floor system).

Issues which need to be considered in assessing the potential failure mechanisms of existing seating connections were discussed. Individual structural detail aspects were highlighted

which can help predict potential failure mechanisms basic on individual seating connection seismic assessment. The predominant details are the strength of the hollowcore unit, the strength and length of the provided seating ledge, the presence of core tie reinforcement, and the strength of the *in-situ* concrete end stubs and topping concrete. However, there is still substantial uncertainty in this assessment, particularly regarding the *in-situ* strength of individual seating connection elements (including the hollowcore units themselves). For this reason it is difficult to determine a hierarchy of strength for existing seating connections.

Therefore, intervention to the seating connection hierarchy of strength through isolation of the floor from the frame system appeals as a retrofit approach. Through this approach, the uncertainty associated with determining the largely 'un-determinable' intrinsic aspects of existing seating connections and the resulting likely failure mechanism could be negated.

4.6 References

Bull D.K, Matthews J.G, 2003, *Proof of concept tests for hollow-core floor unit connections*, Precast NZ report, Feb 2003.

Collins M. P, and Mitchell D. 1991, *Prestressed concrete structures*, Prentice Hall, N.J

Fenwick R.C, Deam B.L, and Bull D. K, 2004. *Failure Modes for Hollowcore Flooring Units*, Journal of the Structural Engineering Society New Zealand Inc. (SESOC), Vol. 17, No 1

Fenwick R.C, Dely, R, Davidson B, 1999, *Ductility Demand for Uni-Directional and Reversing Plastic Hinges in Ductile Moment Resisting Frames,* Bulletin of the New Zealand National Society for Earthquake Engineering, Vol. 32, No. 1

Fenwick R. C and Megget, L. M, 1993, *Elongation and Load Deflection Characteristics of Reinforced Concrete Members Containing Plastic Hinges*. Bulletin of the New Zealand National Society for Earthquake Engineering, Vol. 26, No. 1

Herlihy M. D, 2000, *Precast concrete floor support and diaphragm action:* a thesis submitted in partial fulfilment of the requirements for the degree of Doctor of Philosophy at the University of Canterbury.

Lau D.B.N, 2001, *The influence of precast-prestressed flooring on the seismic performance of reinforced concrete perimeter frame buildings*, Department of Civil and Resource Engineering, University of Auckland, Auckland, New Zealand.

Liew H.Y, 2004, *Performance of hollow-core floor seating connection details*, Masters Thesis, Department of Civil Engineering, University of Canterbury, Christchurch, New Zealand.

Lindsay R.A, 2004, *Experiments on the seismic performance of hollow-core floor systems in precast concrete buildings*, Masters Thesis, Department of Civil Engineering, University of Canterbury, Christchurch, New Zealand.

MacPherson C.J, 2005, *Seismic performance and forensic analysis of a precast concrete hollow-core floor super-assemblage*, Masters Thesis, Department of Civil Engineering, University of Canterbury, Christchurch, New Zealand.

Matthews J.G, 2004, *Hollow-core floor slab performance following a severe earthquake*, PhD Thesis, Department of Civil Engineering, University of Canterbury, Christchurch, New Zealand.

NZS4203:1992, 1992. *Code of practice for general structural design and design loadings for buildings (NZS4203), Parts 1&2*, Standards New Zealand, Wellington, New Zealand

NZS1170.5:2004, 2004. Structural Design Actions Part 5 : Earthquake actions – New Zealand, Standards New Zealand, Wellington, New Zealand

NZS3101:1995, 1995, *Concrete Structures Standard, NZS3101, Parts 1 & 2*, Standards New Zealand, Wellington, New Zealand.

NZS3101:1995, 2004, Amendment No. 3 to 1995 Standard (NZS3101), Standards New Zealand, Wellington, New Zealand.

NZS3101:2006, 2006, *Concrete Structures Standard, NZS3101, Parts 1 & 2*, Standards New Zealand, Wellington, New Zealand.

Restrepo-Posada J. I, Park R, Buchanan A. H, 1993, *Seismic behaviour of connections between precast concrete elements*, Dept. of Civil Engineering University of Canterbury, Christchurch, N.Z.

Taylor L.J, 2004, *Vertical Displacement Incompatibility between Floor Slabs and Seismic Resisting Systems*, Final Year Project, Department of Civil Engineering, University of Canterbury, Christchurch, New Zealand.

5 Retrofit Background and Philosophy

The proposed retrofit strategy aims to improve the performance of existing hollowcore seating connections to emulate the behavioural characteristics exhibited by 'new' amended seating connection details (specified in Amendment 3 of NZS3101:1995 and now in NZS3101:2006). The approach for achieving this considers the observed primary failure mechanisms outlined in Section 4, while also incorporating some of the design philosophy used to improve the seismic performance of the amended seating connections.

Techniques are suggested which could be introduced to existing hollowcore seating connections to target critical structural weaknesses, that lead to the perceived primary failure mechanisms. The strategies are aimed at being simple, practical, non-invasive, *in-situ* retrofit modifications capable of being implemented by hand. Strategies include the addition of external seating to the existing seating ledge, external confinement of the existing seating ledge, selective weakening of the interface between the hollowcore unit and seating beam and the addition of external shear force load paths within the hollowcore unit.

Guidance to the implementation of each retrofit approach and the associated complications of each technique are discussed. Two simple performance levels are suggested with the recommendation that care is required in implementing individual retrofit strategies. A likely requirement to successfully retrofit existing seating connections is to employ a combination of the suggested individual retrofit techniques.

A simple experimental investigation regarding the implementation and performance of introducing external shear reinforcement is presented. The remaining retrofit techniques are demonstrated in a Section 6 through the retrofit of an existing seating connection sub-assembly test specimen (HC4).

5.1 Individual Retrofit Concepts

Following the investigation of the performance of existing hollowcore seating connections, three primary failure mechanisms were identified. For each of the failure mechanisms, specific structural details common in existing seating connections were identified as the main deficiencies which formed the basis of the failure mechanisms. Based on these connection deficiencies, individual retrofit approaches have been developed which aim to target these.

5.1.1 Additional Seating

The problem of loss of support with and without topping delamination (LOSD and LOS) has been identified as a primary failure mechanism of seating deficient hollowcore floor systems. This was illustrated by generally poor performance of the benchmark specimen tests in this investigation. The primary contributing factor to LOSD and LOS was the 'pull-off' effect imposed on the floor system, as a result of beam elongation. The obvious solution to this performance is to provide an additional seating ledge and therefore provide a vertical load path from the floor system to the supporting beam, in addition to the existing seating ledge. This can be easily implemented with the use of a steel section, or similar, fixed to the face of the seating beam underneath the soffit of the hollowcore unit. The aim of this retrofit approach is to increase the provided seating ledge length to exceed the beam elongation 'pull-off' effects. Figure 4-1 illustrates how Equal Angle (EA) or Rectangular Hollow (RHS) steel sections could be used to provide an additional seating ledge. Such an approach mimics the increased seating length outlined in Amendment 3 to NZS3101:1995, and now in NZS3101:2006. The improved performance of the amended seating connection details has since been experimentally verified by Lindsay (2004) and MacPherson (2005).

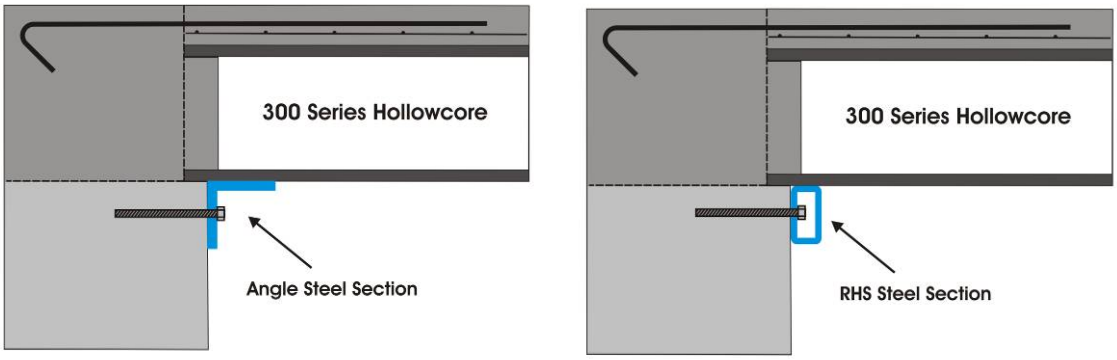

a) EA steel section **b) RHS steel section**

Figure 5-1 Potential additional seating retrofit concepts

There are however considerations which need to be recognised when retrofitting an existing connection in this way. Thought needs to be given to the implications that increasing the seating length will have on the overall seating connection performance. In particular the affect that additional seating may have on the rotational fixity of the connection. Seating connection fixity has been identified as a mechanism causing critical damage to existing hollowcore floor systems (Matthews 2004).

Care should therefore be taken to ensure any additional seating accommodates the rotational movement of the floor system relative to the seating beam. If this is not achieved the clamping action from the additional seating on the hollowcore unit could result in increasing the undesired seating connection fixity (Liew 2004). Furthermore, an additional seating ledge unable to accommodate the floor system rotation could result in increased hogging moments in the floor system (top of the hollowcore unit in tension). This is a result of shifting the point of negative rotation of the hollowcore unit further along the soffit, away from the seating beam as illustrated in Figure 5-2. Depending on the steel section used, the new pivot point could also act like an undesired knife edge on the soffit of the unit.

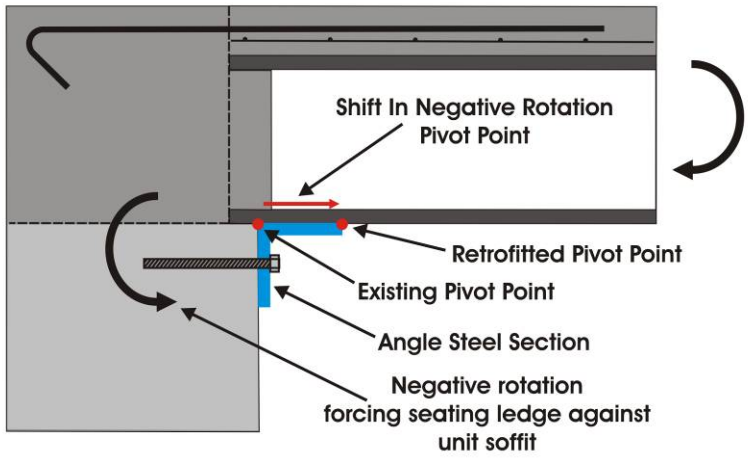

Figure 5-2 Offset in pivot point of the hollowcore unit as a result of an additional seating ledge

These characteristics were observed in a seating connection retrofit test carried out by Liew (2004). A 150x150x12 Equal Angle steel section (150EA) was used as additional seating. As a result, the long (150mm), rigid and square ended flange of the seating pressed directly against the unit soffit. Due to this restraint, the unit 'broke its back' (OFSF – see Section 4.1.3) under increased fixity and hogging demand on the unit. To prevent this, Liew (2004) suggested clearance should be provided between the soffit of the hollowcore unit and additional seating ledge to accommodate the rotation of the unit relative to the seating beam. This suggests that the length and nature of the steel section used to increase seating length can have an adverse affect on connection performance.

The application of a steel section to act as an additional seating ledge would also provide confinement to the existing concrete seating ledge. This would result in maintaining the integrity of the existing seating ledge, increasing the potential for the seating ledge to provide

vertical support to the hollowcore unit. However, confining the existing seating ledge would potentially increase the restraint of the hollowcore unit soffit under positive rotation (resistance to the hollowcore unit soffit from pulling away from the seating beam), resulting in a higher positive connection flexural strength. Experimental tests in this investigation showed that spalling of the seating ledge was seen to act as a release mechanism for the seating connection rupture, therefore accommodating positive rotation of the hollowcore unit relative to the seating beam. Potentially the increased soffit restraint could modify the connection hierarchy of strength to induce flexure-shear failure (FSF – see Section 4.1.2) in the hollowcore unit.

Consequently, this raises the issue of what increase in seismic performance level would be achieved by applying additional seating alone as a retrofit technique. Should only collapse prevention be desired and damage to the hollowcore unit accepted, additional seating alone may be sufficient. However, there is concern regarding the capability of the end of the damaged hollowcore unit to support the vertical load of the floor system (illustrated in Figure 5-3). There is the possibility that the prestressing reinforcement (tendons) in the hollowcore unit would provide vertical support through tying back into trapped hollowcore unit on the seating beam (as seen by Matthews (2004)) or catching on the additional seating ledge. However this possible load path via prestressing tendons acting as dowels should not be relied upon when considering retrofit approaches.

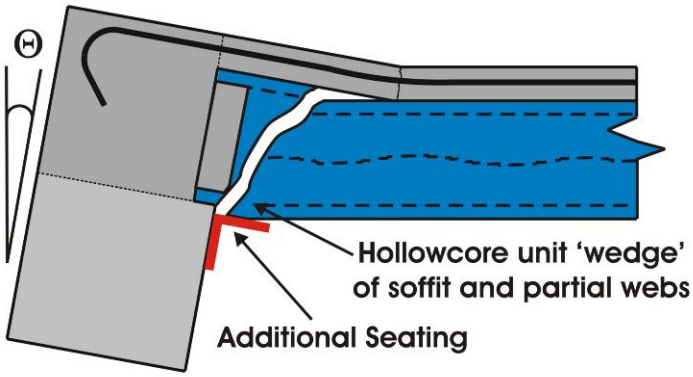

Figure 5-3 Additional seating retrofit application

If protection of the hollowcore unit was desired further retrofit techniques may be required in combination with additional seating. Further to this, there are cases in which additional seating could be by-passed; an illustration of this is in the case of OFSF where the failure

plane occurs some distance from the seating beam, illustrated in Figure 5-4. This illustrates that the nature of the existing seating connection and likely primary failure mechanisms can have a significant bearing on the appropriateness of the retrofit approach.

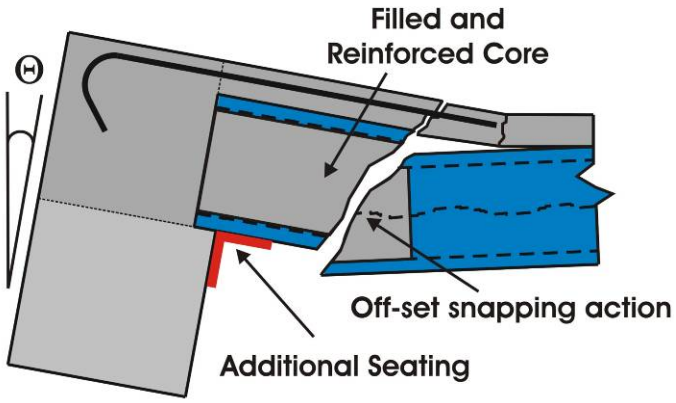

Figure 5-4 Additional seating bypassed by offset flexure-shear failure (OSF)

5.1.2 Existing Seating Confinement

Control specimen tests in this investigation and all previous 'rotation-focused' super-assembly and sub-assembly tests (Bull and Matthews 2003: Matthews 2004; Liew 2004; Lindsay 2004; Trowsdale 2004; MacPherson 2005) observed some degree of spalling of the seating ledge. This spalling was seen to contribute substantially to the loss of support (LOSD and LOS) primary failure mechanisms observed in this investigation. Spalling was seen to be a result of combined bearing and lateral 'pull-off' of the soffit of the hollowcore unit on the provided seating ledge. The unreinforced nature of the seating ledge (typical in existing seating connections) served to increase the susceptibility of the seating ledge to this spalling. For this reason it could be potentially beneficial to prevent this spalling of the existing seating ledge through providing external confinement to the existing seating ledge. By providing confinement and preventing spalling, the existing seating ledge integrity could potentially be maintained. The 'strut and tie' mechanism based on an anchored fixing and additional seating ledge to achieve external confinement is illustrated in Figure 5-5.

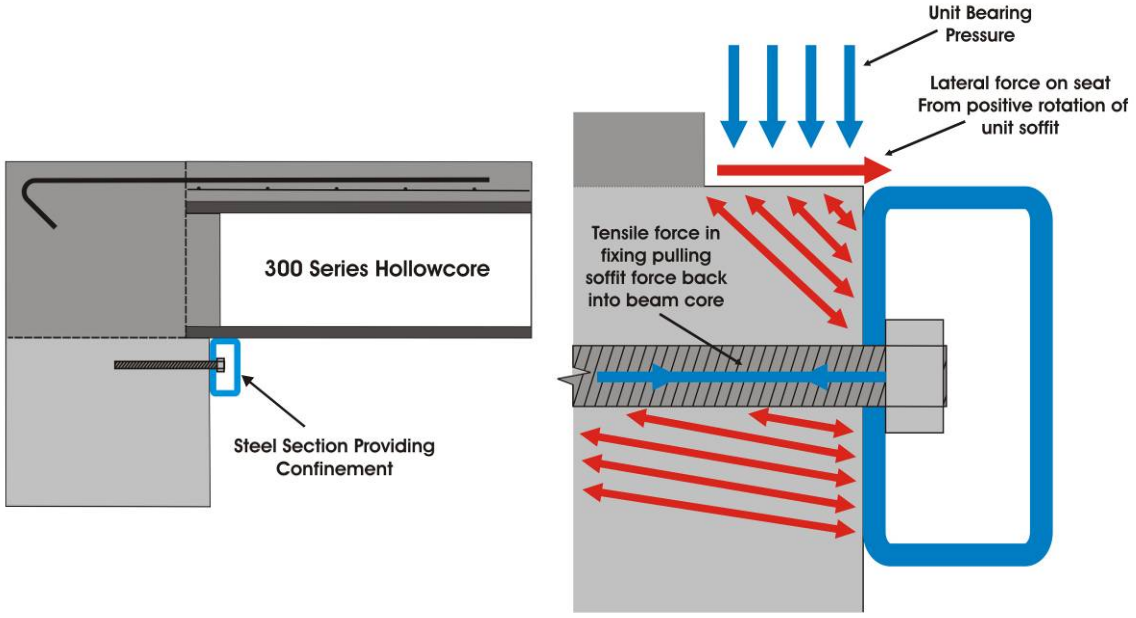

a) Physical representation **b) Provided force transfer mechanism**

Figure 5-5 External confinement mechanism of an existing seating beam

As alluded to earlier, seat spalling was seen to act as a partial release mechanism for the opening of the interface between the hollowcore unit and seating beam (under positive rotation). For this reason, providing confinement will increase the restraint on the unit soffit provided by the seating ledge. As a result, higher connection flexural strength will likely be achieved, and increased force actions imposed on the hollowcore unit. Care will be required to not adversely affect the connection hierarchy of strength through providing external confinement. Again such an approach may require additional modifying retrofit approaches to ensure this. Depending on the steel section used, this approach may not be beneficial if FSF or OFSF is the likely seating connection failure mechanism. This further prompts the need to adapt retrofit approaches to individual seating connections.

5.1.3 Selective Weakening

Excessive flexural strength (fixity) in typical seating connections was identified as a major issue for a retrofit strategy. Issues associated with excessive fixity were exhibited in all three seating connection primary failure mechanisms. This was demonstrated by snapping of hollowcore unit in FSF and OFSF primary failure mechanisms, and by trapped hollowcore unit soffit in the LOSD and LOS primary failure mechanisms. The philosophy proposed to achieve *in-situ* modification of this critical structural weakness is to introduce a plane of

weakness between the end of the hollowcore unit and seating beam (Ireland 2006). By doing so, this isolates the hollowcore unit from the seating beam. Figure 5-6 illustrates the desired idealised behaviour as a result of isolating the end of the hollowcore unit from the seating beam. Such an approach mimics that taken in the use of a compressible backing board in the first amended connection detail specified in NZS 3101:1995 Amendment 3 and now in NZS 3101:2006.

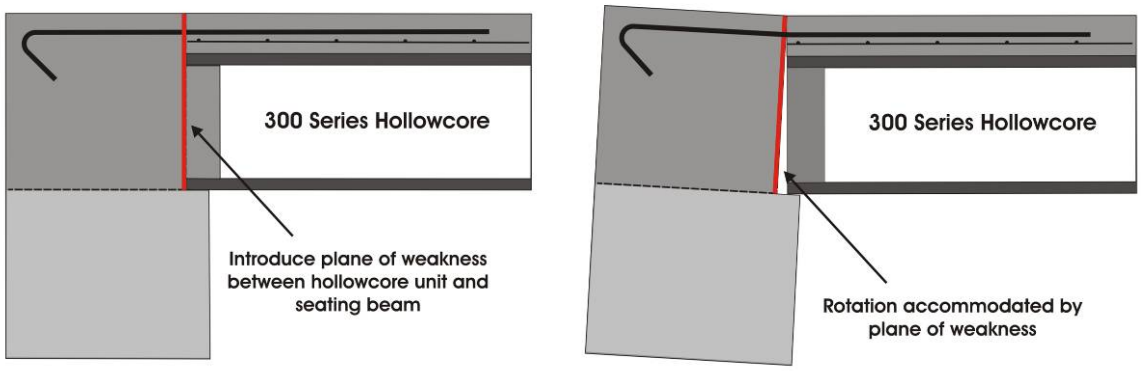

a) Location of induce plane of weakness **b) function of plane of weakness**

Figure 5-6`Selective weakening retrofit concept

The rationale behind the approach is to release the rotational degree of freedom at the seating connection, increasing the potential to accommodate relative rotation between the seating beam and floor system. The main focus in achieving this was to substantially reduce the flexural strength of the *in-situ* concrete stubs in the end of units, which key the hollowcore unit into the seating beam.

The selective weakening approach is considered to be the most effective method of improving performance of typical existing hollowcore seating connections. It is likely this individual approach will be the starting point for most retrofit applications. However, there are practicality issues associated with the implementation of such an approach, these are discussed in Section 5.2.3.

5.1.4 Pseudo-Transverse Reinforcement

The FSF failure mechanism identified by Matthews (2004) and Bull and Matthews (2003) is of concern and regarded as an important retrofit consideration. A conceptual approach being employed is to provide external structural elements through the hollowcore units to facilitate

tensile shear force load paths in the 'shear-truss' model from the soffit of the hollowcore unit to the reinforced topping. The aim of this approach was to replicate the 'shear-truss' force transfer mechanism of traditional transverse reinforcement or 'stirrups' in a reinforced concrete beam. Thereby increasing the shear capacity of the hollowcore unit, Figure 5-7 illustrates the approach of the pseudo-transverse reinforcement retrofit.

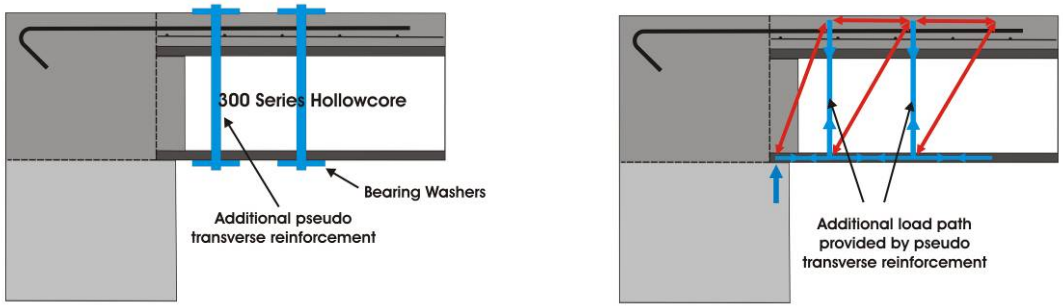

a) Physical representation **b) Provided force transfer mechanism**

Figure 5-7 Pseudo transverse reinforcement retrofit concept

The issue of using this approach is that the strengthening of the hollowcore unit in the seating connection region (as a result of the additional internal load path) could shift the failure plane further out into the unit. This could result in OFSF, similar to that observed in the seating connection tests with reinforced cores carried out by Liew (2004). For this reason care will be required in the application of this technique, particularly in determining how far along the hollowcore unit the additional shear reinforcement will be required. The additional shear reinforcement (capacity) will need to implement to a point along the hollowcore unit where the shear capacity of the hollowcore unit alone can sustain the shear demand. The shear demand is greatest in the support regions of the floor system, and decreases towards the mid-span (under gravity and seismic loading).

The results of the tests of control specimens, in this investigation, suggest using this type of approach to provide vertical support is undesirable. Concerns are held over relying on the vertical supporting loadpaths being provided through the existing starter bars. The combined rotation and elongation strain demand on the starter bars resulted in significantly high tensile strains, leading to rupture of the starter bars in the absence of strain penetration along the starter bars (as discussed in Section 4). In reality, demand will also be placed on the starter bars from the transfer of floor diaphragm lateral forces to the lateral load resisting system (the

primary purpose of starter bars). Therefore, it is not recommended to rely on the starter bars to provide a vertical load path.

5.2 Performance Based Retrofit

Two simple performance levels are suggested for when considering the retrofit of typical existing seating connections. These are firstly, a lower, minimum performance level, described as 'collapse prevention only' and secondly, and a higher level, described as 'collapse prevention and protection of floor system integrity'. It is suggested to target the lower level as a minimum requirement, followed by targeting the higher performance level based on factors such as the cost of the retrofit procedure and structural importance. Traditionally performance based assessment identifies target structural performance levels for increasing levels of seismic excitation. Generally, in structural engineering terms performance levels have been defined by structural parameters such as peak or residual interstorey drift, ductility, or energy dissipation (Pampanin et al 2002).

To define seismic demand or 'excitation' at a hollowcore seating connection level is not simple. This is because the seismic performance is a function of seismic demand in two ways, seating beam rotation and beam elongation 'pull-off'; both of which are indirectly a function of interstorey drift of the supporting frame. It is the relationships between frame drift and individual rotation and elongation which are the cause of this complication and uncertainty. In addition to this, the unpredictable initial rupture of existing hollowcore seating connections occurs at very low drift levels (0.2-0.3%). This drift is well below code drift limits (2.5% for ductile reinforced concrete frames, NZS3101:1995), and even typical frame yield drift levels (0.4-0.5%).

Therefore, it is suggested to put reliance on cost and structural importance to determine the desired performance level rather than the level of seismic excitation. Further to this, in order to achieve even a lower performance level, collapse prevention retrofit, the integrity of the floor system may have to be protected as well, eliminating the need to consider which performance level to target (being connection dependant). For this reason the retrofit approaches were aimed to be simple, cost effective, and applicable for most implementations, based on simple observations the seating connection details.

5.2.1 Practical Application Considerations

A number of considerations need to be made when retrofitting existing hollowcore seating connections. These include issues associated with practicality, implementation and invasiveness of the retrofit strategy. This section discusses ways in which to implement the discussed retrofit approaches and the associated complications.

5.2.2 Additional Seating and Confinement

The application of additional seating and existing seating confinement is non-invasive and could be carried out with relative ease. There are however some considerations which affect the ease of implementation and performance of the retrofit approach.

Locating the 'new' additional seating ledge at the same level or as close as possible to the existing seating ledge is recommended (given the potentially irregular (bowing) profile of the hollowcore unit soffit). If the additional seating ledge obstructs the negative rotation of the hollowcore unit (top of the hollowcore unit in tension), allowances should be made to accommodate this rotation. This can be done through careful selection of length of the additional seating ledge, modification of the profile of the additional seating ledge, or placing a compressible packing material between the seating ledge and the hollowcore unit soffit. It is not recommended to simply provide clearance between the soffit of the unit and additional seating, as this relies on the unit firstly being damaged, and secondly undergo a vertical displacement (drop) to engage the additional seating ledge. In addition, there is no guarantee the damaged end of the unit will provide sufficient vertical load capacity once it has descended onto the additional seating ledge.

One of the complications of implementing additional seating and confinement is the fixing of the steel section to the face of the seating beam. It is important the fasteners pass well into the reinforced concrete core of the seating beam to provide sufficient tensile force to prevent spalling of the existing seating ledge. For this reason the location of the fasteners becomes important and must pass well beyond transverse reinforcement (stirrups) of the seating beam. This creates potential complications in terms of first finding the reinforcement and then secondly, matching fixing points (holes) on the steel section with identified gaps in the beam reinforcement thereby avoiding clashes between stirrups and fasteners. A suggested way of mitigating this complication is to have more fixing points in the steel section than required

and use the fixing points in a 'hit and miss' manner to avoid fixing points which coincide with the beam reinforcement.

A further consideration, in terms of achieving sufficient confinement, is ensuring the steel section is fastened tightly against the face of the seating beam. This may be difficult under typical construction tolerances given the very fine margin of error associated with achieving confinement (continuous, direct contact of the confining element onto the concrete). If this is not achieved, the confinement will be passive in nature and spalling will result. The spalled wedge of seating could, however, be held behind the confinement (steel section), maintaining the seating ledge to a sufficient degree. A potential positive of achieving only passive confinement is the release mechanism associated with seat spalling (as discussed in Sections 5.1.1 and 5.1.2) may still be maintained whilst the seating ledge will not be lost.

5.2.3 Selective Weakening

There are a number of perceived problems associated with the practicality of selective weakening. Ideally to guarantee a complete plane of weakness at the interface between the hollowcore unit and seating beam, a continuous saw cut, or similar, would be required through the combined depth of the hollowcore unit and topping. This would be a laborious, difficult and expensive procedure. In addition, such a procedure would involve cutting through the topping starter bars. These would have to be reinstated; which again is complicated and un-practical. A suggested alternative (Personal Dialogue, NZSEE Conference 2006) was to drill down behind the flooring units, in a 'hit and miss' manner, to generate a perforated plane of weakness along the interface between the hollowcore unit and the seating beam. The advantage of this approach is the implementation would be easier and starter bars can be avoided and left intact as illustrated in Figure 5-8.

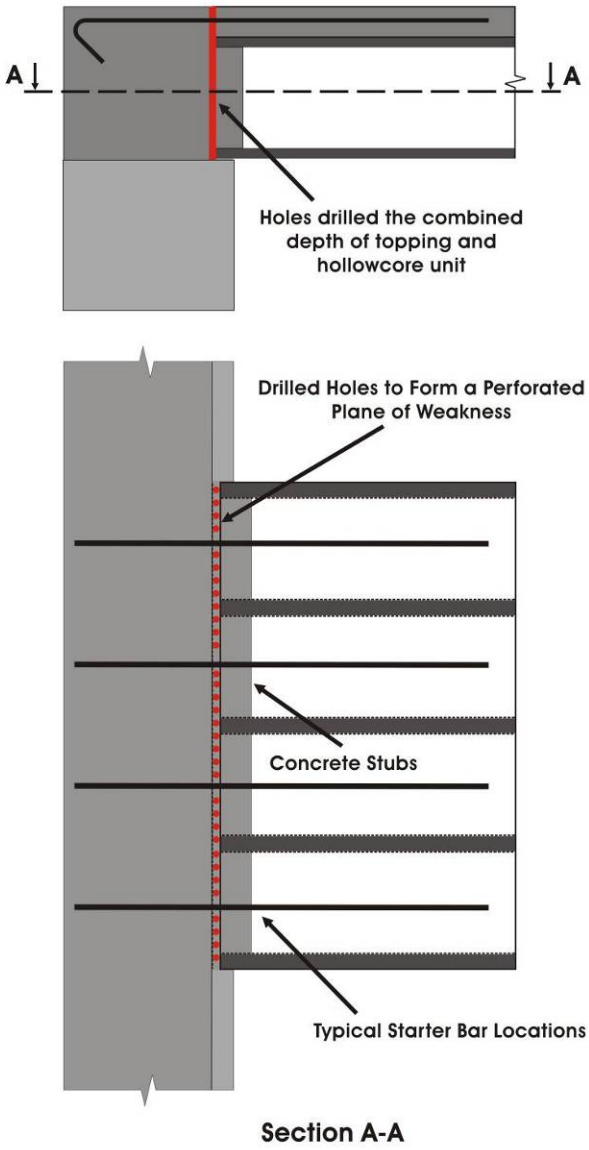

Figure 5-8 Selective weakening approach using a drill hole perforation

It can be seen from Figure 5-8 that such an approach can separate a large proportion of the end of the hollowcore unit and concrete 'stubs' from the seating beam. This will significantly weaken the interface between the hollowcore unit and seating beam. In addition, starter bars remain intact, with structural function maintained. The structural integrity of starter bars is important in maintaining the lateral in-plane diaphragm load paths between the floor and frame systems. If desired it would be possible to reinstate the floor surface by filling the holes with grout or similar for a short depth down the holes.

5.2.4 Pseudo-Transverse Reinforcement

The application of this retrofit technique is essentially practical to implement. However, there are some issues associated with invasiveness and disruption to the buildings function, and the effectiveness of the post-construction reinforcement for shear. The implementation of this approach would require the application of steel ties, or similar, through the cores of the hollowcore unit. The ties would need to be fixed at the hollowcore unit soffit and topping surfaces to provide the clamping force. Fixing the ties at the hollowcore unit soffit would be acceptable, as the fixing will be hidden by suspended ceilings or in exposed cases could be face capped or left exposed without affecting the function of the building. However, the fixing on the topping surface of the floor system will protrude above the finished floor surface raising invasiveness issues. To avoid this, it may be possible to recess the fixing in the topping and reinstate the original floor surface. However, this is potentially time and cost inefficient.

It is suggested that the application of such a retrofit procedure would be applicable to every second core of each hollowcore unit. This is in order to distribute compression load paths through the hollowcore unit webs. Figure 5-9 illustrates the potential application of such an approach with floor surface fixings protruding above the floor surface.

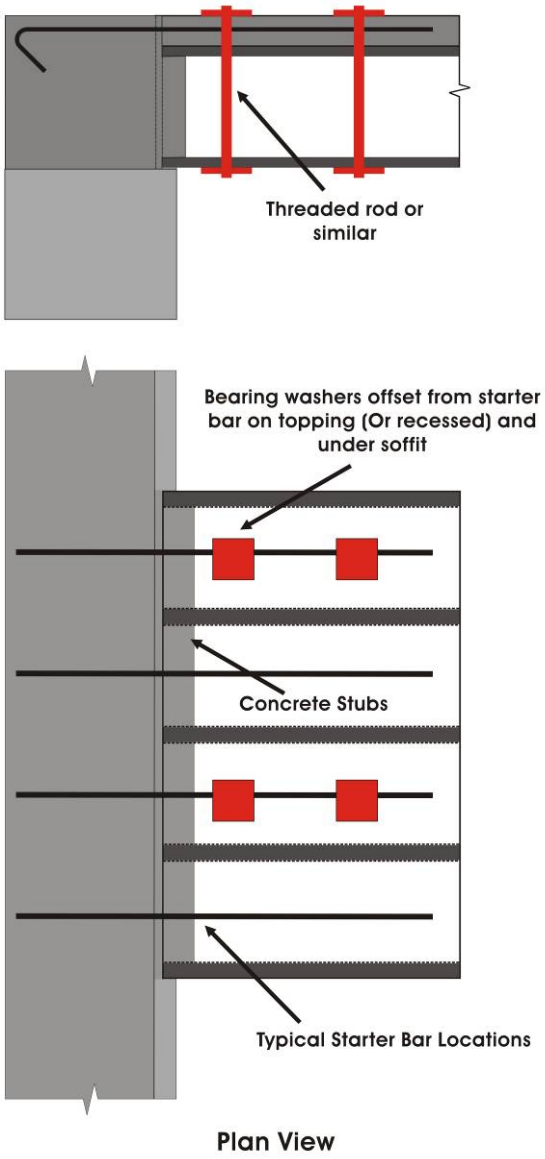

Figure 5-9 Potential layout of pseudo- transverse reinforcement

In terms of effectiveness, the application of such structural additions involves drilling through the brittle hollowcore unit. It is likely such drilling, particularly if through the cores of the hollowcore unit, would result in spalling a cone of concrete from the top and/or soffit of the hollowcore unit. This could potentially lead to creating a weakness in the hollowcore unit and would be undesirable.

5.3 Trial Pseudo-Transverse Reinforcement – 'Pull-Out' Test

In order to investigate the practical application of pseudo-transverse reinforcement, a simple experimental investigation was carried out. The aim of the investigation was to implement the discussed retrofit procedure, to investigate the effectiveness of such an approach and to highlight any potential complications. Of particular interest was the effect of installation method, including drilling into the hollowcore unit, the transfer of forces through the hollowcore unit section and resulting failure mechanism.

5.3.1 Experimental Setup

The retrofit approach was carried out on a hollowcore unit from a previous sub-assembly test (HC2). The test setup aimed to replicate the tensile forces that would be induced in an external tie passing through the cores of the combined hollowcore unit and topping section. Monotonic tension was applied using a hydraulic jack until failure. The tensile force resisted was by the tie fixing on the unit soffit and imposed by a hydraulic jack sitting on the same fixing footprint on the topping surface. Figure 5-10 illustrates the test setup.

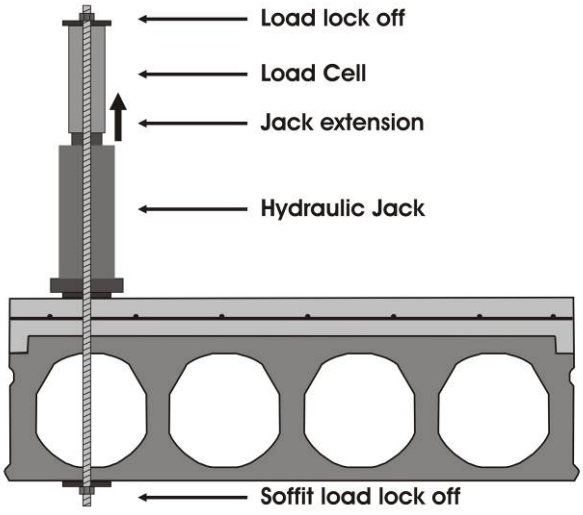

Figure 5-10 Pseudo-transverse reinforcement 'pull-out' test setup

The tie detail consisted of a high tensile M16 threaded rod with 100x100x10mm mild steel washers, top and bottom. Each tie test was carried out independently, allowing four tests to be performed on a 300 series hollowcore and topping section (one tie per core). Initially four tests were carried out on a short off-cut of hollowcore unit, approximately 500mm long. It was expected the short length of the section of unit would have a negative impact on the test

result (that is, produce a lower capacity). For this reason later tests were carried out on the end of a much longer section of hollowcore unit, consistent with the proposed location and conditions in reality.

5.3.2 Results – Installation Observations

To install the ties a standard masonry bit and hammer drill were used. An 18mm drill bit was used to give clearance for the 16mm threaded rod tie. A number of experimental holes were drilled to investigate the effect the drilling process had on the integrity of the hollowcore unit. It was found that due to using the masonry bit and hammer function, cones of concrete were pushed out of the unit and topping on exit of the drill bit. If drilling from the topping down, cones were pushed out of the bottom of the top flange of the hollowcore unit core and soffit of the unit. If drilled in the opposite (upwards) direction, cones were pushed out on the top of the soffit flange of the core and out of the topping floor surface. In all cases the cones were in the order of 100mm in diameter and as deep as 15-20mm at the apex of the cone. Figure 5-11 illustrates the nature and location of the observed cone spalling.

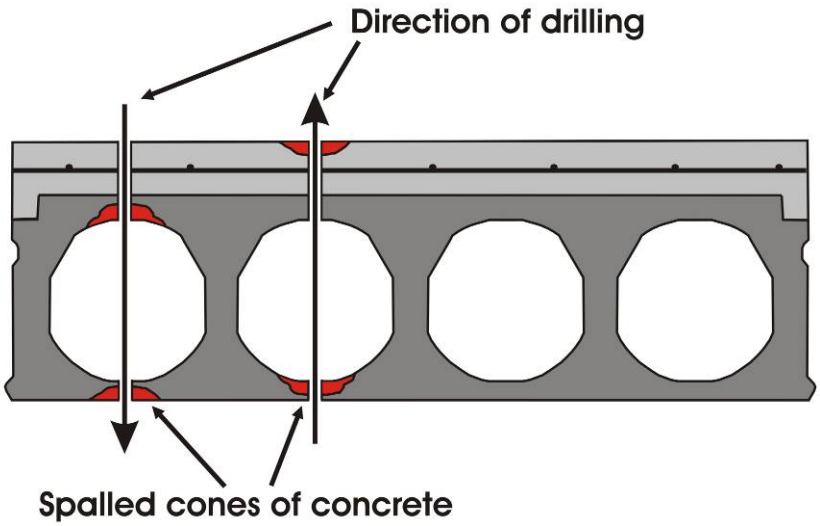

Figure 5-11 Cone spalling as a result of drilling through 300 series hollowcore unit and topping section

The most desired outcome of these (still not ideal) was when drilling the hole from the soffit upwards. The reason for this was the spalling of the cone in the topping surface was preferred, as the spalling did not occur in the top of the hollowcore unit itself. This was beneficial as the hollowcore unit is the delicate element in the floor system. In addition, this option was preferred aesthetically as the spalling of the unit soffit was not visible. Observing these installation issues emphasised the importance of the bearing washers. The bearing

washers will be needed to bear around the spalled cone and spread the load path on the hollowcore unit soffit closer to the origin of the webs. To mitigate the effect of the spalling induced by the drilling, grout could be used to fill the exposed cone areas to replace the spalled concrete. Other than the observed spalling issues, installation of the ties was straight forward and could be easily applied in practice.

5.3.3 Results – Pull-Out Testing

Four pull-out tests were initially carried out on a small off-cut of combined hollowcore unit and topping approximately 500mm in length. All the tests were seen to fail through longitudinal splitting along the soffit of the hollowcore unit segment (along the inside of the core). The failures were premature as a result of the short length of the unit, as shown by later tests on a larger hollowcore unit segment. Figure 5-12 illustrates the longitudinal splitting failure observed in pull out tests on the short segment of hollowcore unit.

Figure 5-12 Typical longitudinal splitting failure for pull out tests 1-4

Figure 5-13 illustrates the force versus displacement relationship from the pull-out tests. The four tests carried out on the short off-cut of hollowcore unit were Test 1 to Test 4. It can be seen the nominal axial strength achieved ranged from 40-60kN which is still in the elastic range of the tie. Forces of these magnitudes would be more than sufficient to resist shear forces and even provide vertical support under typical combined gravity and seismic load

cases (based on 50kN per unit from G&Qu&E load case used in sub-assembly tests). This justification is based on the suggested use of at least four ties per unit in reality, as shown in Figure 5-9. The reason for this is to distribute demand among the tie reinforcement and distribute forces within the hollowcore unit cross section.

The achieved displacements in Figure 5-13 are for the 1500mm unbounded length of the entire pull-out test rig (hydraulic ram and load cell included) and are not representative of achievable tensile strains in the M16 threaded tie (approximately 400mm).

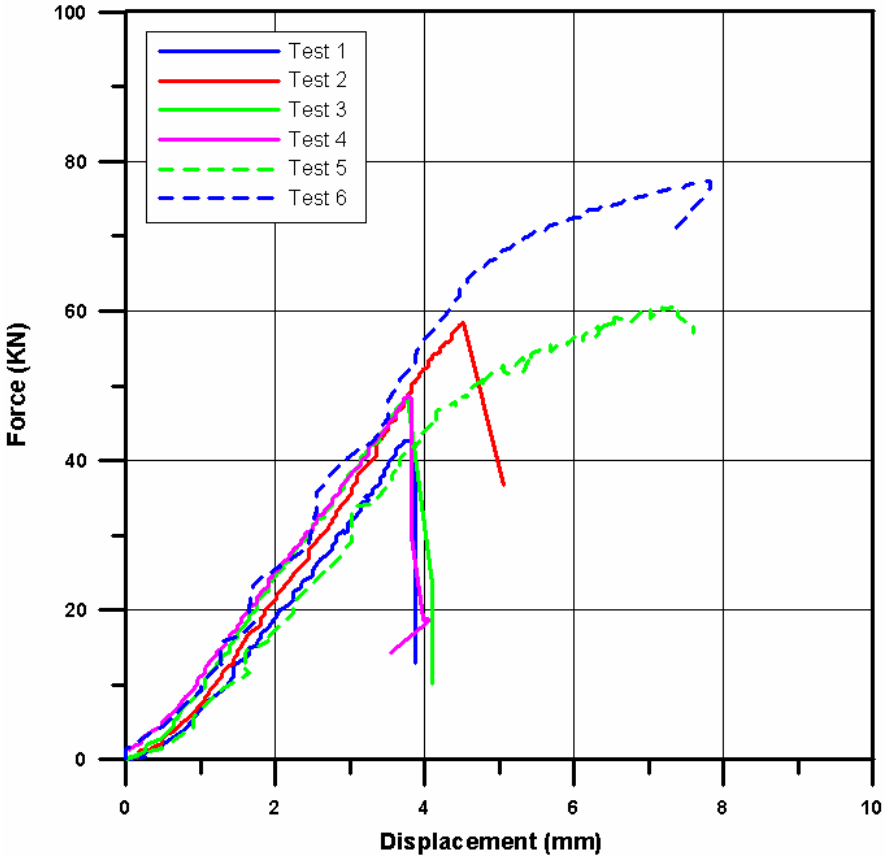

Figure 5-13 Pull-Out test force versus displacement

Test 5 and Test 6 where carried out on the longer section of hollowcore unit and topping. Test 5 achieved an ultimate capacity of 60kN, failure as a result of a cone-type pull-out in the hollowcore unit soffit was observed. The hollowcore unit soffit following the test, shown in Figure 5-14 illustrates the failure mechanism. This failure would be expected in reality, rather than that observed in tests 1 to 4. Test 6 achieved a peak tensile capacity of approximately 78kN at which stage yielding in the tie was apparent and the test ended. No significant damage to the unit was observed. Testing of the longer segment of hollowcore showed higher

tie capacity was achieved in comparison with tests 1 to 4, and far exceeded the expected demand. No further tests were carried out as sufficient tie capacities were achieved even on the conservative off-cut tests.

Figure 5-14 Cone pull out in soffit of unit

Figure 5-15 illustrates the failure mechanism from Test 5 and the proposed 'strut and tie' load path. It was seen that a cone of concrete pulled out along cracks forming along the principle compressive load paths in the unit soffit. A crack was also seen in the top flange as a result of arch action over the core, which was only restrained by the tensile strength of the unreinforced hollowcore unit (resulting in cracking). From this it can be seen that the horizontal components of the compression struts originating from the tie fixing on the hollowcore unit soffit were restrained by the unreinforced hollowcore unit, contributing to the resulting failure mechanism. If larger bearing washers were used to spread the origin of the compression struts closer to the webs of the hollowcore unit, increasing the pitch of the compression struts, the damage causing horizontal tension component of the strut could be substantially reduced.

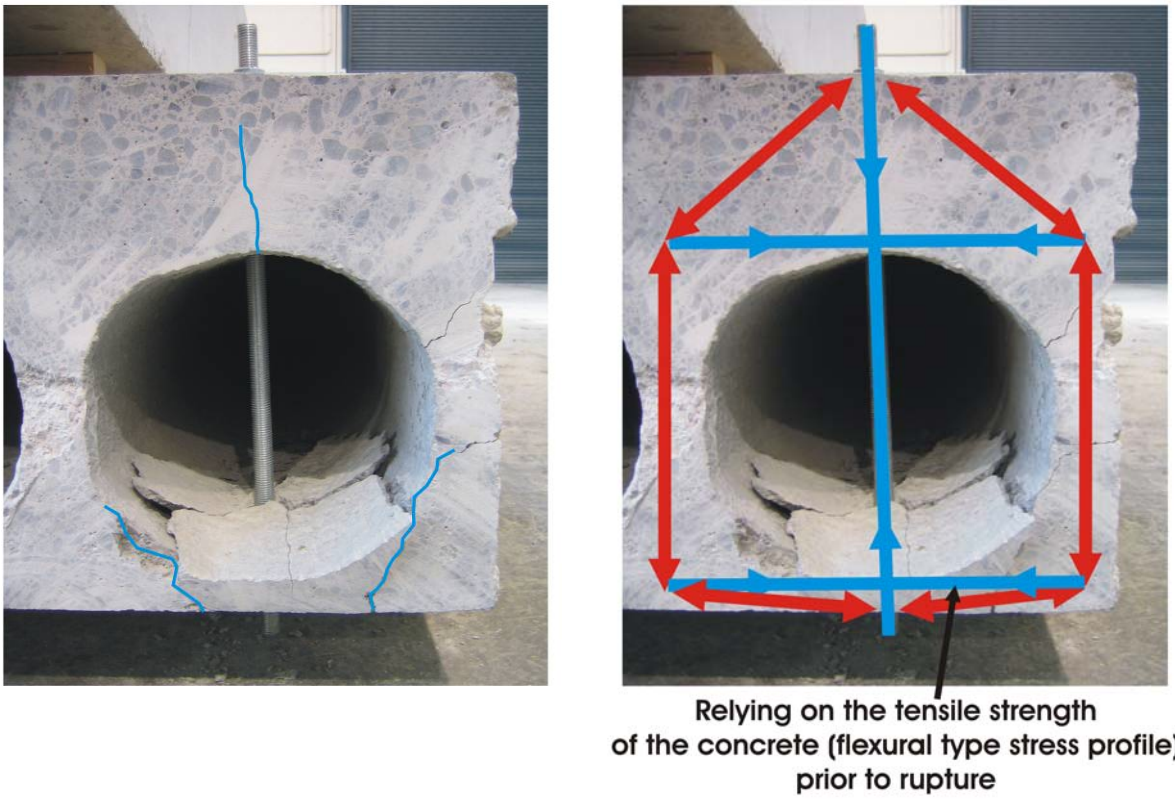

a)Tensile tie failure **b) Tensile 'strut and tie' load path**

Figure 5-15 Failure mechanism observed in pull out Test 5

Figure 5-16 illustrates how the strut and tie load paths described in Figure 5-15 can be expanded to consider the load paths in an entire floor system. The 'strut and tie' load path illustrates how placing a tie in every second core can directly pick up four webs of the hollowcore unit, and the fifth outside web through the tensile strength of the concrete and flexural type stress profiles within the web. As a result of this (and other tensile load paths in the unreinforced hollowcore unit) it becomes evident that there is potential for damage in the hollowcore unit to occur. This is a result of the unreinforced hollowcore unit having to carry tensile tie load paths to maintain equilibrium with compression struts. This emphasises the need to distribute forces by using a number of tensile ties and bearing washers, to reduce the potential for such damage.

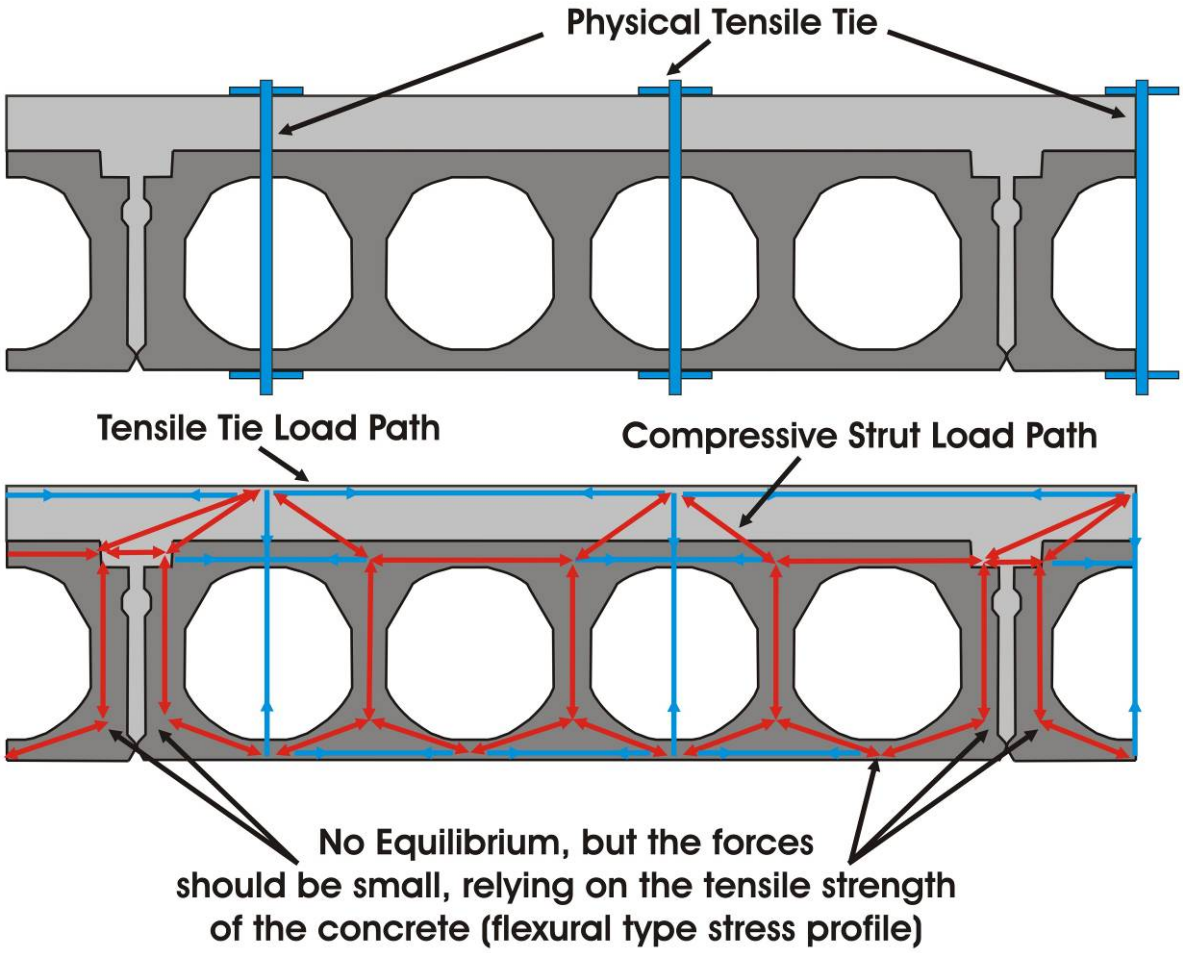

Figure 5-16 Global strut and tie mechanism for pseudo transverse reinforcement

5.4 Conclusions

A suite of conceptual retrofit approaches have been proposed with the aim to provide tools for the practising engineer to retrofit poor performing, existing hollowcore seating connections in a simple, practical, and non-invasive manner. The rationale behind the retrofit techniques was to target critical structural weaknesses observed in experimental tests of existing seating connections. In doing this, the overall theme was to modify the existing connection hierarchy of strength to protect the hollowcore units and floor system, thereby bringing existing seating connection performance closer to that of 'new' amended connections outlined in Amendment 3 of NZS3101:1995 and NZS 3101:2006.

It is anticipated that a combination of these individual retrofit techniques will be required to produce a successful retrofit solution. Retrofit techniques will need to be used in a manner which focuses on individual seating connections, in line with primary failure mechanisms that result in loss of support of the floor system. It is suggested that the selective weakening

retrofit approach is promising in generating the desired retrofit mechanism. This is particularly relevant in negating substantial uncertainty in determining the likely primary failure mechanism.

Simplistic performance based retrofit considerations for the procedure have been suggested with two potential performance levels; simple low level collapse prevention; and higher level collapse prevention and maintaining floor system integrity. It is suggested to use factors such as cost and structural importance (rather than the levels of seismic demand) to determine which performance level to target when implementing a retrofit strategy. This is due to complexity associated with assessing the seismic demand levels on *in-situ* seating connections. In addition to this it is likely that in some cases protection of the floor system integrity may be required to achieve collapse prevention. For this reason the retrofit approaches were aimed to be simple, cost effective and easily implemented. However, if under low levels of seismic demand (ie small rotations and beam elongation 'pull-off') satisfactory seismic performance of the an existing hollowcore seating connection can be justified, not implementing any retrofit techniques may be appropriate.

Practicality issues and potential adverse effects associated with the retrofit procedures have been raised, highlighting the sensitivity of existing seating connections to external modifications. Of particular importance is the modifications made to the existing seating connections and how these affect the rotational fixity of the connection.

The implementation of pseudo-transverse reinforcement was experimentally investigated. The results from this investigation demonstrated the ability of the additional tie reinforcement to transfer forces of sufficient magnitude to facilitate a shear load path within in the hollowcore unit (should a sufficient number of ties be implemented). The strength achieved in the ties was governed by a cone pull-out failure in the soffit of the hollowcore unit. It is suggested that a number of ties be used to distribute forces within the hollowcore unit section (and among a number ties) to reduce the risk of this failure. It is suggested that the implementation of this retrofit technique be approached with caution as to not adversely affect the performance of the seating connection. Potentially the pseudo-transverse reinforcement could strengthen the hollowcore unit in the seating connection region shifting the failure plane further out into the unit (OFSF).

5.5 References

Bull D.K, Matthews J.G, 2003, *Proof of concept tests for hollow-core floor unit connections*, Precast NZ report, Feb 2003.

FEMA, 2000, *Prestandard and Commentary for the Seismic Rehabilitation of Buildings – FEMA 356*, Washington, D.C

Herlihy M.D, 1999, *Precast concrete floor support and diaphragm action*, PhD Thesis, Department of Civil Engineering, University of Canterbury, Christchurch, New Zealand.

Ireland M.G, 2006, *Concept and Implementation of a Selective Weakening Approach for the Seismic Retrofit of R.C. Buildings*, NZSEE Conference Proceedings, Napier, New Zealand.

Liew H.Y, 2004, *Performance of hollow-core floor seating connection details*, Masters Thesis, Department of Civil Engineering, University of Canterbury, Christchurch, New Zealand.

Lindsay R.A, 2004, *Experiments on the seismic performance of hollow-core floor systems in precast concrete buildings*, Masters Thesis, Department of Civil Engineering, University of Canterbury, Christchurch, New Zealand.

MacPherson C.J, 2005, *Seismic performance and forensic analysis of a precast concrete hollow-core floor super-assemblage*, Masters Thesis, Department of Civil Engineering, University of Canterbury, Christchurch, New Zealand.

Matthews J.G, 2004, *Hollow-core floor slab performance following a severe earthquake*, PhD Thesis, Department of Civil Engineering, University of Canterbury, Christchurch, New Zealand.

Meija-McMaster J.C, 1994, Precast *concrete hollowcore floor unit support and continuity*, Masters Thesis, Department of Civil Engineering, University of Canterbury, Christchurch, New Zealand.

NZS1170.5:2004, 2004. Structural Design Actions Part 5: Earthquake actions – New Zealand, Standards New Zealand, Wellington, New Zealand

NZS3101:1995, 1995, *Concrete Structures Standard, NZS3101, Parts 1 & 2*, Standards New Zealand, Wellington, New Zealand.

NZS3101:1995, 2004, Amendment No. 3 to 1995 Standard (NZS3101), Standards New Zealand, Wellington, New Zealand.

NZS3101:2006, 2006, *Concrete Structures Standard, NZS3101, Parts 1 & 2*, Standards New Zealand, Wellington, New Zealand.

NZSEE, 2005, *Assessment and Improvement of the Structural Performance of Buildings in Earthquake*. Study Group Draft. New Zealand Society of Earthquake Engineering.

Oliver S.J, 1998, *The performance of concrete topped precast hollow-core flooring systems reinforced with and without Dramix steel fibres under simulated seismic loading*, Masters Thesis, Department of Civil Engineering, University of Canterbury, Christchurch, New Zealand.

Pampanin S, Christopoulos C, Priestly M.J, 2002, *Residual Deformations in the Performance-Based Seismic Assessment of Frame Structures*, Research Report ROSE – 2002/02, IUSS Press.

Trowsdale J, 2004, *Seismic Performance of Hollowcore Seating Detail Specified by Amendment No 3 NZS 3101:1995*, Final Year Project, Department of Civil Engineering, University of Canterbury, Christchurch, New Zealand.

6 Experimental Observations and Results: Retrofitted Seating Connection

This section discusses the observed behaviour and performance of the retrofitted existing seating connection sub-assembly test (HC4). Results are presented through the discussion of photographs of the specimen during and after testing. Instrumented results consistent with benchmark specimen tests (HC1, HC2 & HC3) are presented for comparison. The aim was to implement retrofit techniques targeting the perceived weaknesses observed in the control specimen tests.

6.1 HC4 – Retrofitted Specimen

The HC4 seating connection detail employed the combined additional seating and seating ledge confinement, and selective weakening retrofit techniques. The existing seating connection detail, prior to retrofit, was consistent with the HC3 specimen (including the use of an 'old' hollowcore unit). This included gravity loading, vertical displacement and elongation loading. The aim of this test was to demonstrate the potential enhancement of performance of the existing seating connection through introducing additional seating in the form of a steel RHS section. The steel RHS also acts as confinement to the existing seating ledge. In addition selective weakening of the interface between the hollowcore unit and seating beam was implemented to reduce flexural force actions imposed on the hollowcore unit. Figure 6-1 illustrates the connection detail and retrofit modifications.

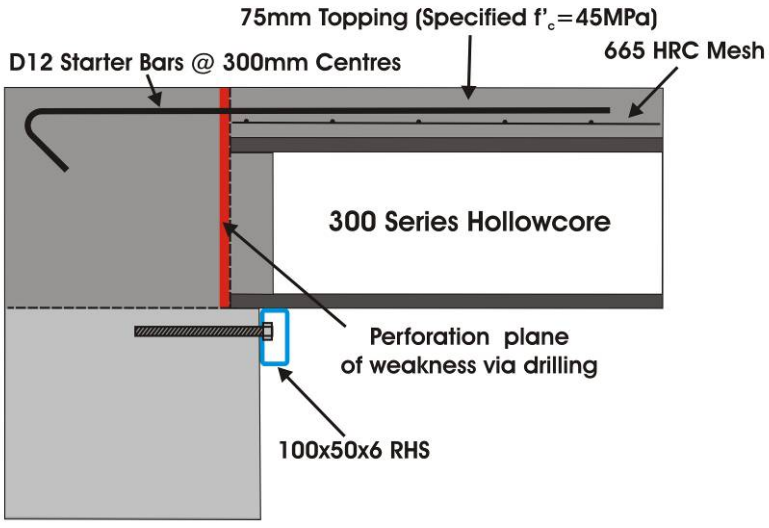

Figure 6-1 HC4 seating connection detail

Figure 6-2 shows the drill holes in a perforation pattern along the length of the seating connection (at the interface between the hollowcore unit and seating beam). The drill holes aim to implement a plane of weakness between the hollowcore unit and seating beam. The drill holes miss the starter bars (underneath potentiometers in Figure 6-2).

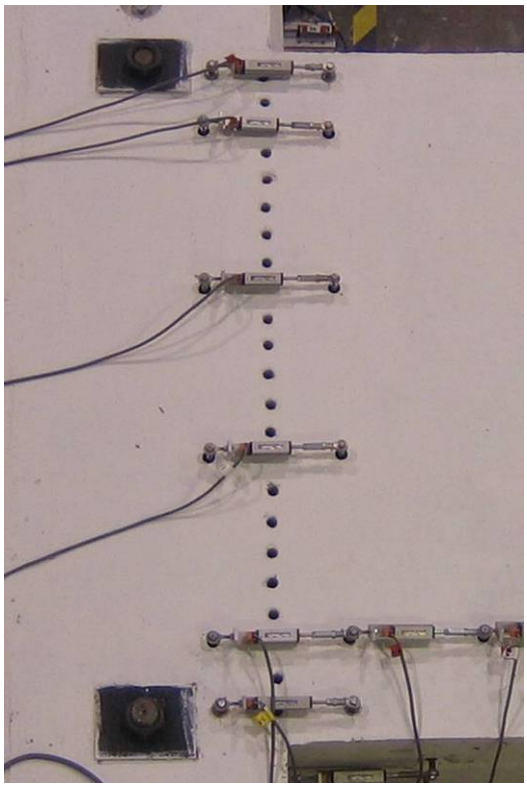

Figure 6-2 Plan view of perforation drill hole plane of weakness

Figure 6-3 shows the steel RHS section in place. The fixings were recessed inside the RHS in order to produce more efficient shear force transfer, to increase the confinement pressure of the inside web of the RHS against the face of the seating beam, and hide the fasteners. Fixing holes were faced off with plastic caps to hide the threaded rod fasteners. A number of alternative steel sections were considered for the additional seating ledge. These can be seen in Appendix C. The main reasons for using the RHS section were:

- Additional seating did not exceed the desired 50mm (other standard sections (angles or channels) could not satisfy without the addition of stiffeners).
- The section was stable, compact and stiff out of plane for confinement reasons.
- The rounded corners formed an ideal pivot point to the soffit of the hollowcore unit.
- the section was deep enough to provide sufficient clearance under the soffit of the unit to install fasteners (drill holes into seating beam etc)

Figure 6-3 Additional RHS seating ledge

6.1.1 Test Visual Performance Indicators

For discussion regarding the seating connection behaviour positive rotation or drift refers to the hollowcore unit soffit pulling away from the seating ledge; conversely, negative rotation or drift refers to the top of the unit pulling away from the seating beam, this is illustrated in Figure 2-9.

The HC4 hollowcore seating connection was seen to behave in a manner consistent with the HC1, HC2 and HC3 benchmark specimens. The interface between the hollowcore unit and seating beam ruptured at a drift of +0.2%, accommodating the imposed rotation of the hollowcore unit relative to the seating beam. The cracked interface was seen to originate from the face of the existing seating beam (behind the steel RHS), through the corner of the soffit of the hollowcore unit, and concrete stubs and topping (shown in Figure 3-2 a). Figure 3-2 b) shows the cracked interface passed through the plane of weakness as intended. At this point there was significant stiffness and strength reduction, consistent with benchmark tests.

Interestingly, initiation of this interface from the topping down occurred when the additional gravity load was placed onto the system. This was observed by cracks forming along the intended plane of weakness, for the length of the seating connection. This suggests the implemented plane of weakness was successful to some degree, particularly in the negative moment direction where the top of the hollowcore unit and the topping are in tension.

a) Initial rupture of the interface between the hollowcore unit and seating beam at +0.5% drift

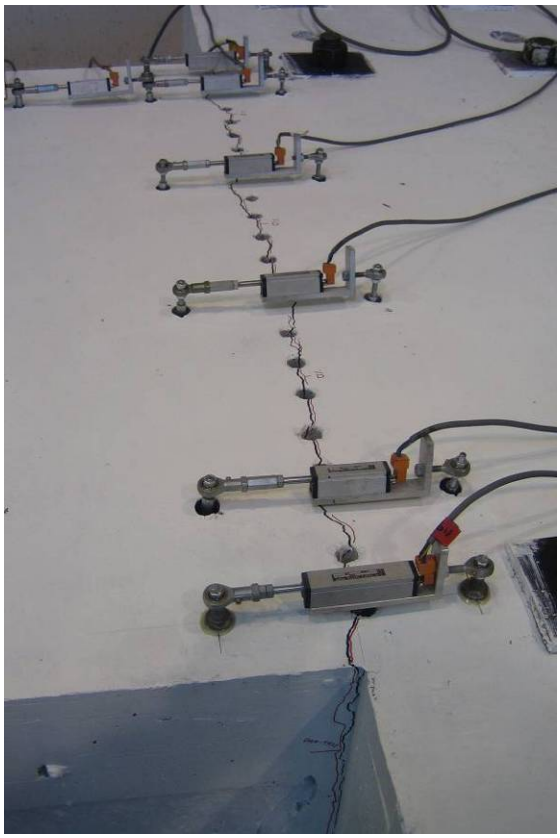

b) Rupture of introduce plane of weakness at -0.5% drift

Figure 6-4 HC4 crack interface between the hollowcore unit and seating beam

Following initial rupture at +0.2% drift, the cracked interface was seen to widen as expected under combined elongation and vertical drift demand. This behaviour was consistent with all benchmark specimens. A small amount of spalling of the seating ledge occurred behind the RHS and in regions directly adjacent to the outside webs of the hollowcore unit. The cracks which formed as a result of the spalling were seen to open and close with reversing tension and compression of the sliding soffit of the hollowcore unit. This spalling was seen to be passively confined by the RHS following cracking and did not worsen. Associated with the sliding of the unit on the confined seating ledge and RHS, a portion of the outside web on the north side of hollowcore unit was seen to be pulled off (illustrated in Figure 6-5 b)).

Figure 6-5 illustrates the unit sitting on the provided RHS seating on both north and south sides of the hollowcore unit. The RHS was seen to begin taking the gravity load of the unit during the +2.5% drift cycle. At this stage the cracked interface was in the order of 15 to 20mm in width, approximately 2mm of vertical displacement (drop) in the unit was observed as a result of the shift in vertical support of the hollowcore unit to the RHS.

a) South side of unit **b) North side of unit**

Figure 6-5 Additional RHS seating ledge providing vertical support at +2.5% drift

Figure 6-5 illustrates the hollowcore unit at peak drift levels of +2.5%, -2.0% and +3.5%. This sequence clearly shows the progressive opening of the interface between the hollowcore unit and seating beam, and transfer of vertical load support from the existing concrete seating ledge to the additional RHS seating. Upon completion of the test, a drop of 2mm of the hollowcore unit, as a result of the load transfer to the RHS, was observed. The crack width of the interface was in the order of 25mm. At this stage (+2.5% drift) the starter bars were still intact and no obvious delamination of the *in-situ* topping from the hollowcore unit was noticed. At higher drift cycles, where significant elongation had been incurred, the starter bars were seen to buckle when unloading from peak negative drifts. This was a result of the interface between the hollowcore unit and seating beam closing at the topping level, compressing the previously stretched starter bars

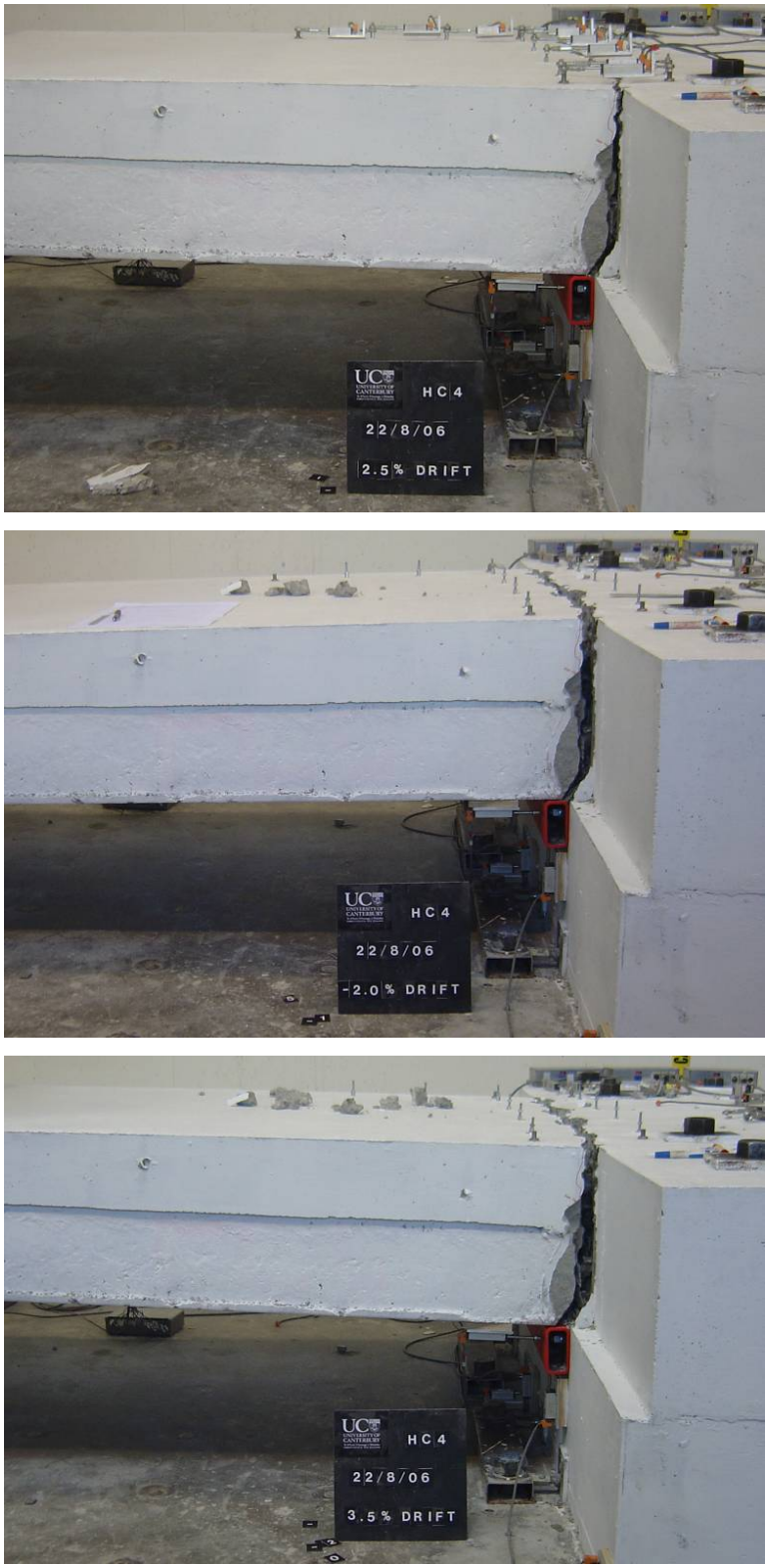

Figure 6-6 Peak drift sequence of HC4 (+2.5%, -2.0%, +3.5%)

Following the completed test sequence, loss of support was prevented due to the presence of the additional RHS seating. In order to gauge just how much elongation would be required to induce loss of seating, increasing monotonic elongation was applied to the hollowcore unit at a constant 0% drift level. Final loss of seating occurred under approximately 95mm of elongation (from the initial position of the hollowcore unit at the start of the test). Figure 6-7 illustrates a sequence of photos from the imposed monotonic elongation loading. During the elongation, rupture of the starter bars was observed at 55-65mm of elongation. A significant amount of strain penetration was seen to occur, firstly through the significant elongation achieved in the starter bars, and also the pot fixings attached to the starter bars were observed to slide within the provided cavities in the topping and seating beam. It was observed during the elongation test that at approximately 80-85mm of elongation, the unit was resting on the embedded prestressing strands which were acting like small dowels protruding from the end of the hollowcore unit where the soffit had spalled away.

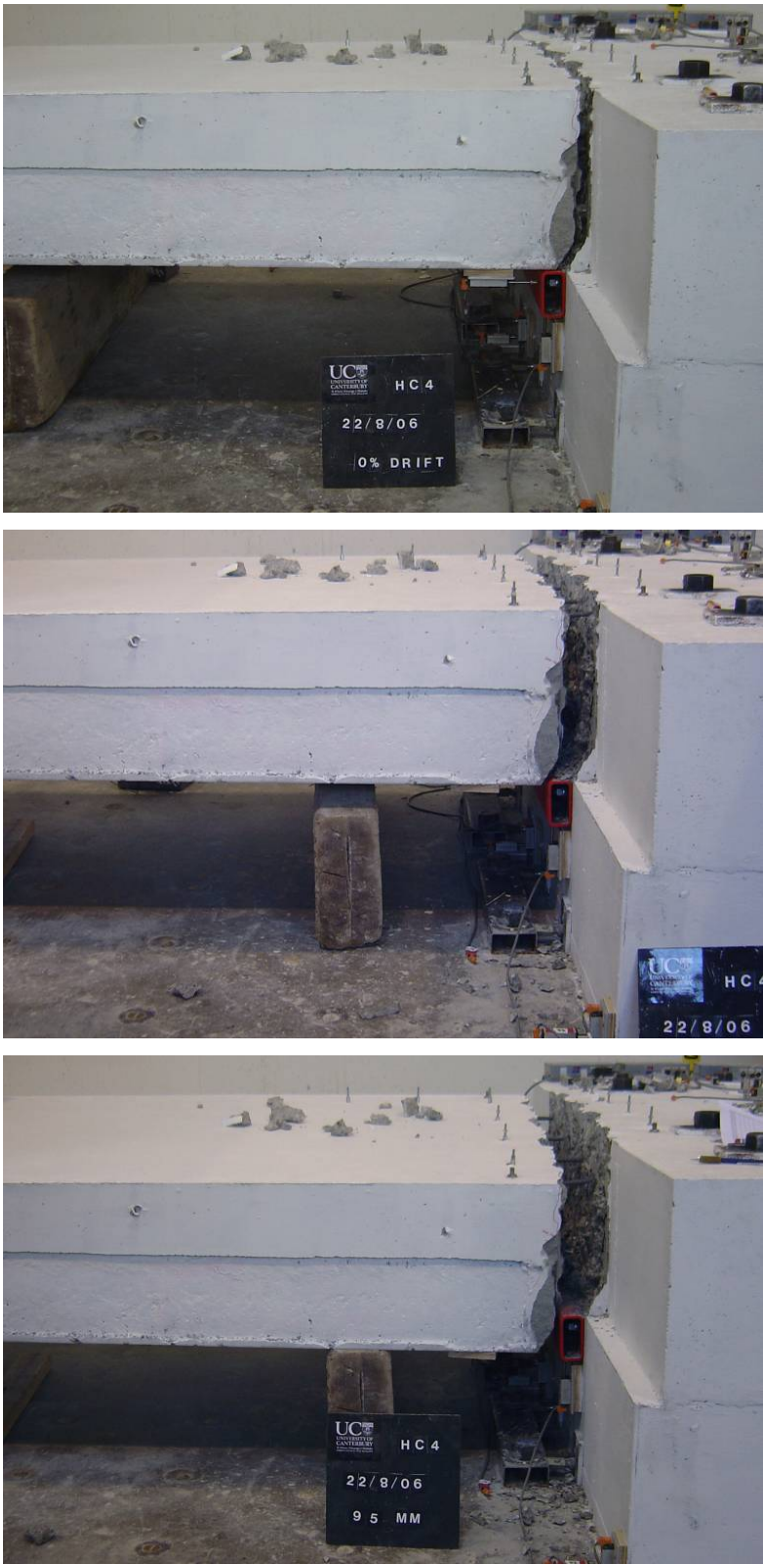

Figure 6-7 Elongation test of unit following initial test sequence

6.1.2 Post-Test Visual Performance Indicators

Following the test, the end of the hollowcore unit and the seating beam sections of the interface between the hollowcore unit and seating beam were exposed. It was observed that the interface cracked along the intended plane of weakness. It can be seen that as a result of the failure plane occurring along the perforated plane of weakness, behind the unit, portions of seating beam concrete have been left on the end of the unit (shown in Figure 6-8). This left exposed drill holes on the seating beam and end of the hollowcore unit, shaded in blue in Figure 6-8 c) and d). In previous tests, a smooth failure surface was observed where the end of the hollowcore unit formed against the *in-situ* seating beam and later pulled away, exposing the smooth end of the hollowcore unit.

Significant portions of the hollowcore unit soffit were trapped on the existing seating ledge, as shown in Figure 6-8 a) and c), shaded in green. Figure 6-8 d) shows the exposed end of the hollowcore unit with the missing portions of hollowcore unit soffit shaded in green. This was likely due to not achieving the plane of weakness the full depth of the hollowcore unit, reducing the effectiveness of isolating the unit. A probable cause of this was the holes forming the plane of weakness were not drilled deep enough, and potentially should have been drilled to just below the level of the existing seating ledge. In additional to this, the confinement of the existing seating ledge would have resulted in greater restriction of the hollowcore unit soffit. In control specimen tests, a significant amount of spalling of the seating ledge was observed and acted as a partial release mechanism for the hollowcore unit soffit under positive drift (hollowcore unit soffit in tension). In this case, rotation release was facilitated by rupture of the hollowcore unit soffit (or trapping) due to increased strength of the seating ledge and absence of spalling (due to confinement).

a) Exposed seating beam

b) Exposed hollowcore unit end

c) Exposed seating beam – critical regions highlighted

d) Exposed hollowcore unit end – critical regions highlighted

Figure 6-8 Damage mechanism and failure surfaces HC4

The addition of the RHS seating ledge was seen to successfully confine the existing seating ledge. Only a small amount of spalling occurred near the end of the RHS and 'nibbling' of the existing square edge of the seating ledge along the length of the seating connection, directly behind the RHS. The spalling of the seating ledge near the end of the additional seating was likely due to the reduced efficiency of the end of the RHS section to restrain the seating ledge. In reality this would not occur as the seating would be continuous along the length of a number of hollowcore units. The observed 'nibbling' of the square edge of the existing seating ledge was due to the bend radius of the RHS not completely confining the very corner of the existing seating ledge. Figure 6-9 illustrates the extent of confinement of the RHS and the resulting significant increase in provided seating when compared with control specimens (shaded in red). Figure 6-8 a) and c) also illustrates the intact face of the seating beam as a result of confinement of the existing seating ledge.

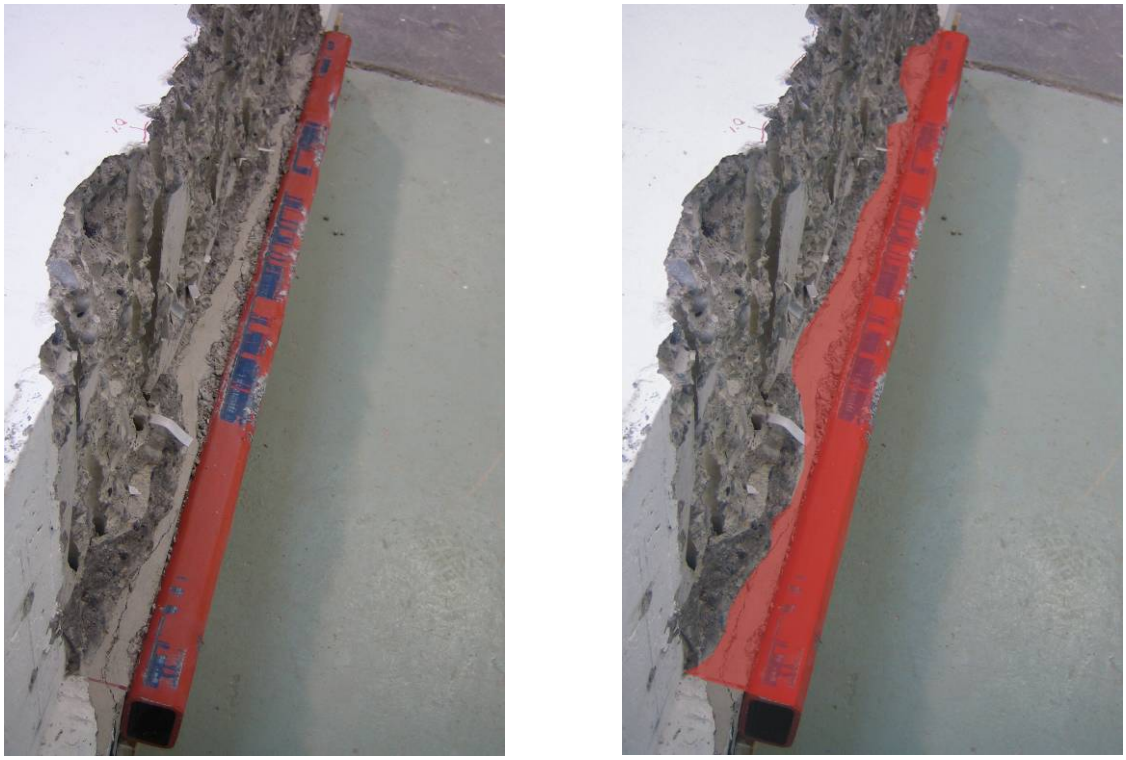

a) Exposed seating beam interface and additional seating

b) Exposed seating beam interface and additional seating: confined and additional seating ledge highlighted (in red)

Figure 6-9 Additional RHS seating ledge and existing seating ledge confinement

6.1.3 Instrumental Performance Indicators

Figure 3-5 shows the horizontal (elongation), vertical (drift) and combined moment versus rotation hysteretic relationships for the retrofitted specimen. The observed hysteretic behaviour was consistent with control specimen tests, with relatively high initial stiffness and initial rupture of the interface between the hollowcore unit and seating beam at approximately +0.2% drift. A peak strength of approximately 80kNm was observed. The plane of weakness was seen to reduce the overall peak strength of the connection by approximately 35% when compared with the equivalent un-retrofitted HC3 specimen (with a peak strength of approximately 125kNm). The reduction was smaller than desired. However, considering the observed increased restriction on the soffit of the hollowcore unit, provided by confinement of the existing seating, the gross reduction was likely to be greater then the net 35% reduction. The restraint on the soffit of the hollowcore unit was illustrated by the significant amount of trapped soffit of the hollowcore unit and the pulling off of a portion of the hollowcore unit web (as illustrated in Figure 6-5 b). Should the plane of weakness not have been implemented the increase in confinement and seating alone would likely have resulting in a peak connection strength higher than the un-retrofitted HC3 connection.

Figure 3-5 a) shows significant positive elongation moment, which was also observed in HC2 and HC3 control specimens. This was likely a result of resistance to unloading from negative drift cycles (partial closing of crack interface at the starter bar level) by the starter bars through compressive yielding and/or buckling (as observed in this test). This was not observed in the HC1 control specimen test, which exhibited extensive delamination of the *in-situ* topping from the hollowcore unit, suggesting the lack of or limited amount of delimitation in HC2, HC3 and HC4 allowed forces to be transferred to the starter bars, giving the observed positive elongation moment capacity.

With little to no vertical displacement (drop) of the hollowcore unit as a result of the additional provided seating ledge, the residual negative moment due to the presence of starter bars crossing the crack interface was much more defined than previous control specimen tests as seen in Figure 3-5 c). Residual moment offset was again observed as a result of shift in gravity load distribution, following initial rupture of the interface between the hollowcore unit and seating beam (as discussed in Section 2).

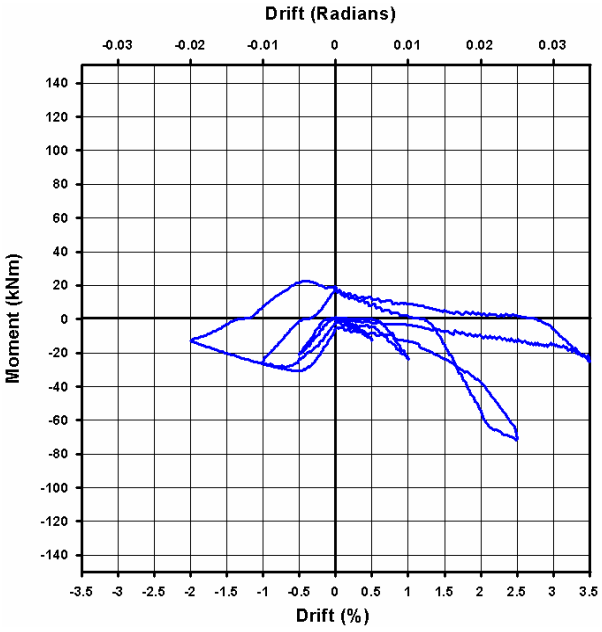

a) Horizontal elongation induced moment versus rotation

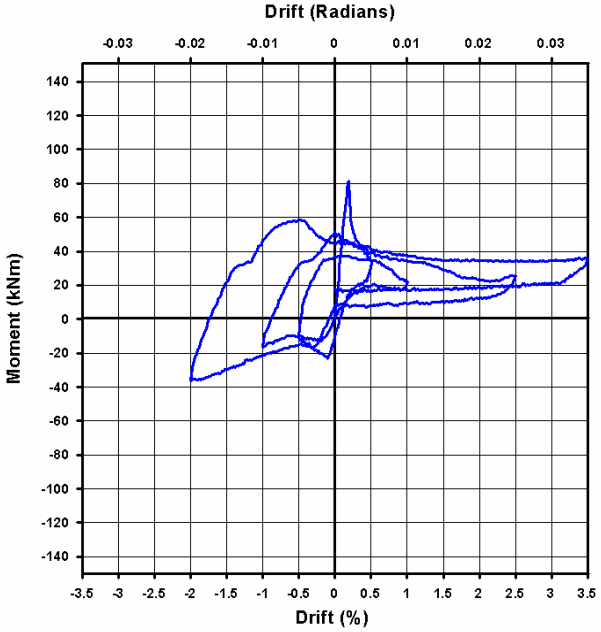

b) Vertical drift induced moment versus rotation

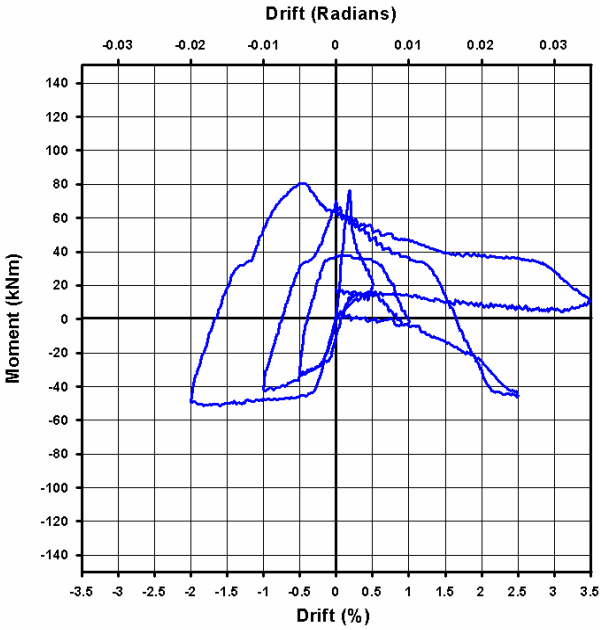

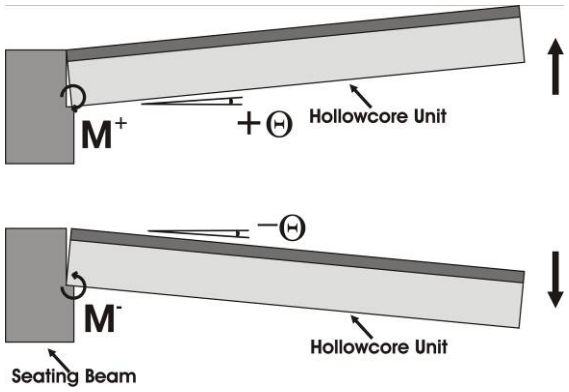

c) Net moment versus rotation

Figure 6-10 HC4 moment versus rotation

Figure 3-6 shows the average strain in the starter bars across the interface between the hollowcore unit and seating beam. The 'walking' nature induced by the combined drift and elongation loading protocol consistent with control specimen tests was observed. Much higher strains were observed when compared with HC1 and HC2 (approximately 100% greater at -1.0% drift), as was the case with HC3. This was due to the lack in early strain

penetration, and associated topping delamination. This was likely due to the stronger topping concrete and the difference in hollowcore unit ('new' versus 'old') resulting in a stronger bond between in-situ topping and the hollowcore unit. HC1 and HC2 were 'new' units and HC3 and HC4 'old' units. Strain penetration was physically observed in higher drift cycles (-2.0% and +3.5% drift cycles), which explained why rupture did not occur at a similar elongation to HC3 (during -2.0% drift cycle).

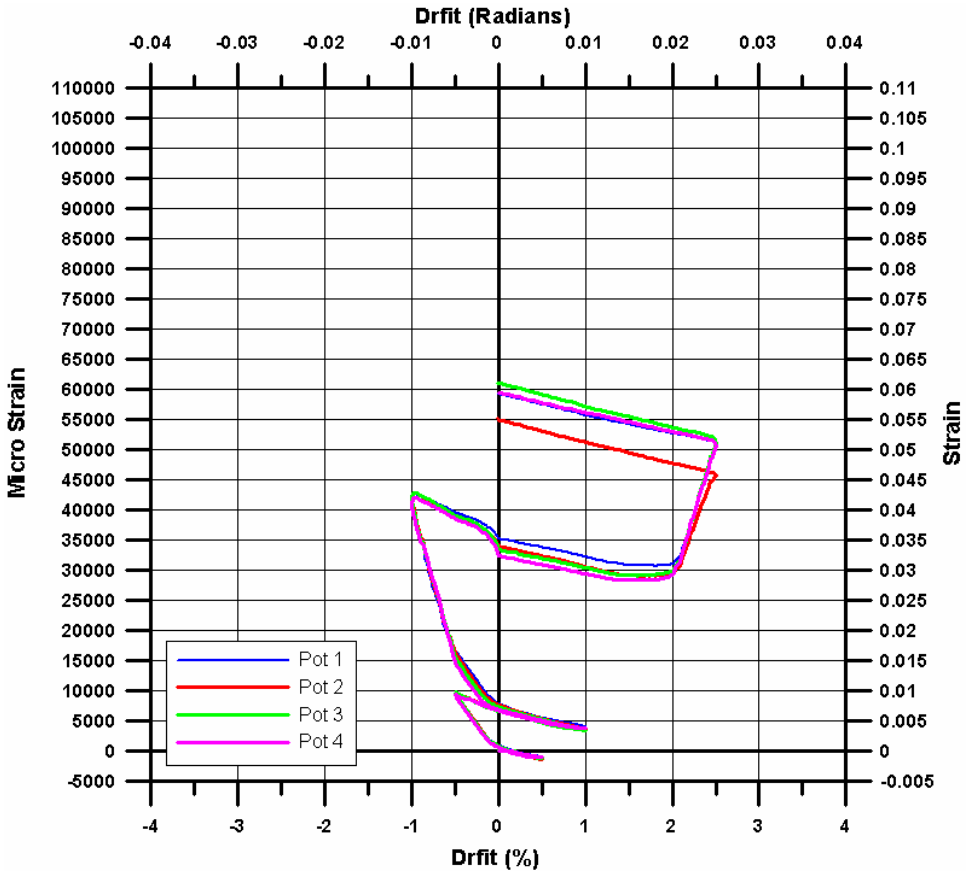

Figure 6-11 HC4 Starter Bar Strain across the interface between the hollowcore unit and seating beam

Because there was no danger of loss of support, instrumentation was maintained up until the -2.0% drift cycle (longer than previous control specimen tests). Figure 3-7 shows the desired ('T') and achieved ('M') displacement profile at the end of the hollowcore unit at peak drift levels. The desired 'T' profile refers to the prescribed rotation and elongation from the determined loading profile, described in Section 2. The vertical axis represents the depth of the combined hollowcore unit and topping section, 0mm corresponds to the level of the hollowcore unit soffit (and seating ledge) and 375mm the level of the topping floor surface. Good agreement was observed between the two, both in terms of elongation and vertical drift, with only a small amount of slack in elongation being observed.

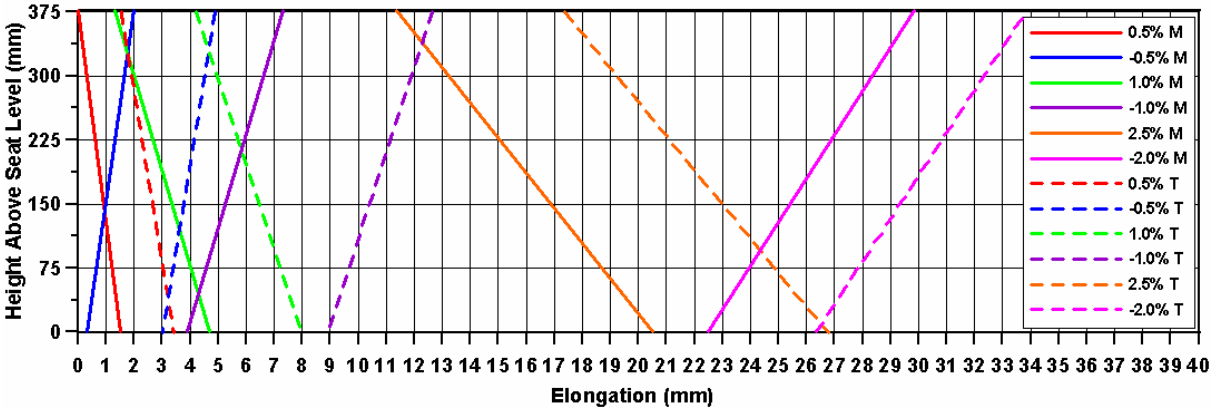

Figure 6-12 HC4 hollowcore unit end displacement profile

6.1.4 Key Implications of Connection Performance

Overall, the behavioural mechanism of the retrofitted seating connection was consistent with control specimen tests. However, the addition of the RHS seating ledge successfully prevented loss of seating. During the 2.5% drift cycle the RHS was seen to provide sole vertical support to the hollowcore unit. Vertical support was maintained to an elongation of approximately 95mm, significantly higher than expected elongation 'pull-off' during even a severe seismic event.

The addition of the RHS seating also aimed to function as confinement for the existing seating ledge. The confinement was seen to be passive in some areas, where low levels of initial spalling were observed. However, overall the confinement was effective, with the extent of spalling significantly reduced when in comparison with control specimen tests. The spalling that did occur was passively confined and held in place by the RHS section, and did not worsen during the test.

The confinement of the RHS was seen to provide more restraint to the soffit of the hollowcore unit under positive drift (unit soffit in tension). This highlighted the strength and length of the concrete seating ledge as a considerable behavioural variable in determining the peak strength of existing hollowcore seating connections. In control specimen tests, the seat spalling acted as a partial fuse or release mechanism for hollowcore unit soffit. This raises concern as to the application of additional seating and associated confinement to the existing seating alone. This is because an increase in the seating connection flexural strength may result in damage to the hollowcore unit. This is undesirable in terms of the effect it has on the hierarchy of

strength of the connection, potentially shifting the initial rupture or weakness into the hollowcore unit.

A reduction of the peak connection strength of approximately 35% was observed as a result of the introduced plane of weakness. This reduction was less than desired, however, considering the likely increase in strength as a result of provided seating confinement; the true reduction was likely to be much higher. This suggests that the perforation plane of weakness contributed in part in the success of the retrofit. The full extent of the benefit of this is hard to quantify without being able to determine a hierarchy of strength for the connection. The reduction would likely have been greater had the drill holes been slightly deeper, potentially passing just below the level of the existing seating ledge to ensure the plane of weakness penetrated the full depth of the hollowcore unit.

No obvious signs of topping delamination where observed during the test. Starter bar strains during the early drift cycles of the test were seen to be much higher than those observed in HC1 and HC2 tests, as was the case in HC3. This suggests the bond between the 'old' units and *in-situ* topping in HC3 and HC4 was higher than in HC1 and HC2, which used 'new' units. This is likely to be due to a combination of the higher topping concrete strength and the more cement rich mix of the older hollowcore units bonding better with the *in-situ* topping. Strain penetration of the starter bars was observed at higher drift levels through sliding of attached pot fixings in the provided cavities. Should this not have occurred starter bar rupture would likely have occurred much earlier, as was observed in HC3.

6.2 Conclusions

For consistency with experimental results reported in Section 3, conclusions for HC4 were made in Section 6.1.4. As a result only brief general conclusions are discussed in this section.

Overall the retrofit approach was successful, particularly in providing additional seating to the hollowcore unit to prevent loss of seating. Loss of seating was prevented to an elongation of approximately 95mm, much higher than expected beam elongation induced 'pull-off' on a floor system in reality.

The application of additional seating needs to be carried out with care in order not to strengthen the overall connection through providing confinement to the existing seating, restraining the soffit of the hollowcore unit. Potentially selective weakening approaches may be important in imposing a net reduction of seating connection flexural strength, and achieving a desired connection hierarchy of strength when applying retrofit approaches.

7 Beam Elongation Investigation

Previous research has shown the interaction between precast hollowcore floor and seismic frame systems to be influential in effecting the performance of the individual structural systems (Matthews 2004; Lau 2001; Lindsay 2004; MacPherson 2005). The dominant interaction was the 'pull-off' effect (from plastic hinge elongation in adjacent longitudinal beams) which jeopardises the vertical support of the simply supported, one-way, precast floor system. This section reviews the beam elongation phenomenon and previous research in the area which describe simple hand calculation (or spreadsheet) models for predicting beam elongation. Following this, the proposed modification of an existing method, to more accurately represent the beam elongation phenomenon is presented. The proposed modifications target aspects of beam elongation which are dependant on the number and magnitude of the rotation cycles undergone by the beam plastic hinges (the loading history). The aim of this section is to further develop a simple hand or spreadsheet type beam elongation model capable of accurately representing the peculiarities of beam elongation and the 'pull-off' effect on precast floor systems.

7.1 Beam Elongation – Review

Beam elongation is an intrinsic behavioural characteristic of ductile beams in seismic resisting frames which conform to a beam sway deformation mechanism (rotational plastic hinging in the beams). As a result of the unique material behaviour of reinforced concrete beam sections (combined concrete and compression reinforcement resisting compressive forces (C_s), and tensile reinforcement (alone) resisting tensile forces (T_s) within the section, ($C_s<T_s$)) the neutral axis depth is generally less than the depth of the centroidal axis of the section. This results in the centreline of the beam having a net tensile strain and therefore geometrically elongates under imposed rotation (drift). Figure 7-1 shows the beam elongation mechanism as a function of neutral axis depth when considering simple flexural section equilibrium of a reinforced concrete beam. When the tension force (T_s) is less than the yield force of the bars, the geometric elongation is recoverable as the applied moment reduces.

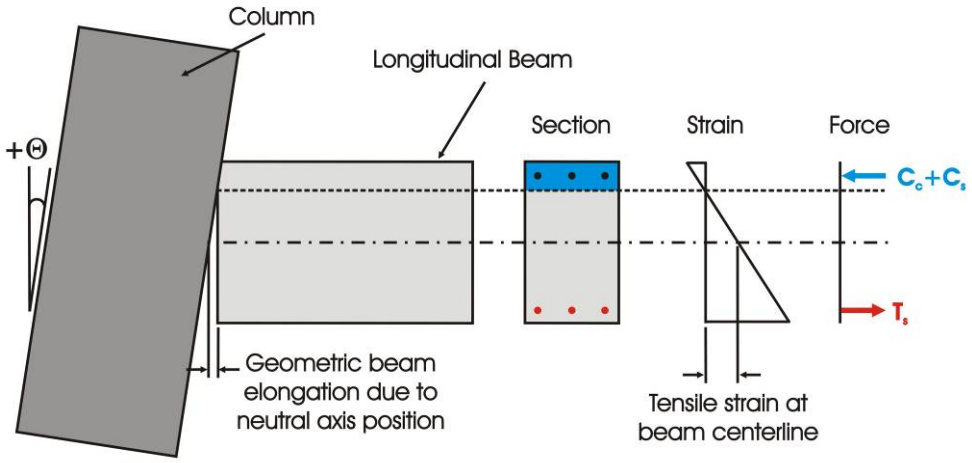

a) Beam elongation under positive rotation

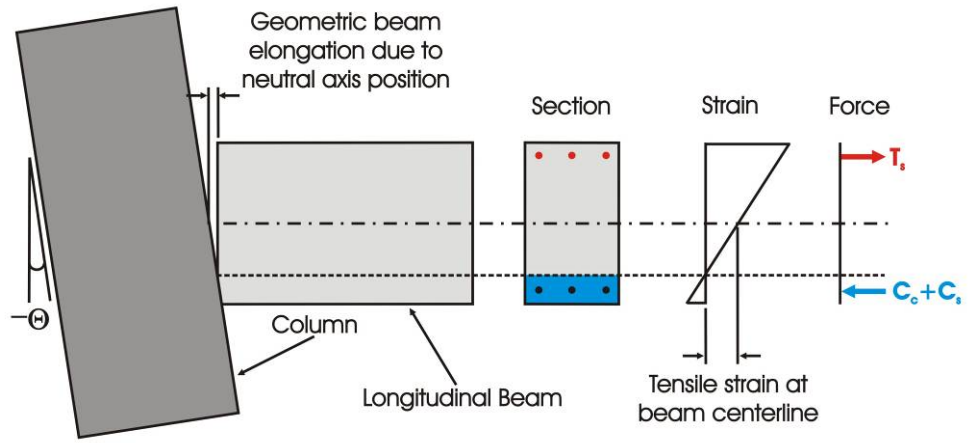

b) Beam elongation under negative rotation

Figure 7-1 Beam elongation resulting from flexure as a function of neutral axis depth

Beam elongation incurred as a result of rotation beyond elastic limits (generally defined as onset of yield strain in the tensile reinforcement), results in residual elongation, or non-recoverable growth upon unloading. The residual elongation is due to the force differential between tensile and compressive reinforcement. This force differential is a result of the concrete contribution to combined compressive forces (C_c+C_s) and not tensile forces, resulting in C_s being less than T_s upon reversal. Therefore the compressive force (C_s) is not large enough to compress the previously stretched reinforcement (T_s) back to its original position.

The force differential can be described further by the simplified truss mechanism of internal load paths in a reinforced concrete beam to provide shear resistance in a plastic hinge (Fenwick and Megget 1993). Due to the presence of the horizontal component of the diagonal concrete compression struts, the compressive force (C) in the compression steel must be less than the tensile force (T) in order to maintain equilibrium. This is illustrated in Figure 7-2 where upon load reversal the smaller compressive force is insufficient to yield in compression the previously extended tensile reinforcement. In addition to the force differential contribution to residual beam elongation, flexural and shear cracks induced in tension regions of the section will not completely close upon unloading. This is due to interference of dislodged aggregate, further preventing full recovery of the tensile strains in the regions that were previously in tension (Fenwick and Megget 1993).

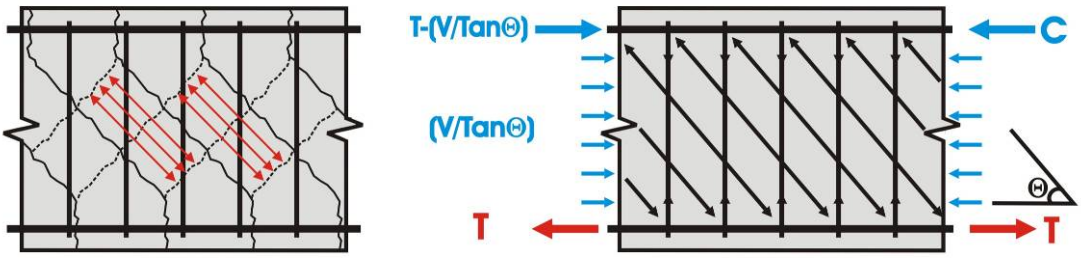

a) Diagonal Compression **b) Truss Mechanism**

Figure 7-2 Truss mechanism providing shear resistance in a plastic hinge zone from Fenwick and Megget (1993)

Beam elongation becomes particularly evident under reverse cyclic loading, where residual elongation is accumulated in each reversing inelastic cycle. Elongation occurs in both bi directional and uni-directional plastic hinges (Fenwick and Megget 1993). Uni-directional plastic hinges are a unique case when the plastic hinge undergoes rotations in only one direction (locally) under reversing drifts of the full frame (globally). This is usually due to gravity load demand dominating the beam behaviour (over the seismic demand), resulting in a plastic hinge forming near the mid-span of the beam rather than at the ends of the beam (as typically is the case for bi-directional plastic hinges). In contrast bi-directional plastic hinges incur reversing rotations (locally) under reversing drifts of the full frame (globally). For this reason bi-directional plastic hinges result in the accumulation of greater amounts of overall beam elongation (Fenwick and Megget 1993). This is due to the reversing neutral axis locations (shown in Figure 7-1) accumulating elongation in each reversing cycle. As a result,

a racketing effect occurs where the beam grows due to alternating stretching of tensile reinforcement and rotation about the neutral axis. Uni-directional hinges result in tensile strains being confined to only one layer of longitudinal reinforcement therefore reducing the elongation accumulation.

The magnitude of beam elongation incurred depends on a number of factors, the most influential of these being the axial force conditions in the beam, and the nature of the loading history. The presence of axial restraint limits the potential for beam elongation through increasing the depth of the neutral axis, reducing the magnitude of tensile strain at the centreline of the beam, as illustrated in Figure 7-3.

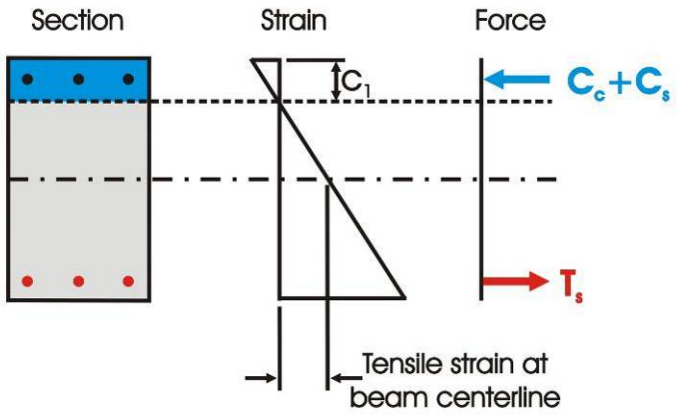

a) Neutral axis depth and resulting elongation without axial restraint

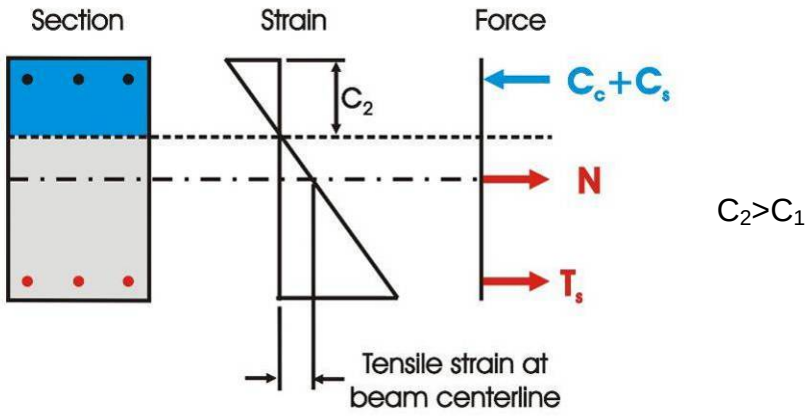

b) Neutral axis depth and resulting elongation with axial restraint

Figure 7-3 - Effect of axial restraint on beam elongation

Axial restraint can come from two sources in full building systems. Firstly the presence of a floor system connected along the length of the beam, and secondly, frame beams of the floors above and below the beam in question (Zerbe and Durrani 1989; Zerbe and Durrani 1990; Lau 2001; Matthews 2004).

The presence of a floor slab also provides additional reinforcement to the beam section, enhancing negative moment capacity (hogging) upon activation and amplified force differential effects due to higher amounts of reinforcement at the floor level. In the case of precast prestressed floor systems spanning past internal columns, the presence of prestressing tendons in the flooring unit can also provide significant axial restraint. Beam elongation restraint of this nature was observed in super-assembly tests carried out by Matthews (2004), Lindsay (2004) and MacPherson (2005).

In terms of the restraint to beam elongation provided by beams on the levels above and below the beam in question, it is unlikely plastic hinges in the beams will form in unison up the height of a frame. This leads to differential amounts of inelastic rotation occurring at different points in time, resulting in beams which elongate to varying amounts. Therefore, beams which elongate less provide axial restraint to those beams around them (through the columns spanning vertically between the beams). Conversely, net tension can also be induced in beams which elongate less than those above and below (Fenwick et al 1996).

The nature of the loading history and rotation of the plastic hinge has a significant effect on the extent of beam elongation. By definition, larger inelastic rotations will result in larger peak and residual elongation. In addition, a larger number of inelastic cycles will also result in larger accumulated elongation. A specific case of this is repeated rotation cycles of the same magnitude, where elongation occurs in subsequent cycles only to a lesser extent in each repeated cycle. The decrease in elongation contribution from repeating cycles has been described as approximately inversely proportional to the number of repeated cycles (Lee and Watanabe 2003).

The influence of the number and magnitude of load (rotation) cycles was summarised by Lee and Watanabe (2003). Four distinct regions describing the longitudinal axial strain behaviour in plastic hinge regions of reinforced concrete beams under reverse cyclic loading were proposed. The four paths are summarised and illustrated in Figure 7-4:

Path 1 ***Pre-flexural yielding and unloading region***, which describes recoverable elastic longitudinal axial strain (elongation), observed up until yielding when loading, and recovered upon unloading.

Path 2 ***Post-flexural yielding region***, where residual longitudinal axial strain (elongation) is generated due to plastic hinge rotation

Path 3 ***Slip region***, where due to the change in direction of loading, little or no change in longitudinal axial strain (elongation) occurs

Path 4 ***Repeated loading region***, where longitudinal axial strain is accumulated upon repeated rotation cycles, the extent of which is described as decreasing approximately inversely proportional to the number of repeated cycles

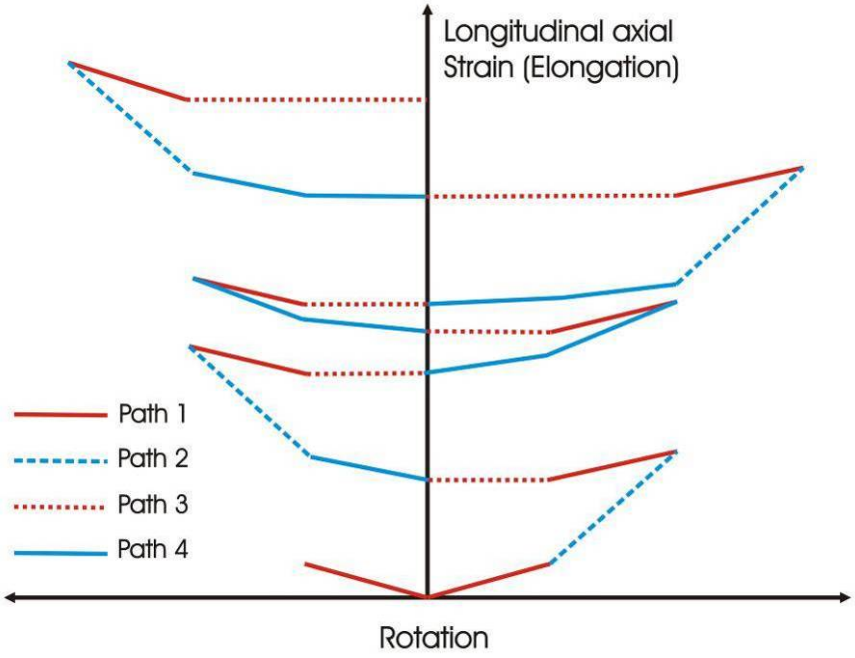

Figure 7-4 Proposed idealization of beam elongation behaviour within plastic hinge regions of reinforced concrete beams after Lee and Watanabe 2003

7.2 Beam Elongation Prediction – Previous Research

A number of numerical approaches have been proposed by previous researchers which predict the expected amount of beam elongation. These fall in two categories: envelope type approaches which predict the maximum beam elongation only (Fenwick and Megget 1993; Restrepo 1993) and more complicated loading history dependant approaches which predict a beam elongation profile from a prescribed loading (rotation) history (Lee and Watanabe 2003; Matthews 2004). All of these methods are rotation based, assuming a neutral axis depth

within the beam section, to infer the amount of beam elongation (or longitudinal axial strain) at the beam centreline. A common agreement between all researchers was the typical plastic hinge elongation was in the order of 2-5% of the beam depth when ductility levels above four were reached. With the exception of Matthews (2004), experimental investigations associated with these numerical approaches have been statically determinate systems without restraint from either a floor slab or adjacent beams above or below. A summary of these techniques describing the benefits and shortcomings of each method is presented.

7.2.1 Envelope Type Beam Elongation Prediction Models

Fenwick and Megget (1993) proposed the concept of uni- and bi-directional plastic hinges (as discussed in Section 7.1) and relationships to predict the accumulated elongation envelope of these hinges. The first of these, for uni-directional plastic hinges is given by Equation (7-1).

$$Extension = \sum \theta (d - d')/2 \qquad \textbf{Equation (7-1)}$$

The net accumulated beam elongation at the centreline of the beam is described in terms of a summation of plastic rotation undergone by the plastic hinges in the beam ($\sum\theta$) over a lever arm of half the distance between centroids of longitudinal reinforcement *(d-d')/2*. Complementary to the uni-directional elongation prediction, a relationship of the same nature was proposed for bi-directional plastic hinges. The difference being, due to the reversing neutral axis position within the beam section due reversing rotation demand, elongation from the previous rotation cycle (e) is added to new rotation as shown in Equation (7-2). The resulting predicted elongation from Equation (7-2) is approximately three times that of Equation (7-1).

$$Extension = e + \sum \theta (d - d')/2 \qquad \textbf{Equation (7-2)}$$

Restrepo (1993) proposed similar upper and lower bound beam elongation envelope prediction relationships. The assumed beam deformation pattern shown in Figure 7-5 illustrates how the two relationships were conceived through geometrical relationships assuming rotation of the plastic hinges occurs about the longitudinal compression reinforcement.

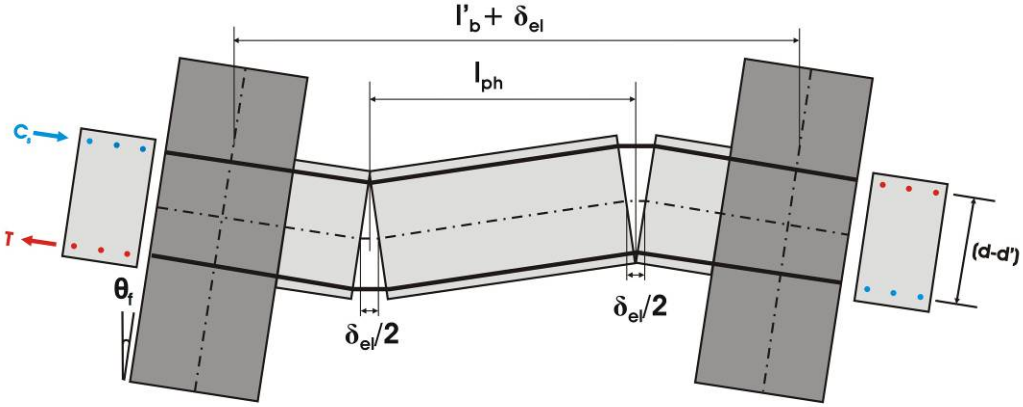

Figure 7-5 Assumed beam deformation attributing to beam elongation adapted from Restrepo et al (1993)

The lower bound formulation given by Equation (7-3) was achieved by assuming a monotonic inelastic push to a prescribed drift level in one direction, resulting in a net elongation. The upper bound was then achieved assuming reversal of rotation in a cyclic manner, resulting in accumulating elongation due to residual tensile strain in compression reinforcement from each previous cycle. As a result, the upper limit given by Equation (7-4) was twice the lower bound.

$$\delta_{el} = \theta_f \frac{l'_b}{l_{ph}}(d - d') \qquad \textbf{Equation (7-3)}$$

$$\delta_{el} = 2\theta_f \frac{l'_b}{l_{ph}}(d - d') \qquad \textbf{Equation (7-4)}$$

Where δ_{el} is the predicted elongation; l'_b is the distance between column centrelines; l_{ph} is the distance between plastic hinges; and *(d-d')* the internal section lever arm. Such an approach does not deal with the loading history and cyclic dependant nature (number of and magnitude of the cycles) of beam elongation. As a result, should the rotation be of a different magnitude in the reversing direction the upper bound relationship is incorrect.

7.2.2 Loading History Depended Beam Elongation Prediction

Lee and Watanabe (2003) proposed a comprehensive model which accounted for the loading dependant nature of beam elongation. Based around a sophisticated numerical section analysis model, loading dependant properties and peculiarities of beam elongation were simplified into four paths to form a continuous, loading dependant longitudinal axial strain

(beam elongation) profile (illustrated in Figure 7-4). The four paths described by Lee and Watanabe (2003) are justified at a section level and described in detail below.

Path1: Pre-flexural yielding or unloading region

The assumed rate of decrease in axial strain is the same as the increasing rate of axial strain in the elastic region. Simplified this equates to determining the longitudinal axial strain (elongation) at the yield rotation (or curvature) through simple section analysis and adding or subtracting that elongation upon onset of load or unloading respectively. This was justified through the observation of stress versus strain behaviour of the top and bottom layers of longitudinal reinforcement from the section analysis from Lee and Watanabe 2003, illustrated in Figure 7-6. Figure 7-4 shows the resulting effect on the longitudinal axial strain (beam elongation) profile. In both figures, Path 1 is illustrated by the solid red line.

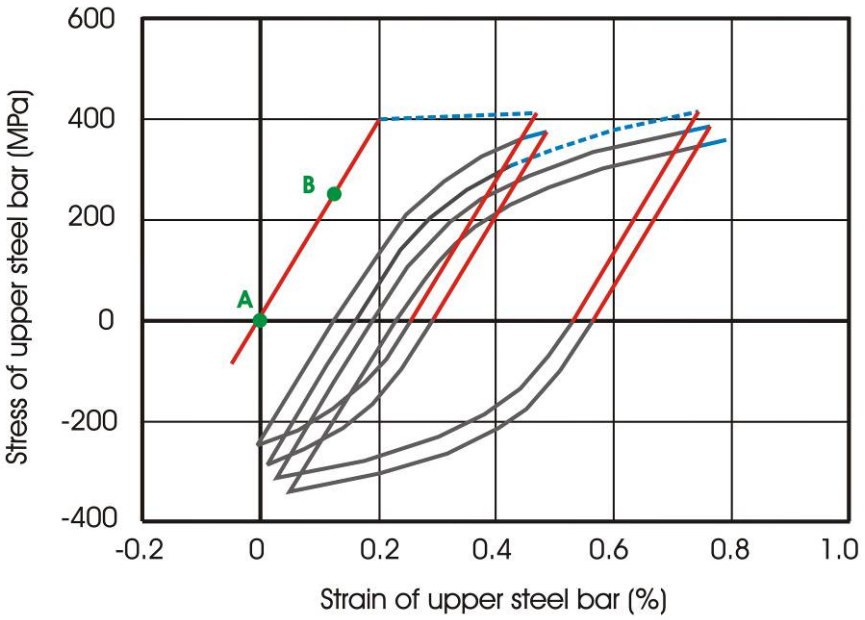

a) Upper reinforcement

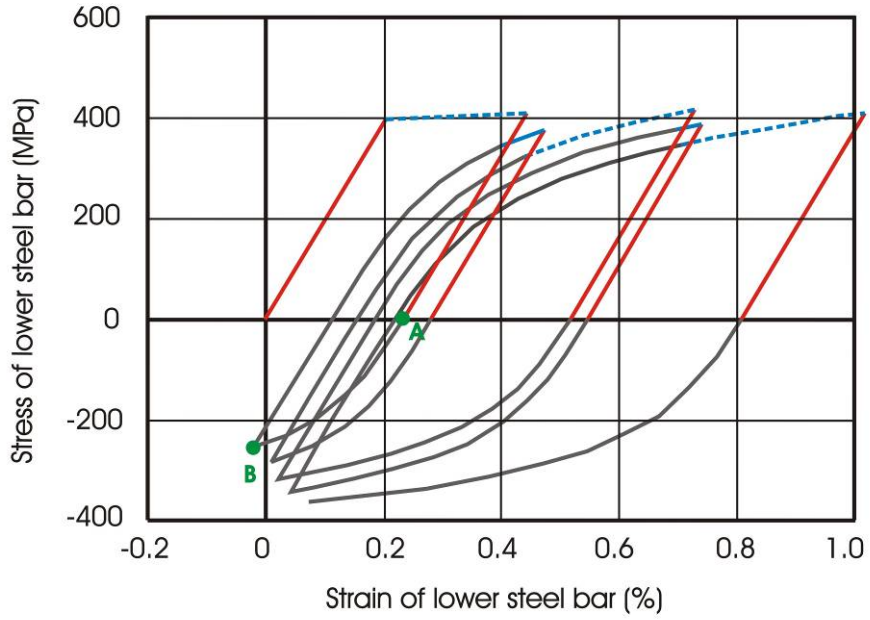

b) Lower reinforcement

Figure 7-6 Stress strain relationship for upper and lower layers of longitudinal reinforcement showing elongation paths after Lee and Watanabe (2003)

Equation (7-5) is the resulting relationship describing Path 1 in a cumulative nature. Where F is the number of unloading cycles beyond flexural yielding and ε_{xf} is the axial strain at flexural yielding.

$$\varepsilon_{Path\,1} = (1 - F)\varepsilon_{xf} \qquad \textbf{Equation (7-5)}$$

Path2: Post-flexural yielding region

Following flexural yielding, longitudinal axial strain increases rapidly, resulting in significant amounts of elongation as the applied rotation increases beyond that for initiation of flexural yielding. This is particularly relevant for the first cycle to a specific inelastic rotation level. This is illustrated in terms of the stress versus strain relationship of the reinforcement from the section analysis in Figure 7-6 and the effect on beam elongation in Figure 7-4, in both figures Path 2 is highlighted by the hashed blue line.

The relationship for longitudinal axial strain resulting from Path 2 is given by Equation (7-6). R_{pmp} and R_{pmn} are the positive and negative inelastic rotations for that cycle respectively, j_d the rotational lever arm within the section, and l_h is the estimated plastic hinge length.

$$\varepsilon_{Path\,2} = \frac{(R_{pmp} + R_{pmn})\,j_d}{2l_h} \qquad \textbf{Equation (7-6)}$$

Path 3: Slip Region

During the change in sign of rotation (and curvature) there is only negligible change in longitudinal axial strain (elongation). This is due to an opposing, similar magnitude change in top and bottom reinforcement strain. This is due to the initial compression of previously tensile reinforcement and extension of previous compression reinforcement. In reality, axial strain actually decreases slightly due to the bauschinger effect on unloading of the previously yielded tensile reinforcement (Lee and Watanabe 2003). The stress versus strain transition from points A to B in Figure 7-6 show the stress strain relationship illustrating Path 3, and red hashed lines in Figure 7-4 illustrate the resulting effect on the longitudinal axial strain (elongation). The resulting relationship for Path 3 is given by Equation (7-7).

$$\varepsilon_{Path\,3} = 0 \qquad \textbf{Equation (7-7)}$$

Path 4: Repeated Loading Region

Under repeated inelastic loading (rotation), the magnitude of longitudinal axial strain (elongation) is described as accumulating in a decreasing manner approximately inversely proportionally to the number of repeated cycles. Path 4 is illustrated in terms of the stress versus strain of longitudinal reinforcement in Figure 7-6 and the effect on the longitudinal axial strain in Figure 7-4 by the solid blue lines. The relationship for Path 4 is given by Equation (7-8) where R_{mi} is the i^{th} rotation component; N_j the number of the j^{th} reload cycle.

$$\varepsilon_{Path\,4} = \sum_{i=1}^{m}\sum_{j=1}^{n}\left(\frac{R_{mi}\,jd}{2l_h}\right)^{0.85}\frac{1}{4N_j}(1 \le N_j \le 5) \qquad \textbf{Equation (7-8)}$$

Finally, the resulting cumulative longitudinal axial strain relationship (elongation profile) is given by Equation (7-9). A summarised envelope of the maximum longitudinal axial strain comprised only of the main elongation contributing Path 2 was also proposed by Lee and Watanabe (2003) as a simpler alternative and is given in Equation (7-10).

$$\varepsilon = (1-F)\varepsilon_{xf} + \frac{(R_{pmp}+R_{pmn})\,jd}{2l_h} + \sum_{i=1}^{m}\sum_{j=1}^{n}\left(\frac{R_{mi}\,jd}{2l_h}\right)^{0.85}\frac{1}{4N_j} \qquad \textbf{Equation (7-9)}$$

$$\varepsilon = \frac{(R_{pmp}+R_{pmn})\,jd}{2l_h} \qquad \textbf{Equation (7-10)}$$

The method proposed by Lee and Watanabe (2003) is comprehensive and describes the important facets of beam elongation. Calibration of the model was carried out with a series of experimental tests which aimed at testing the versatility of the method. Good agreement was found under a variety of monotonic and reverse cyclic rotation loading histories. Like the envelope methods it is rotation based, the important advantage of this method over the envelope methods is the dependence on a loading history (rotation of the plastic hinge). However, the process is complex and is expressed in terms of longitudinal axial strain rather than elongation and does not include any restraint from a floor slab or similar.

Matthews (2004) proposed a method which fitted between the envelope approaches of Fenwick and Megget (1993) and Restrepo (1993), and the approach of

Lee and Watanabe (2003) in terms of complexity. The 'Rainflow' method proposed by Matthews (2004) was also based on rotation of the plastic hinge, which generated rotations from a loading profile, like Lee and Watanabe (2003).

The Rainflow beam elongation prediction method made a simplifying assumption that elongation only occurred under 'new' inelastic rotation. 'New' inelastic rotation was described as being achieved when a previous rotation peak (exceeding elastic limits) was surpassed. Figure 7-7 illustrates the principle of the Rainflow beam elongation prediction in terms of an elongation profile which results from a given loading history.

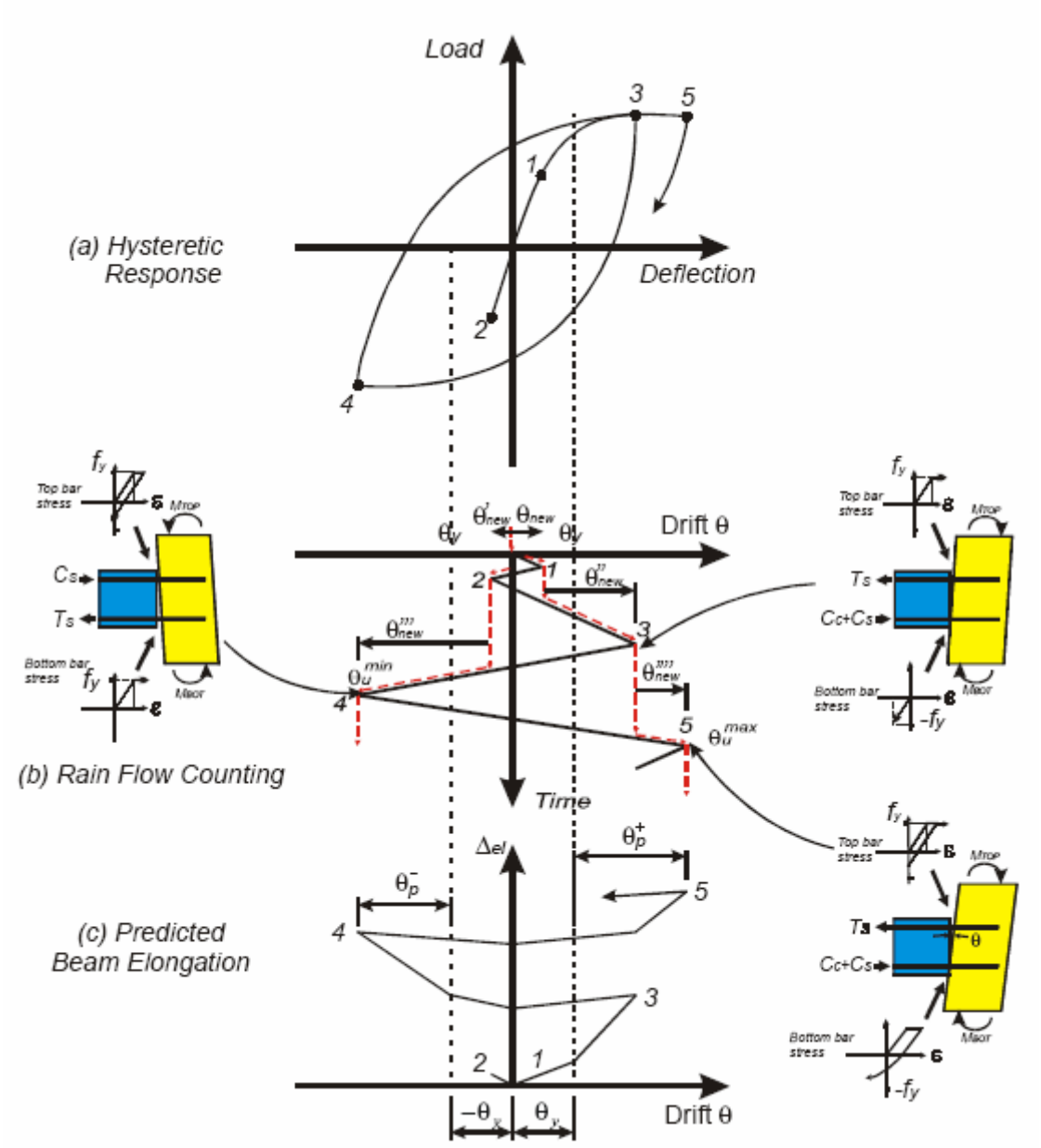

Figure 7-7 Rainflow elongation prediction from Matthews (2004)

Equation (7-11) describes the relationship behind determining elongation using the Rainflow method. θ_p^+ and θ_p^- are the positive and negative plastic rotations, θ_y the yield drift, and $\sum e_{cr}$ the sum of internal lever arms from the neutral axis to centreline of the beam.

$$\Delta_{el} = (\left|\theta_p^{\ +}\right| + \left|\theta_p^{\ -}\right| + \left|\theta_y\right|)\sum e_{cr} \qquad \textbf{Equation (7-11)}$$

The predominant variable or unknown in this relationship is the location of the neutral axis which determines e_{cr} for each hinge. Matthews (2004) calibrated e_{cr} values against measured experimental values for internal and external beam plastic hinges. As a result, the contribution of the hollowcore floor system reinforcement and restraint actions where included. Floor system restraint was particularly applicable for the internal plastic hinges, as the hollowcore flooring units spanned past the internal column in Matthews' (2004) super-assembly test. Figure 7-8 illustrates the internal lever arms (e_{cr}) developed by Matthews (2004).

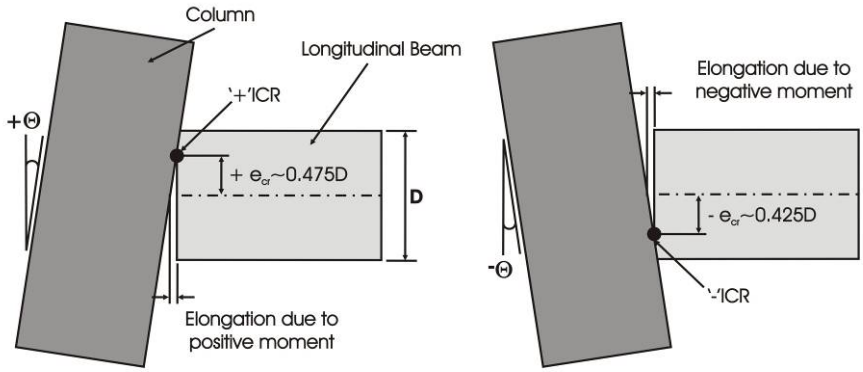

a) Exterior plastic hinge lever arms

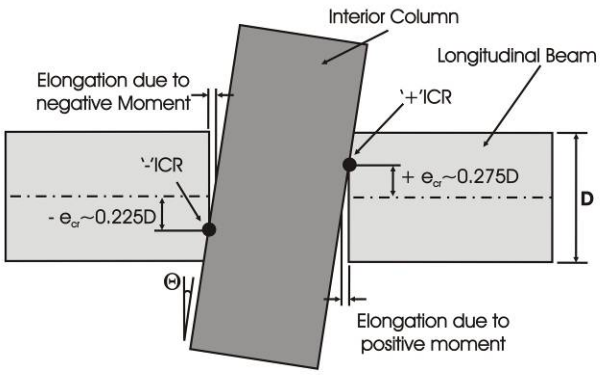

a) Interior plastic hinge lever arms

Figure 7-8 Internal lever arms for interior and exterior beam column joints after Matthews 2004

This approach omits elongation accumulation under repeated rotation cycles of the same magnitude. This facet of beam elongation can contribute significantly to the overall elongation, as described by Lee and Watanabe (2003) (Path 4), and as was observed in a number of experimental tests (MacPherson, 2005; Lindsay, 2004; Lau, 2001; Restrepo, 1993; Fenwick et al 1981). The reason why this was not identified by Matthews (2004) is that the loading profile used had no repeating inelastic drift cycles of the same magnitude.

7.3 Adaptation of Lee and Watanabe/Rainflow

The beam elongation prediction method proposed by Lee and Watanabe (2003) shows good approximation to the beam elongation phenomenon, particularly in recognising the contribution of repeated drift cycles to elongation. However, this approach was complex, in terms of longitudinal axial strain, and did not incorporate the restraint from a floor system. Matthews (2004) proposed a method which was simpler than the method of Lee and Watanabe (2003), and incorporated a floor system. However, Matthews (2004) neglected the elongation contribution of repeated inelastic drift cycles of the same magnitude. In addition to this, the variation in neutral axis position for elastic and inelastic cycles was not recognised. The following section outlines the proposed adaptation of the two methods, which uses simple rigid body rotation like the reviewed prediction methods, accounts for repeated drift cycles of the same magnitude, and has both elastic and inelastic neutral axis positions. The aim of this was to bring the profile generated by the simpler approach of Matthews (2004) to resemble the four paths of elongation proposed by Lee and Watanabe (2003).

7.3.1 Refinement 1 - Drift Cycle Dependence

A significant omission by Matthews' (2004) model was the contribution to beam elongation from repeated inelastic drift cycles of the same magnitude. A number of experimental and analytical investigations have shown that reduced amounts of elongation are incurred for each repeated drift cycle of the same magnitude. Lee and Watanabe (2003) describe this reduction in the incurred longitudinal axial strain in the beam (elongation) as being approximately inversely proportional to the number of repeated cycles.

To incorporate elongation from repeated inelastic drift cycles, reduction factors (k_i) were proposed to apply to the first and second repeated drift cycles of a given magnitude. These factors are applied to the elongation incurred by the first drift cycle (in subsequent cycles) in order to give reduced elongation contribution from the repeating cycles. Only two repeated

cycles are considered, as further elongation contribution would be small and creates unnecessary complication. Table 7-1 summarises the proposed reduction factors. The generation of these values was based on similar values proposed by Lee and Watanabe (2003) and calibration with experimental beam elongation data from Matthews (2004), Lindsay (2004) and MacPherson (2005). The calibration process involved iterative comparisons between the measured beam elongation data sets and the equivalent predictions with varying k_i factors. The main variable for which comparisons were made was the elongation at peak drift levels, particularly at high drifts, where maximum elongations were reached. The reason for this was that the most important aspect for the model to capture was the overall maximum beam elongation or 'pull-off' that would be imposed on the floor system. In addition to this, the final factors of 1.0, 0.5 and 0.25 were selected as they were simple rounded figures.

Table 7-1 Drift cycle reduction factors (k_i)

Drift Cycle Reference	**(i)**	**k_i**
Initial cycle	0	1.00
1st repeated cycle	1	0.50
2nd repeated cycle	2	0.25
3rd repeated cycle	3+	0.00
Elastic unloading cycle	-	1.00

k_i is applied to each positive and negative increment of rotation incurred following first yield. The number of times a drift cycle is repeated is counted (drift cycle reference i) and the appropriate reduction factor applied to give the reduced elongation contribution from that rotation cycle. The first time a rotation increment is incurred the greatest magnitude elongation results (i=0), followed by reducing contributions every repetition after that. In the third repeated cycle (i=3+, the fourth time drift level is reached), slip occurs as described by Path 3 in the approach of Lee and Watanabe (2003). Upon each unloading the recovery of the elastic growth (from the start of that loading cycle) is undergone.

7.3.2 Refinement 2 - Neutral Axis Position

The review of previous research shows that the neutral axis depth of a reinforced concrete beam section is a dominant variable which controls the extent of elongation for a given rotation. There are a number of factors which can affect neutral axis depth: the presence of floor slab reinforcement, unsymmetrical longitudinal beam reinforcement, axial restraint from a floor system and beams of the story above and below, and above all, the ductility demand (magnitude of rotation) on the beam. Given the structural conditions of the beam and floor system, the neutral axis position of the beam will continually change under changing rotation or ductility demand.

Previous envelope elongation prediction methods assumed rotation occurs about the longitudinal compression steel. Matthews (2004) estimated internal lever arm (e_{cr}) values from experimental results as shown in Figure 7-8. The e_{cr} values suggested by Matthews (2004) or very similar values, for bare hinges without a floor system, were used in this investigation. In addition to this, a reduction of the internal lever arm values proposed by Matthews (2004) was implemented for the elastic elongation contribution. The elastic internal lever arm was in the order of 60-70% of that used for the plastic elongation contribution, and this was estimated approximately using simple section analysis. The aim of this was to incorporate a distinction between elastic and plastic elongation contribution due to different neutral axis positions for the two conditions. This was thought to be important due to the accumulating nature of beam elongation and the number of times elastic elongation or recovery occurs under cyclic loading. Figure 7-9 illustrates the typical e_{cr} values used in this investigation.

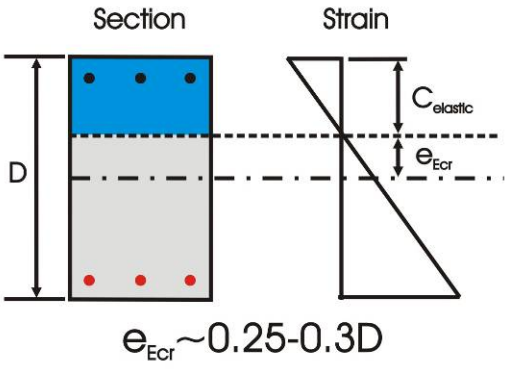

a) Elastic internal lever arm assumption

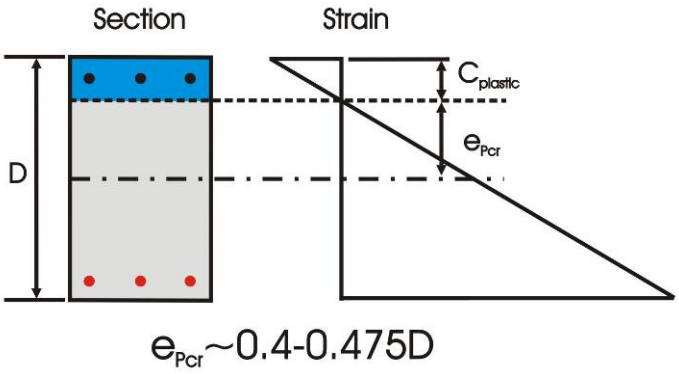

b) Plastic internal lever arm assumption

Figure 7-9 Elastic and plastic e_{cr} assumptions

7.3.3 Adapted Elongation Prediction Procedure

The following process outlines the method for carrying out the elongation prediction. The primary information required is the drift or rotation history of the plastic hinge (or overall frame), the yield drift or rotation of the beam section, and the depth of the beam section (D). The calculation process is stepped out and is represented schematically in Figure 7-10 (an example spreadsheet calculation is also shown in Appendix D):

- **Step 1** From the beam properties determine the yield rotation (θ_y) (generally in the order of 0.4-0.5% drift)

- **Step 2** Break the inelastic (plastic) loading cycles into rotation increments (θ_{pi}). The rotation increments are governed by previous loading peaks, where the increment for a specified drift level is the previous peak subtracted

from the new peak. The reason for this is to enable the application of the appropriate k_i factor to each repeated rotation increment. This results in controlling the transition from maximum elongation (k_i=1.0) contribution of 'new' inelastic rotation, to no elongation or slip once the drift increment has been repeated three times (k_i =0.0)

- **Step 3** Specify the internal lever arms, e_{Ecr} (elastic) and e_{Pcr} (plastic) based on the structural nature of member, presence of activated floor slab and restraint conditions. Values from Matthews (2004) shown in Figure 7-8 and elastic modification from Figure 7-9 or similar values (based on a simple section analysis) are recommended.

- **Step 4** Determine elastic ($\Delta_{elastic}$) and plastic (Δ_{pi}) elongation contributions for positive and negative rotation increments. Equation (7-12) and Equation (7-13) represent the elastic ($\Delta_{elastic}$) and plastic (Δ_{pi}) elongation contributions.

$$\Delta_{elastic} = k_i e_{Ecr} \theta_y \qquad \textbf{Equation (7-12)}$$

$$\Delta_{pi} = k_i e_{Pcr} \theta_{pi} \qquad \textbf{Equation (7-13)}$$

- **Step 5** Sum the individual elongation contributions in a cumulative manner at each elastic and inelastic load increment based on the loading history to form the elongation profile. The elastic recovery upon unloading (change in rotation direction) must be included, followed by slip back to zero rotation position of the plastic hinge. This involves counting the number of repeated cycles to determine how many times a drift increment is incurred. Equation (7-14) and Equation (7-15) represent the cumulative peak and residual (following unloading) elongations as illustrated in Figure 7-10.

$$\Delta_{Peak} = \Delta_{elastic} + \sum \Delta_{Pi}$$ **Equation (7-14)**

$$\Delta_{R\,esidual} = \Delta_{Peak} - \Delta_{elastic}$$ **Equation (7-15)**

Where: Δ_{Peak} is the elongation at a loading cycle peak

$\Delta_{Residual}$ is the unloading and zero rotation elongation

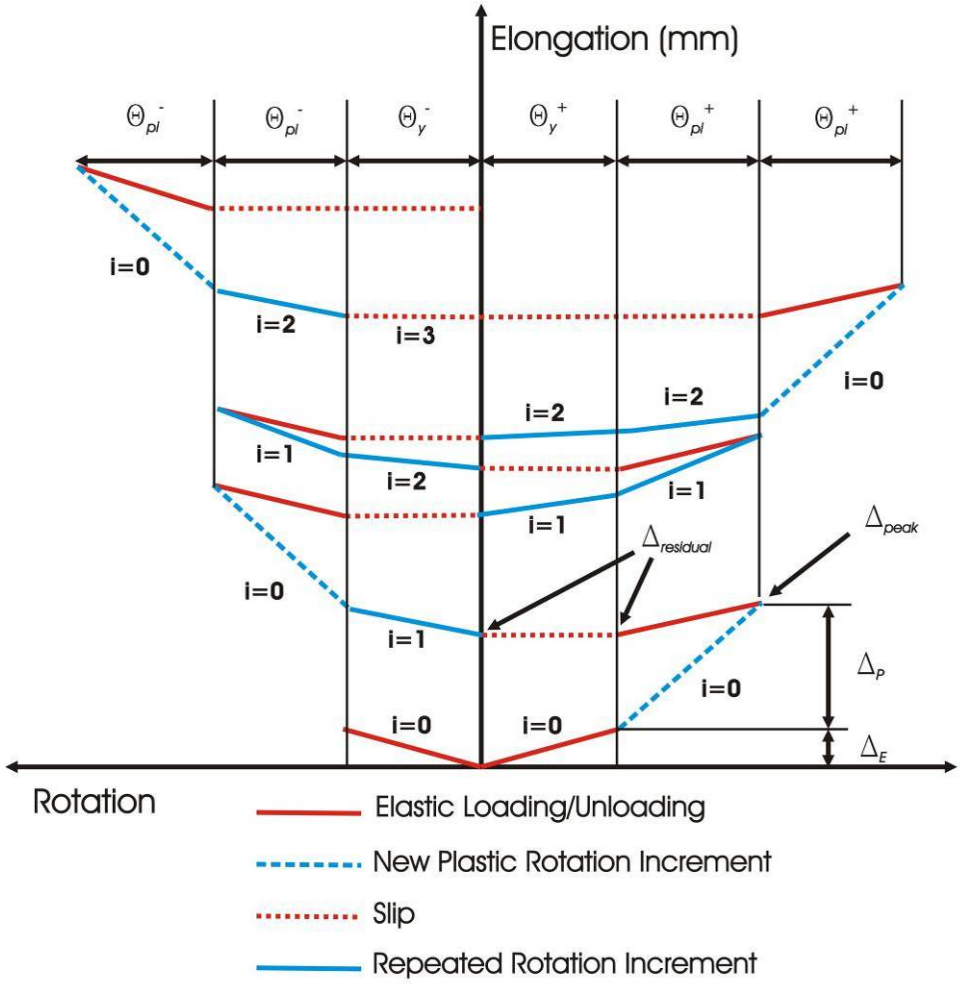

Figure 7-10 Elongation prediction schematic adapted from Lee and Watanabe (2003)

Figure 7-11 below illustrates an example comparison of the method proposed by Matthews (2004) (green plot) and the proposed modified method (blue plot), compared with measured elongation data (red plot). Two example beam elongation predictions are shown in

Figure 7-11. These were from a single hinge, Hinge 7, (see Figure 7-12) from Lindsay (2004) and a combined frame bay, West transverse bay (see Figure 7-12), from MacPherson (2005).

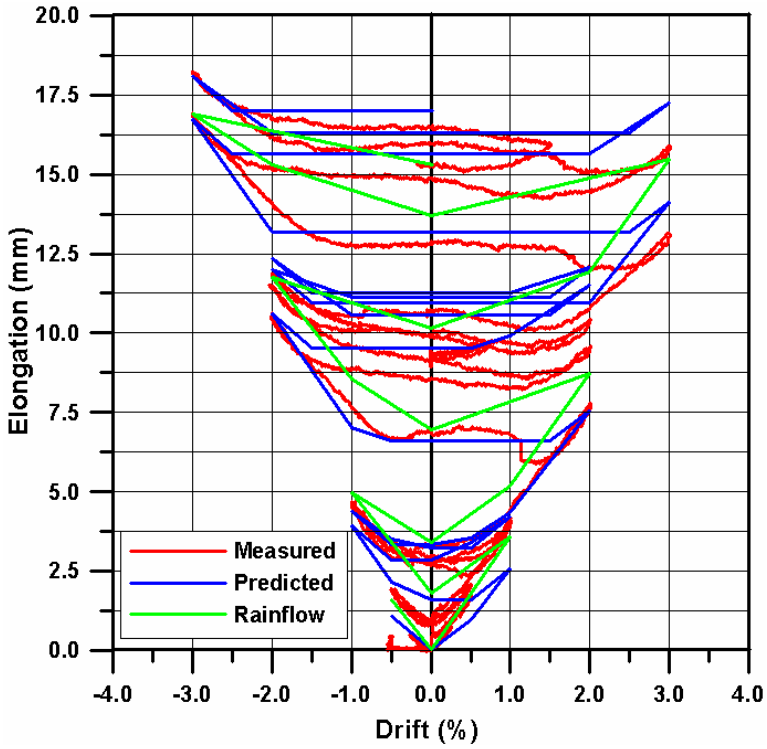

a) Single hinge elongation prediction from Lindsay (2004)

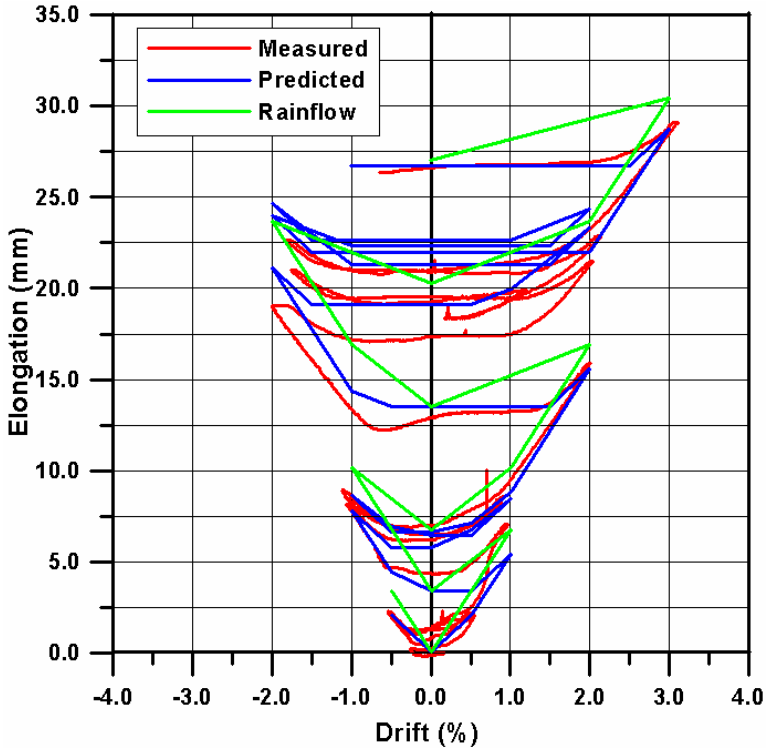

b) Combined bay elongation prediction from MacPherson (2005)

Figure 7-11 Comparison between Rainflow and the modified method beam elongation prediction

There are two important points to note from Figure 7-11. This first of these is the absence of increasing elongation under repeated drift cycles of the green line (Matthews (2004) method). Figure 7-11 shows one green peak representing a number of red peaks (2 or 3, depending on the number of repeated cycles), in contrast to the blue line (adapted method). The second point to note, particularly in Figure 7-11 b) is the better match of the first elastic cycle between the blue and red line (measured elongation data) than the green and red line. These two facets are what have been modified from the original method proposed by Matthews (2004) to improve the representation of the beam elongation phenomenon.

7.3.4 Prediction Simplifications

The proposed beam elongation prediction method is simple and assumes the hinge is detailed sufficiently to allow flexure governed plastic hinge behaviour to occur. There are a number of aspects of real plastic hinge behaviour which are not accounted for as a result of this. Particularly, the nature of the detailing of the plastic hinge is neglected, mainly the nature of the transverse reinforcement. As a result, aspects which can affect the extent of beam elongation, such as shear deformation, confinement, longitudinal bar buckling, strain penetration, and bond slip are not accounted for. It is likely that this will not be an issue for rotations below 2-2.5% given the buildings of interest are post-1970's and should incorporate capacity design principles ductile design and detailing considerations for plastic hinge zones. However, under higher rotations above 2-2.5% the effectiveness of the hinge detailing will likely have a significant effect on the accuracy of the beam elongation prediction. For hinges which are not detailed to achieve high levels of ductility it is likely the prediction method will over estimate the beam elongation.

In this investigation, frame or column interstorey drift was considered to equate directly to beam rotation. This is not explicitly correct, as in reality, the beam will potentially undergo larger rotations that the frame drift due to geometric reasons such as the depth of the column and length of the plastic hinge in the beam. This is illustrated in Figure 7-5, where the rotation of the plastic hinges (locally) is greater than the frame drift (globally). The difference between the two is a function of the distance between the centrelines of the columns divided by the distance between the rotation points of the plastic hinges (l'_b/l_{ph}). For this reason, the depth of the columns and the length of the plastic hinges can affect the magnitude of the difference between the local hinge rotation and the global frame drift (the larger the column depth and plastic hinge length the greater the difference).

There were two reasons for this simplification, firstly in order to reduce computational effort and secondly for consistency. In terms of consistency, the internal lever arms were developed by Matthews (2004) under the same column to beam drift assumption. Therefore, in order to incorporate the structural properties of the super-assembly and utilise the internal lever arms (e_{cr}) from Matthews (2004), this simplification was held.

In a similar manner, no reference was made to the variation in hollowcore seating and longitudinal perimeter floor to frame system connections. These aspects could have an effect on plastic hinge behaviour depending on the extent of interaction between the two structural systems. This aspect was also ignored in the interests of simplicity.

7.4 Comparisons with Measured Experimental Beam Elongation

Comparisons of the adapted elongation prediction model with measured plastic hinge elongation profiles from a number of experimental investigations are made in this section. The first of these was with data from Matthews (2004), Lindsay (2004) and MacPherson (2005), who carried out super-assembly tests which incorporated a hollowcore floor system. This data was used to calibrate the adapted elongation model, particularly the k_i factors for the beam elongation accumulation from repeated drift cycles of the same magnitude. Comparisons were made with the first longitudinal and transverse load cycles for each hinge in the respective directions of the three super-assembly tests. Figure 7-12 illustrates the plastic hinge references and loading directions for the super-assembly comparisons.

Calibration was carried out on transverse beams which spanned orthogonally to the one-way flooring units. The reason for this was the measured elongation profiles were generally less disordered than the plastic hinges of the longitudinal beams, spanning parallel to the floor units. Following this, comparisons were made with bare plastic hinge (no floor system) experimental beam elongation data from Fenwick et al (1981), Restrepo (1993) and Lau (2001). All of these researchers carried out experimental work at a sub- or super-assembly level of some description, which involved cyclic loading of reinforced concrete beams (resulting in beam elongation). Internal lever arms were reduced to 0.4D for the bare beams (plastic hinges) based on the absence of interference from a connected floor system. This was based on simple section analyses which shown in Appendix D.

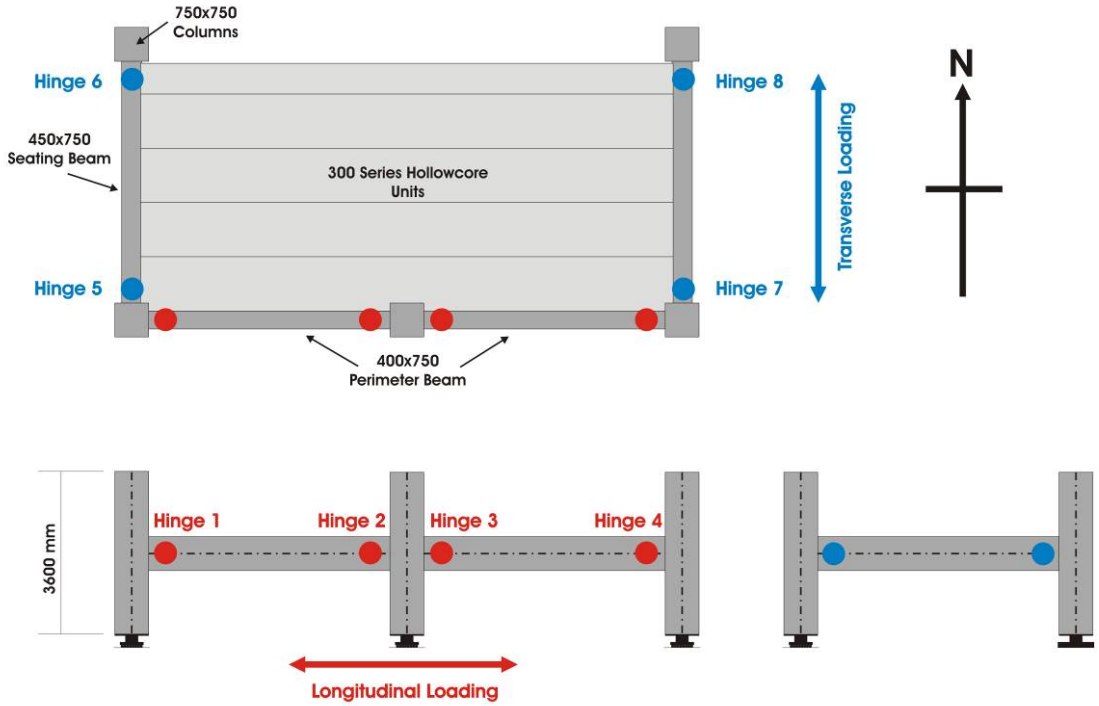

Figure 7-12 Super-Assembly hinge reference locations and loading directions

7.4.1 Matthews (2004) Super-Assembly Test

Figure 7-13 through Figure 7-19 show the comparison between the predicted and measured beam elongation profiles for individual plastic hinges 1 through 4, the combined East and West bays, and the entire frame in the longitudinal loading direction. In addition to each elongation profile (with respect to drift (or rotation)) a summary of the beam elongation at peak drift levels is shown. This includes a percentage difference between measured and predicted beam elongation values with respect to the maximum measured beam elongation. A negative percentage difference represents under-prediction of elongation, and a positive percentage difference over-prediction. This format of presentation is consistent for all the comparisons presented.

Good agreement between the measured and predicted beam elongation was generally seen, with some under and over prediction at higher drifts in hinges 2 and 4. This over prediction was carried through to the West and East bay predictions. Interestingly, over prediction on some hinges and under prediction on others cancelled out to give a good overall frame prediction. This suggests there is potential for variability in the beam elongation of individual hinges, but in general the individual variability is 'ironed' out in the overall global frame

elongation when a number of plastic hinge contributions are combined, and the prediction approach holds.

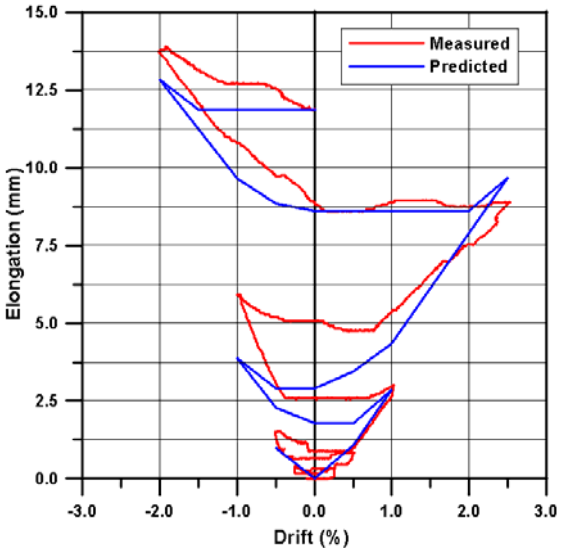

Hinge 1			
Drift (%)	e_{Theory} (mm)	$e_{Measured}$(mm)	$\%_{difference}$
0.5	1.1	0.9	1.2
-0.5	1.0	1.5	-3.9
1.0	2.9	2.6	1.8
-1.0	3.9	5.8	-14.1
2.5	9.7	8.9	5.5
-2.0	12.8	13.8	-7.1
0.0	11.9	12.0	-1.0

Figure 7-13 Hinge 1 beam elongation prediction comparison for Matthews (2004) longitudinal elongation data

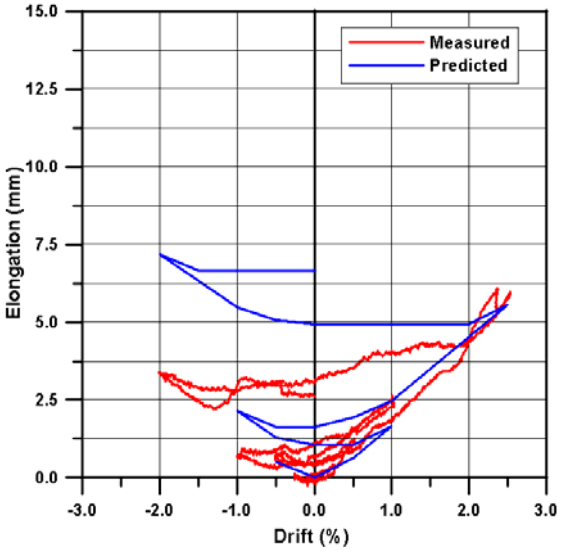

Hinge 2			
Drift (%)	e_{Theory} (mm)	$e_{Measured}$(mm)	$\%_{difference}$
0.5	0.6	1.2	-9.7
-0.5	0.5	0.7	-3.2
1.0	1.7	2.6	-15.8
-1.0	2.1	0.9	20.5
2.5	5.5	6.0	-7.7
-2.0	7.2	3.4	62.6
0.0	6.7	2.6	67.5

Figure 7-14 Hinge 2 beam elongation prediction comparison for Matthews (2004) longitudinal elongation data

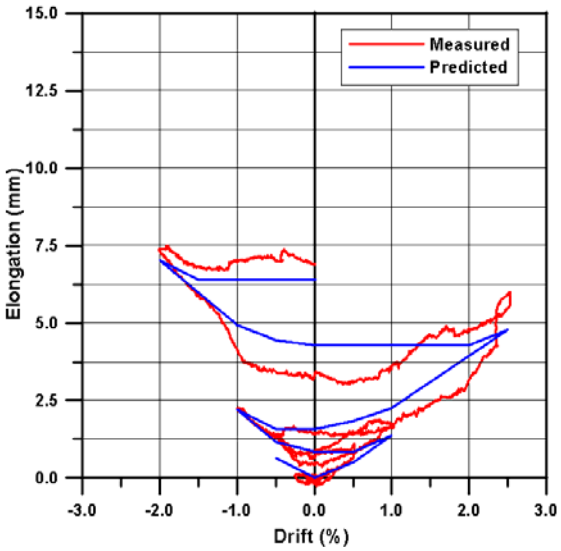

Hinge 3			
Drift (%)	e_{Theory} (mm)	$e_{Measured}$(mm)	$\%_{difference}$
0.5	0.5	1.6	-14.8
-0.5	0.6	1.3	-9.2
1.0	1.4	1.7	-4.7
-1.0	2.2	2.3	-1.6
2.5	4.8	5.9	-15.2
-2.0	7.0	7.4	-5.4
0.0	6.4	6.9	-7.0

Figure 7-15 Hinge 3 beam elongation prediction comparison for Matthews (2004) longitudinal elongation data

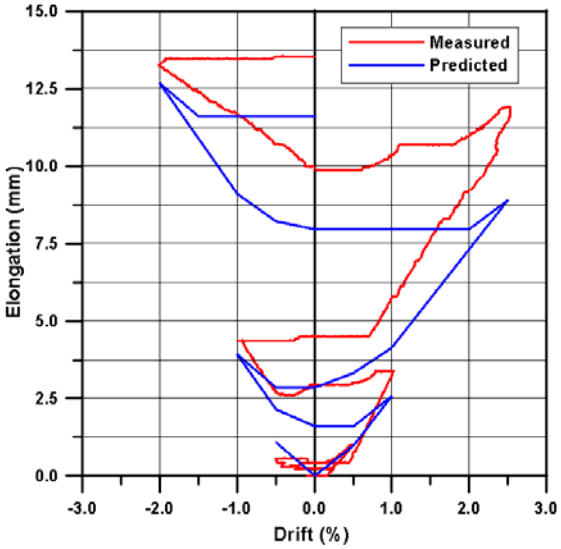

Hinge 4			
Drift (%)	e_{Theory} (mm)	$e_{Measured}$(mm)	$\%_{difference}$
0.5	1.0	1.0	-0.3
-0.5	1.1	0.6	3.5
1.0	2.6	3.4	-6.3
-1.0	3.9	4.4	-3.6
2.5	8.9	11.9	-22.2
-2.0	12.7	13.2	-4.0
0.0	11.6	13.5	-14.1

Figure 7-16 Hinge 4 beam elongation prediction comparison for Matthews (2004) longitudinal elongation data

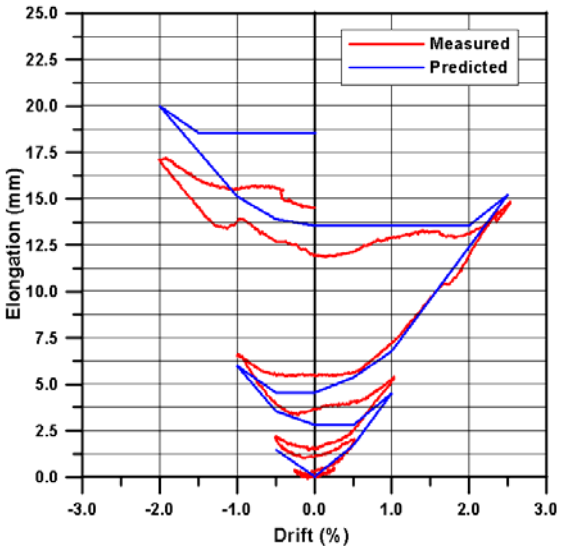

West Bay			
Drift (%)	e_{Theory} (mm)	$e_{Measured}$(mm)	$\%_{difference}$
0.5	1.7	2.6	-4.4
-0.5	1.5	1.9	-2.1
1.0	4.5	5.1	-2.9
-1.0	6.0	6.7	-3.5
2.5	15.2	17.8	-12.6
-2.0	20.0	20.6	-3.0
0.0	18.5	20.4	-9.1

Figure 7-17 West Bay beam elongation prediction comparison for Matthews (2004) longitudinal elongation data

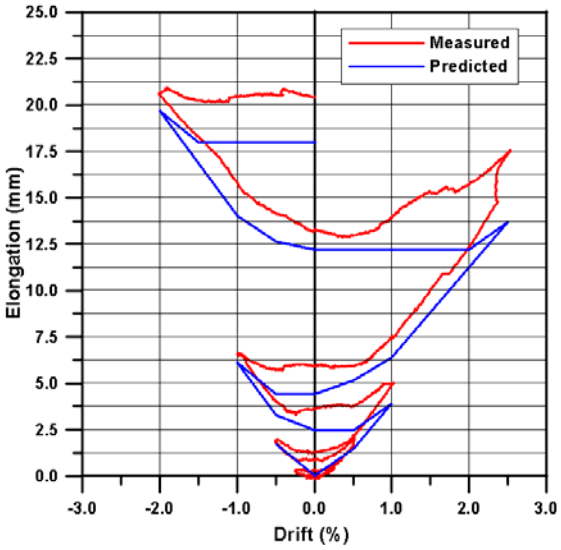

East Bay			
Drift (%)	e_{Theory} (mm)	$e_{Measured}$(mm)	$\%_{difference}$
0.5	1.5	2.1	-3.7
-0.5	1.7	2.2	-3.0
1.0	3.9	5.2	-7.6
-1.0	6.1	6.7	-3.5
2.5	13.7	14.9	-7.2
-2.0	19.7	17.2	14.3
0.0	18.0	14.6	19.6

Figure 7-18 East Bay beam elongation prediction comparison for Matthews (2004) longitudinal elongation data

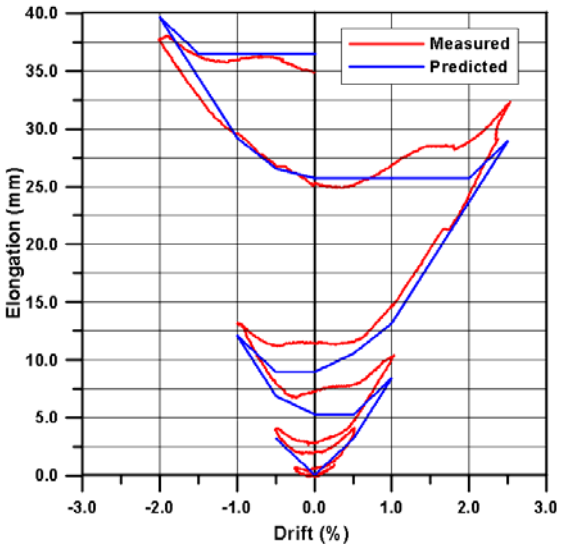

Whole Frame			
Drift (%)	e_{Theory} (mm)	$e_{Measured}$(mm)	$\%_{difference}$
0.5	3.2	4.7	-4.1
-0.5	3.2	4.1	-2.5
1.0	8.4	10.3	-5.0
-1.0	12.1	13.4	-3.5
2.5	28.9	32.7	-10.1
-2.0	39.6	37.8	4.9
0.0	36.5	35.0	3.9

Figure 7-19 Entire Frame beam elongation prediction comparison for Matthews (2004) longitudinal elongation data

Figure 7-20 through Figure 7-25 illustrate the prediction comparison for hinges 5 through 8 and the combined East and West transverse bays. Hinges 6 and 8 showed good agreement; however, hinges 5 and 7 were inaccurate. This inaccuracy filters down into the prediction for each combined East and West bay. This again shows the variable nature of beam elongation of individual hinges.

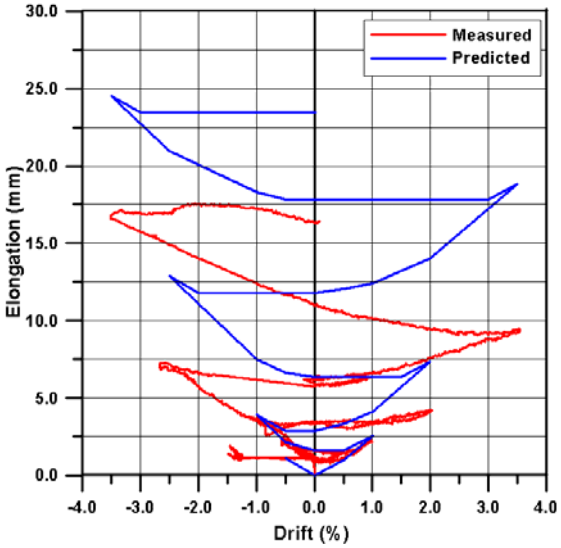

Hinge 5			
Drift (%)	e_{Theory} (mm)	$e_{Measured}$(mm)	$\%_{difference}$
0.5	1.0	1.4	-2.6
-0.5	1.1	2.5	-8.5
1.0	2.6	2.2	2.1
-1.0	3.9	3.4	3.0
2.0	7.3	4.0	19.5
-2.5	12.8	7.3	32.8
3.5	18.8	9.3	56.2
-3.5	24.5	16.9	45.1
0.0	23.4	16.3	42.3

Figure 7-20 Hinge 5 beam elongation prediction comparison for Matthews (2004) Transverse elongation data

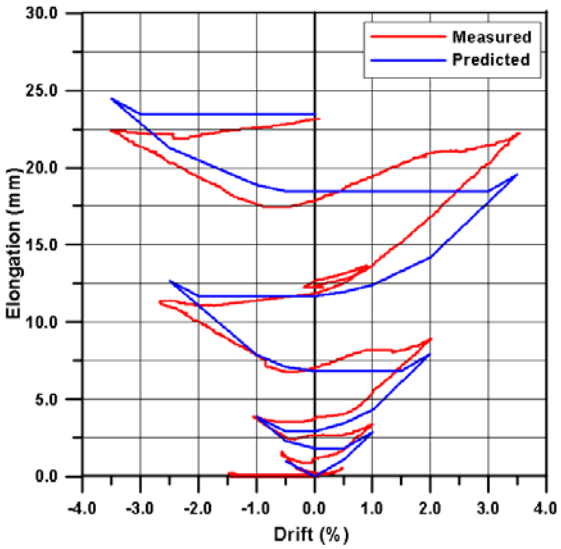

Hinge 6			
Drift (%)	e_{Theory} (mm)	$e_{Measured}$(mm)	$\%_{difference}$
0.5	1.1	0.4	2.9
-0.5	1.0	1.3	-1.5
1.0	2.9	3.2	-1.5
-1.0	3.9	3.8	0.2
2.0	7.9	8.9	-4.4
-2.5	12.6	11.3	5.7
3.5	19.5	22.2	-11.6
-3.5	24.4	22.4	8.7
0.0	23.5	23.2	1.1

Figure 7-21 Hinge 6 beam elongation prediction comparison for Matthews (2004) Transverse elongation data

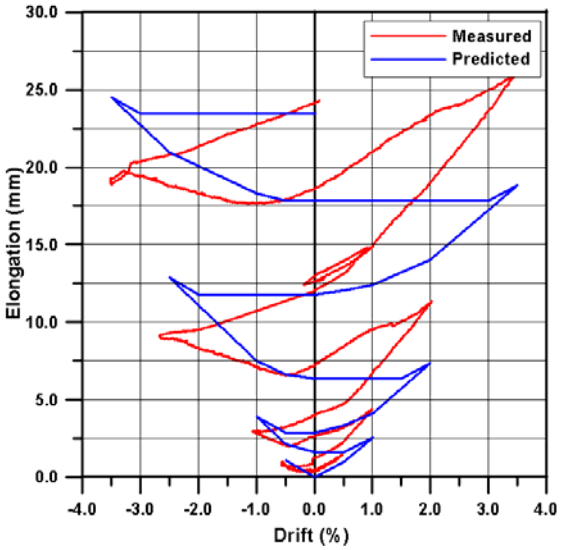

Hinge 7			
Drift (%)	e_{Theory} (mm)	$e_{Measured}$(mm)	$\%_{difference}$
0.5	1.0	1.2	-0.9
-0.5	1.1	0.9	0.6
1.0	2.6	4.2	-6.3
-1.0	3.9	2.9	3.9
2.0	7.3	11.3	-15.3
-2.5	12.8	9.2	14.0
3.5	18.8	26.1	-28.0
-3.5	24.5	18.9	21.5
0.0	23.4	24.3	-3.3

Figure 7-22 Hinge 7 beam elongation prediction comparison for Matthews (2004) Transverse elongation data

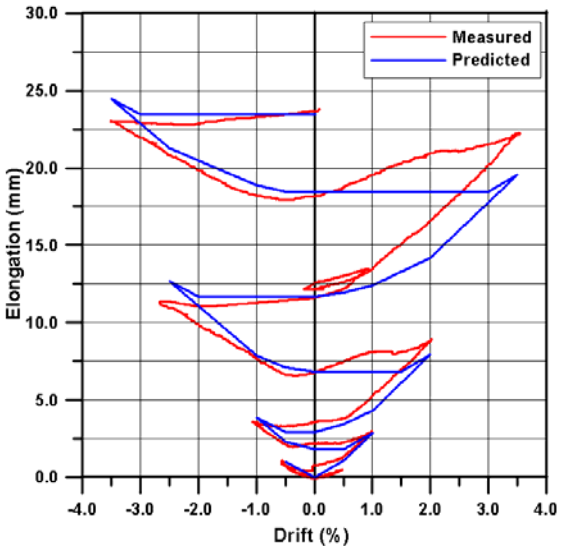

Hinge 8			
Drift (%)	e_{Theory} (mm)	$e_{Measured}$(mm)	$\%_{difference}$
0.5	1.1	0.4	2.8
-0.5	1.0	0.9	0.2
1.0	2.9	2.8	0.2
-1.0	3.9	3.5	1.5
2.0	7.9	8.9	-4.3
-2.5	12.6	11.3	5.6
3.5	19.5	22.2	-11.3
-3.5	24.4	23.0	6.0
0.0	23.5	23.7	-1.0

Figure 7-23 Hinge 8 beam elongation prediction comparison for Matthews (2004) Transverse elongation data

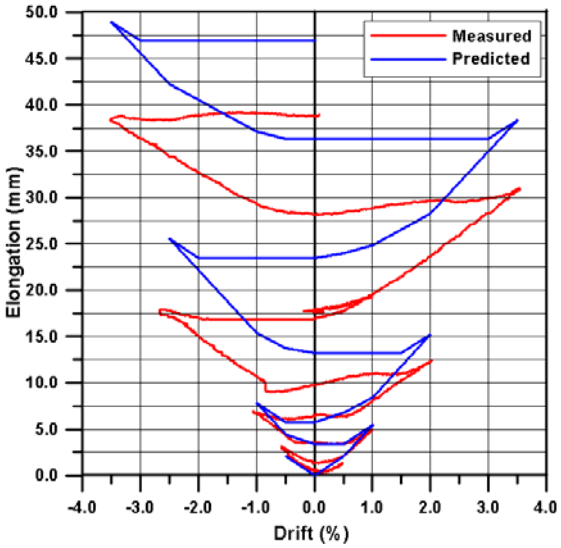

West Bay			
Drift (%)	e_{Theory} (mm)	$e_{Measured}$(mm)	$\%_{difference}$
0.5	2.0	1.8	0.6
-0.5	2.0	3.8	-4.5
1.0	5.4	5.4	0.0
-1.0	7.8	7.2	1.4
2.0	15.2	12.9	5.8
-2.5	25.5	18.6	17.4
3.5	38.3	31.5	17.2
-3.5	48.9	39.3	24.4
0.0	46.9	39.5	18.8

Figure 7-24 West bay beam elongation prediction comparison for Matthews (2004) Transverse elongation data

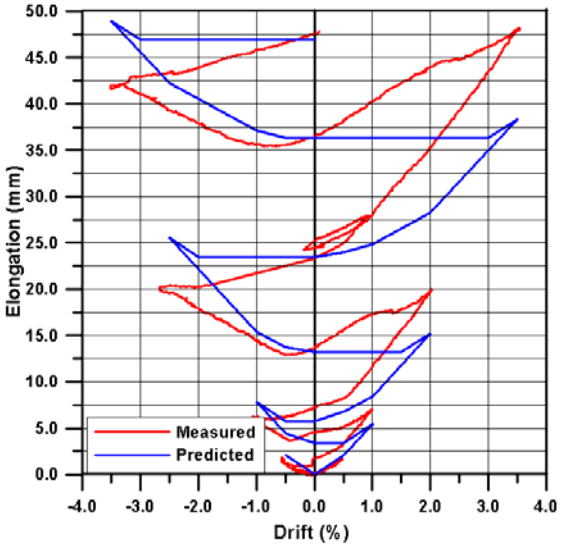

East Bay			
Drift (%)	e_{Theory} (mm)	$e_{Measured}$(mm)	$\%_{difference}$
0.5	2.0	1.6	0.9
-0.5	2.0	2.0	0.1
1.0	5.4	5.4	0.1
-1.0	7.8	7.4	0.7
2.0	15.2	16.2	-2.1
-2.5	25.5	24.1	2.8
3.5	38.3	47.5	-19.4
-3.5	48.9	41.0	16.7
0.0	46.9	47.1	-0.5

Figure 7-25 East bay beam elongation prediction comparison for Matthews (2004) Transverse elongation data

7.4.2 Lindsay (2004) Super-Assembly Test

Observing longitudinal elongation comparisons from Lindsay (2004), shown in Figure 7-26 through Figure 7-32, it can be seen the peak beam elongation values were predicted quite well. However, due to varying degrees of skew between elongation induced by positive and negative drift, the overall predicted elongation profile in terms of shape was quite inaccurate. This was particularly evident for the internal plastic hinges (Hinges 2 and 3), which the floor system spanned passed. This suggests the floor system played a significant role in restraining the beam elongation, more so than was observed by Matthews (2004). Hinge 2 in Matthews (2004) test (Figure 7-14 b)) showed similar restraint against elongation under negative drift. The restraint of elongation was observed when the neutral axis was located in the top of the beam (when the bottom of the beam as trying to open), putting bottom longitudinal reinforcement into tension.

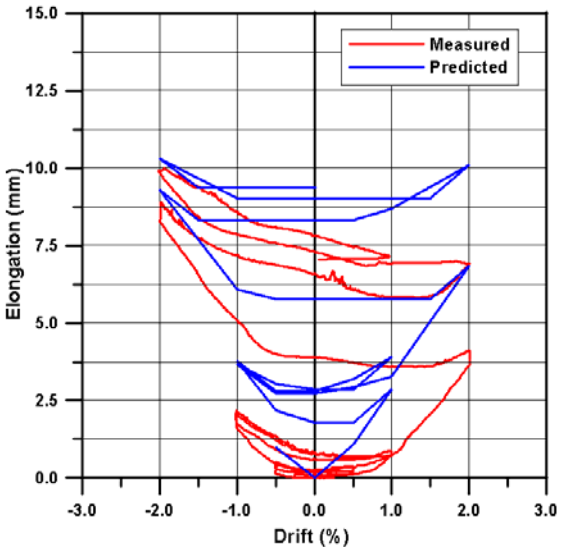

Hinge 1			
Drift (%)	e_{Theory} (mm)	$e_{Measured}$(mm)	$\%_{difference}$
0.5	1.1	0.4	6.8
-0.5	1.0	0.5	4.6
0.5	1.1	0.4	6.8
-0.5	1.0	0.5	4.6
1.0	2.9	0.7	21.7
-1.0	3.8	1.8	19.8
1.0	3.9	0.7	32.3
-1.0	3.7	2.1	15.7
2.0	6.8	4.0	28.6
-2.0	9.3	8.9	3.7
2.0	10.1	6.9	32.3
-2.0	10.3	9.9	4.1
0.0	9.3	7.0	23.7

Figure 7-26 Hinge 1 beam elongation prediction comparison for Lindsay (2004) longitudinal elongation data

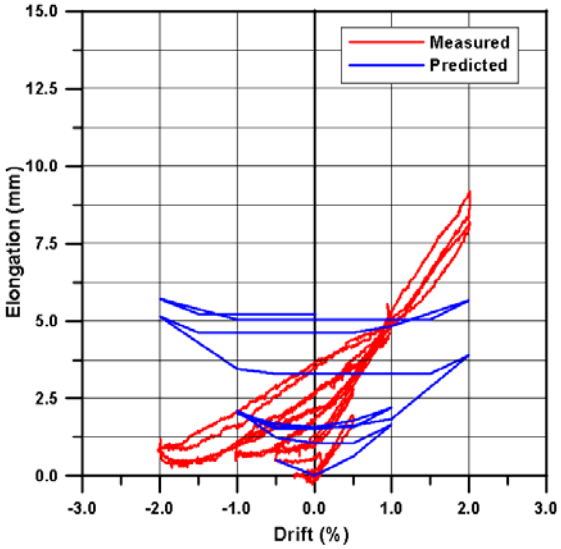

Hinge 2			
Drift (%)	e_{Theory} (mm)	$e_{Measured}$(mm)	$\%_{difference}$
0.5	0.6	2.0	-15.0
-0.5	0.5	0.7	-2.1
0.5	0.6	2.5	-20.4
-0.5	0.5	0.7	-2.1
1.0	1.7	4.5	-31.0
-1.0	2.1	0.8	13.9
1.0	2.2	4.5	-25.1
-1.0	2.0	0.8	13.1
2.0	3.9	7.8	-42.5
-2.0	5.1	0.8	47.1
2.0	5.7	9.2	-38.5
-2.0	5.7	0.8	53.4
0.0	5.2	3.7	16.4

Figure 7-27 Hinge 2 beam elongation prediction comparison for Lindsay (2004) longitudinal elongation data

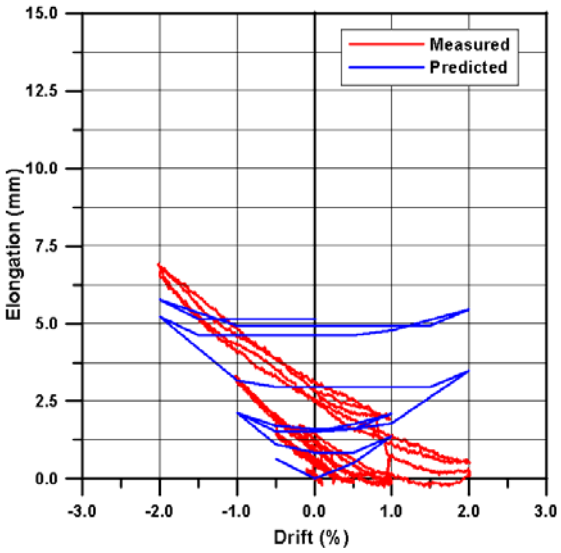

Hinge 3			
Drift (%)	e_{Theory} (mm)	$e_{Measured}$(mm)	$\%_{difference}$
0.5	0.5	0.1	5.9
-0.5	0.6	1.4	-11.3
0.5	0.5	0.1	5.9
-0.5	0.6	1.4	-11.3
1.0	1.4	0.1	18.1
-1.0	2.1	3.2	-15.6
1.0	2.1	0.1	28.8
-1.0	2.1	3.2	-15.7
2.0	3.5	0.2	47.2
-2.0	5.2	6.7	-21.4
2.0	5.4	0.5	71.7
-2.0	5.8	6.9	-16.5
0.0	5.1	3.1	29.6

Figure 7-28 Hinge 3 beam elongation prediction comparison for Lindsay (2004) longitudinal elongation data

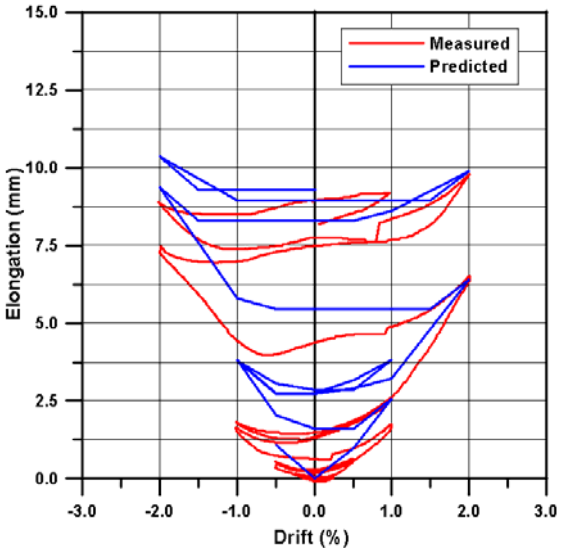

Hinge 4			
Drift (%)	e_{Theory} (mm)	$e_{Measured}$(mm)	$\%_{difference}$
0.5	1.0	0.6	3.7
-0.5	1.1	0.5	5.9
0.5	1.0	0.6	3.7
-0.5	1.1	0.7	3.8
1.0	2.6	1.7	8.8
-1.0	3.8	1.6	22.7
1.0	3.8	2.7	11.3
-1.0	3.8	1.7	21.3
2.0	6.4	6.4	0.0
-2.0	9.4	7.3	21.2
2.0	9.9	9.7	1.9
-2.0	10.4	8.8	16.0
0.0	9.3	8.2	11.2

Figure 7-29 Hinge 4 beam elongation prediction comparison for Lindsay (2004) longitudinal elongation data

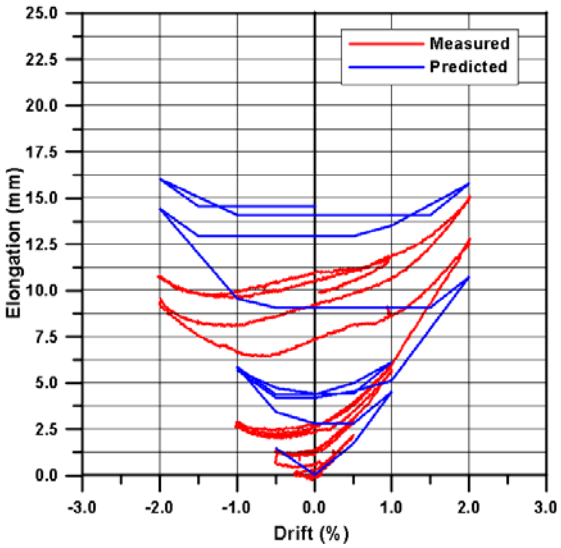

West Bay			
Drift (%)	e_{Theory} (mm)	$e_{Measured}$(mm)	$\%_{difference}$
0.5	1.7	2.4	-4.4
-0.5	1.5	1.2	1.6
0.5	1.7	2.9	-7.5
-0.5	1.5	1.2	1.6
1.0	4.5	5.2	-4.3
-1.0	5.8	2.6	20.1
1.0	6.1	5.2	5.5
-1.0	5.7	2.9	17.2
2.0	10.7	11.8	-6.7
-2.0	14.4	9.7	29.2
2.0	15.8	16.1	-2.2
-2.0	16.0	10.7	33.0
0.0	14.6	10.7	23.9

Figure 7-30 West bay beam elongation prediction comparison for Lindsay (2004) longitudinal elongation data

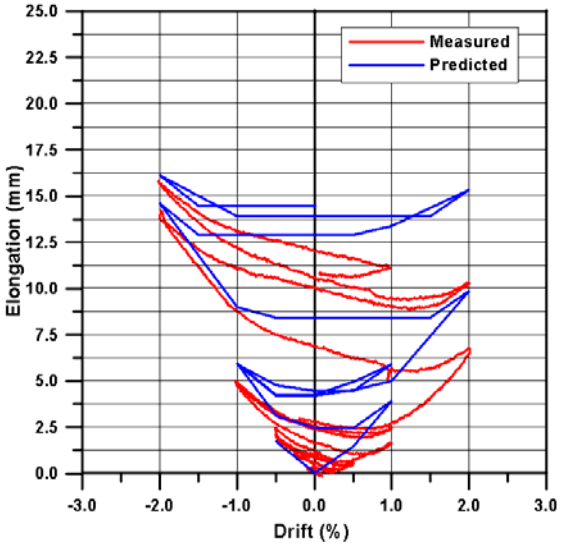

East Bay			
Drift (%)	e_{Theory} (mm)	$e_{Measured}$(mm)	$\%_{difference}$
0.5	1.5	0.7	4.9
-0.5	1.7	1.9	-1.4
0.5	1.5	0.7	4.9
-0.5	1.7	2.1	-2.6
1.0	3.9	1.8	13.4
-1.0	5.9	4.8	7.2
1.0	5.9	2.8	19.7
-1.0	5.9	4.9	6.3
2.0	9.9	6.6	20.7
-2.0	14.6	14.0	3.7
2.0	15.3	10.2	32.7
-2.0	16.1	15.7	2.7
0.0	14.4	11.3	19.9

Figure 7-31 East bay beam elongation prediction comparison for Lindsay (2004) longitudinal elongation data

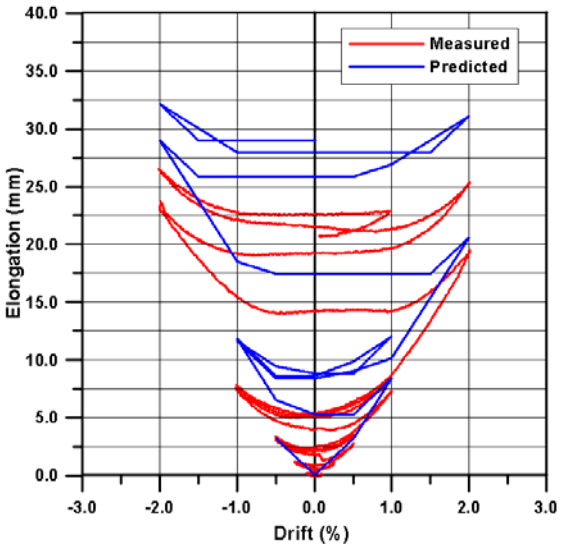

Entire Frame			
Drift (%)	e_{Theory} (mm)	$e_{Measured}$(mm)	$\%_{difference}$
0.5	3.2	3.1	0.2
-0.5	3.2	3.1	0.2
0.5	3.2	3.6	-1.7
-0.5	3.2	3.3	-0.6
1.0	8.4	7.0	5.3
-1.0	11.8	7.4	16.5
1.0	12.0	8.0	15.0
-1.0	11.6	7.8	14.2
2.0	20.6	18.4	8.3
-2.0	29.0	23.7	20.0
2.0	31.1	26.3	18.1
-2.0	32.1	26.4	21.7
0.0	29.0	22.0	26.4

Figure 7-32 Entire frame beam elongation prediction comparison for (2004) longitudinal elongation data

As a result of this restraint of the individual hinges, the inaccuracy of the beam elongation profile was carried through to the predictions for the combined bays. The combination of the restraint in opposing drift direction of individual hinges resulted in an over prediction of elongation for each bay and the entire frame.

Figure 7-33 through Figure 7-38 show the individual plastic hinge and combined East and West bay elongation in the transverse loading direction. The prediction shows good agreement with peak elongation in one direction for each hinge. Again the skewed measured beam elongation profile was observed, resulting in over prediction of elongation in one drift direction for each hinge and overall over estimation for the combined bays. However, the restraint of the floor system was not as pronounced as in the longitudinal direction. This suggests the units themselves played a large part in the restraint, in addition to activation of the topping reinforcement (common for both loading directions).

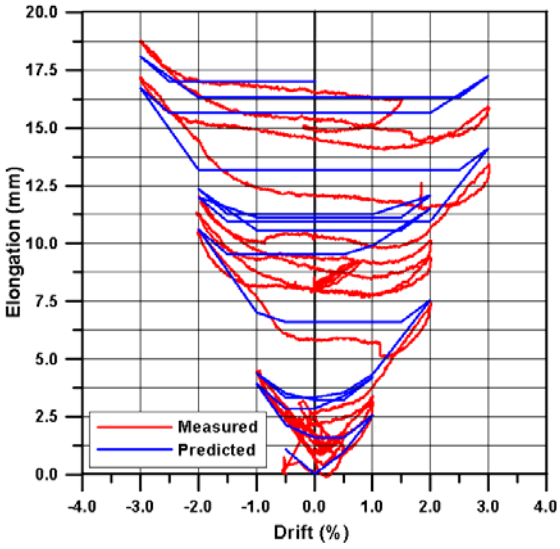

Hinge 5			
Drift (%)	e_{Theory} (mm)	$e_{Measured}$(mm)	$\%_{difference}$
0.5	0.9	1.9	-5.4
-0.5	0.8	1.4	-3.2
0.5	0.9	1.9	-5.4
-0.5	0.8	1.4	-3.2
1.0	2.7	3.2	-2.8
-1.0	3.8	4.3	-2.8
1.0	4.3	3.2	5.7
-1.0	4.4	4.3	0.4
2.0	7.8	7.4	2.2
-2.0	10.5	10.3	1.1
2.0	11.9	9.5	13.1
-2.0	12.6	11.3	7.2
2.0	12.7	10.1	14.1
-2.0	12.6	11.8	4.5
3.0	15.4	13.1	12.4
-3.0	17.7	17.1	3.2
3.0	18.7	15.8	15.5
-3.0	19.4	18.6	4.2
0.0	18.6	16.5	11.2

Figure 7-33 Hinge 5 beam elongation prediction comparison for Lindsay (2004) transverse elongation data

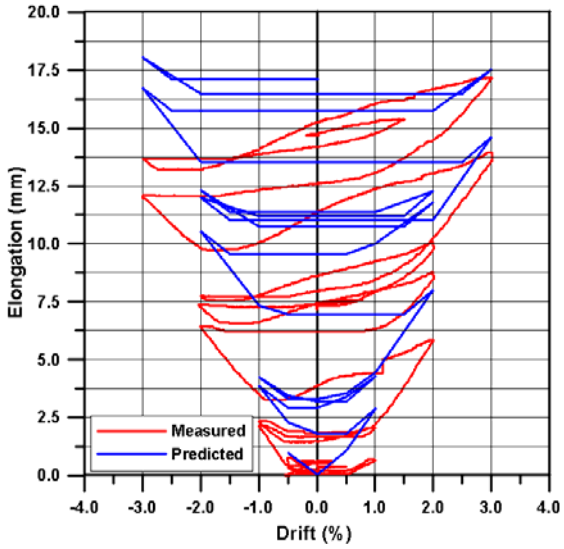

Hinge 6			
Drift (%)	e_{Theory} (mm)	$e_{Measured}$(mm)	$\%_{difference}$
0.5	0.8	0.6	1.2
-0.5	0.9	0.7	1.1
0.5	0.8	0.3	2.9
-0.5	0.9	0.7	1.1
1.0	2.4	0.6	10.5
-1.0	3.8	2.2	9.5
1.0	4.2	2.2	11.5
-1.0	4.5	2.3	12.8
2.0	7.4	5.8	9.3
-2.0	10.6	6.4	24.5
2.0	11.7	8.7	17.5
-2.0	12.7	7.4	30.9
2.0	12.6	10.6	11.6
-2.0	12.7	7.7	29.1
3.0	15.0	13.9	6.3
-3.0	17.7	12.1	33.0
3.0	18.4	17.1	7.9
-3.0	19.4	13.7	33.5
0.0	18.5	14.2	25.4

Figure 7-34 Hinge 6 beam elongation prediction comparison for Lindsay (2004) transverse elongation data

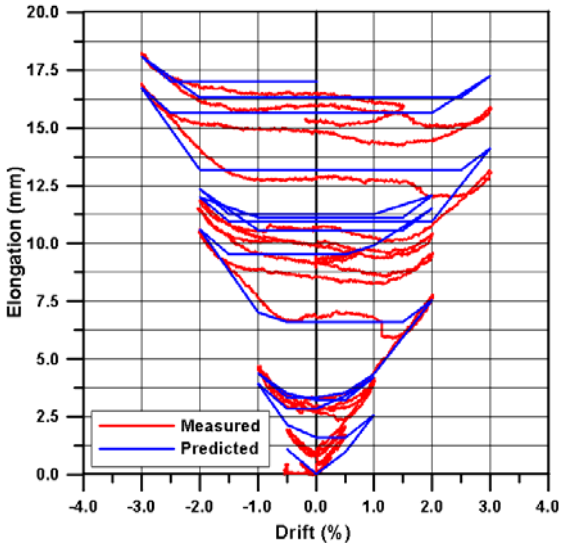

Hinge 7			
Drift (%)	e_{Theory} (mm)	$e_{Measured}$(mm)	$\%_{difference}$
0.5	0.9	1.6	-3.9
-0.5	0.8	1.8	-5.5
0.5	0.9	2.3	-7.7
-0.5	0.8	1.8	-5.5
1.0	2.7	4.4	-9.5
-1.0	3.8	4.5	-4.0
1.0	4.3	4.4	-0.7
-1.0	4.4	4.5	-0.7
2.0	7.8	7.6	1.1
-2.0	10.5	10.3	1.1
2.0	11.9	9.4	13.9
-2.0	12.6	11.4	6.8
2.0	12.7	10.3	13.3
-2.0	12.6	11.7	5.1
3.0	15.4	12.9	13.7
-3.0	17.7	16.8	4.9
3.0	18.7	15.8	15.8
-3.0	19.4	18.2	6.5
0.0	18.6	16.5	11.5

Figure 7-35 Hinge 7 beam elongation prediction comparison for Lindsay (2004) transverse elongation data

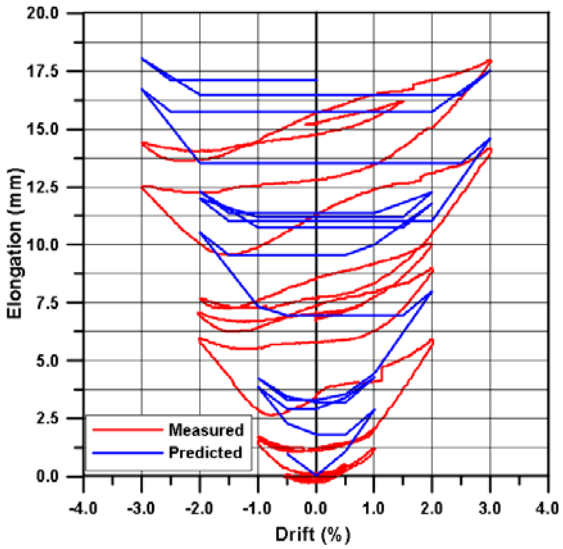

Hinge 8			
Drift (%)	e_{Theory} (mm)	$e_{Measured}$(mm)	$\%_{difference}$
0.5	0.8	0.3	2.8
-0.5	0.9	0.4	2.7
0.5	0.8	0.3	2.8
-0.5	0.9	0.4	2.7
1.0	2.4	1.2	6.7
-1.0	3.8	1.6	12.4
1.0	4.2	2.1	11.6
-1.0	4.5	1.7	15.6
2.0	7.4	5.8	8.8
-2.0	10.6	5.9	26.2
2.0	11.7	8.9	15.6
-2.0	12.7	7.0	31.7
2.0	12.6	10.0	14.4
-2.0	12.7	7.7	27.8
3.0	15.0	14.1	4.9
-3.0	17.7	12.5	29.3
3.0	18.4	17.9	3.0
-3.0	19.4	14.4	28.1
0.0	18.5	14.7	21.4

Figure 7-36 Hinge 8 beam elongation prediction comparison for (2004) transverse elongation data

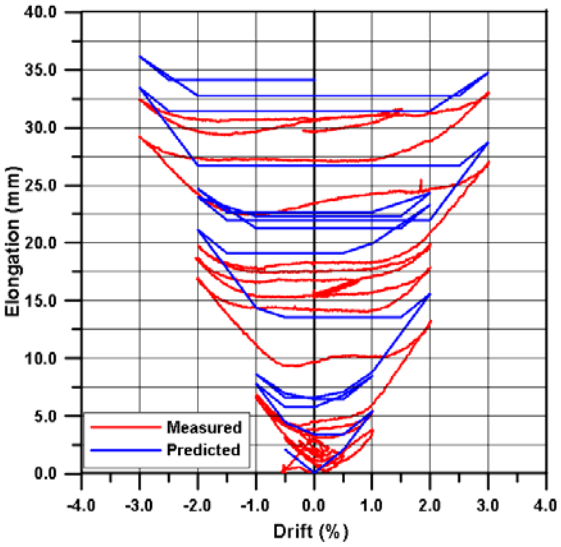

West Bay			
Drift (%)	e_{Theory} (mm)	$e_{Measured}$(mm)	$\%_{difference}$
0.5	1.7	2.5	-2.5
-0.5	1.7	2.1	-1.3
0.5	1.7	2.2	-1.6
-0.5	1.7	2.1	-1.3
1.0	5.1	3.8	3.8
-1.0	7.6	6.5	3.3
1.0	8.4	5.4	9.2
-1.0	8.9	6.6	6.9
2.0	15.2	13.2	6.0
-2.0	21.1	16.7	13.4
2.0	23.6	18.2	16.5
-2.0	25.3	18.7	20.1
2.0	25.3	20.7	14.0
-2.0	25.3	19.5	17.7
3.0	30.4	27.0	10.3
-3.0	35.4	29.2	19.0
3.0	37.1	32.9	12.8
-3.0	38.8	32.3	19.8
0.0	37.1	30.7	19.5

Figure 7-37 West bay beam elongation prediction comparison for Lindsay (2004) transverse elongation data

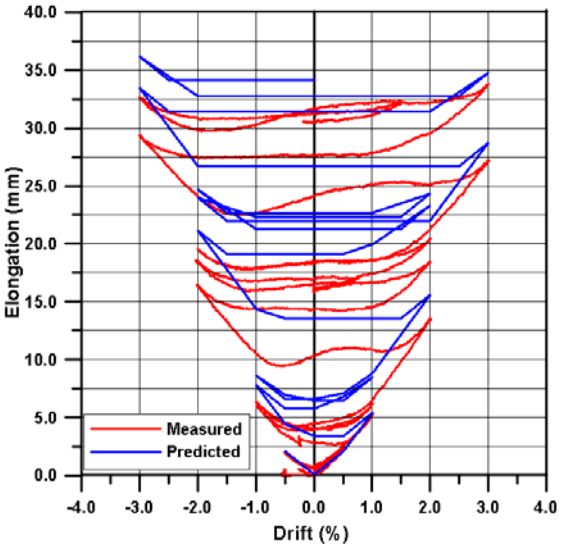

East Bay			
Drift (%)	e_{Theory} (mm)	$e_{Measured}$(mm)	$\%_{difference}$
0.5	1.7	1.9	-0.6
-0.5	1.7	2.2	-1.5
0.5	1.7	2.6	-2.7
-0.5	1.7	2.2	-1.5
1.0	5.1	5.6	-1.6
-1.0	7.6	6.1	4.4
1.0	8.4	6.5	5.7
-1.0	8.9	6.2	7.9
2.0	15.2	13.4	5.3
-2.0	21.1	16.2	14.5
2.0	23.6	18.3	15.8
-2.0	25.3	18.4	20.5
2.0	25.3	20.3	14.9
-2.0	25.3	19.4	17.5
3.0	30.4	27.0	10.0
-3.0	35.4	29.3	18.2
3.0	37.1	33.7	10.2
-3.0	38.8	32.6	18.4
0.0	37.1	31.2	17.6

Figure 7-38 East bay beam elongation prediction comparison for Lindsay (2004) transverse elongation data

Overall good agreement between the measured and predicted beam elongation profiles in the transverse direction (perpendicular to the floor system) was seen. However, the predicted elongation profile was seen to slightly over estimate the magnitude of beam elongation for combined East and West transverse bays. In general, it can be seen that the introduction of the elongation reduction factors (k_i) has improved the overall shape of the elongation profile significantly. This is particularly evident under repeated drift cycles of the same magnitude.

7.4.3 MacPherson (2005) Super-Assembly Test

Figure 7-39 through Figure 7-45 show the beam elongation comparison with measured beam elongation data from longitudinal super-assembly test phase from MacPherson (2005). The measured elongation profiles were seen to be quite disordered. As a result, there was little correlation between the predicted and measured elongation profiles in the longitudinal loading direction. Hinge 1 was an exception to this, which showed reasonable agreement between the predicted and measured beam elongation profiles.

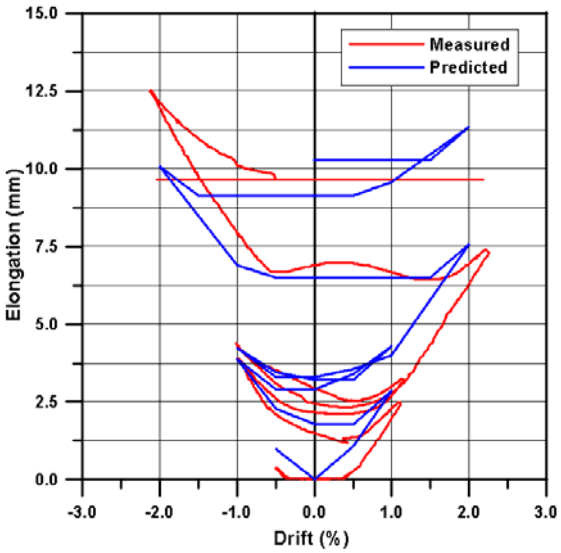

Hinge 1			
Drift (%)	e_{Theory} (mm)	$e_{Measured}$(mm)	$\%_{difference}$
0.5	1.07	0.3	6.2
-0.5	0.96	0.4	4.5
0.5	1.07	0.3	6.2
-0.5	0.96	0.4	4.5
1.0	2.85	2.5	2.8
-1.0	3.85	3.8	0.4
1.0	4.27	3.2	8.6
-1.0	4.23	4.2	0.3
2.0	7.55	7.4	1.2
-2.0	10.07	12.4	-18.8
2.0	11.34	-	-
-2.0	11.86	-	-
0.0	10.91	9.7	9.7

Figure 7-39 Hinge 1 beam elongation prediction comparison for MacPherson (2005) longitudinal elongation data

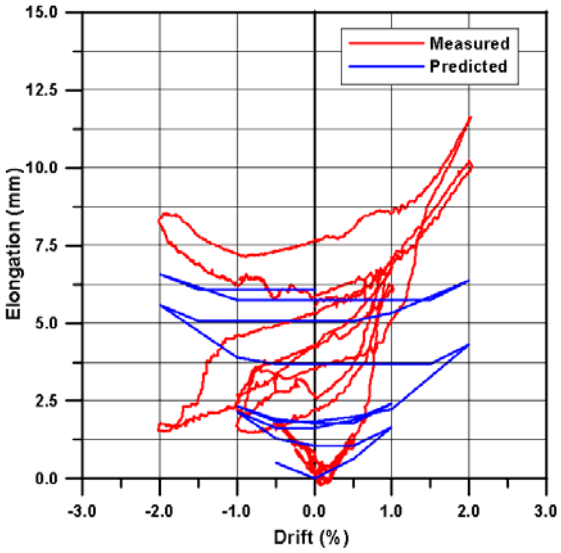

Hinge 2			
Drift (%)	e_{Theory} (mm)	$e_{Measured}$(mm)	$\%_{difference}$
0.5	0.62	1.5	-7.6
-0.5	0.51	1.8	-11.2
0.5	0.62	1.5	-7.6
-0.5	0.51	1.8	-11.2
1.0	1.65	6.0	-37.5
-1.0	2.13	1.6	4.6
1.0	2.39	6.9	-38.9
-1.0	2.32	2.4	-0.7
2.0	4.29	10.2	-51.0
-2.0	5.57	1.7	33.4
2.0	6.35	11.6	-45.2
-2.0	6.58	8.4	-15.7
0.0	6.07	5.6	4.1

Figure 7-40 Hinge 2 beam elongation prediction comparison for MacPherson (2005) longitudinal elongation data

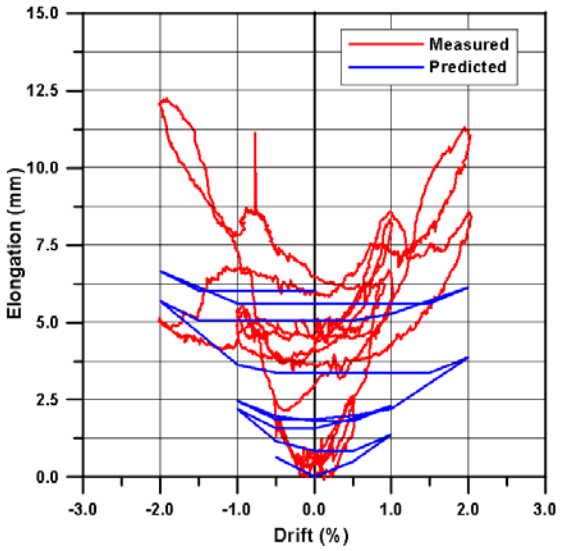

Hinge 3			
Drift (%)	e_{Theory} (mm)	$e_{Measured}$(mm)	$\%_{difference}$
0.5	0.51	2.6	-17.4
-0.5	0.62	1.8	-9.8
0.5	0.51	2.6	-17.4
-0.5	0.62	1.8	-9.8
1.0	1.35	6.6	-43.8
-1.0	2.18	5.4	-26.8
1.0	2.30	8.2	-49.2
-1.0	2.46	5.4	-24.5
2.0	3.87	8.6	-39.4
-2.0	5.68	5.0	5.7
2.0	6.12	11.0	-40.7
-2.0	6.64	12.0	-44.6
0.0	6.02	6.4	-3.1

Figure 7-41 Hinge 3 beam elongation prediction comparison for MacPherson (2005) longitudinal elongation data

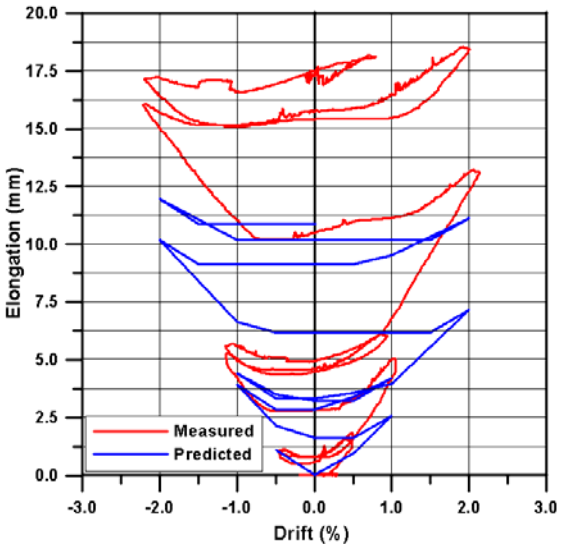

Hinge 4			
Drift (%)	e_{Theory} (mm)	$e_{Measured}$(mm)	$\%_{difference}$
0.5	0.96	1.5	-2.9
-0.5	1.07	1.1	-0.2
0.5	0.96	1.5	-2.9
-0.5	1.07	1.1	-0.2
1.0	2.55	5.0	-13.2
-1.0	3.91	5.4	-8.1
1.0	4.17	6.0	-9.9
-1.0	4.37	5.6	-6.6
2.0	7.13	13.1	-32.3
-2.0	10.18	16.0	-31.5
2.0	11.10	18.5	-40.0
-2.0	11.93	17.2	-28.5
0.0	10.86	17.4	-35.3

Figure 7-42 Hinge 4 beam elongation prediction comparison for MacPherson (2005) longitudinal elongation data

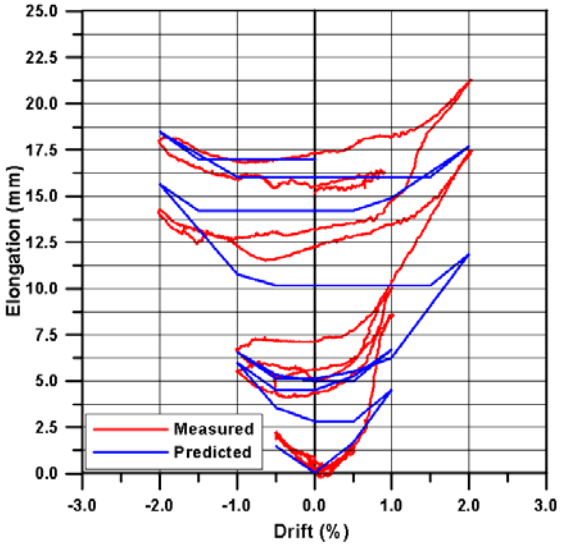

West Bay			
Drift (%)	e_{Theory} (mm)	$e_{Measured}$(mm)	$\%_{difference}$
0.5	1.7	1.8	-0.5
-0.5	1.5	2.2	-3.5
0.5	1.7	1.8	-0.5
-0.5	1.5	2.2	-3.5
1.0	4.5	8.5	-18.8
-1.0	6.0	5.4	2.7
1.0	6.7	10.1	-16.2
-1.0	6.6	6.6	-0.2
2.0	11.8	17.6	-27.0
-2.0	15.6	14.1	7.2
2.0	17.7	21.3	-16.9
-2.0	18.4	18.1	1.6
0.0	17.0	15.3	7.9

Figure 7-43 West bay beam elongation prediction comparison for MacPherson (2005) longitudinal elongation data

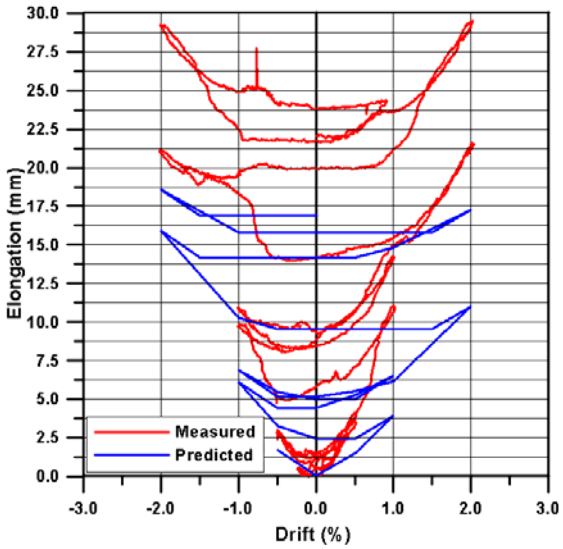

East Bay			
Drift (%)	e_{Theory} (mm)	$e_{Measured}$(mm)	$\%_{difference}$
0.5	1.5	4.1	-8.9
-0.5	1.7	2.9	-4.1
0.5	1.5	4.1	-8.9
-0.5	1.7	2.9	-4.1
1.0	3.9	11.6	-26.1
-1.0	6.1	10.8	-16.0
1.0	6.5	14.2	-26.2
-1.0	6.8	11.0	-14.1
2.0	11.0	21.7	-36.3
-2.0	15.9	21.0	-17.4
2.0	17.2	29.5	-41.6
-2.0	18.6	29.2	-36.0
0.0	16.9	23.8	-23.4

Figure 7-44 East bay beam elongation prediction comparison for MacPherson (2005) longitudinal elongation data

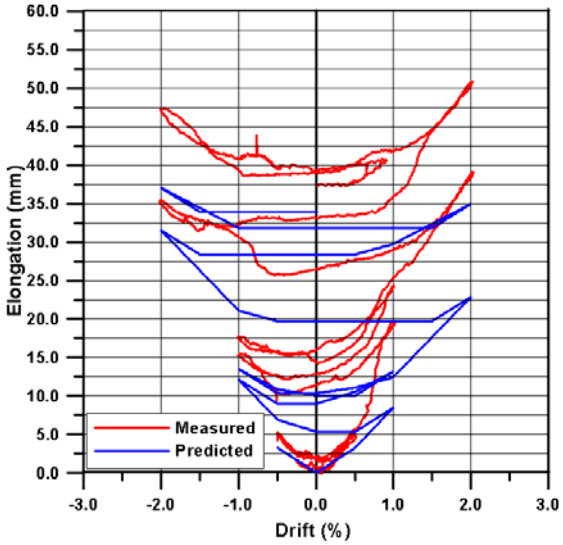

Entire Frame			
Drift (%)	e_{Theory} (mm)	$e_{Measured}$(mm)	$\%_{difference}$
0.5	3.2	5.9	-5.4
-0.5	3.2	5.1	-3.8
0.5	3.2	5.9	-5.4
-0.5	3.2	5.1	-3.8
1.0	8.4	20.1	-23.0
-1.0	12.1	16.2	-8.1
1.0	13.1	24.3	-22.0
-1.0	13.4	17.6	-8.3
2.0	22.8	39.3	-32.4
-2.0	31.5	35.1	-7.1
2.0	34.9	50.8	-31.3
-2.0	37.0	47.3	-20.3
0.0	33.9	39.1	-10.3

Figure 7-45 Entire frame beam elongation prediction comparison for MacPherson (2005) longitudinal elongation data

Figure 7-46 through Figure 7-51 show the beam elongation profile comparison for the transverse loading phase of the super-assembly test carried out by MacPherson (2005). Good agreement was seen between the measured and predicted elongation profile, both in terms of magnitude and beam elongation profile shape.

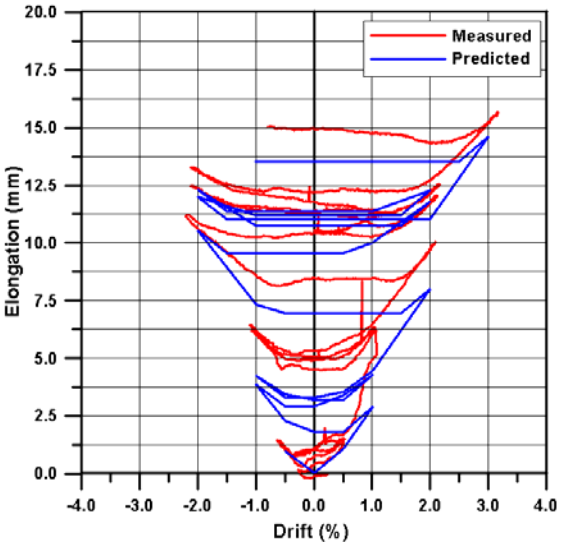

Hinge 5			
Drift (%)	e_{Theory} (mm)	$e_{Measured}$(mm)	$\%_{difference}$
0.5	1.1	1.7	-4.1
-0.5	1.0	1.4	-2.9
0.5	1.1	1.7	-4.1
-0.5	1.0	1.4	-2.9
1.0	2.9	6.5	-23.5
-1.0	3.9	6.2	-15.1
1.0	4.3	6.5	-14.4
-1.0	4.2	6.2	-12.7
2.0	8.0	9.9	-12.3
-2.0	10.5	11.2	-4.4
2.0	11.8	11.9	-0.7
-2.0	12.3	12.4	-0.6
2.0	12.2	12.5	-1.7
-2.0	12.0	13.3	-8.6
3.0	14.6	15.5	-5.9
0.0	13.5	14.9	-9.0

Figure 7-46 Hinge 5 beam elongation prediction comparison for MacPherson (2005) transverse elongation data

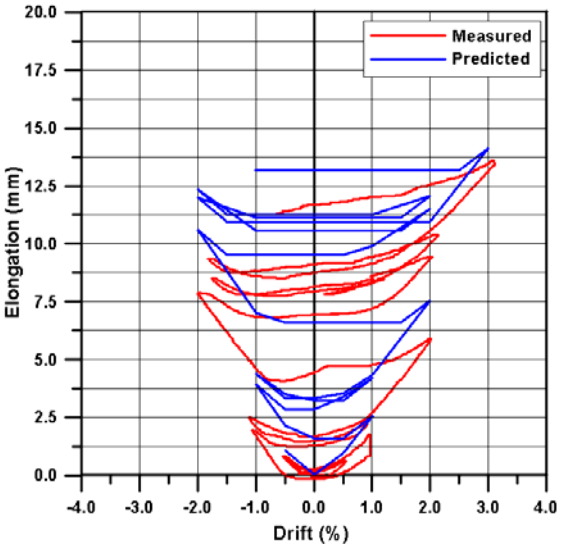

Hinge 6			
Drift (%)	e_{Theory} (mm)	$e_{Measured}$(mm)	$\%_{difference}$
0.5	1.0	0.8	1.1
-0.5	1.1	0.8	2.0
0.5	1.0	0.8	1.1
-0.5	1.1	0.8	2.0
1.0	2.6	1.8	5.5
-1.0	3.9	1.9	14.8
1.0	4.2	2.5	12.3
-1.0	4.4	2.4	14.5
2.0	7.5	5.9	12.0
-2.0	10.6	7.8	20.4
2.0	11.5	9.4	15.5
-2.0	12.3	8.5	28.1
2.0	12.1	10.4	12.2
-2.0	12.0	9.3	19.8
3.0	14.1	13.6	3.7
0.0	13.2	11.7	10.7

Figure 7-47 Hinge 6 beam elongation prediction comparison for MacPherson (2005) transverse elongation data

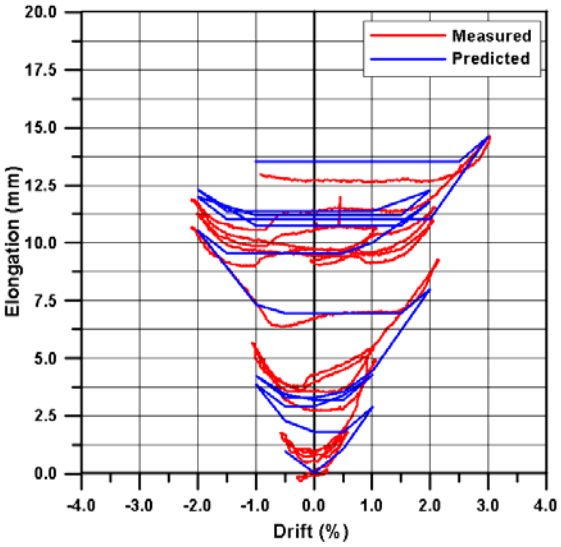

Hinge 7			
Drift (%)	e_{Theory} (mm)	$e_{Measured}$(mm)	$\%_{difference}$
0.5	1.1	1.9	-5.7
-0.5	1.0	1.7	-5.1
0.5	1.1	1.9	-5.7
-0.5	1.0	1.7	-5.1
1.0	2.9	4.6	-12.0
-1.0	3.9	5.2	-9.2
1.0	4.3	5.5	-8.5
-1.0	4.2	5.6	-9.4
2.0	8.0	9.2	-8.2
-2.0	10.5	10.6	-0.6
2.0	11.8	10.9	6.1
-2.0	12.3	11.4	6.2
2.0	12.2	11.4	5.8
-2.0	12.0	11.8	1.2
3.0	14.6	14.6	-0.1
0.0	13.5	12.7	5.5

Figure 7-48 Hinge 7 beam elongation prediction comparison for MacPherson (2005) transverse elongation data

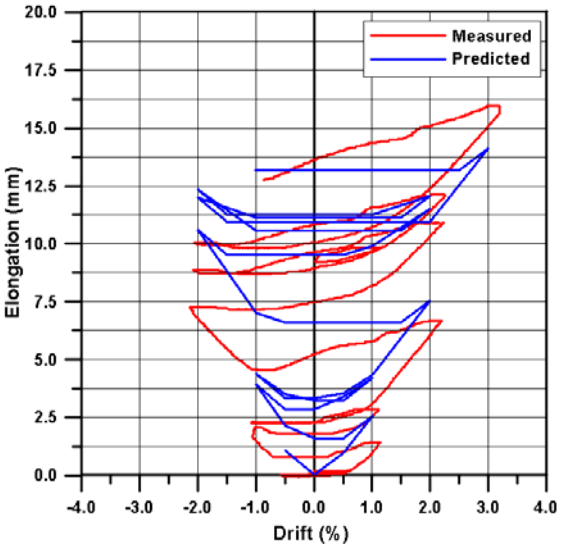

Hinge 8			
Drift (%)	e_{Theory} (mm)	$e_{Measured}$(mm)	$\%_{difference}$
0.5	1.0	0.1	5.4
-0.5	1.1	0.1	6.1
0.5	1.0	0.1	5.4
-0.5	1.1	0.1	6.1
1.0	2.6	1.4	7.2
-1.0	3.9	2.0	12.0
1.0	4.2	2.8	8.6
-1.0	4.4	2.7	10.5
2.0	7.5	6.6	5.8
-2.0	10.6	7.3	20.6
2.0	11.5	10.9	3.8
-2.0	12.3	8.9	21.6
2.0	12.1	12.1	-0.3
-2.0	12.0	10.0	12.5
3.0	14.1	15.9	-11.3
0.0	13.2	13.6	-2.8

Figure 7-49 Hinge 8 beam elongation prediction comparison for MacPherson (2005) transverse elongation data

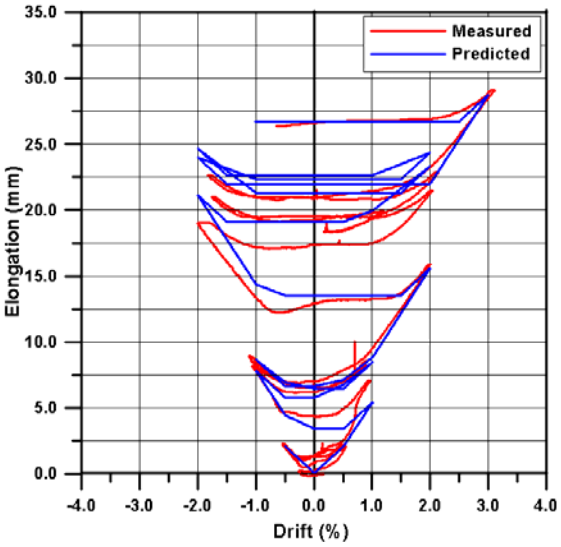

West Bay			
Drift (%)	e_{Theory} (mm)	$e_{Measured}$(mm)	$\%_{difference}$
0.5	2.0	2.5	-1.6
-0.5	2.0	2.2	-0.6
0.5	2.0	2.5	-1.6
-0.5	2.0	2.2	-0.6
1.0	5.4	8.3	-10.0
-1.0	7.8	8.1	-1.2
1.0	8.4	9.0	-1.9
-1.0	8.6	8.6	0.0
2.0	15.5	15.8	-0.9
-2.0	21.1	19.0	7.2
2.0	23.3	21.3	6.8
-2.0	24.6	20.9	12.8
2.0	24.3	22.9	4.8
-2.0	24.0	22.6	4.7
3.0	28.7	29.1	-1.4
0.0	26.7	26.6	0.2

Figure 7-50 West bay beam elongation prediction comparison for MacPherson (2005) transverse elongation data

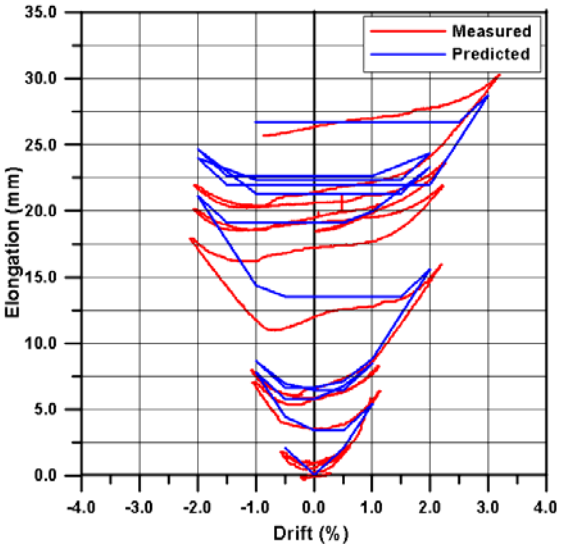

East Bay			
Drift (%)	e_{Theory} (mm)	$e_{Measured}$(mm)	$\%_{difference}$
0.5	2.0	2.0	0.1
-0.5	2.0	1.8	0.7
0.5	2.0	2.0	0.1
-0.5	2.0	1.8	0.7
1.0	5.4	6.0	-2.0
-1.0	7.8	7.2	1.8
1.0	8.4	8.3	0.5
-1.0	8.6	8.3	1.0
2.0	15.5	15.8	-0.9
-2.0	21.1	17.9	10.5
2.0	23.3	21.8	4.9
-2.0	24.6	20.3	14.2
2.0	24.3	23.5	2.6
-2.0	24.0	21.8	7.1
3.0	28.7	30.5	-5.9
0.0	26.7	26.3	1.2

Figure 7-51 East bay beam elongation prediction comparison for MacPherson (2005) transverse elongation data

7.4.4 Fenwick et al (1981) Beam Tests

Figure 7-52 through Figure 7-55 show the predicted and measured beam elongation comparison for four bare reinforced concrete beam sub-assembly tests (with no floor system) carried out by Fenwick et al (1981). Good agreement was seen, with some overestimation of the predicted beam elongation at high drift levels. This was likely due to the ductility demand deteriorating the performance of the plastic hinge, introducing factors such as bar slip, bar buckling, higher shear deformation and general 'sloppiness' of the hinge reducing the potential for stretching of the longitudinal reinforcement and potential for beam elongation to occur.

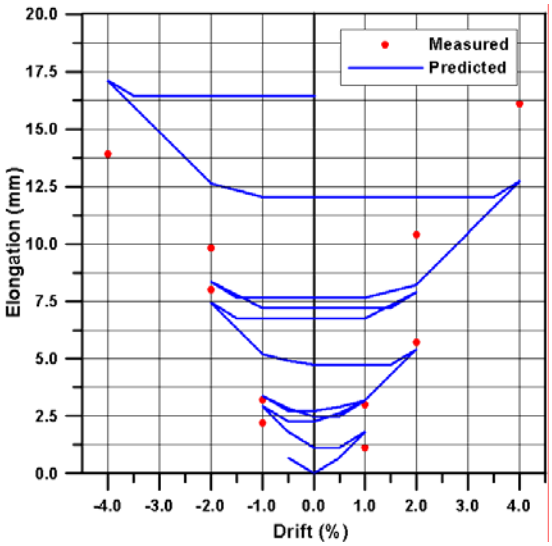

Unit - 1A			
Drift (%)	e_{Theory} (mm)	$e_{Measured}$(mm)	$\%_{difference}$
0.5	0.7	0.0	4.2
-0.5	0.7	0.0	4.2
0.5	0.7	0.0	4.2
-0.5	0.7	0.0	4.2
1.0	1.8	1.1	4.3
-1.0	2.9	2.2	4.5
1.0	3.2	3.0	0.9
-1.0	3.4	3.2	1.1
2.0	5.4	5.7	-1.9
-2.0	7.4	8.0	-3.6
2.0	7.9	10.4	-15.7
-2.0	8.3	9.8	-9.2
4.0	12.7	16.1	-21.0
-4.0	17.1	13.9	19.9

Figure 7-52 Specimen 1A beam elongation prediction comparison for Fenwick et al (1981) elongation data

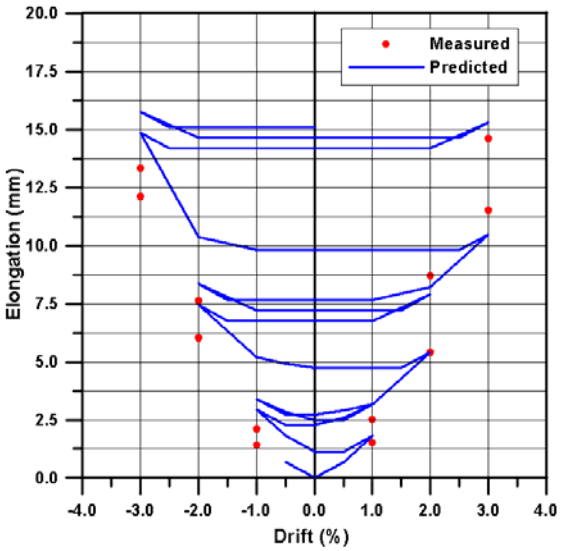

Unit - 1B			
Drift (%)	e_{Theory} (mm)	$e_{Measured}$(mm)	$\%_{difference}$
0.5	0.7	0.0	4.6
-0.5	0.7	0.0	4.6
0.5	0.7	0.0	4.6
-0.5	0.7	0.0	4.6
1.0	1.8	1.5	2.1
-1.0	2.9	1.4	10.4
1.0	3.2	2.5	4.5
-1.0	3.4	2.1	8.7
2.0	5.4	5.4	0.0
-2.0	7.4	6.0	9.8
2.0	7.9	8.7	-5.7
-2.0	8.3	7.6	5.0
3.0	10.5	11.5	-7.1
-3.0	14.9	12.1	18.8
3.0	15.3	14.6	4.8
-3.0	15.8	13.3	16.8

Figure 7-53 Specimen 1B beam elongation prediction comparison for Fenwick et al (1981) elongation data

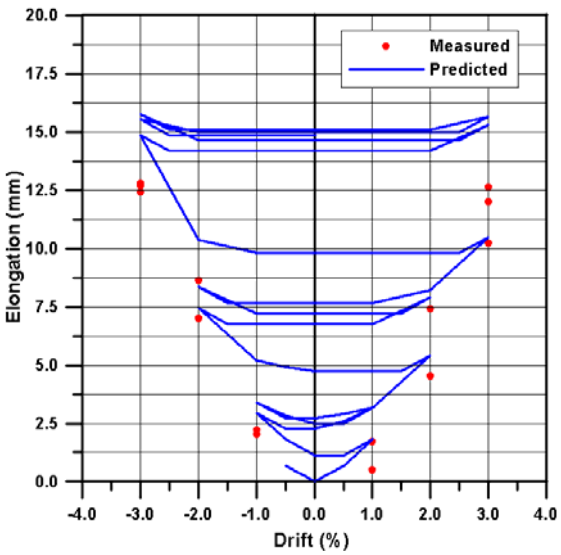

Unit - 2A			
Drift (%)	e_{Theory} (mm)	$e_{Measured}$(mm)	$\%_{difference}$
0.5	0.7	0.0	5.3
-0.5	0.7	0.0	5.3
0.5	0.7	0.0	5.3
-0.5	0.7	0.0	5.3
1.0	1.8	0.5	10.2
-1.0	2.9	2.0	7.2
1.0	3.2	1.7	11.3
-1.0	3.4	2.2	9.2
2.0	5.4	4.5	7.0
-2.0	7.4	7.0	3.3
2.0	7.9	7.4	3.7
-2.0	8.3	8.6	-2.1
3.0	10.5	10.2	2.1
-3.0	14.9	12.7	16.8
3.0	15.3	12.6	21.1
-3.0	15.8	12.8	23.0
3.0	15.6	12.0	28.4
-3.0	15.5	12.4	24.4

Figure 7-54 Specimen 2A beam elongation prediction comparison for Fenwick et al (1981) elongation data

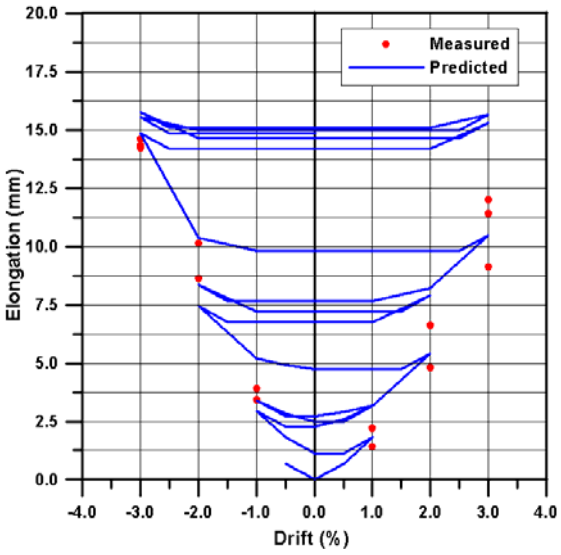

Unit - 2B			
Drift (%)	e_{Theory} (mm)	$e_{Measured}$(mm)	$\%_{difference}$
0.5	0.7	0.0	4.6
-0.5	0.7	0.0	4.6
0.5	0.7	0.0	4.6
-0.5	0.7	0.0	4.6
1.0	1.8	1.4	2.7
-1.0	2.9	3.4	-3.3
1.0	3.2	2.2	6.5
-1.0	3.4	3.9	-3.6
2.0	5.4	4.8	4.1
-2.0	7.4	8.6	-8.0
2.0	7.9	6.6	8.7
-2.0	8.3	10.1	-12.2
3.0	10.5	9.1	9.3
-3.0	14.9	14.6	1.7
3.0	15.3	11.4	26.7
-3.0	15.8	14.2	10.6
3.0	15.6	12.0	24.9
-3.0	15.5	14.3	8.4

Figure 7-55 Specimen 2B beam elongation prediction comparison for Fenwick et al (1981) elongation data

7.4.5 Restrepo (1993) Sub-Assembly Tests

Figure 7-56, Figure 7-57, and Figure 7-58 show predicted and measured beam elongation comparisons with elongation data from three bare reinforced concrete frame sub-assembly tests (no floor system) carried out by Restrepo (1993). Again good agreement was seen between the measured and predicted results. An exception to this was Unit 1 (Figure 7-56), where beam elongation at higher drift levels (2.5% drift cycle) was over predicted.

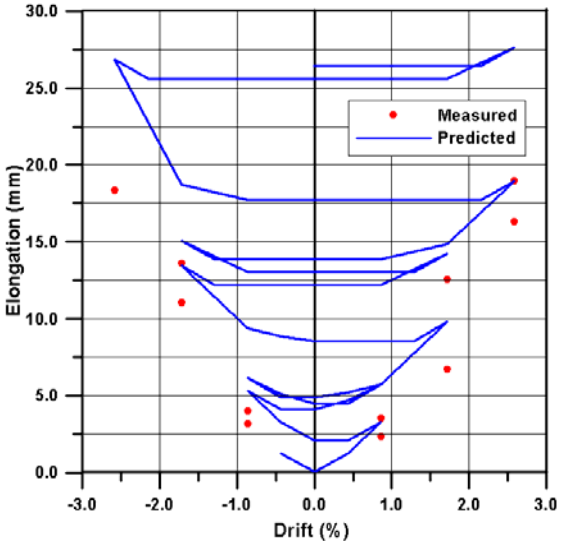

Unit 1			
Drift (%)	e_{Theory} (mm)	$e_{Measured}$(mm)	$\%_{difference}$
0.43	1.63	0.00	6.4
-0.43	1.63	0.00	6.4
0.43	1.63	0.70	3.7
-0.43	1.63	1.40	0.9
0.86	4.33	3.10	4.9
-0.86	7.04	4.20	11.2
0.86	7.59	4.70	11.4
-0.86	8.13	5.30	11.2
1.72	13.00	8.90	16.2
-1.72	17.88	14.70	12.6
1.72	18.96	16.70	8.9
-1.72	20.05	18.10	7.7
2.58	25.19	21.70	13.8
-2.58	35.76	24.40	44.9
2.58	36.84	25.30	45.6

Figure 7-56 Unit 1 beam elongation prediction comparison for Restrepo (1993) elongation data

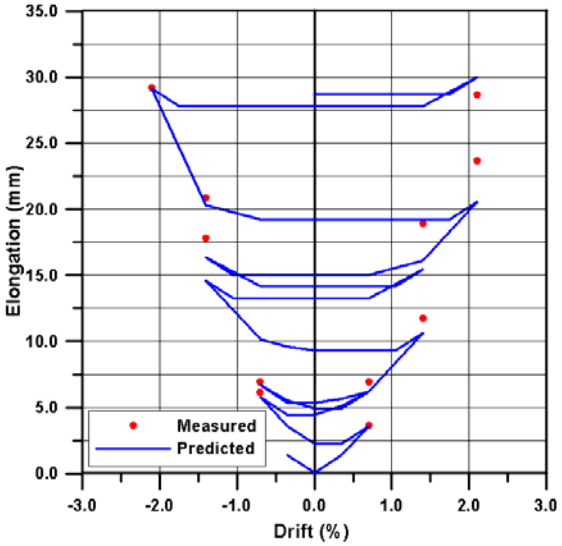

Unit 2			
Drift (%)	e_{Theory} (mm)	$e_{Measured}$(mm)	$\%_{difference}$
0.35	1.32	0.00	4.5
-0.35	1.32	0.00	4.5
0.35	1.32	0.60	2.5
-0.35	1.32	1.40	-0.3
0.70	3.53	3.60	-0.2
-0.70	5.73	6.10	-1.3
0.70	6.17	6.90	-2.5
-0.70	6.62	6.90	-1.0
1.40	10.58	11.70	-3.8
-1.40	14.55	17.80	-11.1
1.40	15.44	18.90	-11.9
-1.40	16.32	20.80	-15.4
2.10	20.51	23.60	-10.6
-2.10	29.11	29.20	-0.3
2.10	29.99	28.60	4.8

Figure 7-57 Unit 2 beam elongation prediction comparison for Restrepo (1993) elongation data

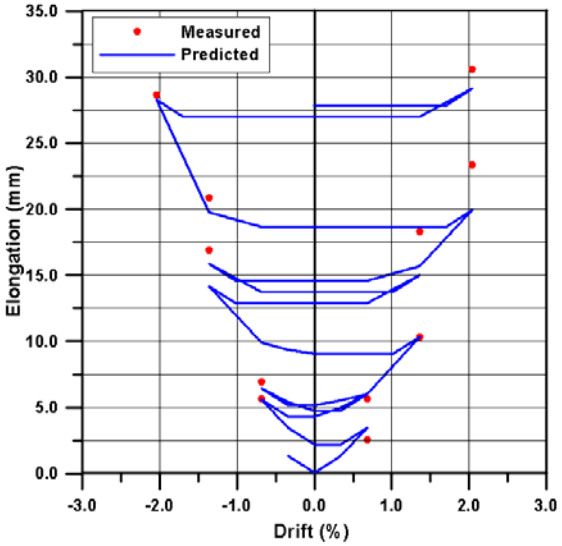

Unit 3			
Drift (%)	e_{Theory} (mm)	$e_{Measured}$(mm)	$\%_{difference}$
0.34	1.29	0.00	4.2
-0.34	1.29	0.00	4.2
0.34	1.29	0.30	3.2
-0.34	1.29	1.10	0.6
0.68	3.43	2.50	3.0
-0.68	5.57	5.60	-0.1
0.68	6.00	5.60	1.3
-0.68	6.43	6.90	-1.5
1.36	10.28	10.30	-0.1
-1.36	14.14	16.90	-9.0
1.36	14.99	18.30	-10.8
-1.36	15.85	20.80	-16.2
2.04	19.92	23.30	-11.0
-2.04	28.27	28.60	-1.1
2.04	29.13	30.60	-4.8

Figure 7-58 Unit 3 beam elongation prediction comparison for Restrepo (1993) elongation data

7.4.6 Lau (2001) Super-Assembly Test

Figure 7-59 shows the predicted versus measured beam elongation profile comparison for a bare frame super-assembly experimental test carried out by Lau (2001). Reasonable agreement was seen up to a drift of 2.5% however, again the beam elongation values at the 2.5% drift level were over estimated.

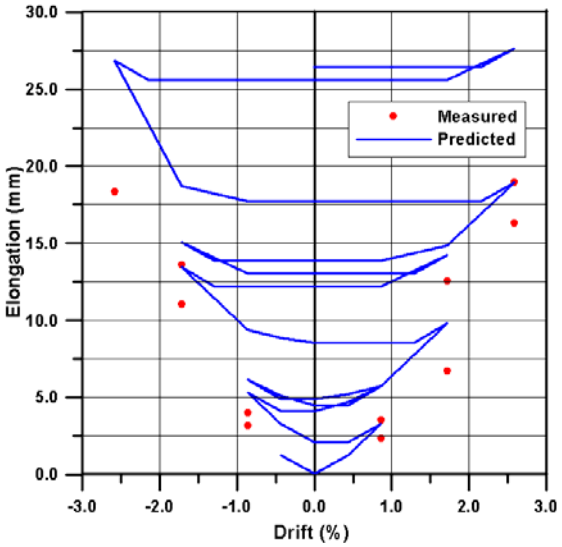

Bare Frame			
Drift (%)	e_{Theory} (mm)	$e_{Measured}$(mm)	$\%_{difference}$
0.5	1.4	0.0	4.4
-0.5	1.4	0.0	4.4
0.5	1.4	0.0	4.4
-0.5	1.4	0.0	4.4
1.4	5.8	5.0	2.3
-1.4	9.4	6.8	7.9
1.4	10.8	9.3	4.6
-1.4	11.9	10.0	5.8
2.7	18.1	18.0	0.4
-2.7	24.0	21.4	8.0
2.7	25.7	24.0	5.2
-2.7	27.4	25.9	4.5
4.0	33.7	30.5	9.9
-4.0	40.1	32.5	23.3

Figure 7-59 Beam elongation prediction comparison for Lau (2001) elongation data

7.5 Conclusions

The elongation of a plastic hinge (or beam) is a variable and complex phenomenon, which a number of local material and structural detailing factors can influence. Elongation results from Matthews (2004), Lindsay (2004) and MacPherson (2005) show significant amounts or variability under the presence of a hollowcore floor system. This was particularly evident where the floor system spanned passed elongating plastic hinges, providing varying amounts of restraint to elongation and activation of topping reinforcement in tension. This was seen to interfere significantly with the elongation profile of the plastic hinges, making prediction difficult for internal plastic hinges (restrained by the hollowcore units).

The beam elongation model proposed in this investigation was a development of the method proposed by Matthews (2004). Matthews' (2004) model was further developed because it was simple and captured the individual components of plastic hinge elongation for a given rotation well. However, the approach lacked some critical aspects of an overall 'realistic' beam elongation profile and for this reason two modifications were made to the method. Firstly the recognition of the elongation contribution from repeated inelastic rotations of the same magnitude, and secondly the recognition of different neutral axis depths for elastic and inelastic conditions in the plastic hinge.

To incorporate the elongation contribution from repeated rotation cycles, elongation reduction factors (k_i) were proposed. The k_i factors were used for the first two repeating cycles of a specific level of rotation, following which no elongation or 'slip' was said to occur. This provided a transition from maximum elongation as a result of 'new' inelastic rotation, to slip once a rotation had been repeated three times. Internal lever arms for inelastic rotations were taken from Matthews (2004) and reduced by approximately 60% to give internal lever arms for elastic rotations. This was only an approximate estimation, based on simple section analysis assessment.

Comparisons were made between the proposed elongation model and a number of experimental beam elongation data sets. Initial comparisons and calibration of the k_i elongation reduction factors were made with elongation profiles measured from super-assembly tests carried out by Matthews (2004), Lindsay (2004) and MacPherson (2005). These data sets included the effect of a hollowcore floor system to

varying degrees. Calibration was carried out on transverse plastic hinges (in beams spanning orthogonally to the one-way floor system) to reduce interference from the floor system. Following this, a number of comparisons were made with bare super- and sub-assemblies without a floor system.

Good agreement was seen between predicted and measured elongation profiles, both in terms of peak elongation and overall elongation profile shape. Elongation prediction was particularly good for plastic hinges, which were not significantly affected by the presence of a floor system. The local variability of elongation for individual hinges was seen to be high; however, when combined bays or frames of two or more hinges were made this variability was generally 'ironed' out. This shows the general rigid body rotation philosophy based on geometric properties of frame and hinge rotation holds well.

The proposed model was simplistic and easily implemented by hand or spreadsheet, as a result some limitations of the proposed model were observed. Firstly the slope or skew between elongation induced by negative and positive hinge rotation was observed in some of the plastic hinge elongation profiles from the super-assembly tests with a hollowcore floor system. This skew was particularly evident in internal hinges which the floor system spanned passed. In these cases the peak elongation was predicted within reasonable and acceptable limits. However, the elongation profile shape was not particularly accurate.

Overestimation of elongation at higher drift levels in excess of approximately 2.5% was observed in a number of the comparisons. This was a result of the model assuming well detailed, flexural dominated, ideal plastic hinge behaviour. In reality plastic hinge behaviour is not ideal (particular at high drift/ductility levels) and is significantly reliant on the detailing of transverse reinforcement in the plastic hinge region to generate sufficient ductility. Therefore, it is likely the overestimation is due to induced 'sloppiness' in the plastic hinges, limiting tensile strains in the longitudinal reinforcement, and hence limiting the beam elongation. Such aspects which could affect this are, shear deformation, bar buckling, bond slip and loss of confinement. Overestimation of elongation at higher drifts would be a safer outcome for avoidance of collapse of the floor system. Particularly when the prediction method is simplistic and does not account for torsional rotation of the supporting beam, between the plastic hinges which form in those beams

7.6 References

Fenwick R.C, Davidson B.J, 1995, *Elongation in ductile seismic-resistant reinforced concrete frames*, Recent Developments in Ductile Moment Resisting Frames in Buildings, Thomas Paulay Symposium, ACI SP-157.

Fenwick R.C, Davidson B.J, McBride A, *The Influence of Slabs on Elongation in Ductile Seismic Resistant Concrete Frames*, 1995, Proceedings NZNSEE Technical Conference, Ne2 Plymouth, March 1995

Fenwick R.C, Dely, R, Davidson B, 1999, *Ductility Demand for Uni-Directional and Reversing Plastic Hinges in Ductile Moment Resisting Frames,* Bulletin of the New Zealand National Society for Earthquake Engineering, Vol. 32, No. 1

Fenwick R.C, Ingham J.M, Wuu P.J.Y, 1996, *The Performance of Ductile R/C Frames Under Seismic Loading*, Proceedings NZNSEE Technical Conference, New Plymouth, March 1996

Fenwick R. C and Megget, L. M, 1993, *Elongation and Load Deflection Characteristics of Reinforced Concrete Members Containing Plastic Hinges*. Bulletin of the New Zealand National Society for Earthquake Engineering, Vol. 26, No. 1

Fenwick R.C, Tankut A.T, Thom C.W, 1981, *The Deformation of Reinforced Concrete Beams Subjected to Inelastic Cyclic Loading – Experimental Results*, Department of Civil and Resource Engineering, University of Auckland, Auckland, New Zealand.

Kim J, Stanton J.F, MacRae G.A, 2004, *Effect of Beam Growth on Reinforced Concrete Frames*, ASCE Journal of Structural Engineering, Vol. 130, No. 9, September

Lau D.B.N, 2001, *The influence of precast-prestressed flooring on the seismic performance of reinforced concrete perimeter frame buildings*, Department of Civil and Resource Engineering, University of Auckland, Auckland, New Zealand.

Lee J.Y and Watanabe F, 2003, *Predicting the longitudinal axial strain in the plastic hinge regions of reinforced concrete beams subjected to reversed cyclic loading*, Engineering Structures, Vol. 25, No. 7, June

Lindsay R.A, 2004, *Experiments on the seismic performance of hollow-core floor systems in precast concrete buildings*, Masters Thesis, Department of Civil Engineering, University of Canterbury, Christchurch, New Zealand.

MacPherson C.J, 2005, *Seismic performance and forensic analysis of a precast concrete hollow-core floor super-assemblage*, Masters Thesis, Department of Civil Engineering, University of Canterbury, Christchurch, New Zealand.

Matthews J.G, 2004, *Hollow-core floor slab performance following a severe earthquake*, PhD Thesis, Department of Civil Engineering, University of Canterbury, Christchurch, New Zealand.

Restrepo-Posada J. I, Park R, Buchanan A. H, 1993, *Seismic behaviour of connections between precast concrete elements*, Dept. of Civil Engineering University of Canterbury, Christchurch, N.Z.

Zerbe H.E and Durrani A.J, 1989, *Seismic Response of Connections in Two-Bay R/C Frame Sub-assemblies*, Journal of Structural Engineers, ASCE, Vol. 115, No.11, November 1989.

Zerbe H.E and Durrani A.J, 1990, *Seismic Response of Connections in Two-Bay R/C Frame Sub-assemblies with a Floor*, Structural Journal, ACI, Vol. 87, No.4, July-August 1990.

8 Summary, Conclusions and Recommendations

8.1 Summary

This investigation was part of a greater research initiative regarding the seismic performance of precast concrete hollowcore floor systems. The focal point of the greater research programme was the interaction of the floor system with the supporting seismic resisting frame system, the connection details between the two systems and how these affected the global building performance. Previous facets of the research programme focussed on the assessment of existing configurations and validation of new improved connection details for current practice. Particular focus was given to the connection between the floor and beam supporting the vertical loads of the floor. The result of which has led to the significantly improved understanding of the poor performing details for the existing seating connection and the implementation of alternative, superior performing details for the seating connection into current practice. However, very little consideration has been given to retrofit procedures for the already existing buildings with potentially poor performing seating connection details.

A two-dimensional sub-assembly test of a single hollowcore unit seated on a supporting beam was used to experimentally investigate existing and retrofitted seating connection details. Both the rotation of the supporting seating beam relative to the floor system and beam elongation induced 'pull-off' deformations were imposed on the hollowcore unit. These two deformations were previously identified as the predominate damage causing demands that can jeopardise the structural integrity of existing hollowcore seating connections. The aim of the investigation was to further develop the understanding of the perceived structural deficiencies of existing hollowcore floor seating connections. Following which, the collective information from this and previous existing seating connection experimental tests was used to develop a suite of retrofit procedures. The individual retrofit approaches were later experimentally verified through implementation on a sub-assembly test of an existing seating connection.

The 'pull-off' effect on one-way precast floor systems was identified as having a major influence on the integrity of existing hollowcore seating connections. Therefore, an investigation was carried out into available simple, hand-type calculation, reinforced concrete beam (plastic hinge) elongation models capable of estimating the 'pull-off' effect. From this a modification was made to an existing method developed by Matthews (2004) to more

accurately represent the beam elongation phenomenon, without substantially sacrificing the attractive simplicity of the model. Good agreement between a range of predicted and experimental beam elongation data sets was observed.

8.2 Conclusions

Based on the experimental and numerical investigations in this research project the following conclusions were made:

8.2.1 Existing Seating Connection Investigation

1. Three single hollowcore unit and seating beam sub-assembly experimental tests with existing seating connection details were carried out. Loss of vertical support with and without delamination of the *in-situ* topping from the hollowcore unit (LOSD & LOS primary failure mechanisms), resulting in collapse of the floor system was observed in two of the three tests. This was primarily a result of spalling of the unreinforced concrete seating ledge and trapping and breaking off of portions of the hollowcore unit soffit. The result of these features was the formation of a near vertical failure plane behind the end of the hollowcore unit, negating the vertical support of the seating ledge. This resulted in loss of support under beam elongation 'pull-off' actions much less than the original available seating length. The loss of support (LOSD and LOS) failure mechanism demonstrated the importance of not relying on topping starter bars to provide a vertical load path for the floor system. This was a result of either breaking of the bond between the *in-situ* topping concrete and the hollowcore unit (delamination), or rupture of the starter bars at the interface between the hollowcore unit and seating beam under elongation demand, in the absence of delamination.

2. The loss of support (LOSD and LOS) failure mechanism observed in this investigation varied from previous existing hollowcore seating connection investigations (Matthews 2004; Bull and Matthews 2003; Liew 2004). Previous tests observed flexure-shear failure (FSF) in the hollowcore units as result of the seating connection flexural strength exceeding that of the hollowcore unit. The variation in the observed failure mechanism was likely a result of increased unit strength and quality from that of the previous investigations. This was demonstrated by overall connection strengths in this investigation exceeding those observed by Bull and Matthews (2003) (which resulted in rupture of the hollowcore unit) by up to 75% (in the case of the HC3 test specimen).

The comparisons between the two investigations were justified by the fact that at first rupture and peak flexural strength (+0.2-0.25% drift) the tests in this investigation were yet to experience significant elongation 'pull-off' forces (tension in the hollowcore unit). This is consistent with the Bull and Matthews (2003) tests which had no 'pull-off' applied to the hollowcore unit.

3. Existing seating connection tests in this investigation had the hollowcore unit seated directly on the bare concrete seating ledge. Previous tests of existing details seated the hollowcore unit on a wet mortar bedding material. This raised concern as to the possible increasing affect the mortar bed had on the restraint of the soffit and damage causing seating connection flexural strength. Seating connection strengths achieved in this investigation exceeded previous equivalent mortar bedded connections. From this it can possibly be concluded that the mortar bed had little adverse effect on previous tests. In addition to this, bare concrete seating ledges could potentially provide sufficient restraint of the hollowcore unit soffit and connection fixity to induce flexure-shear failure in the hollowcore unit.

8.2.2 Retrofit Philosophy and Implementation

1. A suite of simple and low-invasive individual retrofit techniques were suggested which target the observed structural deficiencies of typical existing hollowcore seating connections. The retrofit concepts focused on preventing the loss of vertical support of the floor system and addressing the problem of excess flexural strength (fixity) of the seating connection. The general retrofit strategy incorporated a combination of the individual techniques aimed at demonstrating intervention in the seating connection hierarchy of strength to result in desirable seismic behaviour. The techniques included the implementation of an additional seating ledge, confinement of the existing seating ledge and selective weakening of the interface between the hollowcore unit and seating beam.

2. A retrofit strategy was carried out on an existing seating connection sub-assembly specimen through two *in-situ* modifications. Firstly, an RHS steel section was fixed to the face of the seating beam to provide additional seating and confine the existing seating ledge. Secondly, a plane of weakness was introduced behind the end of the hollowcore unit to isolate the hollowcore unit from the seating beam attempting to

limit the flexural strength capacity of the seating connection. A superior performance resulted when compared with the equivalent existing seating connection test. Loss of seating was prevented up to an elongation of 85-95mm (significantly more 'pull-off' than could be expected in reality). A flexural strength reduction at the seating connection of approximately 35% was achieved, this was less than desired. However, the extent of weakening was likely larger than observed as a result of opposing increase in the flexural strength of the connection due to the confinement of the existing seating ledge providing more restraint to the soffit of the hollowcore unit.

3. Existing hollowcore seating connections are very sensitive to external modifications, and what can be achieved from simple retrofit approaches is limited given the delicate and *in-situ* nature of the existing connections. In addition to this, the peak strength of the connection is reliant on a number of intrinsic properties of the connection (some difficult to determine); namely, the strength and length of the unreinforced concrete seating ledge, the strength of *in-situ* concrete cores in the end of the hollowcore unit, and the strength of hollowcore unit itself. There is substantial uncertainty regarding the *in-situ* strength of these individual seating connection elements (including that of the hollowcore units). For this reason it is difficult to determine a hierarchy of strength for existing seating connections. This makes the selective weakening retrofit approach attractive as these uncertainties could potentially be negated.

8.2.3 Beam Elongation Investigation

1. A modification was presented to the simple, rigid body rotation based beam elongation model proposed by Mathews (2004) was presented. The reason for this modification was to introduce the elongation contribution from repeated rotation cycles of the same magnitude (not considered by the Matthews (2004) method). Elongation reduction factors (k_i) were introduced to provide a transition from maximum elongation as a result of 'new' inelastic rotation, to no elongation or 'slip' once a specific magnitude of rotation had been repeated three times. In addition, the recognition that the neutral axis position is substantially different for elastic and inelastic beam behaviour was introduced.

2. A series of comparisons were made with a number of experimental beam elongation data sets. These included plastic hinges with and without the influence of a precast

concrete hollowcore floor system. Good agreement between the predicted and measured peak beam elongation values was observed. A significant improvement in the overall elongation profile shape compared with the Matthews (2004) method was also observed. However, in the presence of the floor system significant variability was observed in the measured beam elongation behaviour, resulting in inaccurate elongation predictions. The model was simplistic, and assumed ideal flexural plastic hinge behaviour by neglecting the detailing and resulting hysteretic behaviour of the plastic hinge. For this reason over prediction of elongation was observed in some cases due to the influence of 'sloppiness' (bar slip, bar buckling and shear deformation) in the actual, built plastic hinge associated with the detailing issues. When estimating the amount 'pull-off' imposed a floor system (as a result of beam elongation), geometric considerations need to be made. This is to relate the elongation of the centreline of the beam to the resulting 'pull-off' that would imposed at the level of the seating ledge. This is particularly important when the level of the seating ledge does not coincide with the centreline of the elongating beam, as discussed in Section 2.2.

8.3 Recommendations for Further Research

Following the completion of this investigation, the greater research program has asked a number of questions, and provided solutions for these problems regarding the seismic performance of precast hollowcore floor systems. However, there are some gaps remaining in the information database and room for advancement, particularly in terms of developing analytical methods for understanding hollowcore floor and seismic frame system interaction.

Concern was raised regarding how representative the hollowcore units used in the sub-assembly tests were of typical existing hollowcore units in practice. The importance of this issue was also highlighted by the effect the concrete strength of the hollowcore unit has on the seating connection hierarchy of strength and potential failure mechanism. For this reason, the implementation of retrofit procedures and the quality and strength of the existing hollowcore units needs to be investigated. This investigation could also encompass an assessment of how many 'at-risk' hollowcore buildings there are. This would have to be carried out with the knowledge developed from this and previous investigations in this greater research programme to be accurate.

At this stage only one sub-assembly test has been carried out on a smaller 200 series hollowcore unit. This leaves a gap in the experimental database representing a substantial proportion of existing building stock. It is also recommended that a series of sub-assembly tests be carried out, repeating the previously tested negative seated (hollowcore unit supported off the ledge by a section of reinforced, *in-situ* concrete, which is part of the finishing pour of the supporting beam and topping) hollowcore seating connections, with reinforced and filled cores (previously tested by Liew (2003)). These tests were previously carried out without beam elongation induced 'pull-off' effects imposed on the specimen. The 'pull-off' demand on such connection configurations could have a negative effect on performance due to the imposed elongation demand on the tie reinforcement (which provides the vertical load path for the floor system). This will involve determining an appropriate or realistic density of tie reinforcement to use as previous tests carried out by Liew (2003) were considered over-reinforced.

When considering the investigation of existing hollowcore seating connections using the two-dimensional sub-assembly approach, all specimens were loaded in a manner which resulted in first rupture under positive rotation (hollowcore unit soffit pulling across the seating ledge). This resulted in the connection not imposing maximum negative rotation demand on the hollowcore unit due to the rupture in the previous cycle. It would be interesting to see the first loading cycle beyond first rupture being negative.

In addition to the vertical support providing end floor-to-frame seating connection, seismic performance issues associated with the longitudinal perimeter connection (running parallel to the floor system, orthogonal to the seating connection) have also previously been raised. Current code requirements (NZS 3101:1995 Amendment 3 (2004); NZS 3101:2006) are to offset the first adjacent hollowcore unit from the longitudinal perimeter frame. Prior to work by Matthews (2004) this was not normally the case, with the first hollowcore unit being placed directly against the parallel beam. There is therefore a need for an investigation regarding how to quantify acceptable limits of vertical displacement incompatibility, and how to retrofit the existing buildings which exceed those limits.

The most potential for advancement in research regarding the seismic performance of hollowcore floor systems is in the analytical areas. Numerous experimental investigations have been carried out at both sub- and super-assembly levels investigating both existing and

new floor and frame structural configurations. As a result, a significant database of physical hollowcore floor system behaviour, both at a connection level and globally as a full building system has been accumulated. This database should be utilised to develop and calibrate numerical models capable of representing the hollowcore floor system and the connections between the floor and frame system. The achievement of which could significantly reduce the reliance on laboratory testing, particularly the size, time and cost limitations associated with this. By utilising a numerical investigation approach, full building investigations could be carried out, requiring much less time and financial expense, and with the major advantage of repeating a number of structural configuration variations. Such research could encompass a number of numerical approaches of varying complexity, these include:

- A finite element model focused locally at the end seating connection to predict the rupture mechanism observed in the existing seating connection primary failure mechanisms. This would be complicated as the model would be required to represent the hollowcore unit and surrounding concrete elements accurately at a material level.

- On a larger scale, a model should be developed to encompass the floor and frame system, including representation of the connection details between the two systems. This would be beneficial in investigating not only issues with the hollowcore floor system, but also issues associated with seismic frame behaviour to include the influence of a floor system, such as the induced overstrength effects on the frame system.

- Such a model could also be used to induce more realistic loading to a hollowcore floor and seismic frame systems. Previous super-assembly experimental investigations used one-way quasi static loading independently in longitudinal and transverse directions. The performance of such systems could be significantly affected if combined bi-directional loading was applied, or even more advanced, earthquake ground motions (pseudo dynamic loading). It would be interesting to use a near field type loading history to get large rotation and elongation in a large early push cycle.

8.4 References

Bull D.K, Matthews J.G, 2003, *Proof of concept tests for hollow-core floor unit connections*, Precast NZ report, Feb 2003.

Fenwick R.C, Deam B.L, Bull D.K, 2004, *Failure Modes for Hollowcore Flooring Units,* Journal of the Structural Engineering Society of New Zealand (SESOC), Vol. 17, No. 1.

Liew H.Y, 2004, *Performance of hollow-core floor seating connection details*, Masters Thesis, Department of Civil Engineering, University of Canterbury, Christchurch, New Zealand.

Lindsay R.A, 2004, *Experiments on the seismic performance of hollow-core floor systems in precast concrete buildings*, Masters Thesis, Department of Civil Engineering, University of Canterbury, Christchurch, New Zealand.

MacPherson C.J, 2005, *Seismic performance and forensic analysis of a precast concrete hollow-core floor super-assemblage*, Masters Thesis, Department of Civil Engineering, University of Canterbury, Christchurch, New Zealand.

Matthews J.G, 2004, *Hollow-core floor slab performance following a severe earthquake*, PhD Thesis, Department of Civil Engineering, University of Canterbury, Christchurch, New Zealand.

NZS3101:1995, 1995, *Concrete Structures Standard, NZS3101, Parts 1 & 2*, Standards New Zealand, Wellington, New Zealand

Appendix A Experimental Design

This section outlines details associated with the development of the hollowcore seating connection experimental test rig.

A1 Hollowcore Unit Design

Figure A-1 and Figure A-2 are the design calculations for the hollowcore units from Stresscrete.

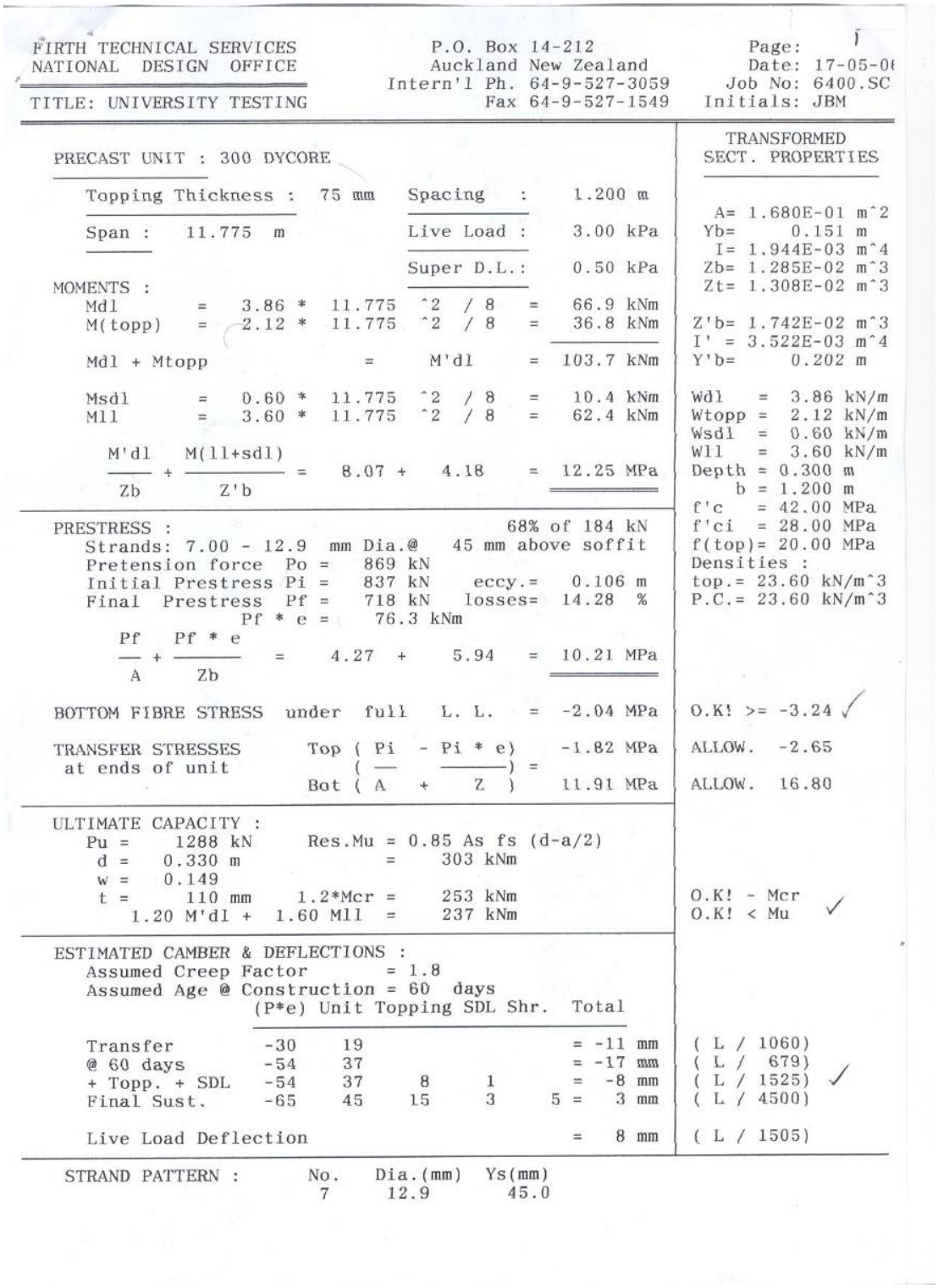

FIRTH TECHNICAL SERVICES
NATIONAL DESIGN OFFICE
P.O. Box 14-212
Auckland New Zealand
Intern'l Ph. 64-9-527-3059
Fax 64-9-527-1549
Page:
Date: 17-05-0
Job No: 6400.SC
Initials: JBM

TITLE: UNIVERSITY TESTING

PRECAST UNIT : 300 DYCORE

Topping Thickness : 75 mm
Spacing : 1.200 m
Span : 11.775 m
Live Load : 3.00 kPa
Super D.L.: 0.50 kPa

MOMENTS :

Mdl	=	3.86 *	11.775	^2 / 8	=	66.9	kNm
M(topp)	=	2.12 *	11.775	^2 / 8	=	36.8	kNm
Mdl + Mtopp			=	M'dl	=	103.7	kNm
Msdl	=	0.60 *	11.775	^2 / 8	=	10.4	kNm
Mll	=	3.60 *	11.775	^2 / 8	=	62.4	kNm

$$\frac{M'dl}{Zb} + \frac{M(ll+sdl)}{Z'b} = 8.07 + 4.18 = 12.25 \text{ MPa}$$

TRANSFORMED SECT. PROPERTIES

A= 1.680E-01 m^2
Yb= 0.151 m
I= 1.944E-03 m^4
Zb= 1.285E-02 m^3
Zt= 1.308E-02 m^3
Z'b= 1.742E-02 m^3
I' = 3.522E-03 m^4
Y'b= 0.202 m

Wdl = 3.86 kN/m
Wtopp = 2.12 kN/m
Wsdl = 0.60 kN/m
Wll = 3.60 kN/m
Depth = 0.300 m
b = 1.200 m
f'c = 42.00 MPa
f'ci = 28.00 MPa
f(top)= 20.00 MPa
Densities :
top.= 23.60 kN/m^3
P.C.= 23.60 kN/m^3

PRESTRESS : 68% of 184 kN
Strands: 7.00 - 12.9 mm Dia.@ 45 mm above soffit
Pretension force Po = 869 kN
Initial Prestress Pi = 837 kN eccy.= 0.106 m
Final Prestress Pf = 718 kN losses= 14.28 %
Pf * e = 76.3 kNm

$$\frac{Pf}{A} + \frac{Pf * e}{Zb} = 4.27 + 5.94 = 10.21 \text{ MPa}$$

BOTTOM FIBRE STRESS under full L. L. = -2.04 MPa — O.K! >= -3.24 ✓

TRANSFER STRESSES at ends of unit
Top $\left(\frac{Pi}{A} - \frac{Pi * e}{Z}\right)$ = -1.82 MPa — ALLOW. -2.65
Bot $\left(\frac{Pi}{A} + \frac{Pi * e}{Z}\right)$ = 11.91 MPa — ALLOW. 16.80

ULTIMATE CAPACITY :
Pu = 1288 kN
d = 0.330 m
w = 0.149
t = 110 mm
Res.Mu = 0.85 As fs (d-a/2) = 303 kNm
1.2*Mcr = 253 kNm
1.20 M'dl + 1.60 Mll = 237 kNm

O.K! - Mcr
O.K! < Mu ✓

ESTIMATED CAMBER & DEFLECTIONS :
Assumed Creep Factor = 1.8
Assumed Age @ Construction = 60 days

	(P*e)	Unit	Topping	SDL	Shr.	Total	
Transfer	-30	19				= -11 mm	(L / 1060)
@ 60 days	-54	37				= -17 mm	(L / 679)
+ Topp. + SDL	-54	37	8	1		= -8 mm	(L / 1525) ✓
Final Sust.	-65	45	15	3	5	= 3 mm	(L / 4500)
Live Load Deflection						= 8 mm	(L / 1505)

STRAND PATTERN :

No.	Dia.(mm)	Ys(mm)
7	12.9	45.0

Figure A-1 - Flexure design of hollowcore unit from Stresscrete

SHEAR DESIGN TO NZS 3101:1995 Date 17-05-06 2
Time 12:06:54

UNIVERSITY TESTING
Span = 11.775 m
300 DYCORE 42.00 MPa
Topping thickness 75 mm 20.00 MPa
Strands 7.00 No. 12.9 mm diameter @ 45 mm above soffit

SUPERIMPOSED LOAD DATA

SDL & LL UDL's from design

SDL = 0.60 kN/m DL LF = 1.200
LL = 3.60 kN/m LL LF = 1.600

SHEAR DESIGN

Precast unit dead load	=	3.86	kN/m
Topping dead load	=	2.12	kN/m
Precast unit spacing	=	1.200	m
Line dead load on P.C. unit	=	0.00	kN/m
Web width	=	242	mm
d in shear equations	=	330	mm
Concrete strength	=	42.00	MPa
Strength reduction factor ø	=	0.750	
0.14 x √(f'c)	=	0.91	MPa
Minimum stirrup requirement	=	282	mm^2/m (Eq. 9-12)
ditto	=	190	mm^2/m (Eq. 9-13)
Maximum stirrup spacing	=	281	mm
Stirrup yield stress	=	300	MPa

U.D. LIVE LOAD DL LF = 1.2
LL LF = 1.6

Posn/L ratio	Max. Mll kNm	Corr. Vll kN	Max. Vll kN	Vsdl kN	Total Vu kN	Shear stresses vu MPa	vcw MPa	vci MPa	Avge. 2 Leg Stirrups reqd. mm^2/m	size mm	spacing mm
0.016	3.9	20.5	20.5	3.4	77.9	1.30	2.58	15.01	190	6	281
0.050	11.9	19.1	19.1	3.2	72.4	1.21	2.69	4.78	nil by cl. 9.3.4.1		
0.100	22.5	17.0	17.0	2.8	64.3	1.07	2.83	2.39	nil by cl. 9.3.4.1		
0.150	31.8	14.8	14.8	2.5	56.3	0.94	2.96	1.58	190	6	281
0.200	39.9	12.7	12.7	2.1	48.2	0.81	3.07	1.18	190	6	281
0.250	46.8	10.6	10.6	1.8	40.2	0.67	3.16	0.92	190	6	281
0.300	52.4	8.5	8.5	1.4	32.2	0.54	3.24	0.91	190	6	281
0.350	56.8	6.4	6.4	1.1	24.1	0.40	3.30	0.91	nil by cl. 9.3.4.1		
0.400	59.9	4.2	4.2	0.7	16.1	0.27	3.34	0.91	nil by cl. 9.3.4.1		
0.450	61.8	2.1	2.1	0.4	8.0	0.13	3.37	0.91	nil by cl. 9.3.4.1		
0.500	62.4	0.0	0.0	0.0	0.0	0.00	3.38	0.91	nil by cl. 9.3.4.1		
0.550	61.8	2.1	2.1	0.4	8.0	0.13	3.37	0.91	nil by cl. 9.3.4.1		
0.600	59.9	4.2	4.2	0.7	16.1	0.27	3.34	0.91	nil by cl. 9.3.4.1		
0.650	56.8	6.4	6.4	1.1	24.1	0.40	3.30	0.91	nil by cl. 9.3.4.1		
0.700	52.4	8.5	8.5	1.4	32.2	0.54	3.24	0.91	190	6	281
0.750	46.8	10.6	10.6	1.8	40.2	0.67	3.16	0.93	190	6	281
0.800	39.9	12.7	12.7	2.1	48.2	0.81	3.07	1.18	190	6	281
0.850	31.8	14.8	14.8	2.5	56.3	0.94	2.96	1.59	190	6	281
0.900	22.5	17.0	17.0	2.8	64.3	1.07	2.83	2.39	nil by cl. 9.3.4.1		
0.950	11.9	19.1	19.1	3.2	72.4	1.21	2.69	4.79	nil by cl. 9.3.4.1		
0.984	3.9	20.5	20.5	3.4	77.9	1.30	2.58	15.02	190	6	281

$v_u/\phi < 0.85$ ∴ nil.

Figure A-2 - Shear design of hollowcore unit from Stresscrete

A2 Seating Beam Base Block Design

The seating beam used for the experimental investigation was based directly off the Matthews (2004) super-assembly test specimen. However, in order to create a more stable base block and improve the time efficiency of the experimental investigation, one base block was comprised of two seating beams back-to-back (illustrated in Figure A-3and Figure A-4). This allowed two tests to be carried out on one base block by rotating the base through 180 degrees for the second test. A tie stirrup within the half-beam was used to tie the two beams together. The tie stirrup was specified consistent with beam transverse reinforcement (the same size and spacing) for simplicity, and checked using a strut and tie approach as illustrated in Figure A-3 and Figure A-4.

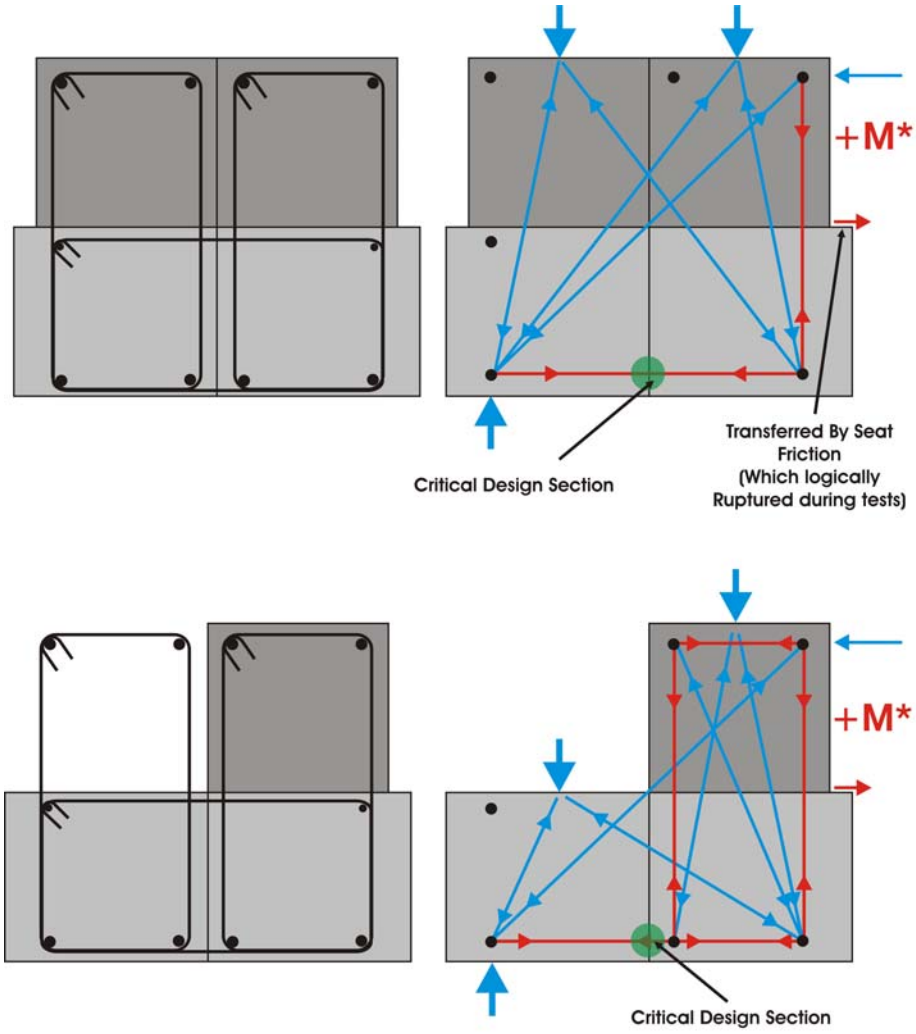

Figure A-3 - Positive hollowcore drift seating beam design

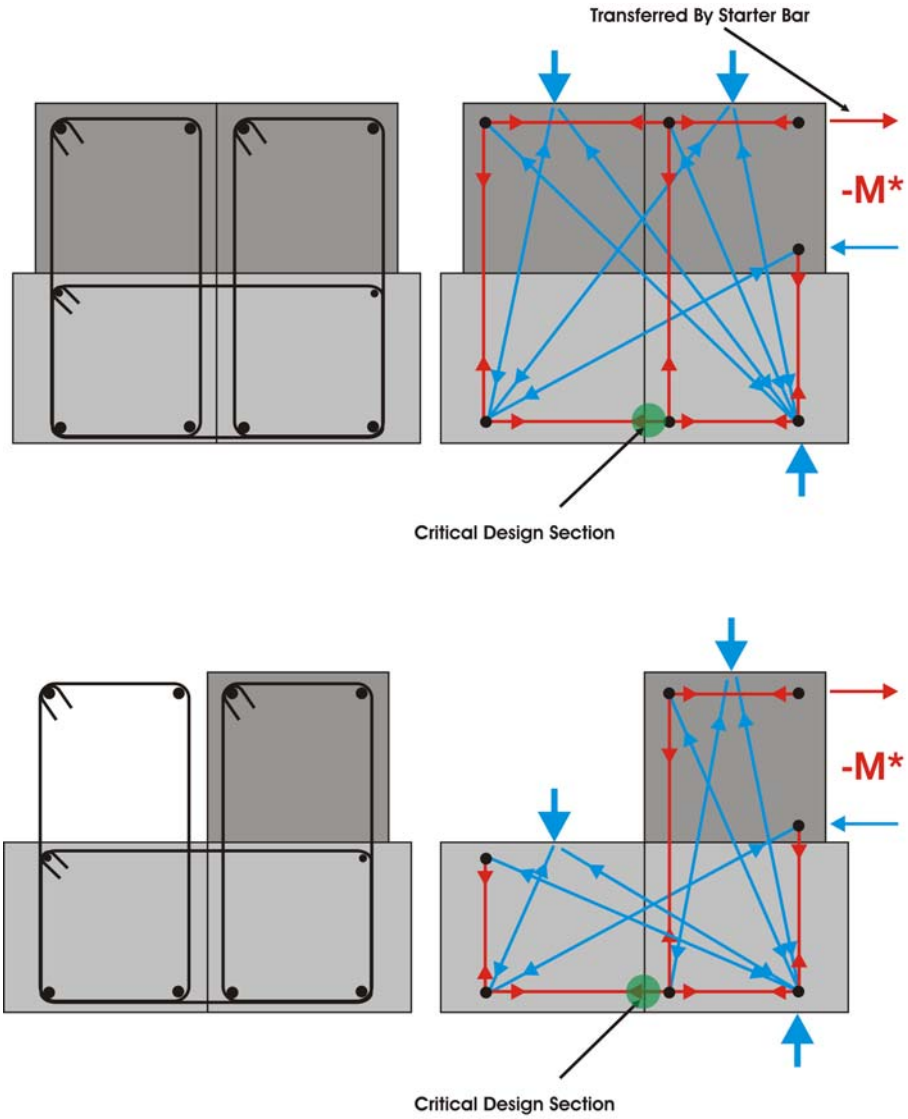

Figure A-4 – Negative hollowcore drift seating beam design

A3 Shear Gradient Adjustment – Gravity Load

This section outlines the method for determining the appropriate gravity load demand for the half-span sub-assembly test specimen, as outlined in Section 2.2. Two alternative gravity load demand options were used one representing the self weight only of the floor system (consistent with previous tests), and one to include superimposed dead load and seismic live load (G&Q_u&E). The reason for this was to determine the amount of additional gravity load to apply to the sub-assembly specimen to represent the load conditions at the seating connection of the full-span floor system. Figure A-5 illustrates the comparison between full-span and half-span shear force diagrams. The addition of a point load (large mass of concrete) was used to modify the sub-assembly shear gradient to represent the full-span in the vicinity of the seating connection.

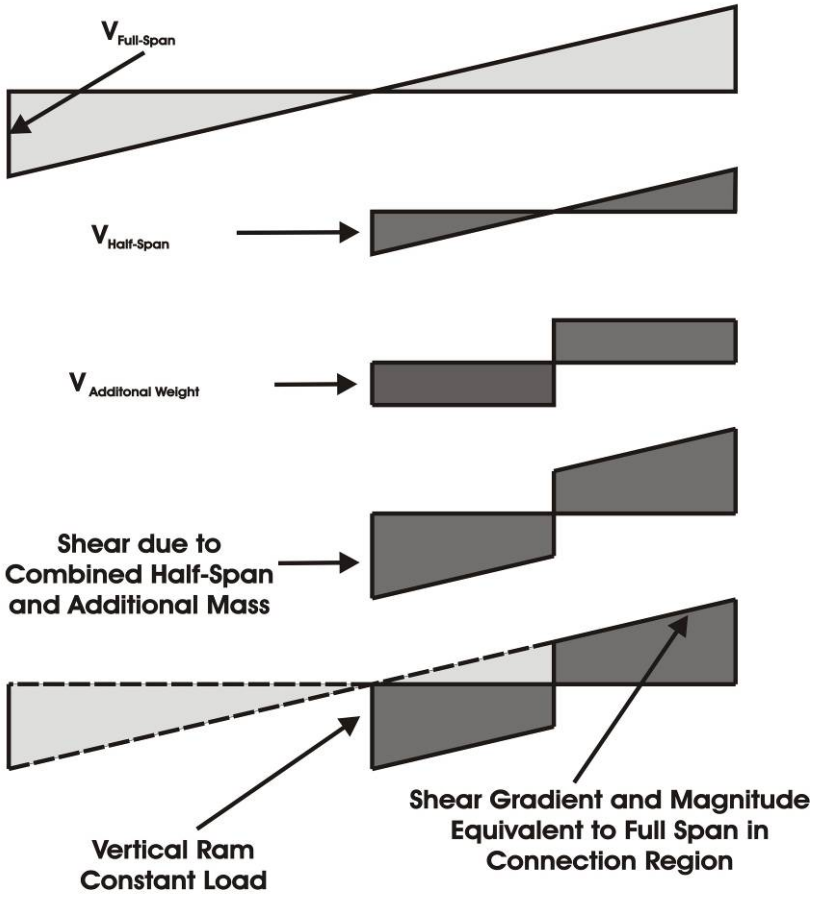

Figure A-5 - Shear gradient modification

Loads:

The basic gravity loads are as followed (as used in design of the hollowcore units):

$$G_{Hollowocre\,unit} = 3.2KPa$$
$$G_{Topping} = 2.1KPa$$
$$G_{Superimposed} = 0.5KPa$$
$$Q = 3.0KPa$$
$$Q_u = 1.2KPa$$

Self-weight dead load only:

Full- and half-span reactions are shown below

$$V_{Full-Span} = \frac{WL}{2}$$

$$W = (3.2 + 2.1)kPa \times 1.2m$$
$$= 6.4kNm^{-1}$$

$$L = 12m$$

$$V_{Full-Span} = \frac{6.4 \times 12}{2}$$
$$= 38.4kNm$$

$$V_{Half-Span} = \frac{WL}{2}$$

$$L = 6m$$

$$V_{Half-Span} = \frac{6.4 \times 6}{2}$$
$$= 19.2kNm$$

A 50kN concrete weight was used to implement the additional gravity load, for which the position of the weight was determined to give the correct proportional addition of the 50kN load at the seating connection. The seating connection had a significant degree of fixity until initial cracking, however for simplicity a simple connection was assumed to match post cracking behaviour (which occurs very early in the testing). This was justified by the majority of the test and importance of vertical gravity load support weighted towards post cracking behaviour.

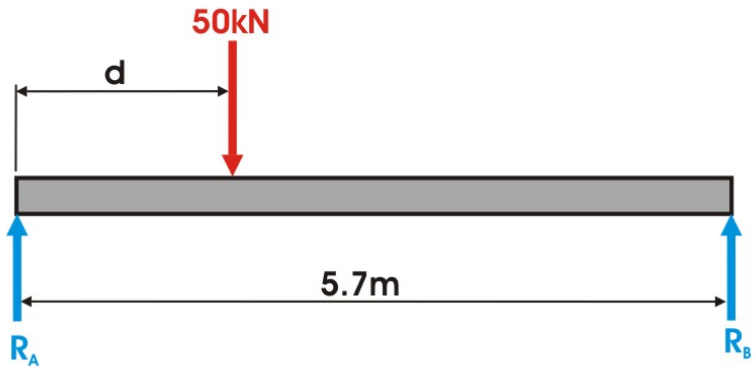

Figure A-6 - Simple schematic used to determine location of additional gravity weight

R_A represents the vertical support for which the vertical hydraulic actuator supports and R_B the seating connection reaction. The reduction to 5.7m is a result of the ram pin being located approximately 0.3m from the end of the 6m unit.

$$R_{B(Desired)} = V_{Full-Span} - V_{Half-Span}$$
$$= 38.4 - 19.2$$
$$= 19.2kN$$

$$R_{A(Desired)} = 50 - 19.2$$
$$= 30.8kN$$

$$\sum M_A = 0$$
$$19.2kN \times 5.7m = 50kN \times d$$
$$d = 2.2m$$

Therefore, the location of the 50kN additional gravity load is 2.2m from the vertical hydraulic ram support to achieve the desired gravity load modification.

Superimposed dead and seismic live load (G&Q_u&E):

$$V_{Full-Span} = \frac{WL}{2}$$

$$W = (3.2 + 2.1 + 0.5 + 1.2)kPa \times 1.2m$$
$$= 8.4kNm^{-1}$$

$$L = 12m$$

$$V_{Full-Span} = \frac{8.4 \times 12}{2}$$
$$= 50.4kN$$

$$V_{Half-Span} = \frac{WL}{2}$$

$$L = 6m$$

$$V_{Full-Span} = \frac{8.4 \times 6}{2}$$
$$= 25.2kN$$

Therefore an additional 25.2kN is required to account for the addition of superimposed gravity and seismic live loads.

$$R_{B(Desired)} = V_{Full-Span} - V_{Half-Span}$$
$$= 50.4 - 25.2$$
$$= 25.2kN$$

$$R_{A(Desired)} = 50 - 25.2$$
$$= 24.8kN$$

$$\sum M_A = 0$$
$$25.2kN \times 5.7m = 50kN \times d$$
$$d = 2.9m$$

Therefore, the location of the 50kN gravity load is 2.9m from the vertical ram support to achieve the desired gravity load modification.

A4 Construction Drawings and Photographs

Shown below are the construction drawings for the seating beam and connection details for the four seating connection test specimens. A selection of construction photographs are shown to illustrate the general construction process for the sub-assembly test specimens.

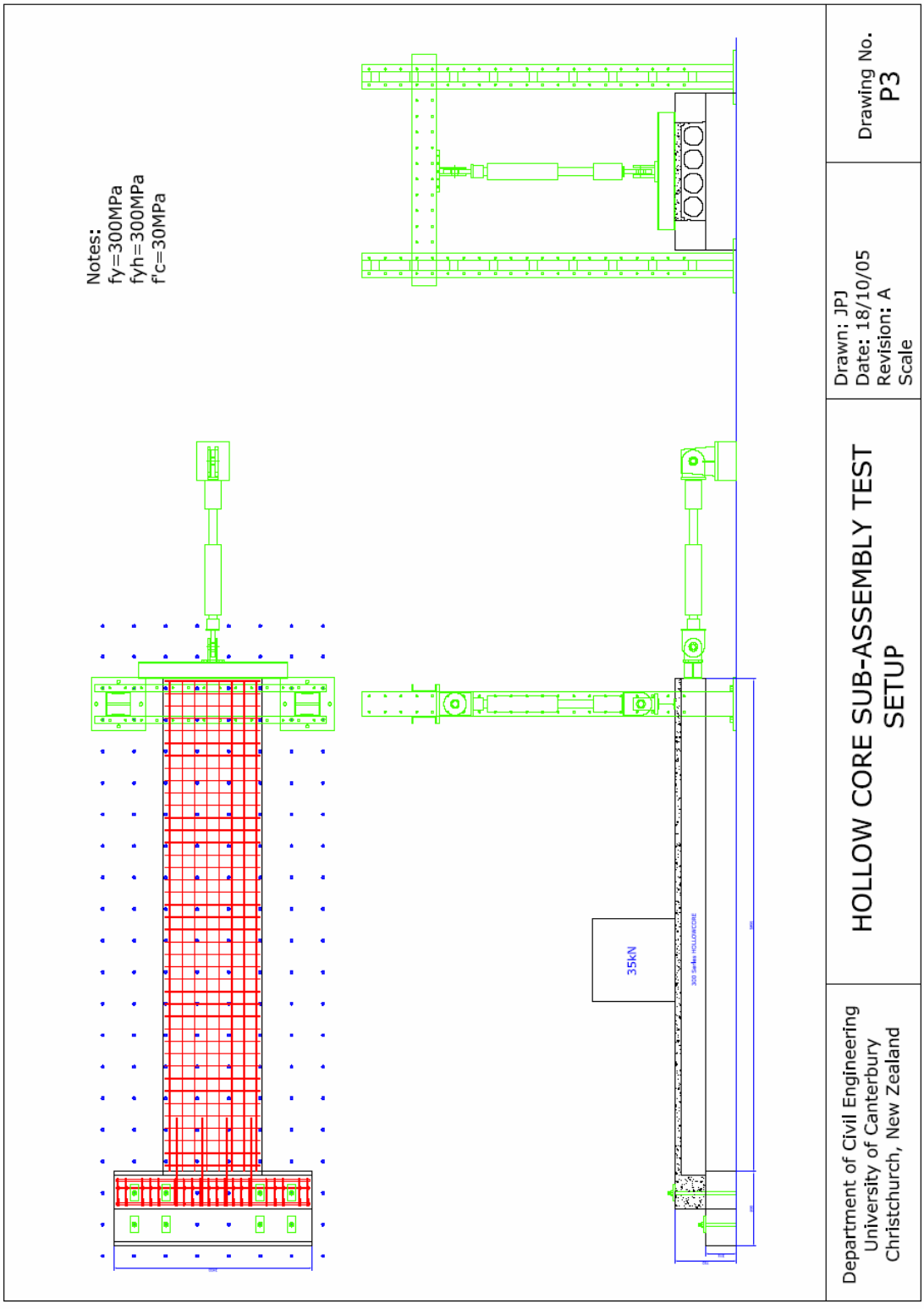

Figure A-7 Hollowcore sub-assembly test setup

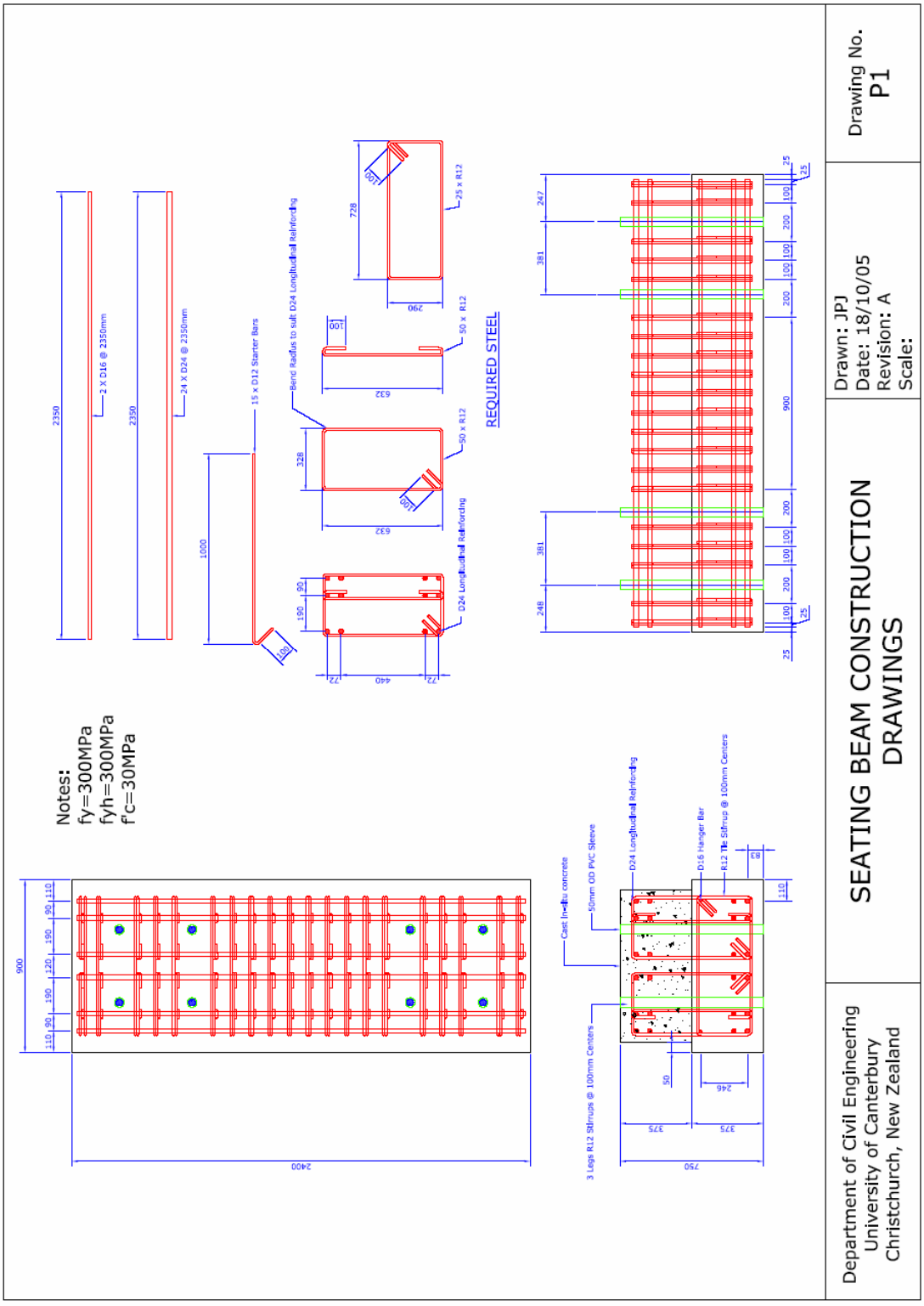

Figure A-8 Seating beam construction drawings

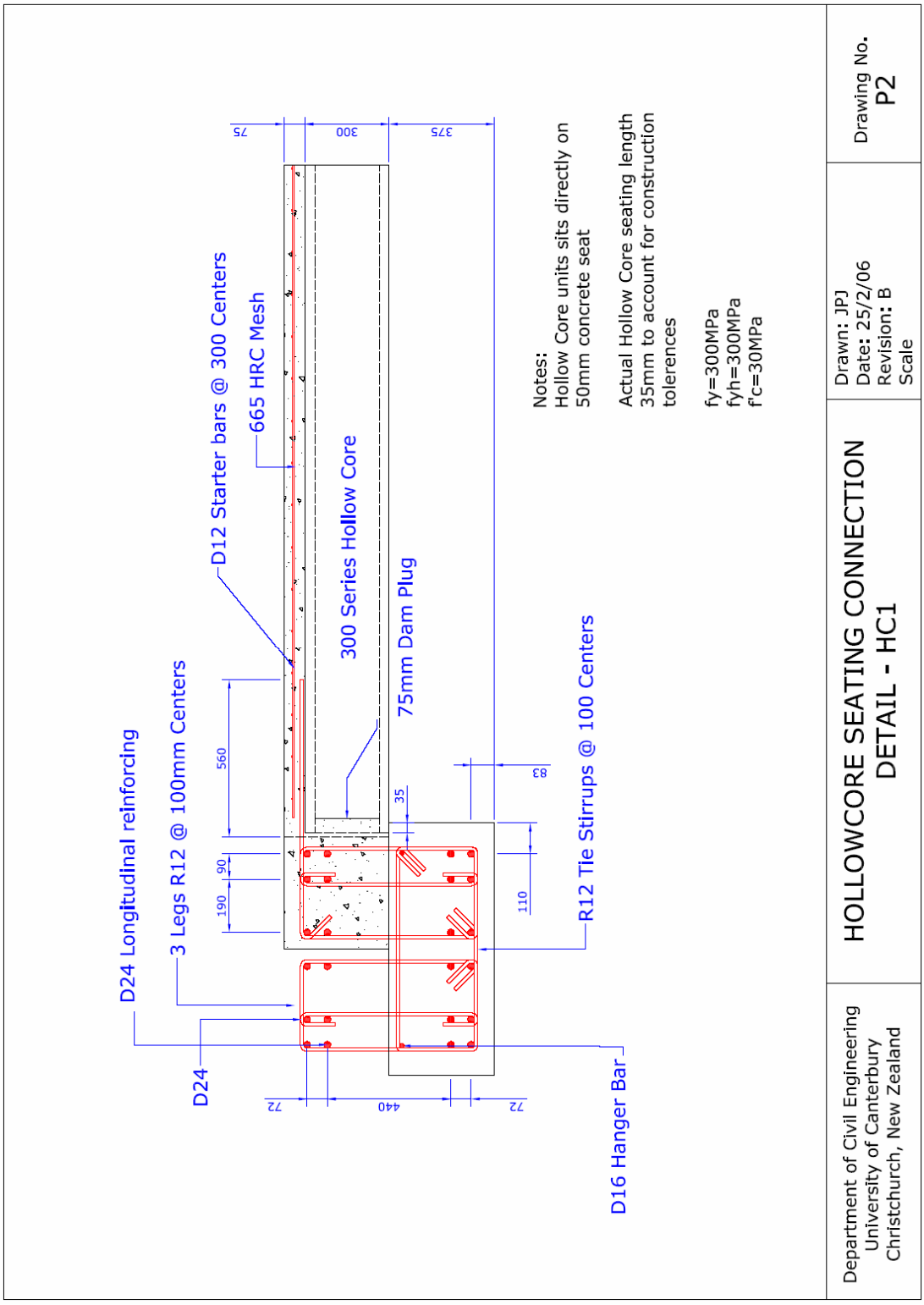

Figure A-9 HC1 seating connection detail

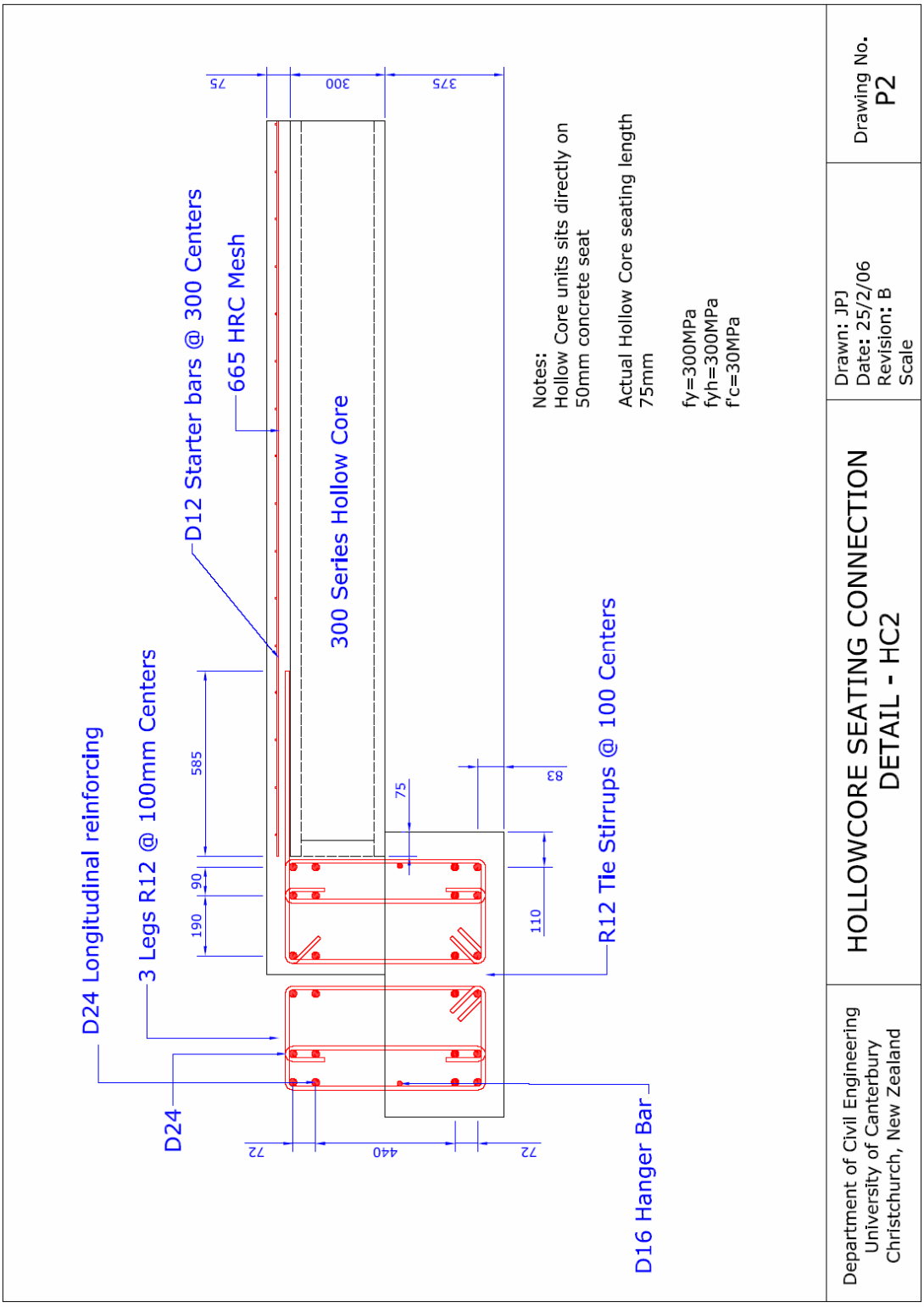

Figure A-10 HC2 seating connection detail

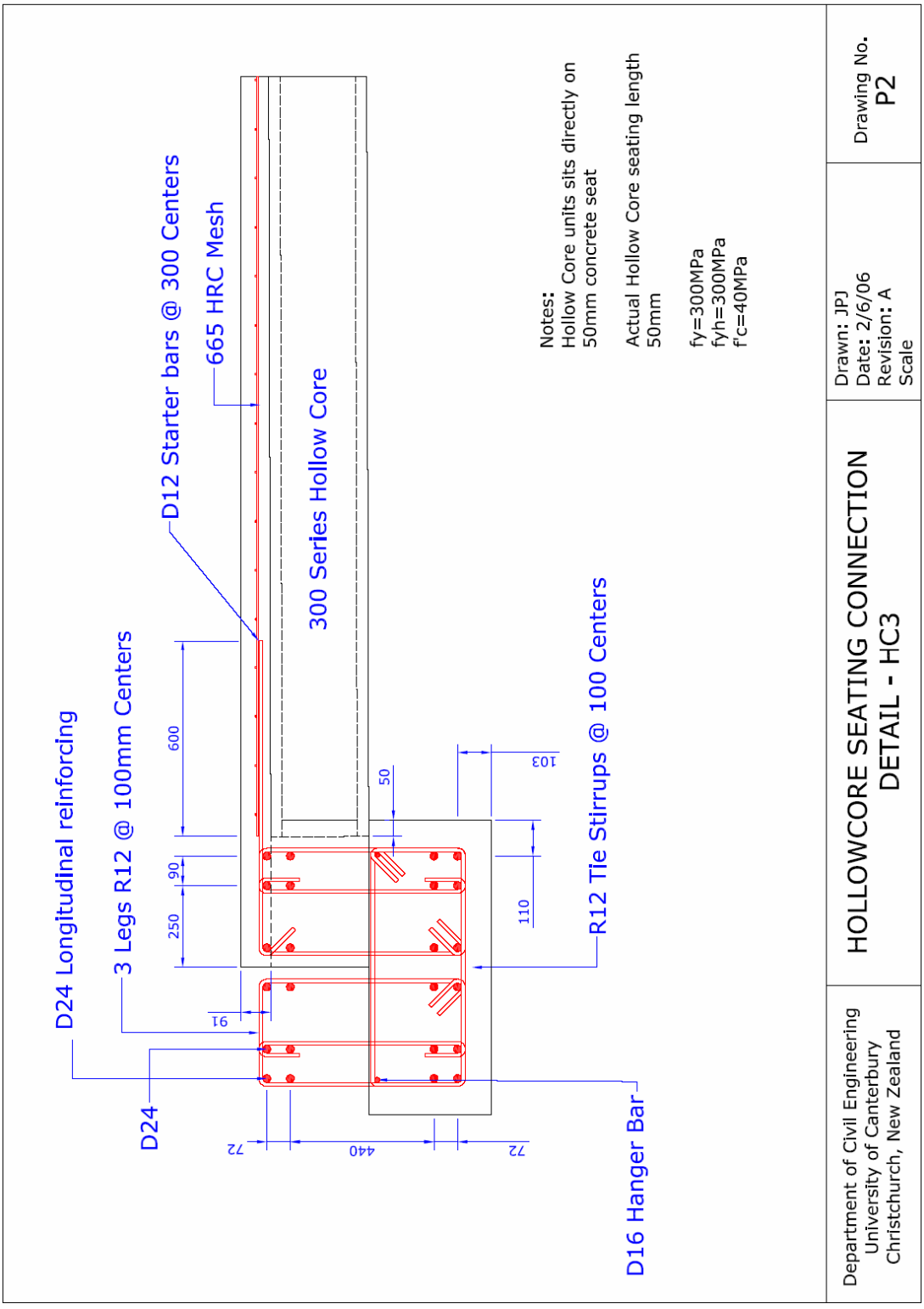

Figure A-11 HC3 seating connection detail

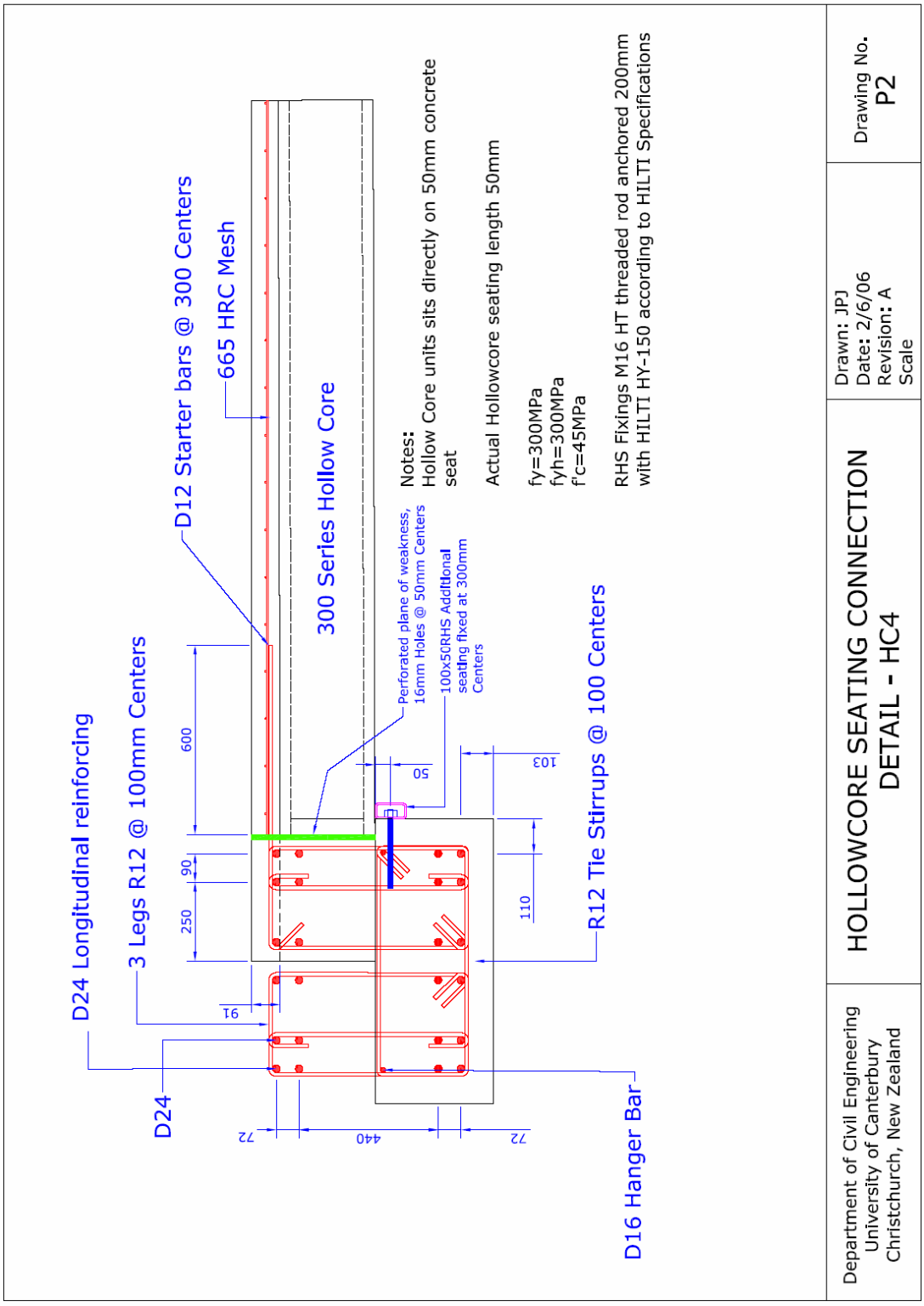

Figure A-12 HC4 seating connection detail

Figure A-13 Seating beam formed up ready for half beam concrete pour

Figure A-14 Seating beam following half beam concrete pour

Figure A-15 Hollowcore unit in position on half beam

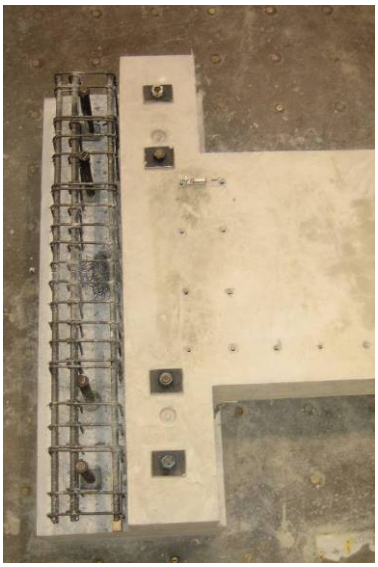

Figure A-16 Final specimen ready for instrumentation

Figure A-17 Topping mesh and starter bars in place and hollowcore unit formed for topping concrete pour

Figure A-18 Typical ready to test seating connection specimen

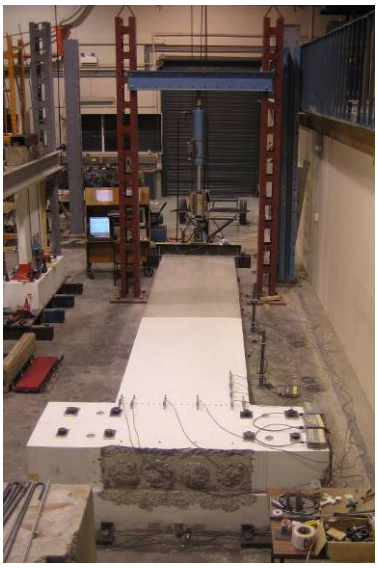

Figure A-19 Full specimen rig for second test on seating beam

Figure A-20 Loading beams attached to end of unit

A5 Material Testing

This section outlines the details regarding various material tests carried out on the test specimen elements (summaries were given in Section 2). The following material properties were tested:

- Topping Reinforcement – D12 Starter bar and 665 HRC Mesh
- Half and full beam concrete properties
- 'New' (HC1 and HC2) and 'Old' (HC3 and HC4) hollowcore unit concrete properties

Topping Reinforcement:

Figure A-21 shows the stress versus strain relationships for the topping reinforcement. This was carried out using the standard monotonic tensile test. The characteristic stress and strain values are shown in Table A-1.

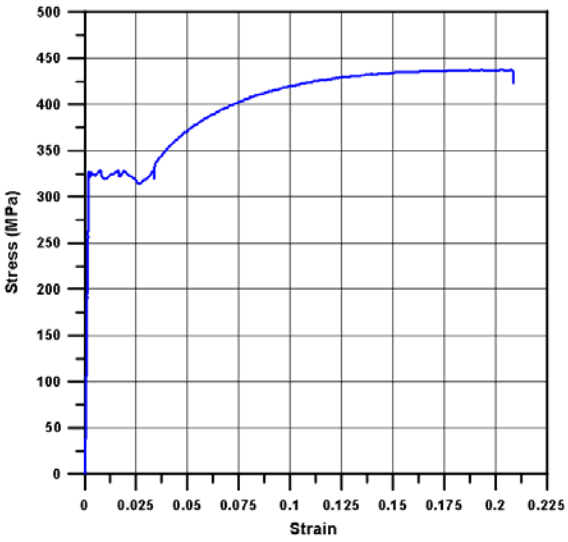

a) Stress versus strain relationship for D12 starter bars

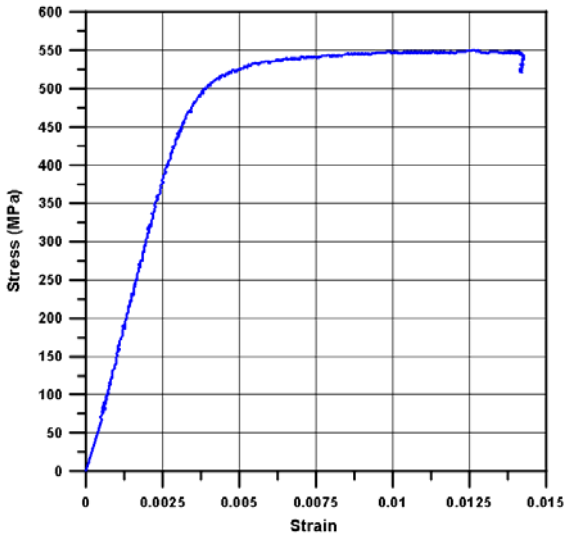

a) Stress versus strain relationship for 665HRC welded wire mesh

Figure A-21 Reinforcing steel stress versus strain relationships

Table A-1 Reinforcement material properties

Type	Location	f_y(MPa)	f_{sh}(MPa)	f_u(MPa)	E_s(GPa)	ε_y	ε_{sh}	ε_{su}
D12	Starter Bars	326	337	436	190	0.003	0.035	0.21
665 HRC Mesh	Topping Mesh	-	-	548	157	-	-	0.014

Half and Full Beam Concrete:

The mean compressive strength of the concrete (f'_c) was determined from standard compressive tests of 100mmx200mm test cylinders.

Hollowcore Unit Concrete:

The compressive strength (f'_c) and modulus of rupture (f_r) of the concrete were estimated for the two types of hollowcore unit used in the experimental investigation. The compressive strength was determined by compression tests on core samples taken from the units. The two data sets for the 'new' and 'old' units are shown in Figure A-22 and Figure A-23.

Sample	f'c (MPa)
1	52.9
2	48.9
3	48.6
4	50.9
5	44.7
6	51.8
7	48.6
8	51.5
9	44.1

Mean f'c (MPa)	49.1
SD (MPa)	3.1

a) Raw Data

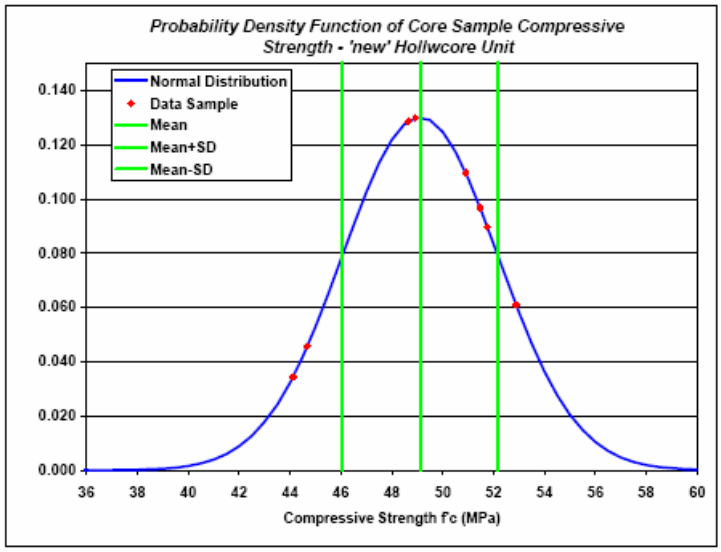

b) Statistical Representation

Figure A-22 'New' core sample test results

Sample	f'c (MPa)
1	90
2	91
3	97
4	92
5	83
6	74
7	82

Mean f'c (MPa)	86
SD (MPa)	6.6

a) Raw Data

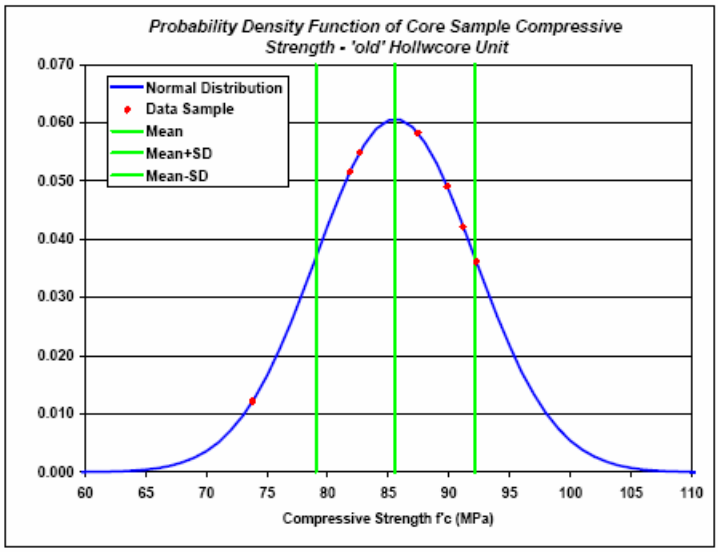

b) Statistical Representation

Figure A-23 'Old' core sample test results

The modulus of rupture (f_r) for the 'new' and 'old' hollowcore units was determined using a two point beam test on small segments of the hollowcore units. 500mm long segments were cut out of the top of hollowcore units and loaded to rupture as illustrated in Figure A-24.

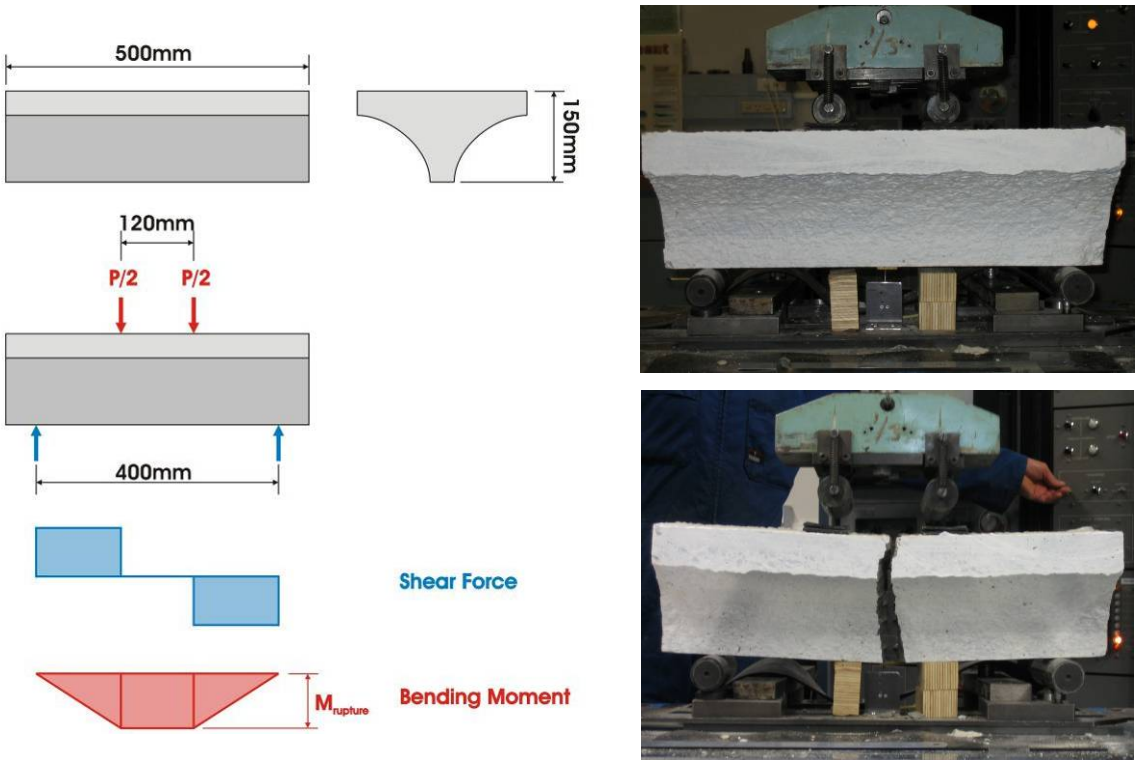

a) Test procedure schematic **b) test photos**

Figure A-24 Two point loading test of hollowcore unit segments

Figure A-25 and Figure A-26 below summarise the results form the modulus of rupture tests.

Sample	f_r (MPa)
1	6.49
2	6.13
3	5.22
4	5.80
5	6.39
6	5.99

Mean fr (MPa)	6.00
SD (MPa)	0.46

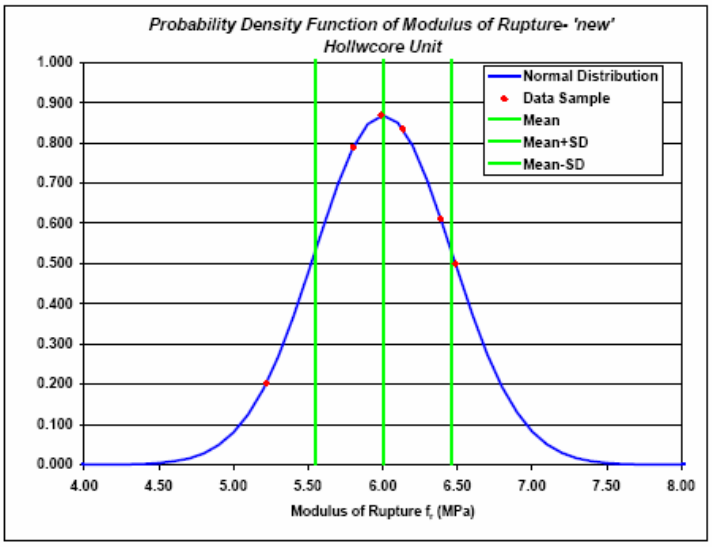

a) Raw data **b) Statistical representation**

Figure A-25 'new' hollowcore unit modulus of rupture test results

Sample	f_r (MPa)
1	7.61
2	7.87
3	7.35
4	7.87
5	6.96
6	8.00

Mean fr (MPa)	7.60
SD (MPa)	0.39

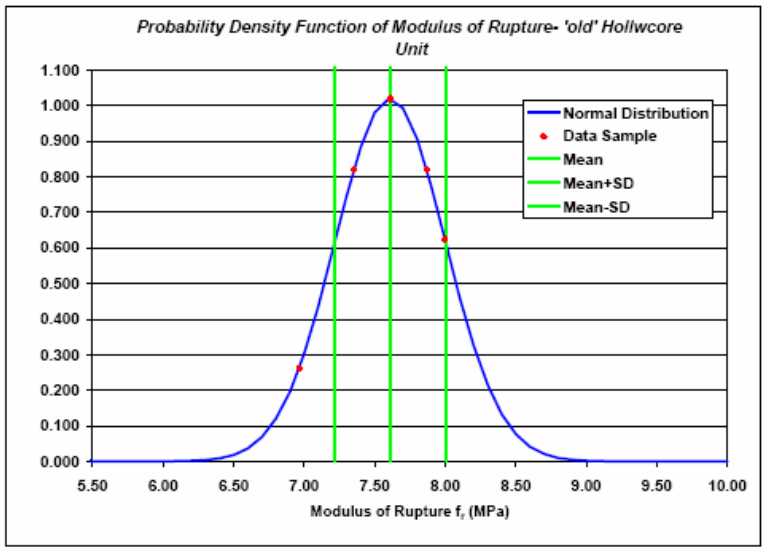

a) Raw data **b) Statistical representation**

Figure A-26 'old' hollowcore unit modulus of rupture test results

Appendix B Experimental Testing

This section outlines additional data and photos from the HC1, HC2, HC3 and HC4 seating connection experimental tests.

B1 Strain Gauge Readings

Strain gauge measurements were taken at six locations along the length of all the starter bars. The six locations were labelled 1 through 6, from left to right along each starter bar as shown in Figure B-. The four starter bars were labelled A, B, C and D, each strain gauge reading is referenced A1, A2, etc. The strain readings are shown at discrete peak drift levels only.

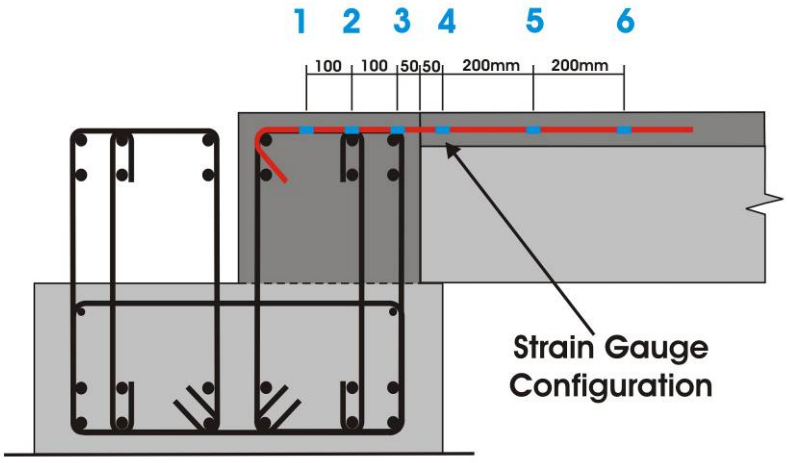

Figure B-1 Strain gauge locations

Figure B- below illustrates the way in which a rough integration of discrete strain gauge strain values was used to verify the average stain across the interface between the hollowcore unit and seating beam (determined by potentiometers across the interface).

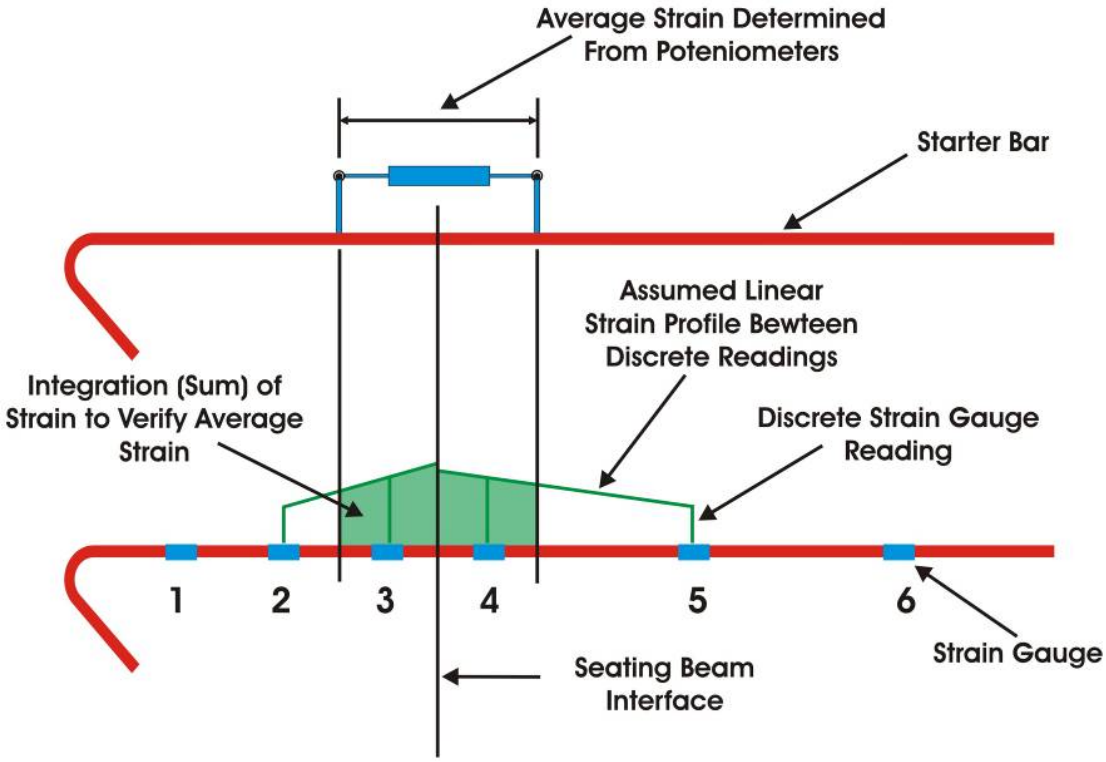

Figure B-2 Strain integration of strain gauge data to verify average strain

Based on this approximation, if the strain integration equates roughly to the average strain the average strain was assumed to be representative.

HC1 Strain readings:

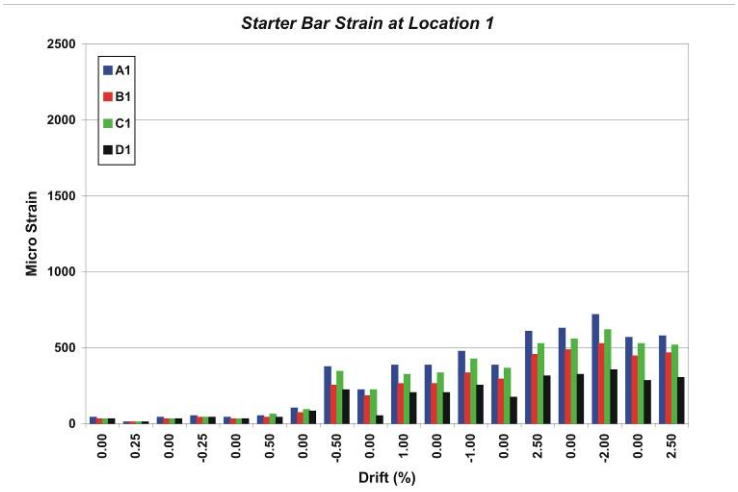

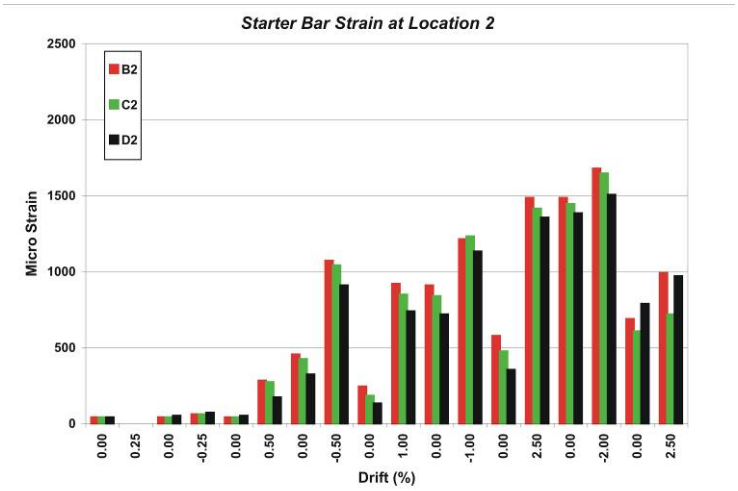

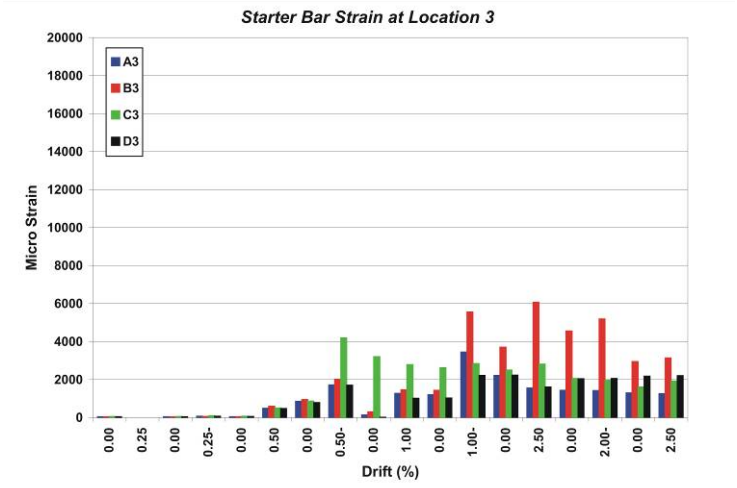

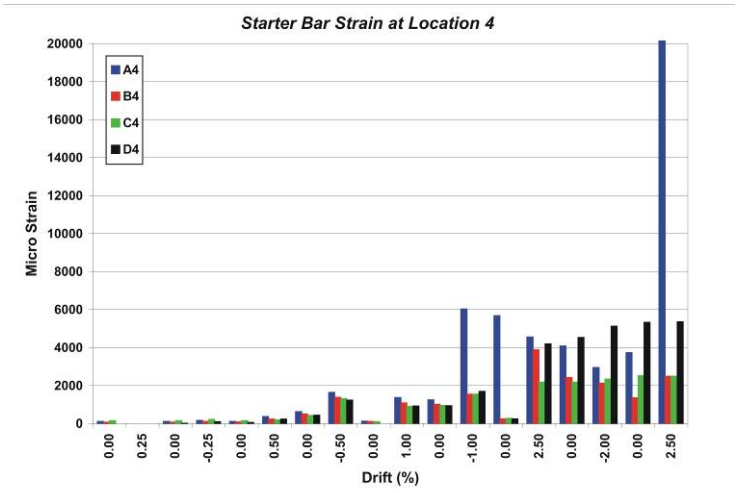
Starter Bar Strain at Location 4
A4
B4
C4
D4
Micro Strain
20000
18000
16000
14000
12000
10000
8000
6000
4000
2000
0
0.00
0.25
0.00
-0.25
0.00
0.50
0.00
-0.50
0.00
1.00
0.00
-1.00
0.00
2.50
0.00
-2.00
0.00
2.50
Drift (%)

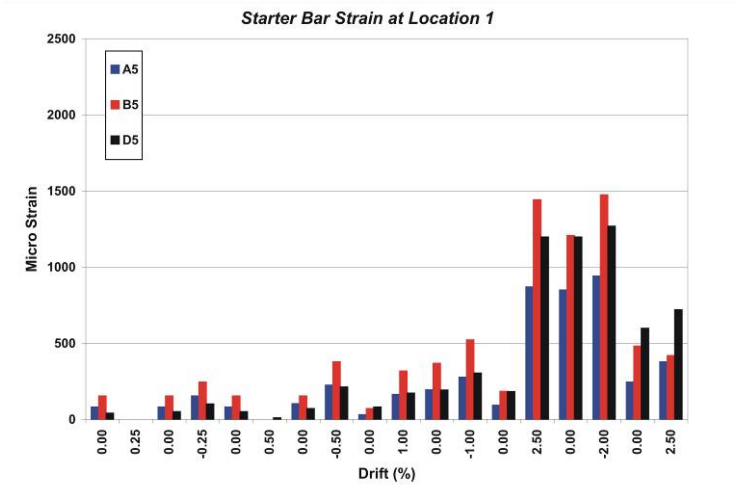
Starter Bar Strain at Location 1
A5
B5
D5
Micro Strain
2500
2000
1500
1000
500
0
0.00
0.25
0.00
-0.25
0.00
0.50
0.00
-0.50
0.00
1.00
0.00
-1.00
0.00
2.50
0.00
-2.00
0.00
2.50
Drift (%)

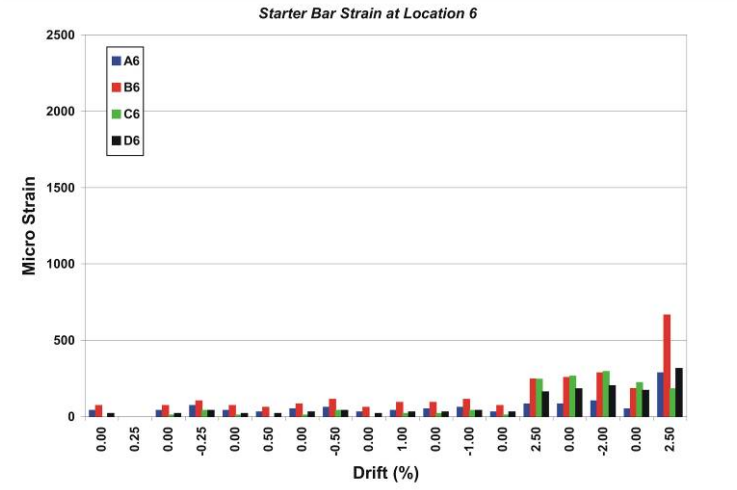
Starter Bar Strain at Location 6
A6
B6
C6
D6
Micro Strain
2500
2000
1500
1000
500
0
0.00
0.25
0.00
-0.25
0.00
0.50
0.00
-0.50
0.00
1.00
0.00
-1.00
0.00
2.50
0.00
-2.00
0.00
2.50
Drift (%)

HC2 Strain readings:

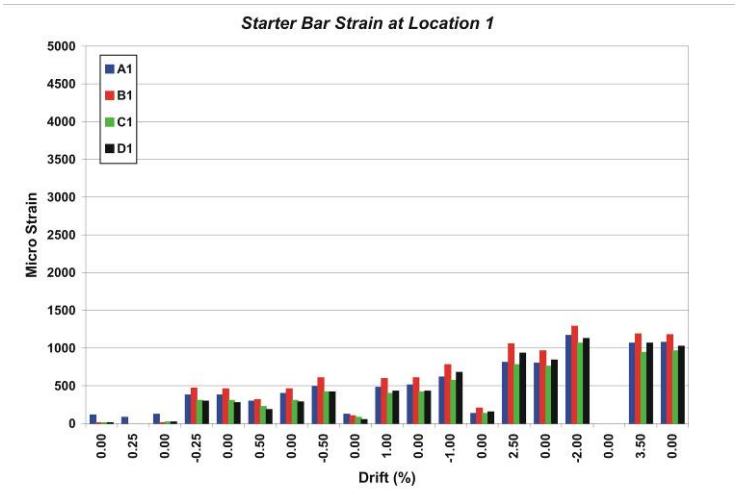

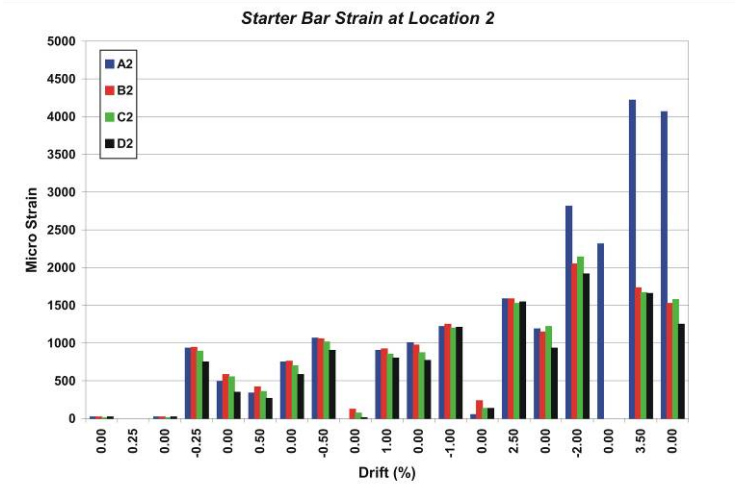

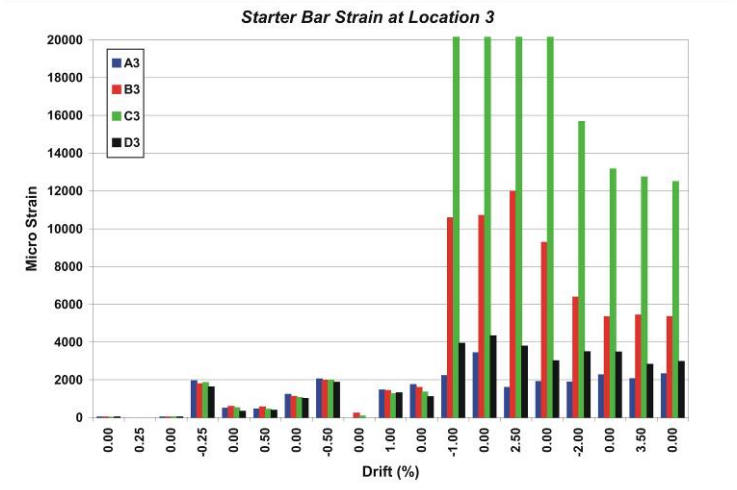

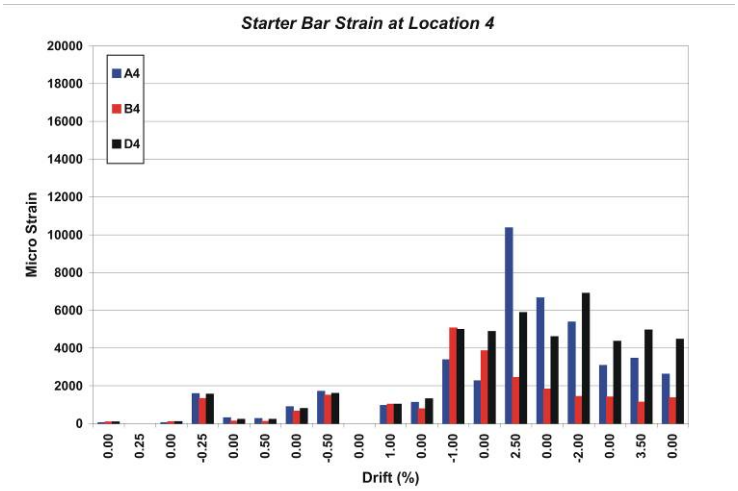
Starter Bar Strain at Location 4
A4
B4
D4
Micro Strain
20000
18000
16000
14000
12000
10000
8000
6000
4000
2000
0
0.00 0.25 0.00 -0.25 0.00 0.50 0.00 -0.50 0.00 1.00 0.00 -1.00 0.00 2.50 0.00 -2.00 0.00 3.50 0.00
Drift (%)

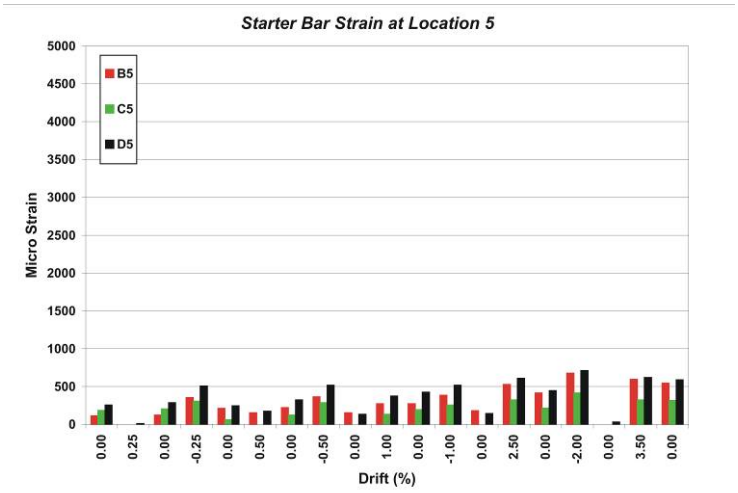
Starter Bar Strain at Location 5
B5
C5
D5
Micro Strain
5000
4500
4000
3500
3000
2500
2000
1500
1000
500
0
0.00 0.25 0.00 -0.25 0.00 0.50 0.00 -0.50 0.00 1.00 0.00 -1.00 0.00 2.50 0.00 -2.00 0.00 3.50 0.00
Drift (%)

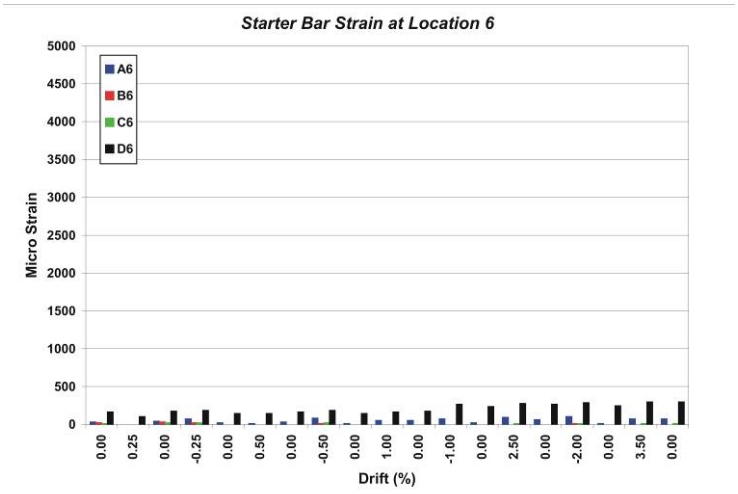
Starter Bar Strain at Location 6
A6
B6
C6
D6
Micro Strain
5000
4500
4000
3500
3000
2500
2000
1500
1000
500
0
0.00 0.25 0.00 -0.25 0.00 0.50 0.00 -0.50 0.00 1.00 0.00 -1.00 0.00 2.50 0.00 -2.00 0.00 3.50 0.00
Drift (%)

HC3 Strain readings:

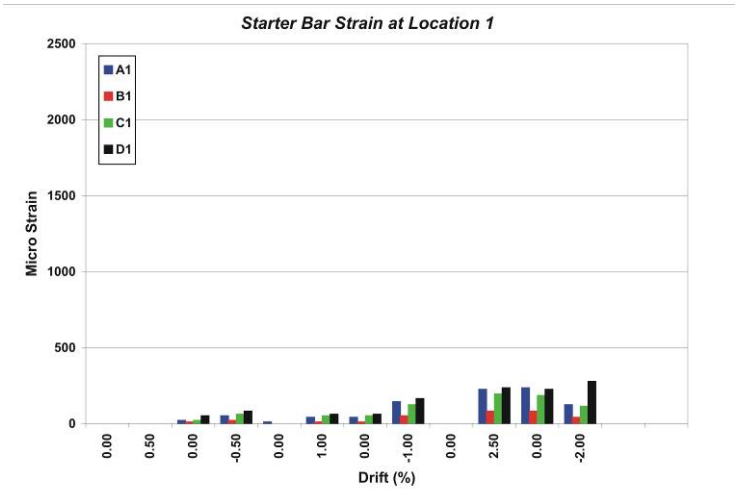

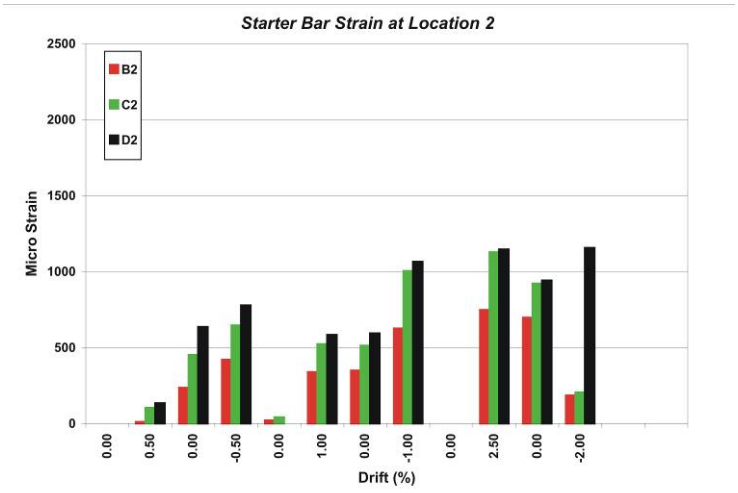

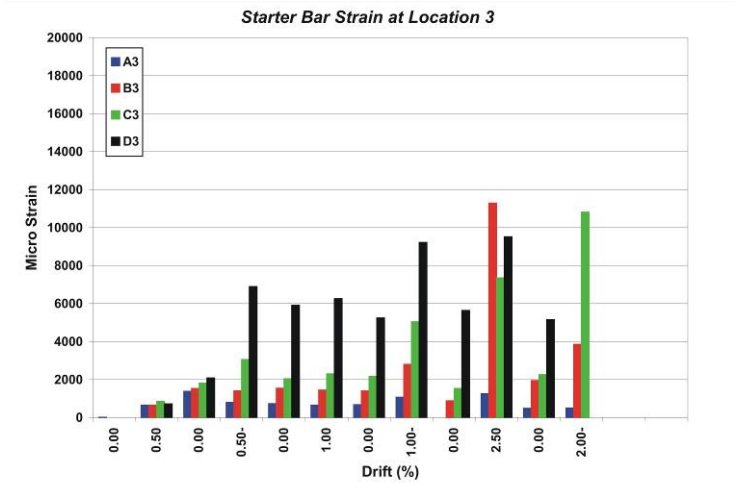

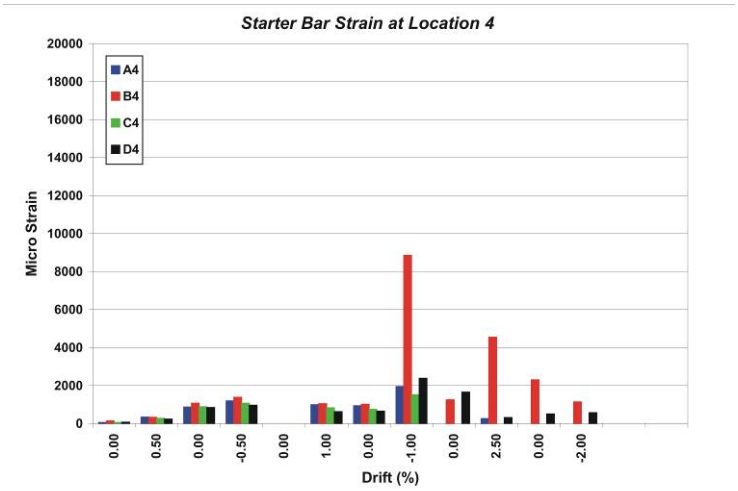
Starter Bar Strain at Location 4
A4
B4
C4
D4
Micro Strain
20000
18000
16000
14000
12000
10000
8000
6000
4000
2000
0
0.00
0.50
0.00
-0.50
0.00
1.00
0.00
-1.00
0.00
2.50
0.00
-2.00
Drift (%)

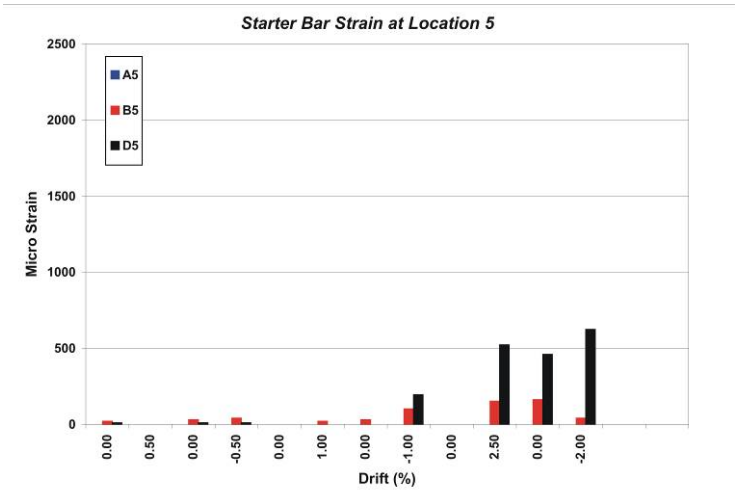
Starter Bar Strain at Location 5
A5
B5
D5
Micro Strain
2500
2000
1500
1000
500
0
0.00
0.50
0.00
-0.50
0.00
1.00
0.00
-1.00
0.00
2.50
0.00
-2.00
Drift (%)

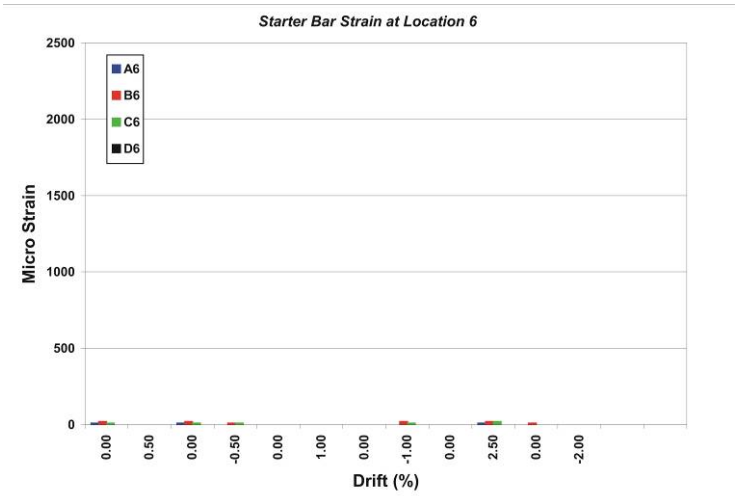
Starter Bar Strain at Location 6
A6
B6
C6
D6
Micro Strain
2500
2000
1500
1000
500
0
0.00
0.50
0.00
-0.50
0.00
1.00
0.00
-1.00
0.00
2.50
0.00
-2.00
Drift (%)

HC4 Strain readings:

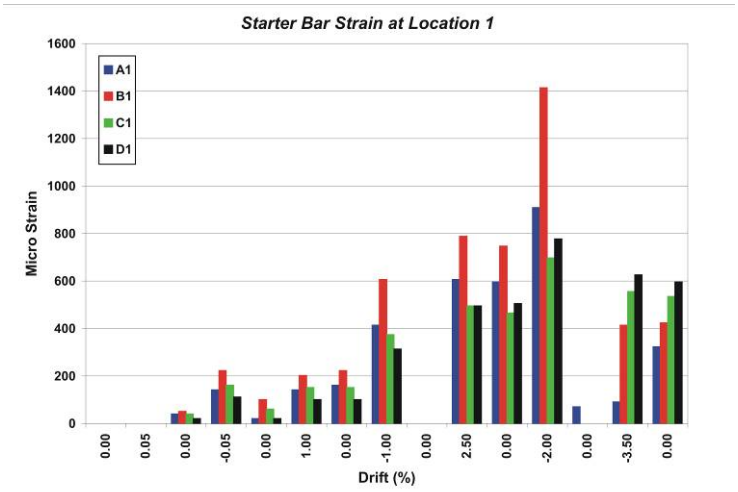

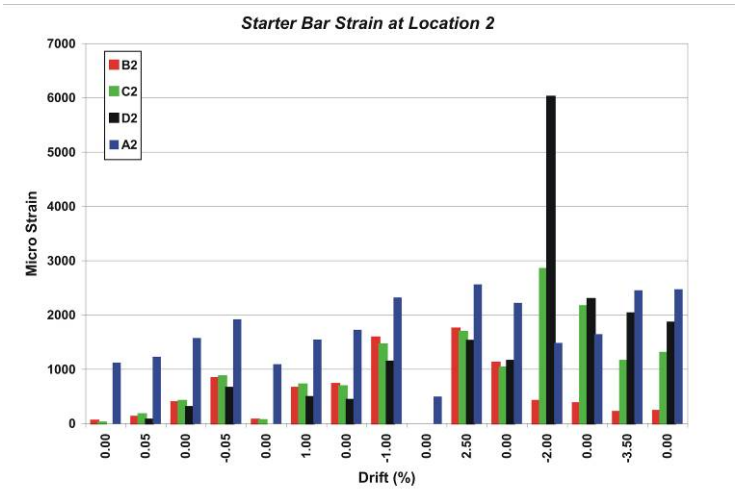

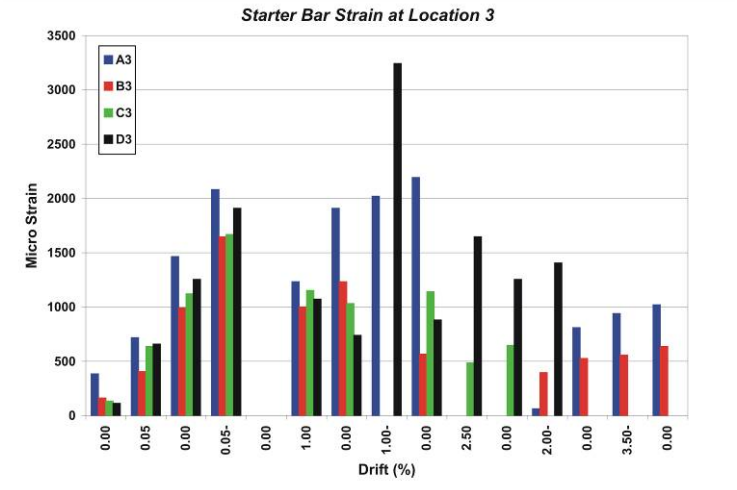

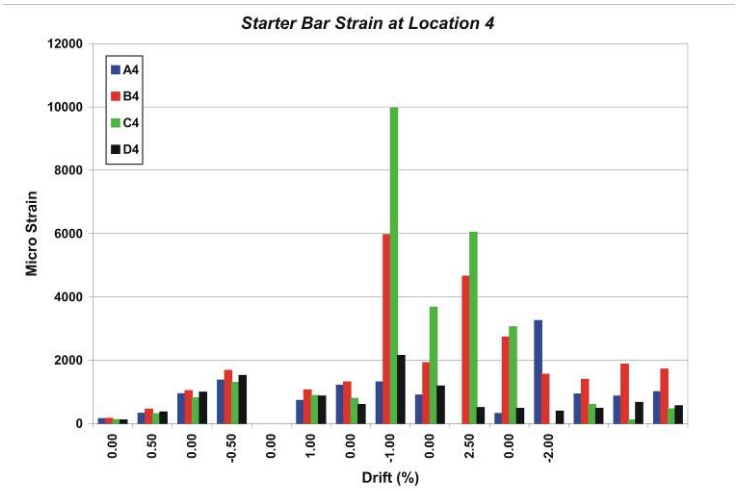

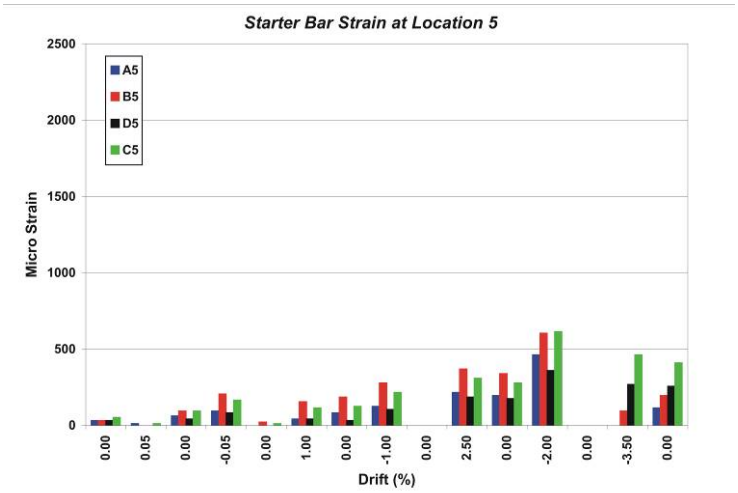

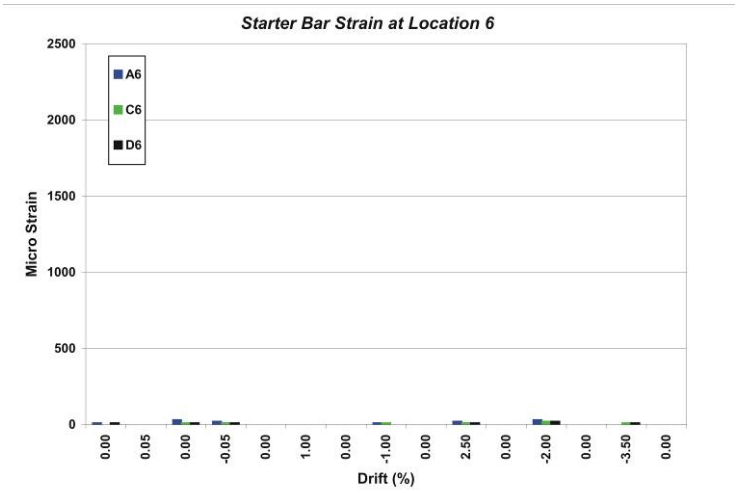

B2 Test Photos

The following photos were taken during the testing of each specimen. The reason for including them was to give further representation of the tests, other than the photos presented in Section 3 (HC1, HC2 and HC3) and Section 6 (HC4).

HC1 – Control Specimen:

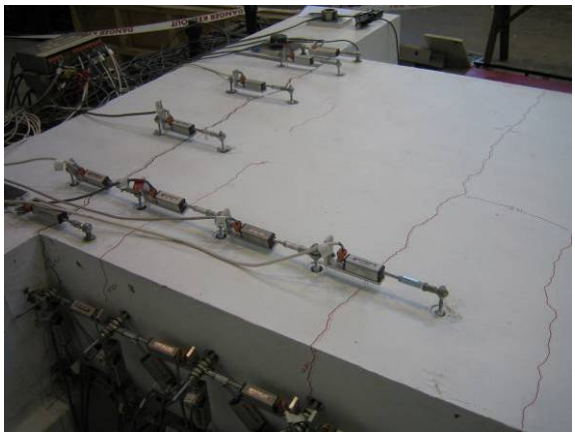

Figure B-3 HC1 lateral topping cracks at -0.25% drift

Figure B-4 HC1 seat spalling at -1.0% drift

Figure B-5 HC1 hollowcore to seating beam interface at -2.0% drift

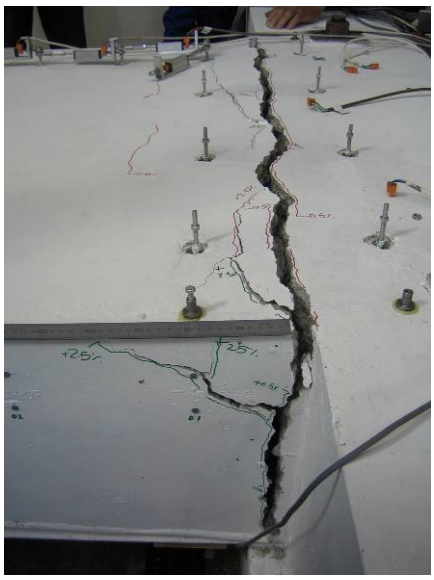

Figure B-6 HC1hollowcore to seating beam interface at -2.0% drift

Figure B-7 HC1 topping delamination, unit dropping at -2.0% drift

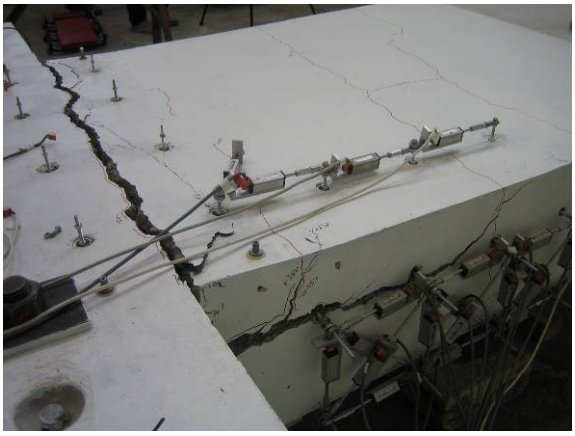

Figure B-8 HC1 seating beam interface and topping delamination at -2.0% drift

Figure B-9 HC1 unit dropping, delamination at +2.5% drift

Figure B-10 HC1 final collapse at +3.0% drift

HC2 – Control Specimen:

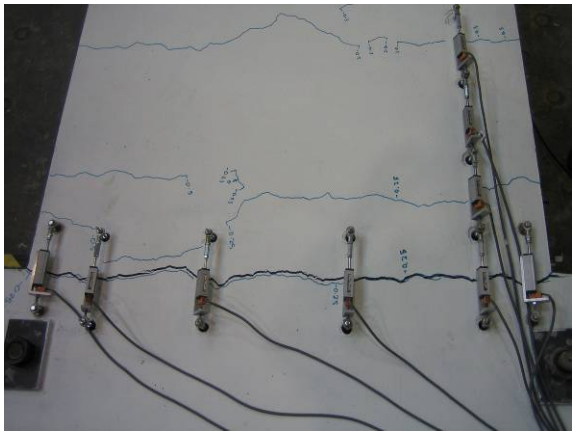

Figure B-11 HC2 interface crack and lateral topping cracks at -1.0% drift

Figure B-12 HC2 seating beam interface at +2.5% drift

Figure B-13 HC2 seat spalling at +2.5% drift

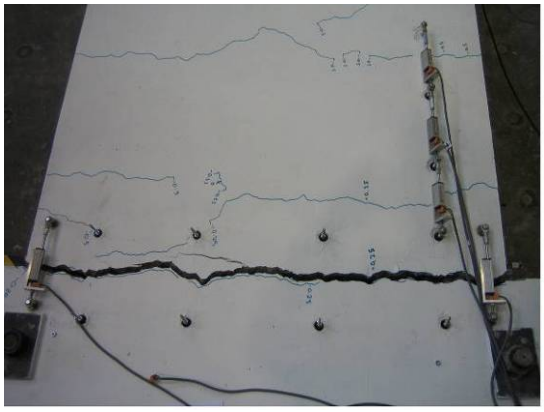

Figure B-14 HC2 seating beam interface at -2.0% drift

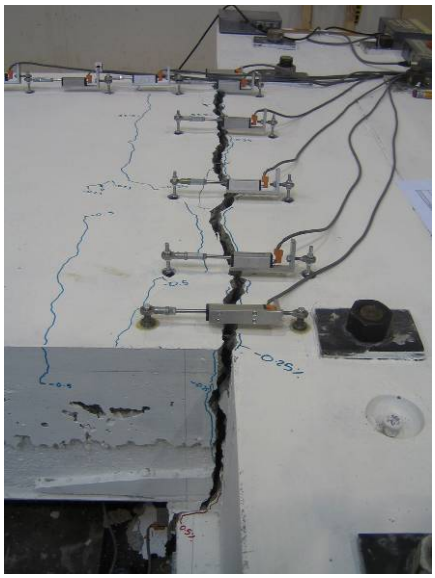

Figure B-15 HC2 seating beam interface at -2.0% drift

Figure B-16 HC2 seating beam interface at +3.5% drift

Figure B-17 HC2 Collapse under 55-60mm elongation

Figure B-18 HC2 Collapse under 55-60mm elongation

HC3 – Control Specimen:

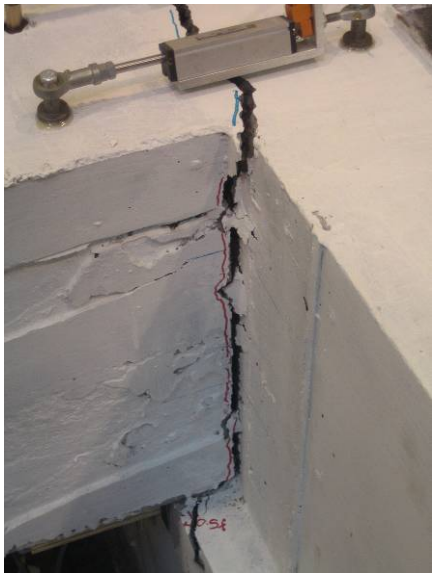

Figure B-19 HC3 seating beam interface at -1.0% drift

Figure B-20 HC3 seating beam interface at -1.0% drift

Figure B-21 HC3 Seating beam interface at +2.5% drift

Figure B-22 HC3 Seat spalling at +2.5% drift

Figure B-23 HC3 seat spalling at +2.5% drift

Figure B-24 HC3 final collapse at -2.0% drift

Figure B-25 HC3 final collapse at -2.0% drift

Figure B-26 HC3 final collapse at -2.0% drift

HC4 – Control Specimen:

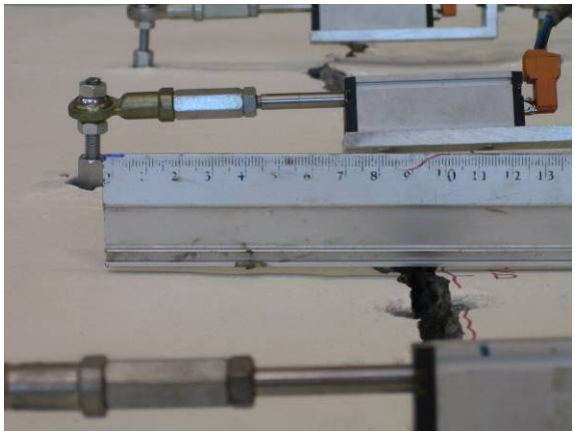

Figure B-27 HC4 unit drop from shift in support to additional seating at 2.5% drift

Figure B-28 HC4 additional seating providing support at 2.5% drift

Figure B-29 HC4 seating beam interface north at 2.5% drift

Figure B-30 HC4 seating beam interface south at 2.5% drift

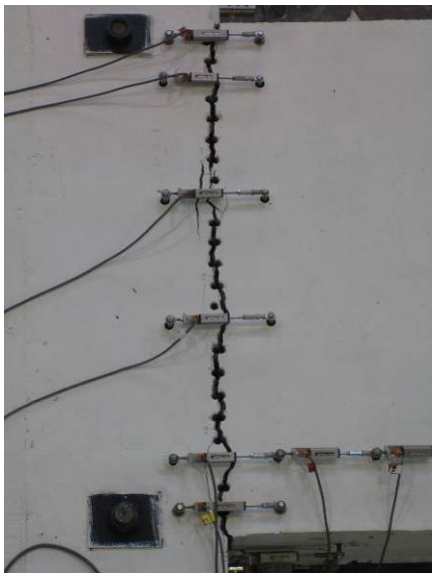

Figure B-31 HC4 seating beam interface/weakened plane

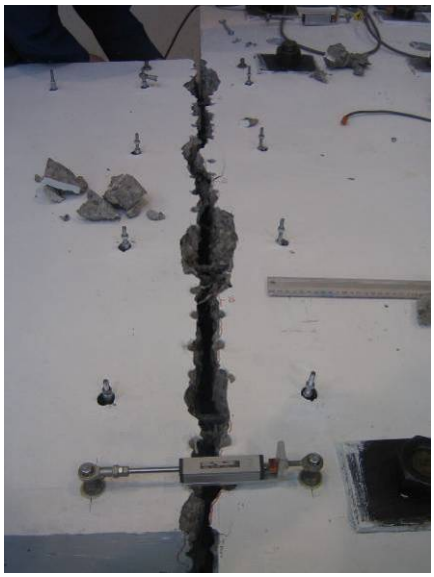

Figure B-32 HC4 seating beam interface/weakened plane at 2.5% drift

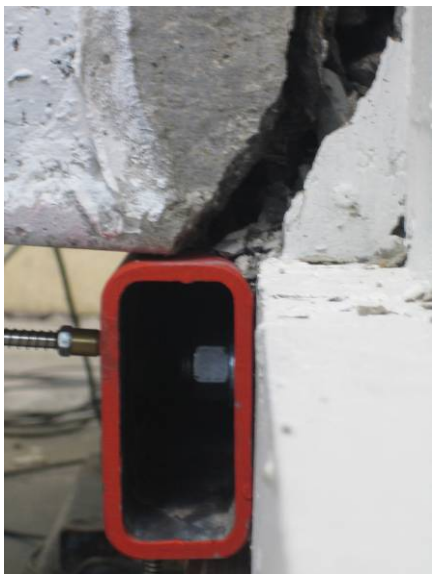

Figure B-33 HC4 additional seating support at 2.5% drift

Figure B-34 HC4 additional seating support at 2.5% drift

Appendix C Retrofit Considerations

This section outlines further details associated with design and testing of the retrofitted seating connection test specimen.

C1 Additional Seating Design

Outlined below is the design summary for the additional seating ledge (RHS steel section). Based on geometry and layout of reinforcing in the seating beam (PPHZ) four fixing points will be used at 300mm centres.

Design Load: $P = 50kN(G \,\&\, Q_u \,\&\, E)$

Steel Section: 100x50x6 RHS

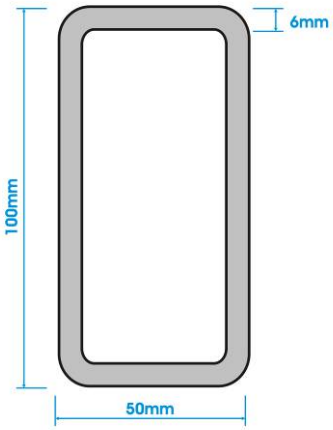

$$\phi M_{sx} = 18.3kNm$$
$$\phi V_v = 292kN$$

Section Design Check:

Section design check carried out assuming worst case un-even bearing resulting in bending and shear of a simply support assumption between two fixing points – this is a very conservative approach.

Section Bending:

$P = 50kN$

$$W_{Fixing} = \frac{P}{S_{Fixing}}$$

$$W_{Fixing} = \frac{50}{0.3}$$

$$W_{Fixing} = 167kNm^{-1}$$

$$M^* = \frac{W_{Fixing} \times S_{Fixing}^{\ 2}}{8}$$

$$M^* = \frac{167 \times 0.3^2}{8}$$

$$M^* = 1.9kNm$$

Section fixed to beam face and fully restrained

$\phi M_{sx} = 18.3kNm$

$M^* \le \phi M_{sx}\ OK$

Section Shear:

$P = 50kN$

$$V^* = \frac{W_{Fixing} \times S_{Fixing}}{2}$$

$$V^* = \frac{167 \times 0.3}{2}$$

$$V^* = 25kN$$

$\phi V_V = 292kNm$

$V^* \le \phi V_v\ OK$

Section Individual Element Design Check:

Individual design elements were considered for bending of the RHS section flange and bearing of fixing bolts in section web.

Flange Bending:

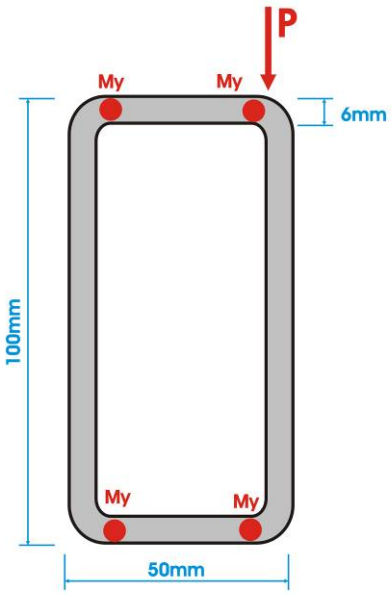

$$M^* = P \times L$$
$$M^* = 50 \times 0.05$$
$$M^* = 2.5$$

$$\phi M_N = \phi \times f_y \times Z_{Flange}$$

Z taken for half the length of seat for uneven bearing

$$Z_{Flange} = \frac{bd^2}{6}$$
$$Z_{Flange} = \frac{600 \times 6^2}{6}$$
$$Z_{Flange} = 3600mm^3$$

Web Bearing(fixing bolts):

$$V_b^* = \frac{P}{2}$$
$$V_b^* = \frac{50}{2}$$
$$V_b^* = 25kN$$

$$V_b = 3.2 d_f t_p f_{up}$$

$$d_f = 16mm$$
$$t_p = 6mm$$
$$f_{up} = 450MPa$$

$$V_b = 3.2 \times 16 \times 6 \times 450$$
$$V_b = 138kN$$

$V_{b(pull-out)}$ *ignored as not flat plate and not critical*

$$C_1 = 1.0$$
$$\phi = 0.9$$

$$C_1 \phi V = 1.0 \times 0.9 \times 138kN$$
$$C_1 \phi V = 124kN$$

$$V_b^* \le C_1 \phi V_b \; OK$$

$f_y = 450MPa$

$\phi M_n = 0.9 \times 450 \times 3600$
$\phi M_n = 1.5kNm$

$At\ least\ 2\ yeild\ lines\ must\ occur$
$for\ fialure\ therefore \phi M_n = 3kN$
$(conservative)$

$M^* \leq \phi M_{sx}\ OK$

Section Fixing Design:

Adhesive anchored fixings were designed according to the Hilti Fastening Technology Manual specifications. The spacing of the fasteners was governed by spacing of the stirrups in the seating beam and the anchorage depth by the extent of beam cover and desire to anchor into the core concrete within the beam section.

Bolt Anchorage Design Check: From HILTI Design Manual

Hole Diameter: 18mm, 16mm Fixing diameter

Pull-out:

$N_{ru,m} = 77.9kN(PerFixing)$

$N_{ru,m} = 4x77.9$
$N_{ru,m} = 311.6kN(Total)$

$N^* = unkown, but\ very\ small$

$N^* \leq N_{ru,m}\ OK$

Shear:

$V_{ru,m} = 46.7kN(PerFixing)$

$V_{ru,m} = 4x46.7$
$V_{ru,m} = 186.8kN(Total)$

$V^* = 50kN$

$V^* \leq V_{ru,m}\ OK$

Bolt Shear Design Check:

Bolt Shear: M16 HT Threaded Rod

$$V_f^* = \frac{P}{2}$$
$$V_f^* = \frac{50}{2}$$
$$V_f^* = 25kN$$

$$V_f = 0.62 f_{uf} k_r (n_n A_c + n_x A_0)$$

$$f_{uf} = 830MPa$$
$$n_n = 1$$
$$n_x = 0$$
$$A_c = A_0 = 144mm^2$$
$$\phi = 0.8$$

$$\phi V_f = 0.8 \times 830 \times 1 \times 144$$
$$\phi V_f = 95.6kN$$

$$V_f^* \le \phi V_f \; OK$$

C2 Alternative Steel Seating Sections

A number of potential steel sections were considered for the additional seating ledge. The 100x50x6RHS was the final section used. The reasons for this were discussed in Section 6, generally the RHS required minimal modification, where other open sections required the addition of stiffeners.

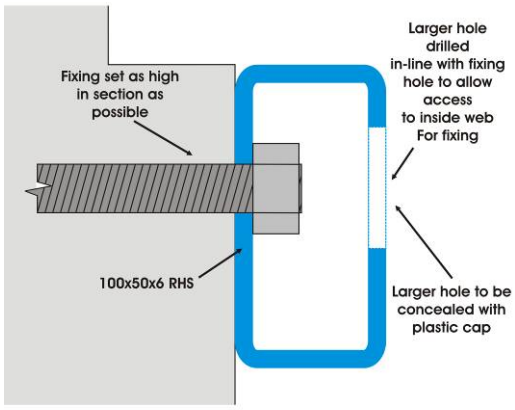

a) 100x50x6 RHS (final solution used)

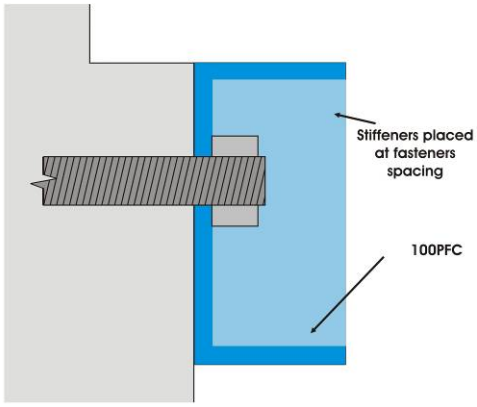

b) 100PFC

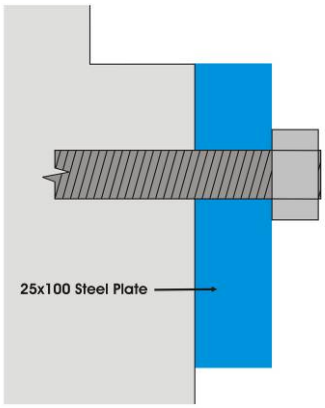

c) 25x100 Steel Plate

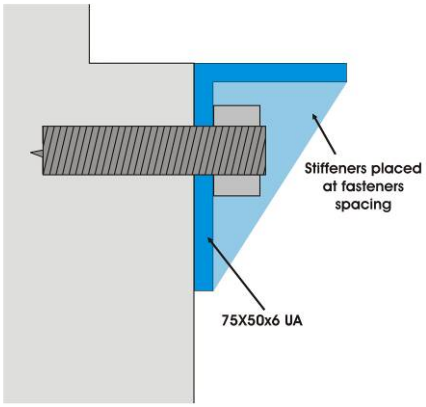

d) 75x50x6UA

Figure C-1 Alternative steel sections for additional seating ledges

Appendix D Beam Elongation Investigation

This section outlines further details associated with adaptation of the Lee and Watanabe (2003) and Mathews (2004) Beam elongation models.

D1 Internal Lever Arm Estimation

To avoid using the internal lever arms (e_{cr}'s) adopted for the University of Canterbury super-assembly for other bare beam comparisons, Response2000 section analysis software was used to estimate elastic and inelastic e_{cr}'s. This section outlines the respective strain profiles used to estimate representative e_{cr}'s for the bare beam comparisons.

Fenwick et al (1981):

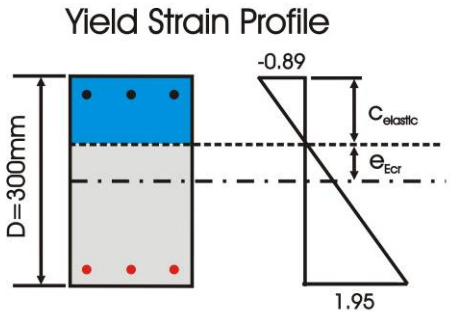

$$\frac{c_{elastic}}{0.89} = \frac{300}{0.89+1.95}$$
$$c_{elastic} = 157mm$$

$$e_{Ecr} = \frac{150-157}{300}xD$$
$$e_{Ecr} = 0.19D$$

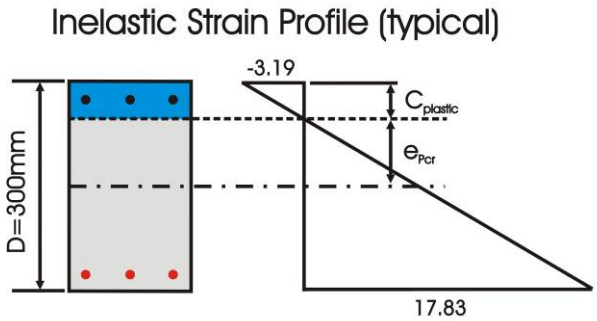

$$\frac{c_{plastic}}{3.19} = \frac{300}{3.19+17.83}$$
$$c_{plastic} = 76mm$$

$$e_{Ecr} = \frac{150-76}{300}xD$$
$$e_{Ecr} = 0.35D$$

a) strain profile **b) Calculations**

Figure D-1 Fenwick et al (1981) internal lever arm estimation

Restrepo (1993):

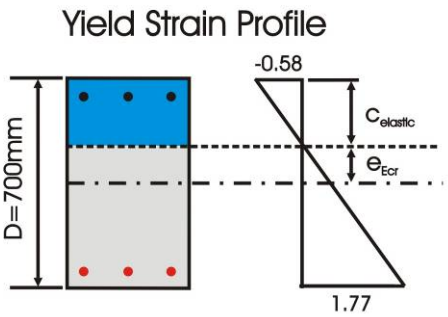

$$\frac{c_{elastic}}{0.58} = \frac{700}{0.58 + 1.77}$$
$$c_{elastic} = 173mm$$

$$e_{Ecr} = \frac{350 - 173}{700} xD$$
$$e_{Ecr} = 0.25D$$

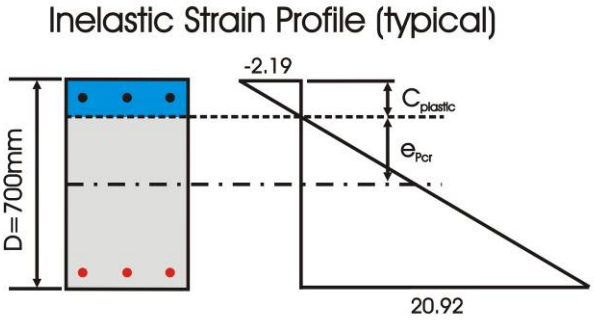

$$\frac{c_{plastic}}{2.19} = \frac{700}{2.19 + 20.92}$$
$$c_{plastic} = 67mm$$

$$e_{Ecr} = \frac{350 - 67}{700} xD$$
$$e_{Ecr} = 0.4D$$

a) strain profile **b) Calculations**

Figure D-2 Restrepo (1993) internal lever arm estimation Unit 1 & 2

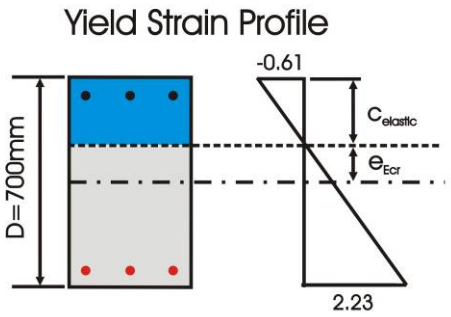

$$\frac{c_{elastic}}{0.61} = \frac{700}{0.61 + 2.23}$$
$$c_{elastic} = 150mm$$

$$e_{Ecr} = \frac{350 - 150}{700} xD$$
$$e_{Ecr} = 0.29D$$

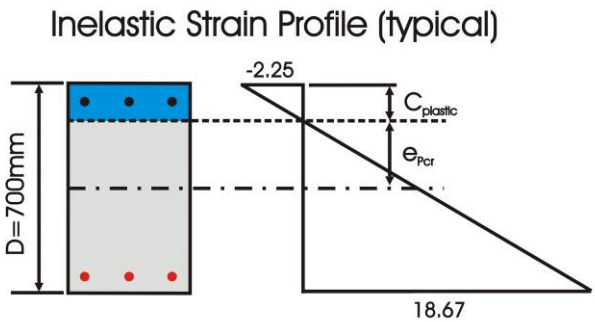

$$\frac{c_{plastic}}{2.25} = \frac{700}{2.25 + 18.67}$$
$$c_{plastic} = 75mm$$

$$e_{Ecr} = \frac{350 - 75}{700} xD$$
$$e_{Ecr} = 0.39D$$

a) strain profile **b) Calculations**

Figure D-3 Restrepo (1993) internal lever arm estimation Unit 3

Lau (2001):

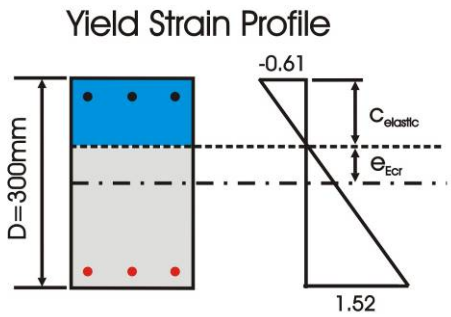

$$\frac{c_{elastic}}{0.61} = \frac{300}{0.61+1.52}$$
$$c_{elastic} = 86mm$$

$$e_{Ecr} = \frac{150-86}{300}xD$$
$$e_{Ecr} = 0.21D$$

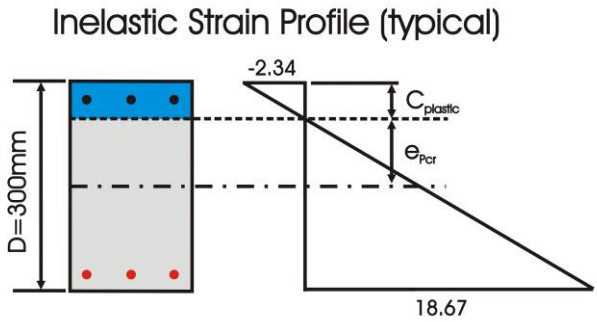

$$\frac{c_{plastic}}{2.34} = \frac{300}{2.34+18.67}$$
$$c_{plastic} = 34mm$$

$$e_{Ecr} = \frac{150-34}{300}xD$$
$$e_{Ecr} = 0.39D$$

a) strain profile **b) Calculations**

Figure D-4 Lau (2001) internal lever arm estimation

D2 Example Beam Elongation Calculation

Figure D- and Figure D- show the loading profile and resulting elongation calculation (spread sheet) for the transverse loading direction (Phase 2) of the super-assembly test carried out by Lindsay (2004). Figure D- illustrates the hinge references and loading directions for the super-assembly test specimen.

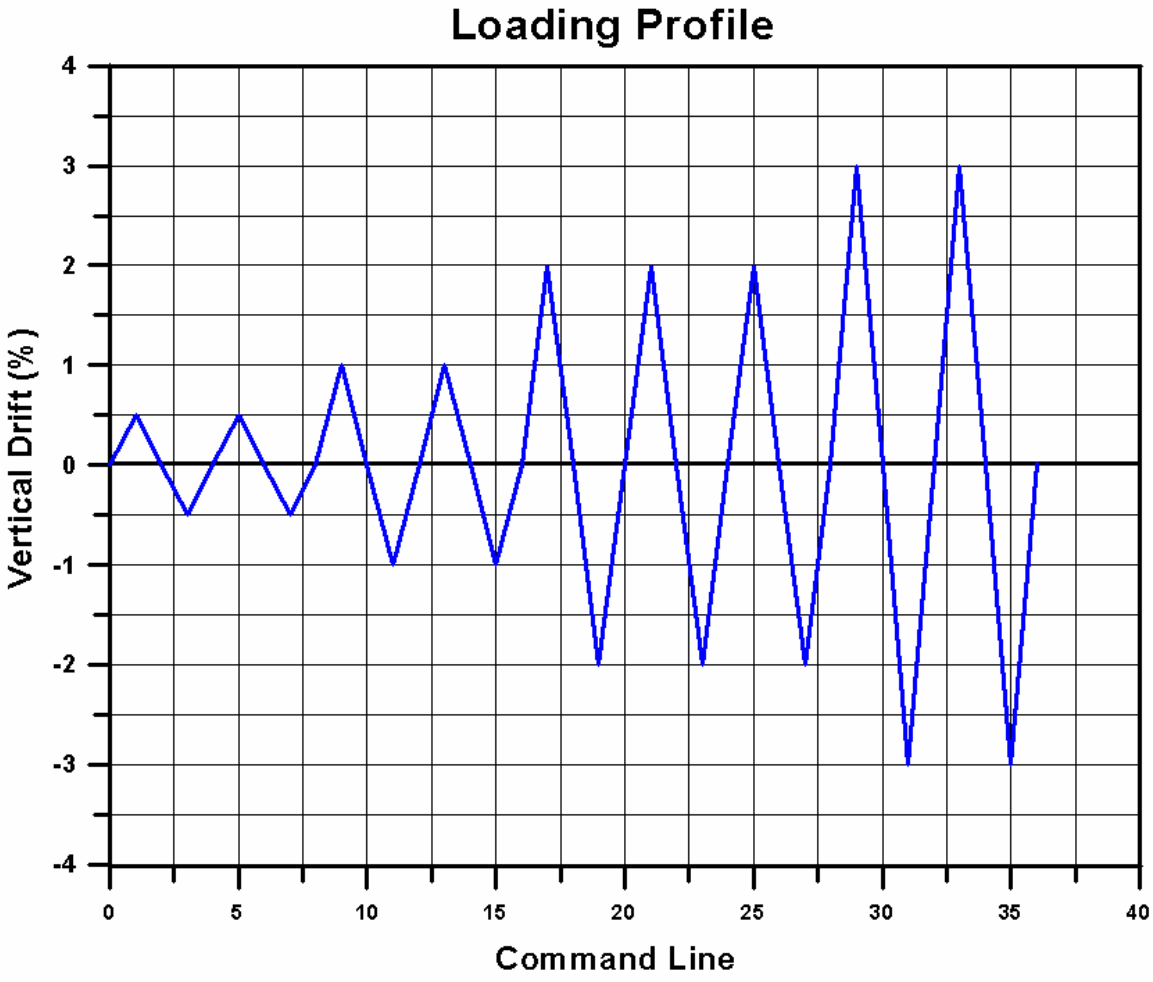

Figure D-5 Loading profile for Lindsay (2004) in Transverse direction

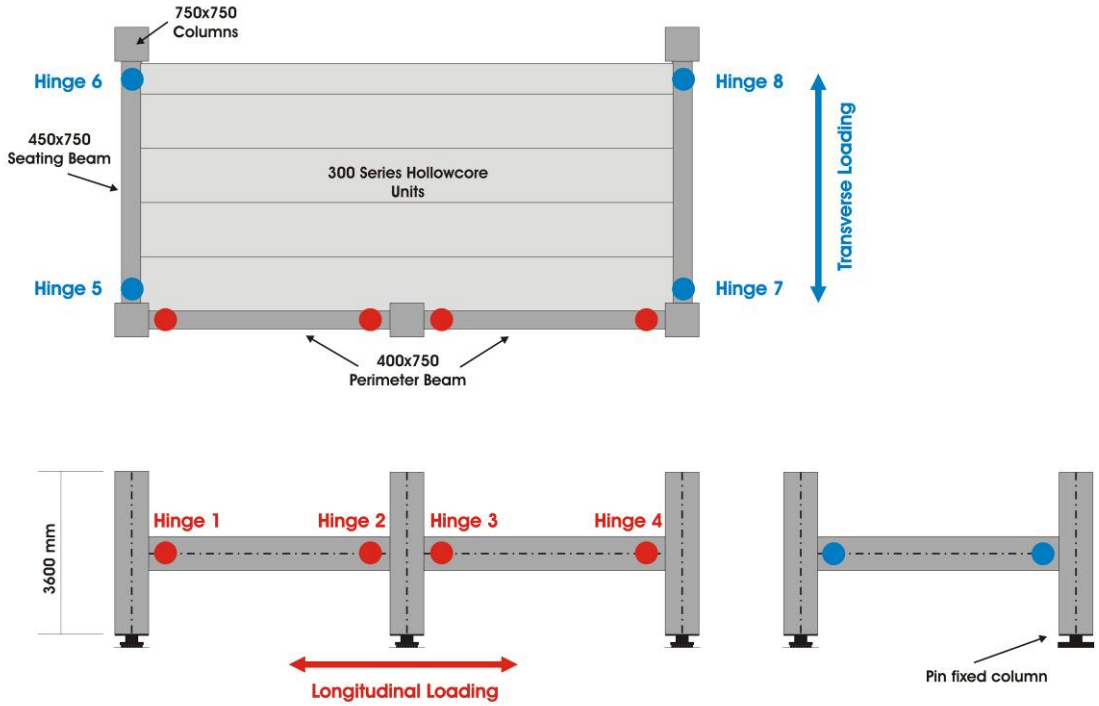

Figure D-6 Super-assembly hinge numbering and loading directions

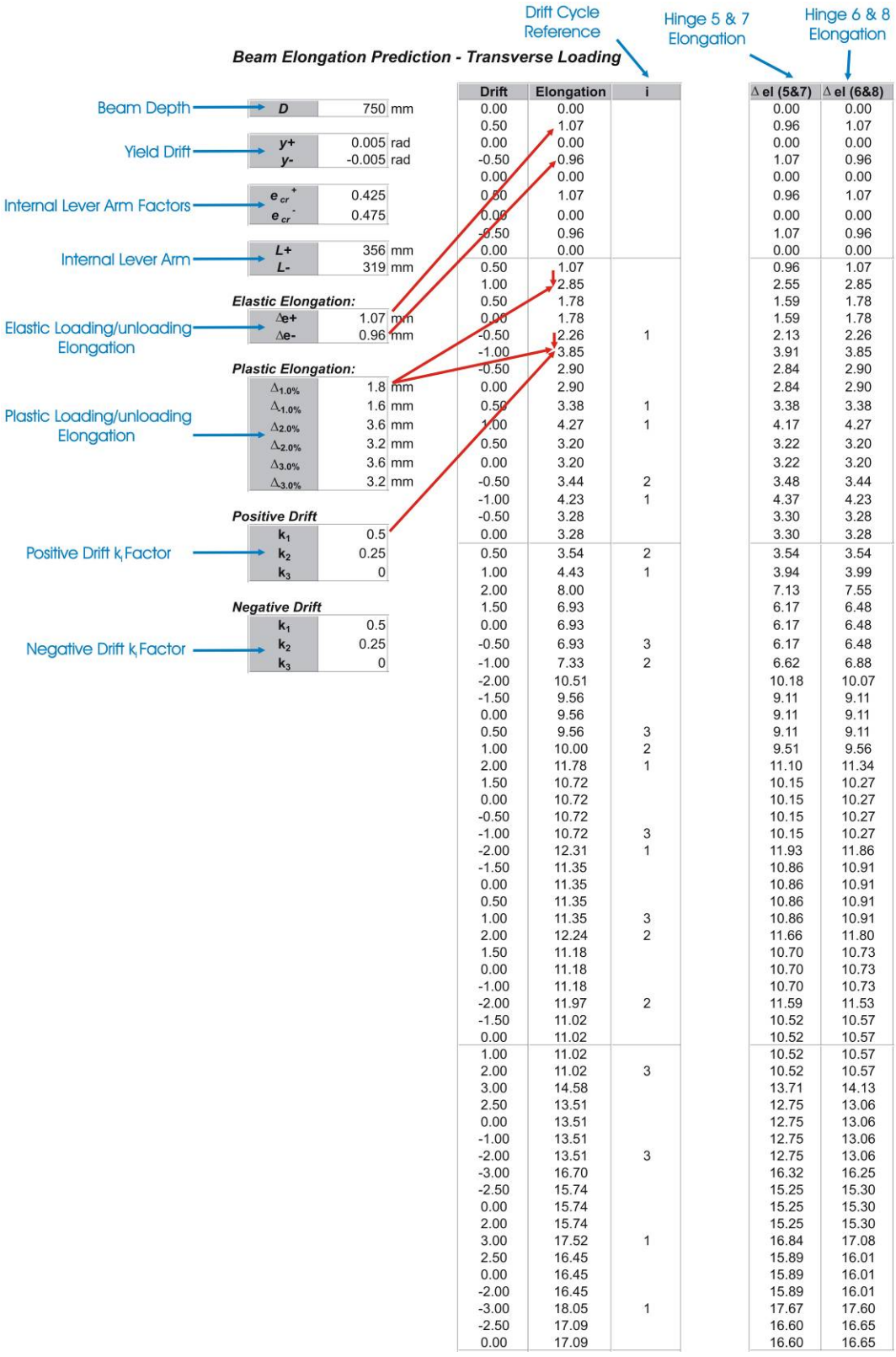

Drift	Elongation	i	Δ el (5&7)	Δ el (6&8)
0.00	0.00		0.00	0.00
0.50	1.07		0.96	1.07
0.00	0.00		0.00	0.00
-0.50	0.96		1.07	0.96
0.00	0.00		0.00	0.00
0.50	1.07		0.96	1.07
0.00	0.00		0.00	0.00
-0.50	0.96		1.07	0.96
0.00	0.00		0.00	0.00
0.50	1.07		0.96	1.07
1.00	2.85		2.55	2.85
0.50	1.78		1.59	1.78
0.00	1.78		1.59	1.78
-0.50	2.26	1	2.13	2.26
-1.00	3.85		3.91	3.85
-0.50	2.90		2.84	2.90
0.00	2.90		2.84	2.90
0.50	3.38	1	3.38	3.38
1.00	4.27	1	4.17	4.27
0.50	3.20		3.22	3.20
0.00	3.20		3.22	3.20
-0.50	3.44	2	3.48	3.44
-1.00	4.23	1	4.37	4.23
-0.50	3.28		3.30	3.28
0.00	3.28		3.30	3.28
0.50	3.54	2	3.54	3.54
1.00	4.43	1	3.94	3.99
2.00	8.00		7.13	7.55
1.50	6.93		6.17	6.48
0.00	6.93		6.17	6.48
-0.50	6.93	3	6.17	6.48
-1.00	7.33	2	6.62	6.88
-2.00	10.51		10.18	10.07
-1.50	9.56		9.11	9.11
0.00	9.56		9.11	9.11
0.50	9.56	3	9.11	9.11
1.00	10.00	2	9.51	9.56
2.00	11.78	1	11.10	11.34
1.50	10.72		10.15	10.27
0.00	10.72		10.15	10.27
-0.50	10.72		10.15	10.27
-1.00	10.72	3	10.15	10.27
-2.00	12.31	1	11.93	11.86
-1.50	11.35		10.86	10.91
0.00	11.35		10.86	10.91
0.50	11.35		10.86	10.91
1.00	11.35	3	10.86	10.91
2.00	12.24	2	11.66	11.80
1.50	11.18		10.70	10.73
0.00	11.18		10.70	10.73
-1.00	11.18		10.70	10.73
-2.00	11.97	2	11.59	11.53
-1.50	11.02		10.52	10.57
0.00	11.02		10.52	10.57
1.00	11.02		10.52	10.57
2.00	11.02	3	10.52	10.57
3.00	14.58		13.71	14.13
2.50	13.51		12.75	13.06
0.00	13.51		12.75	13.06
-1.00	13.51		12.75	13.06
-2.00	13.51	3	12.75	13.06
-3.00	16.70		16.32	16.25
-2.50	15.74		15.25	15.30
0.00	15.74		15.25	15.30
2.00	15.74		15.25	15.30
3.00	17.52	1	16.84	17.08
2.50	16.45		15.89	16.01
0.00	16.45		15.89	16.01
-2.00	16.45		15.89	16.01
-3.00	18.05	1	17.67	17.60
-2.50	17.09		16.60	16.65
0.00	17.09		16.60	16.65

Figure D-7 Spreadsheet for the transverse loading direction of the Lindsay (2004) super-assembly test